

UNCLASSIFIED

AD NUMBER
AD254022
NEW LIMITATION CHANGE
TO Approved for public release, distribution unlimited
FROM Distribution authorized to U.S. Gov't. agencies and their contractors; Administrative/Operational Use; MAR 1961. Other requests shall be referred to Air Force Cambridge Research Laboratories, Hanscom AFB, MA.
AUTHORITY
AFCRL ltr, 3 Nov 1971

THIS PAGE IS UNCLASSIFIED

UNCLASSIFIED

AD 254 022

*Reproduced
by the*

**ARMED SERVICES TECHNICAL INFORMATION AGENCY
ARLINGTON HALL STATION
ARLINGTON 12, VIRGINIA**



UNCLASSIFIED

NOTICE: When government or other drawings, specifications or other data are used for any purpose other than in connection with a definitely related government procurement operation, the U. S. Government thereby incurs no responsibility, nor any obligation whatsoever; and the fact that the Government may have formulated, furnished, or in any way supplied the said drawings, specifications, or other data is not to be regarded by implication or otherwise as in any manner licensing the holder or any other person or corporation, or conveying any rights or permission to manufacture, use or sell any patented invention that may in any way be related thereto.

CATALOGED BY ASI/H

AS AD NO.

254022

DTIC

Geophysics Research Directorate

PROJECT FIREFLY 1960

VOLUME I

MASS TRANSPORT
SPECTROPHOTOMETRY
RELEASE CHEMICAL PHYSICS

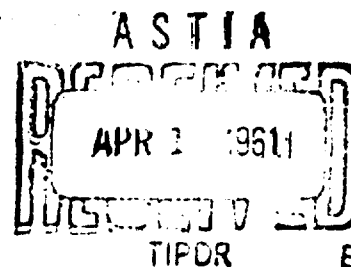
SEMI-ANNUAL REPORT UNDER
ARPA ORDER 42-60
DASA MIPR 528-61

PERIOD COVERED
1 JULY - 31 DECEMBER 1960

SUBMITTED
1 MARCH 1961

XON

AIR FORCE CAMBRIDGE RESEARCH LABORATORIES
AIR FORCE RESEARCH DIVISION (ARDC)
LAURENCE G. HANSCOM FIELD
BEDFORD, MASSACHUSETTS



Best Available Copy

**Best
Available
Copy**

Requests for additional copies by Agencies of the Department of Defense, their contractors, and other government agencies should be directed to the:

Armed Services Technical Information Agency
Arlington Hall Station
Arlington 12, Virginia

Department of Defense contractors must be established for ASTIA services, or have their 'need-to-know' certified by the cognizant military agency of their project or contract.

All other persons and organizations should apply to the:

U. S. DEPARTMENT OF COMMERCE
OFFICE OF TECHNICAL SERVICES,
WASHINGTON 25, D. C.

Chemical Physics Branch
Photochemistry Laboratory
Geophysics Research Directorate
Air Force Cambridge Research Laboratories
Air Force Research Division (ARDC)
Laurence G. Hanscom Field
Bedford, Massachusetts

APRL 256 (I)

PROJECT FIREFLY 1960

VOLUME I

MASS TRANSPORT

SPECTROPHOTOMETRY

RELEASE CHEMICAL PHYSICS

Part I, Semi-annual Report
under ARPA Order 42-60
DASA MIPR 528-61

Period Covered
1 July - 31 December 1960

Submitted
1 March 1961

Project Scientist
N. W. Rosenberg

PROJECT FIREFLY 1960

TABLE OF CONTENTS

PAGE

VOLUME I (U)

Summary - Project Firefly (U) N. W. Rosenberg, AFCRL	7-39
<u>1. EARLY TIME MASS TRANSPORT</u>	
Growth from Photography H. D. Edwards, Ga. Tech.	1001-1006
Short Time Growth and Photometry Measurements R. B. Holt, Device Dev. Corp.	1007-1035
Early-Time Cloud Growth and Energy Distribution as Measured by Doppler Frequency Shift Methods R. A. Barnes, P. B. Gallagher, Stanford U.	1037-1054
Experimental and Theoretical Results on Electron Cloud Growth 0 - 10 Seconds after Release J. F. Paulson, AFCRL	1055-1064
Symposium Discussion	1065-1075
<u>2. LATER TIME MASS TRANSPORT</u>	
Position, Drift and Growth from Photography H. D. Edwards, Ga. Tech.	2001-2024
Molecular and Turbulent Diffusion in the Upper Atmosphere S. P. Zimmerman, K. S. W. Champton, AFCRL	2025-2029
See also Summary: Position, Drift and Growth of Electron Clouds J. W. Wright, NBS Boulder	(5069-5073)
Symposium Discussion	2031-2041
<u>3. SPECTRO PHOTOMETRY</u>	
Filter Photography and Photometry H. D. Edwards, J. L. Brown, Ga. Tech.	3001-3013
Spectrographic Data H. D. Edwards, Ga. Tech.	3015-3017
Firefly 1960 Spectrographic Data C. D. Cooper, U. Georgia	3019-3026

Near Infrared Photometry of Artificial Clouds 3027-3047
 R. G. Eldridge, Tech. Op.; J. D. Armitage, Jr., AFCRL;
 J. J. Freymouth, J. L. Streete, SWU Memphis

See also Short Time Growth and Photometry Measurements (1007-1035)
 R. B. Holt, Device Dev. Corp.

Symposium Discussion 3049-3059

4. RELEASE CHEMICAL PHYSICS

Research Directed toward a Theoretical Study of
Physical Processes Associated with Chemical Releases 4001-4070
 Chemistry of Upper Atmosphere Releases 4004
 Mathematical Models for Chemical Release Studies 4007
 Optical Properties of Chemical Releases 4039
 RF Propagation Studies 4058
 Summary 4065
 F. F. Marmo, et al., GCA

Rocket Measurement of Charge Densities 4071-4072
 R. C. Sagalyn, AFCRL

See also Condition of the Ionosphere (5006-5027)
 J. W. Wright, NBS Boulder

Particle Size Analysis of Some of the Solar Scatter
Materials Used in Project Firefly 1960 4073-4078
 J. L. Brown, Ga. Tech.

VOLUME II (C)

Summary - Project Firefly (C)
 N. W. Rosenberg, AFCRL 7-69

4. RELEASE CHEMICAL PHYSICS (contd)

Chemicals and Release Mechanisms for Upper Atmosphere Investigations 4079-4120
 Electron and High Explosive Point Release Experiments 4082
 Cesium Trail Release Studies 4100
 Addendum 4108
 Fluid Release Studies 4113
 Aerosol Release Studies 4117
 A. C. Baker, H. J. Fisher, S. B. Kilner,
 C. Kuckar, Aerojet

Symposium Discussion 4121-4129

5. RF BACKSCATTER STUDIES

Ionosonde Observations of Artificially Produced Electron Clouds	5001-5006
Condition of the Ionosphere	5006
Details of the Individual Experiments	5025
Summary: Position, Drift and Growth of Electron Clouds	5089
J. W. Wright, NBS Boulder	
Sweep Frequency Ionosonde Observations	5087-5097
D. J. Spencer, USASRPA	
Backscatter Reflection Characteristics of Cesium Cloud Releases	5099-5128
P. B. Gallagher, Stanford U.	
Acania Radar Observations of 1960 Firefly Experiments	5129-5136
R. A. Long, SRI	
Addendum on Forward Scatter of Acania Transmissions	5139-5141
R. A. Long, SRI	
Long Range Backscatter	5143-5155
E. W. Irre, ACF	
Symposium Discussion	5157-5160

6. RF FORWARD SCATTER STUDIES

Summary of Data Collected by DOD in Firefly 1960 Series	6001-6036
J. B. Norvell, E. V. Marsh, R. E. Mallon, DOD	
Radar Communication Experiments Using Ionized Clouds	6037-6057
E. L. Blackwell, USASRD L	
Ion Cloud Propagation Test Results	6059-6082
D. Sukhia, R. Hollis, Martin Co.	
See also Addendum on Forward Scatter of Acania Transmissions	(5139-5141)
R. A. Long, SRI	
Symposium Discussion	6083-6099

VOLUME III (S)

7. MISSILE TRAIL MECHANISMS

High-Altitude Visible Missile Trails	7001-7097
Instrument Selection	7005
Field Observations	7007
Spectrometry	7061
Equipment and Operating Technique	7085
N. W. Rosenberg, W. M. Hamilton, AFCRL; D. J. Lovell, B. A. Bang, Bendix	
Missile Launch Spectra Recorded by Television Techniques	7099-7113
D. J. Lovell, Bendix	
High Altitude Missile Plume	7115 -7125
R. Marriott, Radiation Inc. *	
Missile Exhaust Ionization in the Upper Atmosphere	7127 -7140
L. T. Dolphin, Jr., SRI *	
Some Comments on the Fluid Dynamics of Missile Trails	7141 -7153
A. Thomson and F. Harshbarger, Convair *	
Symposium Discussion	7155 -7162

* Symposium guest speakers

PROJECT FIREFLY 1960 - A SUMMARY REPORT

N. W. Rosenberg

**Headquarters, Air Force Cambridge Research Laboratories
Air Force Research Division (ARDC), Geophysics Research
Directorate, L. G. Hanscom Field, Bedford, Massachusetts**

ABSTRACT

Project Firefly 1960, the upper atmosphere chemical release program of the Geophysics Research Directorate, in cooperation with other participating agencies, has provided a systematic study of several types of upper atmosphere perturbations. Reports on reduced and interpreted data from a number of optical and radio-frequency stations have been prepared by participants, and published as a GRD special report. A preliminary crosscorrelation of that information is presented in this summary. The summary consists of an introduction, special sections on missile trails and weapons effects, and sections on groups of releases:

night point electron	high explosive	cobalt particles
sunlit point electron		hydrocarbon
cesium trail	electron removal	alumina particles

The summary section for each group of releases includes a statement of objectives, observations, conclusions, recommended further data analysis, and recommended further experiments.

1. SCOPE AND OBJECTIVE OF PROGRAM

Upper atmosphere studies, prior to the availability of rockets, were accomplished largely through ground-based observations of natural perturbations, by radio frequency sensors which detect electron inhomogeneities, and optical sensors which detect light scattered and/or emitted by atoms, molecules, ions, and particulate matter. With rockets and satellites available, the upper atmosphere is now being studied with vehicle-borne sensors. An alternate approach to upper atmosphere studies has also been made possible by such vehicles. This is the artificial perturbation of the upper atmosphere by release of vehicle-borne chemicals. Experiments of increased versatility are therefore possible since the study is no longer restricted to unpredictable natural perturbations. Chemical release studies of composition (e.g. by release of nitric oxide or ethylene), of temperature (e.g. by sodium spectral resonance broadening), of electron processes (e.g. by cesium releases), of diffusion and winds (e.g. by solar-illuminated sodium and potassium releases) have been previously reported by this and other laboratories.

Controlled chemical releases provide a unique technique for analysis of those upper atmosphere processes which have a physical scale larger than can be measured by point sampling of vehicle-borne sensors. Natural perturbations such as sporadic E and artificial perturbations such as missile trails inherently involve this large physical scale. The chemical release program of the Geophysics Research Directorate (Project Firefly) has provided a systematic determination of some of the basic variables of such perturbations, so that they can be controlled or simulated as required.

The Project Firefly 1960 experiments were carried out to study the physical and chemical properties of electrons, ions, gases and particulate matter following their release at high velocity and at high altitude. The releases were designed to evaluate (a) the early explosive expansion of these species prior to pressure equilibrium, (b) the later expansion when molecular diffusion or turbulent processes are important, (c) the processes leading to dissipation of the perturbed region through interaction with the ambient, (d) models describing the nature of electron inhomogeneities, (e) mechanisms for light emission under sunlit and under dark conditions, and (f) communication capabilities of artificially created high electron densities.

The field program included two basic areas: (1) the observation of missile targets on the Atlantic Missile Range (AMR), and (2) the controlled release of selected chemicals into the upper atmosphere. Both of these efforts have been integrated with theoretical and laboratory experimental studies (both by GRD and by other agencies) in order to provide the fullest interpretation of the observed phenomena. Volumes I and II of this report cover the chemical release program conducted in 1960, which consisted of a series of 33 chemical releases (listed in Table I) from verticle probe rockets at Eglin AFB during July and August 1960; and Volume III covers missile trail observations on the Atlantic Missile Range.

The chemical release experiment consists of the release itself, and observation, data reduction and data interpretation by participating groups. The participants (named in the Table of Contents of this report) included many groups making simultaneous observations, each studying the aspects of most pertinence

to its own interests. The resulting large pool of information has permitted cross-correlation in a number of ways both for basic geophysics data and for specific military applications. Optical equipment included (a) cameras with framing rates from 500 frames per second¹⁰⁰⁷ to one frame per 10 seconds,²⁰⁰¹ (some equipped with narrow band interference filters),³⁰⁰¹ (b) television light amplifiers¹⁰⁵⁵ in the visible and near I.R., and (c) spectrometers and photometers in the visible³⁰⁰¹,¹⁰⁰⁷ and infrared.³⁰²⁷ Radiofrequency equipment included^{5001, 5087} (a) 2 - 20 mc ionosondes and (b) multiple fixed frequency sounders recording forward and back-scatter above 6 mc., including Doppler and phase shift displays,^{5089, 5129} and (c) modulated forward scatter radiofrequency transmissions at VHF.^{6001, 6037, 6059, 5139}. The program was carried out in a single field trip so that the equipment was set up only once for all thirty-three releases.

The present report is in fact a collection of individual reports made by each of the groups of observers on the entire test series; and the main purpose of this summary section is a preliminary cross correlation of their observations for each type of release (or missile phenomenon). Panel discussions held during a symposium on Project Firefly (31 Jan and 1 Feb 1961) at AFCRL are also included in the report. Over the next months, further cross correlations of the existing data will be made by several of the participating groups to provide more detailed models of upper atmosphere perturbations.

NOTE: Superscript numbers are references to pertinent page numbers in Volumes I, II, and III.

HEAVY POSITION DATA, Revised 1 March 1961

Experiment		Payload		Date	Release time, CST	Solar horizon, km	Release			A-10 range, km
		Net, kg	Added, Na ²				Altitude, km	Latitude, deg	Longitude, deg	
Margie	PEC	60	800 ²	8/13	0437:00.60	62	74.8	30.10	88.08	81
Mario	PEC	18	200 ²	8/9	0438:25.2	50	81.4	30.12	88.03	83
Lola	PEC	60	800 ²	8/15	0438:00.12	62	83.5	30.20	88.62	83
Zelda	PEC	49.5	800 ²	8/25	0830:40	0	102	30.23	88.55	108
Peggy	PEC	18	200 ²	8/16	0441:50.75	53	102.7	30.03	88.53	111
Olive	PEC	18	200 ²	8/18	0441:50.15	57	108.2	29.93	88.46	120
Jeanne	PEC	18	200 ²	8/10	0436:40.80	58	108.7	30.19	88.38	111
Susan	PEC	22	1100 ²	8/17	0443:49.33	45	114.3	30.02	88.52	123
Dolly	PEC	18	800 ¹	7/27	0421:45.84	73	115.2	29.66	88.41	144
Cathy	PEC	18	160 ¹	7/29	0253:44.95	>500	93.9	29.72	88.46	123
Betsy	PEC	18	520 ²	8/8	0416:40.62	123	108.6	30.29	88.69	109
Amy	PEC	18	160 ¹	7/28	0232:45.27	>500	111.0	29.62	88.45	143
Ruthy	PEC	18	160 ¹	8/1	0232:29.35	>500	113.3	29.89	88.59	127
Gerta	PEC	18	745 ²	8/6	0303:00	>500	138.0	30.03	88.47	146
Janet	TEC	16	---	7/26	0419:30	78	118.9	29.84	88.52	138
Hilda	TEC	16	---	8/1	0426:31.2	71	126.0	29.83	88.52	141
Carry	HEX	19	---	7/18	0403:27	114	129.9	30.04	88.66	134
Arlene	HEX	18	---	8/15	1945:34	260	104.2	30.12	88.48	111
Annie	ARC	---	---	8/13	0121:24	>500	97.7	29.92	88.62	132
Norma	ARC	---	---	8/13	0349:24	>500	96.7	30.17	88.51	122
Bena	SHF	14	---	8/19	1356:40	0	105	30.20	88.62	108
Linda	MET	22	---	8/17	2045:00	700	133	30.10	88.57	138
Mavis	SS3	3.2	---	7/29	0415:32	100	67.2	30.31	88.69	67.9
Frances	SS1	7.7	---	7/14	0408:20	88	148.2	30.08	88.81	184
Lily	SS2	8.1	---	7/21	0405:16	115	150.7	30.17	88.83	154
Hedy	CDS	18	---	7/22	0412:47	80	108.3	30.15	88.65	112
Ida	KER	10	---	7/20	1932:30	80	129.6	29.93	88.60	140
Vicky	PEC *	16	800 ²	8/25	1906:19.53	150	2	30.34	88.70	5
Wendy	PEC *	19	200 ²	8/18	0418:40.62	160	14	30.24	88.70	11
Ethel	TEC *	18	---	7/25	NR	>500	NR (No Release)			
Dotty	SS3 *	5	---	7/15	NR	105	NR (No Release)			
Edith	SS2 *	8	---	7/12	NR	55	NR (No Release)			
Trudy	NH ₃ *	11	---	8/17	NR	230	Below Sea Level			

* Not released at altitude

1. Grams NaNO₃

2. Grams mixture

63% NaNO₃ - 37% Al

3. 1959 composition

PEC - point electron cloud

TEC - trail electron cloud

HEX - high explosive

SHF - sulfur hexafluoride

KER - synthetic kerosene

NH₃ - ammonia

MET - 2 μ cobalt powder

SS1 - 0.5 μ Al₂O₃

SS2 - 3 μ Al₂O₃

SS3 - 0.03 μ Al₂O₃

CDS - 3 μ cadmium sulfide powder

2. ARPA SPONSORED STUDIES OF MISSILE PHENOMENA

2.1 Introduction

All existing or proposed ICBM vehicles are launched by engines which release large quantities of chemicals - electrons, ions, gases, and particulate matter - at high velocities and over a wide range of altitudes (up to 150 km for the Minuteman, 300 km for the Atlas). It is improbable that the 1000 - 100,000 cubic kilometers occupied by these exhaust species with their radically different composition from the ambient atmosphere can be hidden from an adequate surveillance system.

2.2 Objectives

The Geophysics Research Directorate has carried out a program under ARPA Order 42 directed towards answering the following six questions:

- (1) What atmospheric characteristics are modified and what phenomena are produced by the passage of a missile through the upper atmosphere?
- (2) What are the chemical and physical mechanisms responsible for the modification of atmospheric characteristics and for the phenomena produced?
- (3) Which of these are general to all vehicles, times, and/or places and which are specific to specific vehicle types, specific times of observation, and/or specific observer-vehicle positions?
- (4) Which of these effects are subject to control (enhancement or attenuation) by missile designers or launchers, by means of additives, changes in engine design, time of launch, decoys, or masks?

- (5) Which phenomena can be effectively used, and in what manner, in:
- (a) surveillance, detection, track, and discrimination
 - (b) prevention of surveillance, detection, track, and discrimination by an AICBM system
 - (c) design of decoys and false alarms

3. DASA SPONSORED STUDIES OF CHEMICAL RELEASES

Nuclear detonations in the upper atmosphere produce artificial upper atmosphere perturbations. It has been suggested that some of these effects can be studied by releasing suitable materials in the upper atmosphere. DASA MIPR 528-61, dated 11 August 1960, initiated a program:

- (1) to evaluate which nuclear effects can be appropriately studied by chemical releases
- (2) to analyze existing data on chemical releases where applicable
- (3) to design and execute specific experiments

4. NIGHT POINT ELECTRON CLOUDS

Five point electron clouds were released at night: Cathy, Amy, Betsy, Ruthy and Gerta, ranging in altitude from 90 to 140 km, each with an identical net payload of 20 kilograms of cesium-containing mixture.

4.1 Objectives

The objectives of this group of releases were (1) to create a region of local high electron density for over-horizon communication; (2) to study mass transport, chemiluminescence and thermal emission from gases and solids ejected at high velocity in the absence of sunlight and (3) to determine the rate of decay of electron density in the absence of ionizing sunlight.

4.2 Discussion

Experimental ground studies were conducted on a CsNO_3/Al mixture with an organic chemical binder to maximize the initial ionization achieved in the release, since in the absence of solar photoionization this initial ionization represents the only source of electrons for the night releases. The ground studies led to a composition ⁴⁰⁹⁰ of lower sensitivity⁴⁰⁸⁸ than the charges of the previous 1959 series. Furthermore, the higher mass density led to a faster reaction rate, ⁴⁰⁹⁰ Whether this was translated into increased yields has not yet been fully assessed.

The composition ⁴⁰⁸³ of each of the point releases produced, at altitude, a 3500 °K plasma mixture of 10 kg of finely divided aluminum oxide, 300 moles of inert gases (including carbon monoxide and hydrogen), 30 moles of cesium and sodium vapors, and a small fraction of cesium ions and free electrons.

In visual observations following release, the chemical cloud expanded to form a circle of light which grew in the first two seconds to about one degree in diameter (2 km) with an orange tint due to 5893A radiation from the small sodium content. The tint disappeared after about ten seconds, leaving a low-intensity but clearly visible white circle, which slowly developed a hole in its center and faded over 30-300 seconds while growing to a diameter of 3° (6 km). The hole in the center suggests that the luminescence occurs at the surface of a diffusing sphere of gaseous products. The highest-altitude cloud (140 km) failed to develop the central hole, suggesting that rapid diffusion at this altitude prevented formation of a defined surface.

The optical observations in the first seconds showed in three cases a single expanding sphere of gas reaching 200-500 meters radius at 0.2 seconds, and 400-1000 meters in 1 second, gradually fading over 10-30 seconds.¹⁰⁵⁵ In the other two cases, a double expanding sphere, one at higher velocity, the other matching those above, was recorded in the first second.¹⁰⁵⁵ A photometer aimed at a point 5 km away from one of the double sphere bursts³⁰⁰¹ showed a transient light wave at 1.2 seconds, suggesting a 4 km/sec average velocity for the outer wave. The outer sphere, possibly radiating solids, disappeared at about the one second mark at a radius of 1 - 2 km. Black body radiation from solid Al_2O_3 would result in a temperature given by $250 (D/t)^{1/3}$ where D is the particle diameter in microns and t the time in seconds. The temperature of a 1 micron particle will drop from $1100^\circ K$ at 0.01 sec to $500^\circ K$ at 0.1 sec; so that black body radiation will be negligible at 0.1 sec. On the other hand, a 10 micron particle will still have a temperature of 1100°

K at 0.1 second and black body radiation will be significant for such size particles.

No adequate spectral data on the persistent luminous cloud was obtained because of the low intensity, estimated as 10^{-9} watt/cm² ster. However, the continued emission over 500 seconds at low intensity totalled 2×10^{13} ergs of luminous energy. Since the entire payload contained only 10×10^{13} ergs, and conversion efficiencies for chemical energy to light emission rarely exceed a fraction of one per cent, it is probable that a source of ambient energy was tapped, possibly oxygen atom recombination. The luminescence probably was not line emission, since it was not recorded by the sensitive spectrograph. 3019

The r.f. observations showed initial radial growth of the electron front approximately ¹⁰⁴³ matching the optical growth, but sufficiently transparent so that both the near and far electron gradients could be separately recorded; i.e., both increasing and decreasing Doppler shifts were simultaneously recorded, tapering off after about one or two seconds at diameters of 1 - 3 km, depending on altitude. ¹⁰⁴³ There was a consistent pattern of more rapid electron density decay at the highest altitude (140 km) than at the lowest altitude studied (94 km). ⁵⁰⁴⁹

The electron drift could be followed by ionosondes for about 1000 seconds, ⁵⁰⁵⁰ typically as a westerly drift at about 50 meter/sec. Optical data confirmed the initial ionosonde position, but was not available for times sufficient to record drift in these night releases.

4.3 Conclusions are as follows:

- (1) Sufficient electron yields can be achieved in the absence of sunlight for over-horizon r.f. reflections.⁶⁰¹³
- (2) Visible luminescence from the surface of a reacting gas mass is present for some minutes
- (3) Radial expansions of electrons and gas front are at similar velocities, the gas reaching ambient pressure within 1 - 3 seconds.^{1059, 1043}
- (4) Electron decay to ambient densities is slower than would be expected in the absence of ionizing sunlight.⁵¹⁰⁹

4.4 Further data analysis is required to answer the following:

- (1) How closely do optical and r.f. growths match?
- (2) How closely do r.f. cross sections measured by different equipment agree?
- (3) Is a consistent model possible for all observations?
- (4) Is the model of ionization suggested by observed internal cloud motions sufficiently accurate to define an electron yield?
- (5) What are the controlling processes and rates for electron density decay?

4.5 Further experiments are required to answer the following:

- (1) Would a multiple point release be⁴⁰⁰⁵ more effective than a single point release as an r.f. reflector?

- (2) What is the cause of a single sphere versus a double sphere from otherwise identical releases?
- (3) What is the chemiluminescent spectrum and the mechanism?
- (4) Can higher altitude persistence of high electron densities be increased by magnetic field entrapment?
- (5) What is the lower altitude limit for effective reflections?
- (6) What processes involving reactions with ambient are important?

5. SUNLIT POINT ELECTRON CLOUDS

Nine sunlit point electron clouds were released, ranging in altitude from 74-115 km. Five of these releases, Marie, Peggy, Olive, Jeannie and Dolly, had identical payloads of 20 kilograms of a cesium-containing mixture; three, Margie, Lola, and Zelda, had the same composition but larger payloads of 50 - 80 kilograms; and one, Susan, utilized the same composition but at a 33% lower mass density, which had been used in the previous year.

5.1 Objectives

The objectives of this group of releases were: (1) to create a region of local high electron density for r.f. communication; (2) to study mass transport, and solar scatter and resonance radiation from solids and gases in the presence of sunlight and (3) to determine the rate of decay of electron density in the presence of ionizing sunlight.

5.2 Discussion

Laboratory data gives a time constant for solar photoionization

of cesium vapor of the order of two thousand seconds. Thus, one percent ionization may be expected in approximately twenty seconds. If the ionization achieved in the initial release, before photoionization, was one percent, then reflectivity of the cloud at times much shorter than twenty seconds would not be affected by photoionization and would be similar in night and sunlit releases. If the initial ionization was less, then night and sunlit clouds should, of course, be similar in behavior for shorter times. Therefore, the time of similarity between night and sunlit releases should allow an estimate of the ionization achieved in the initial release, which cannot be measured in ground tests. At longer times the daylight releases are expected to enter a second phase of ionization due to the presence of sunlight.

The composition of ⁴⁰⁹⁰ these releases was identical to the night point electron clouds.

Visual observations following release indicate a rapidly growing series of two concentric circles of light, the innermost of which showed the sodium orange resonance radiation. Rapid radial growth of the outer circle was to 5° (10 km) in three seconds, the inner circle to 1° (2 km) in the same time. The low altitude releases (70-90 km) rapidly lost any orange tint, and became brilliant white (due to chemical reaction with ambient?) developing a ragged outer edge. In the high altitude releases (above 90 km) the outer circle developed into a fuzzy white portion (solids) which separated from the inner sharper edged portion (gases) which usually retained the sodium color.

Optical observations of the early time growth are too complex to be adequately summarized, but they generally show an asymmetric outer (solids)

wave at 2-10 km per second¹⁰¹⁷, and¹⁰⁰³, a¹⁰⁵⁹ symmetric inner (gas) cloud which becomes separate from the outer wave at 0.3 kilometers and then grows more slowly to perhaps 1 km at 1 second.¹⁰⁰³ An early time upward drift totals about 5 km in 50 seconds and then stops, whether or not the vehicle had an upward velocity component at release.²⁰²³ It is therefore believed that the upward motion is due to temperature difference and/or hydrodynamic forces, slowing as the cloud mixes with a substantial amount of ambient gas.

R.f. observations of the early time Doppler growth¹⁰⁴¹, are⁵¹³⁵ essentially the same as in the nighttime releases, and match reasonably the calculated gaseous radial growth. R.f. cross sections at early times also are similar to the nighttime release cross sections.⁵¹³⁴

Optical observations at longer times show that the cloud as a whole moved in a direction determined by the ambient winds and wind shears. Because of the cloud rise its material was distributed at a series of altitudes, each with a different horizontal motion, which resulted in twisting and shearing of the released gases. Eddy formation was noted at altitudes below about 115 km as a very significant feature of the cloud structure.²⁰²⁷ At altitudes below about 100 km the fuzzy portion of the cloud mentioned above was considerably brighter than above these altitudes, undoubtedly due to formation of substantial quantities of solid oxides of the alkali metals.²⁰⁰⁸, ³⁰⁰⁹ The drift of the cloud after the first minute, showed each part of the cloud, moved essentially in a single horizontal direction determined by shears at different altitudes⁵⁰⁷² but slowly rising and falling by two or three kilometers.²⁰⁰⁸

Radio frequency ionosonde position data at longer times in general agreed with the optical position data.⁵⁰⁴⁶ The optical data were available

for 5 - 20 minutes while r.f. position data were available for much longer periods, up to one or two hours.⁵⁰⁴⁸ At such later times the cloud grows so large⁵⁰³⁶ that it is impossible to assign a single position from slant range given by ionosondes. In placing four ionosondes in the field, it was planned to use the disagreement in position triangulation to give an indication of the physical cloud size, since each ionosonde would measure the slant range to the nearest reflection portion of the cloud.⁵⁰⁸¹

The r.f. reflectivity of the released clouds was in general found to be high and to depend very strongly on altitude,

Other notes on special cases include one release of particular interest, "Betsy". In this case, the initial release was made approximately five minutes before visible sunrise at the release altitude and approximately ten minutes before ionizing sunrise at the release altitude. As expected the luminosity of the cloud resembled that of night releases in the first minute.¹⁰²⁷ The cloud then disappeared until sunlight reached the cloud five minutes after release.²⁰¹⁰ The initial ionization decay was followed by a rise after ionizing radiation reached the cloud roughly ten minutes following release.⁵⁰⁹¹

In the high payload experiments the vehicles failed to reach the desired altitude of 100 km. At the 75 km to 85 km reached in the first two of these releases very rapid chemical consumption was seen to occur with the formation of a very brilliant white cloud thought to be cesium oxide.³⁰²⁴ The third of these releases at 102 km was carried out well after sunrise, and did not have as high r.f. reflectivity as a dawn shot at this altitude.

It was the only release carried out under these conditions and it is quite possible that the daylight ambient pressure corresponded to that of a lower altitude at dawn.

5.3 Conclusions

- (1) A localized area of high electron density can be achieved for r.f. communication.
- (2) The r.f. scatter cross sections are not particularly geographically selective^{5129, 6001}
- (3) An outer wave of small particulate matter,¹⁰¹⁷ seen by solar scatter, moves with the velocity of the initial contact surface (7 km/sec) to distances of several kilometers¹⁰⁰⁵ outrunning the gaseous front after about 0.2 seconds. It is much brighter and larger in forward scatter than in side scatter.¹⁰⁰⁴⁻⁶ Aluminum oxide gas (AlO) acts as a significant resonance scatterer.³⁰²⁶
- (4) The gases expand to ambient pressure in a non-reversible near-adiabatic expansion, working against an effective pressure (due to shock wave generation) substantially higher than the ambient pressure in reaching their final state.
- (5) The ionosondes⁵⁰⁰⁹ and sweep sounders show much less difference than expected between night and dawn releases, i.e. in the absence and presence of solar ionization.

5.4 Further data analysis is required to answer the following:

- (1) Can densitometry distinguish between solids and gaseous motions at early times?
- (2) Can a clear measure of diffusion processes show the different levels of inhomogeneity as suggested from r.f. phase patterns?
- (3) Can a study of optical vs incoherent drift show which cloud regions are the best reflectors?
- (4) Is the model of ionization⁵¹¹⁷ suggested by observed internal cloud motions sufficiently accurate to define an electron yield?
- (5) How closely do optical and r.f. growths match?
- (6) How closely do r.f. cross sections measured by different equipment agree?
- (7) Is a consistent model possible for all observations?

5.5 Further experiments are required to determine

- (a) What is the time of day dependence?
- (b) What is the latitude and the seasonal dependence?
- (c) What payload design is most effective in maximizing reflection?

6. CESIUM TRAIL RELEASES

Two sunlit trail electron clouds were released, Janet and Hilda, at altitudes of 104 and 129 km, with identical payloads of 20 kilograms of a composition designed to release cesium vapor plus inert gases over a 30 second period.

6.1 Objectives

The objectives of this group of releases were: (1) to create a region of local high electron density for r.f. communication; (2) to study solar scatter from gases and solids in the presence of sunlight and (3) to determine the rate of decay of electron density in the presence of ionizing sunlight.

One distinction between the trail releases and the point releases previously described was that the trail releases were to be released with a minimum disturbance of the ambient. The net gas velocity with respect to the ambient is negligible if the rearward velocity of the gases is closely matched to the forward velocity of the vehicle. An additional reason for trail release of cesium in the upper atmosphere is that the electron yield from the low pressure trail release might be higher than the electron yield from the high pressure point release, discussed in a theoretical report.⁴⁰⁰⁴

Another factor was the desirability of creating a trail over a range of altitudes so that the altitude sensitivity of the point releases might be minimized, since the gas would be continuously deposited over a range of altitudes

6.2 Discussion

The ground experimentation⁴¹⁰³ prior to the launches of this type of package showed reasonable burning rates. A first release package failed to ignite and therefore a redesign of the initiating circuit was made. This failure was not a chemical problem, but an electrical circuit problem. Two further releases were made; each gave a small cloud of cesium-containing gas but did not give a long filament trail. The remaining payloads of this type were therefore returned to the laboratory for evaluation where it was found that ignition of the full-size package was difficult, and that nozzle plugging probably resulted in cutoff before complete release was achieved.⁴¹⁰⁸ However, optical observations and r.f. observations were made on these two clouds. Because of the small payload fraction released (probably 1%) neither cloud gave good r.f. returns, but both were useful clouds for optical observations of wind shear and turbulence, and are being studied for this data.²⁰⁰⁹

6.3 Further studies of trail releases first in the laboratory and then at altitude are desired to answer the following questions:

- (1) Can a suitable payload be fabricated having the high electron yield calculated to be obtainable?⁴⁰⁰⁵

- (2) Will the antenna-like filament offer advantages in reflectivity?
- (3) Will the minimum disturbances of the ambient on release result in a smoother contour, ⁵¹⁰⁸ hence a more coherent reflectivity?

7. HIGH EXPLOSIVE RELEASES

Two high explosive clouds were released, Arlene and Carry, at altitudes of 104 and 129 km, with identical payloads of 18 kilograms of RDX, a commercial high explosive.

7.1 Objectives

The objectives of these releases were (1) to determine the r.f. reflectivity of a high velocity gaseous expansion without cesium, (2) the luminescence of the explosion products, primarily carbon monoxide and water, (3) the effect of an ionized vs un-ionized ambient on the density gradient established by an explosion.

7.2 Discussion

The first of these releases, Carrie, was made at dawn when the solar horizon was 114 km. The payload was released at 129 km, in a region which was sunlit by visible light but had seen no UV light for 12 hours. Because of ozone screening, ionizing radiation did not reach the region until three minutes after the release. A typical particle wave was seen to expand at several kilometers per second velocity for perhaps two seconds, leaving a residual whitish glow which persisted in the sky for a period of ten minutes. There were no r.f. returns, and so there was no evidence in

this release that any ionization or electron inhomogeneity was created.

The second of the two high explosive releases, Arlene, was released at 104 km after sunset when the solar horizon had already reached 260 km. The cloud release was therefore made in the dark; however, residual ionization from the daytime was still present in the release region. In this release a brief flash was observed with no particle wave of any significance and a very low level of residual glow, not sufficient to record on the equipment used. However a transient r.f. signal for 0.6 seconds following release was very significant.¹⁰⁵⁰ It indicated a Doppler growth quite similar to that of the cesium releases, which have much higher total ionization. R.f. returns were not received from Firefly Arlene after one second.⁵¹⁰⁷

The interesting distinction between Carrie and Arlene is that a transient r.f. return was obtained in the non-sunlit release made under conditions where there was ambient ionization while no return was obtained from the sunlit release in a non-ionized ambient condition. It is also the case that a rapidly moving outer wave was observed in the sunlit release¹⁰³¹ but not in the ionizing release. This is one of the reasons for inferring that the rapidly moving radial wave is indeed a particle wave rather than an ionizing shock wave. It also suggests that the ionization may well be a pile-up effect which occurs at the front edge of a non-visible non-ionizing shock wave,

which creates a density gradient, both of neutral species and of electrons, permitting r.f. reflections which will presumably be strong during daylight, or under early nighttime conditions when ambient ionization remains from the earlier sunlight.

A visible glow lasted for ten minutes in the sunlit case, Carrie, in a relatively small volume which did not grow as much as the cesium gas releases. This glow is probably caused by solids since the night high explosive release did not show chemiluminescences remaining such as were observed after the point electron cloud releases. The further study of this phenomena with adequate spectral sensitivity is desirable.

It is noted that the two high explosive releases were similar in effects to those of the 1959 series, where a night release showed no evidence of an outer wave or of a residual cloud whereas a dawn release showed both the rapidly moving particle wave and the residual light emitting phenomena. In further experiments higher altitude releases are also desired since there appears to be a significant variation in luminescence with altitude. A recent French release of 80 kilograms of high explosive at dusk at 160 km resulted in excitation of the 6300A oxygen line at the outer rim of a spherical luminescence.

An attempt to define the mechanism for this energy deposition and continued emission of the forbidden oxygen line is important. The 6300 A line was also present in three of the point electron clouds.³⁰²⁶

7.3 Conclusions are as follows:

- (1) The high explosive release can create a transient electron

gradient by creating a density gradient at a shock front without actually ionizing the ambient.

- (2) The continued light emission under dawn condition but not in the dark is probably solar scatter from particulate matter explosive residues.

7.4 Further data analysis is required to compare r.f. transient with shock wave calculations of increased ambient density.

7.5 Further experiments are required

- (1) to study further the light emission or scatter persistent after release, with better spectral recorders.
- (2) to study altitude effect, particularly at high altitudes where the oxygen line is activated.

8. ELECTRON REMOVAL FROM THE E-REGION

One electron removal trail, Rena, released a payload of 14 kilograms of sulfur hexafluoride over a 30 second period covering an altitude from 105 to 120 kilometers.

8.1 Objectives

The objectives of this experiment were (1) to create a region of local low electron density in the E-region, (2) to study the r.f. effects of this electron-depleted region in scatter reflection or transmission, and (3) to determine the rate of return of the region to normal by photoionization or by diffusion from outside the region.

9.2 Discussion

It was necessary that the E-region release be carried out under daylight conditions since the ionosondes were unable to record the presence of any significant E-region ionization at night. In such a daylight release, of course, solar photoionization and photodetachment compete with the electron removal mechanisms. The payload was equipped with a telemetry unit to indicate when the pressure in the canister of sulphur hexafluoride dropped by 90%, thereby confirming that release had occurred.

The release was confirmed in this way, and the ionosonde directly under the release region recorded a perturbation at the time of the release.

5063 It is not certain that this perturbation was due to the release. However, it is described as a region of turbulence imbedded in the normal E-region, with persistence of several minutes beginning at the time of release itself. 5066 It reflected up to frequencies of several megacycles and appeared similar to a sporadic E. 5067 The time and the slant range suggest that a real effect was observed. At least one additional experiment of this type must be carried out to eliminate the possibility that a coincidental sporadic E is the source of the r.f. reflection.

It is also our intention to attempt F region removal, where the continued electron density throughout the nighttime permits observation in the absence of competing sunlight. It has been postulated that recombination in the F region is controlled by the depletion of oxygen molecules, through the charge exchange between oxygen molecules and oxygen ions, O^+ , followed by recombination of the molecular ion O_2^+ with free electrons giving disso-

ciated oxygen atoms in an excited state. This could be confirmed by release of molecular oxygen into the F region at night⁵⁰⁸⁵ where the removal process, normally limited by lack of molecular oxygen, can be accelerated. If the gradients are reasonably sharp, r.f. reflections may be expected from the electron depleted region. Furthermore, emission from the excited oxygen atoms following recombination may be observed optically.

It is noted in this type of experiment that the quantity of removal agent required for electron removal from very large regions of space can be carried on a relatively small vehicle. For example, a $10^6/\text{cm}^3$ electron density which is the maximum formed in the F region, represents 10^{21} electrons per cubic kilometer. A three kilogram payload of molecular oxygen should suffice to remove all of the electrons from about 50,000 cubic kilometers if properly distributed through that large region. In fact the problem of electron removal is more a problem of distribution of the removal agent than one of carrying an adequate payload to the desired altitude.

9.3 Conclusions

- (1) E-region electron removal was probably accomplished by SF_6 release.
- (2) The r.f. effects of the electron-depleted region were similar to those seen from an electron-rich sporadic E-region, probably because of scatter from electron density gradients.
- (3) The region returned to normal in about 500 seconds following the release.

8.4 Further data analysis is suggested to determine

- (1) optimum observer equipment for determining model of electron-depleted region.
- (2) optimum time and altitude for removal experiments.

8.5 Further experiments are suggested

- (1) To confirm that the observation was not a coincidence due to appearance of sporadic E.
- (2) To make F region releases to confirm proposed geophysical mechanism for F region persistence.
- (3) To obtain further r.f. signatures of electron-depleted regions, for comparison with r.f. returns following missile passage through the ionosphere.

9. COBALT METAL POWDER

One cloud, Linda, of cobalt powder of about one micron particle size was released at night at an altitude of 135 km. The net payload of 22 kilograms was sufficient to provide 10^8 cm^2 surface.

9.1 Objectives

The objectives of this experiment were: (1) to observe r.f. reflectivity of dispersed finely divided metal particles, and (2) to study possible chemiluminescence at the surface of metal due to the presence of nitrogen and oxygen active species.

9.2 Discussion

Laboratory studies on the efficiency of cobalt powder as a catalyst for N atom - O atom reactions suggested that one collision in 10^4 would be effective, and this would not result in an observable emission. If the laboratory data were not applicable, i. e., if every collision was effective, and if all nitrogen present in the altitude region was in the atomic form, the release would be observed. No optical effects were observed.

The r. f. return expected from a metal powder due to Rayleigh scattering decreases as the fourth power of the ratio of the wavelength used to the particle diameter, so a very low r. f. cross section for 1 -1000 mc radars would be expected from the micron-sized metal in the missile exhaust. A weak return at 3 mc on the ionosonde was noted from the release time, signalled by a telemeter sensing canister pressure, for a six minute period, at the correct slant range. However the higher frequencies of a battery of equipment ranging up to several thousand mc failed to detect the release; their sensitivity was to ten square meters of effective scatter surface.

9.3 Conclusions

- (1) The presence of an active catalyst surface of 10^8 cm^2 failed to produce any luminescence in the 130 km region. Velocity effects were not evaluated.
- (2) The metal surface of 10^8 cm^2 present as one micron particles had a negligible scatter cross section for sensitive radars to several thousand megacycles.

- (3) The weak 3 mc return for six minutes is unexplained. A further experiment suggested is release of metal powder at lower altitudes where confinement by ambient pressures might give an effective denser scatter surface.

10 KEROSENE

One cloud, 1da, of 10 kg of synthetic kerosene was released under dusk conditions at an altitude of 130 km.

10.1 Objectives

The objectives of this experiment were (1) to determine if any fluorescence or chemiluminescence would be observed from release of hydrocarbons under sunlit conditions at high altitudes, and (2) to determine what persistence would occur by solar scatter from a vaporizing liquid

10.2 Discussion

Laboratory studies suggested a synthetic mixture containing equal quantities of single paraffin, cycloparaffin, and aromatic compounds. Toluene, cyclohexane, and n-hexane were selected. The synthetic "kerosene" was heated to 200°F and pressurized with nitrogen to 1200 psi, then at altitude, was vented through an orifice over a thirty second period.

Visual observation following ejection showed a large spiral with a 10 km radius caused by jetting of the fuel into the low pressure ambient, while the vehicle spun at about 1 rps, over the thirty second release period.

Persistence of a given position of released material never exceeded 3 - 10 seconds, and following the ejection, the visible structure disappeared within 10 seconds.

Optical observations¹⁰⁰² showed the same spiral, but intensity was too low to obtain any spectral resolution. No significant residual emission from the vaporized gas was evident on any records after ten seconds following the emptying of the payload.

No r.f. reflections were observed.

10.3 Conclusions

- (1) No persistent chemiluminescence or fluorescence was obtained by release of hydrocarbon fuel components at altitude.
- (2) Vaporization or dispersion of the liquid droplets was so rapid that residual solar scatter did not exceed 10 seconds.

10.4 Suggested further data analysis

- (1) Computation of effective optical scatter surface.

11. SOLAR SCATTER FROM SMALL-PARTICLE SOLIDS

Four clouds of micron size inert solids, Frances, Lily, Mavis, and Hedy, were released at altitudes from 69 - 150 km, with payloads of 3 - 18 kg, under sunlit conditions.

11.1 Objectives

The objectives of this group of experiments were

- (1) to determine the optical scatter cross section of micron particles at wavelengths longer and shorter than the particle size, viewed from various scatter angles between the sun, the solids cloud, and the observer.
- (2) to determine the rate of dissipation of a mass of small particles released into a low-pressure ambient.
- (3) to determine experimentally the drag on very small particles by a gas; first the expanding release gas, then the ambient gas, and to relate this to expected theoretical drag.

11.2 Discussion

The payloads consisted⁴⁰⁷³ of particles of measured size distribution loosely packed in a cylinder pressurized with nitrogen to about 6 atmosphere; release Mavis contained 3 kg of 0.03 micron aluminum oxide, with a calculated cross section of $3 \times 10^8 \text{ cm}^2$; release Frances contained 8 kg of 0.35 micron aluminum oxide with a cross section of $7 \times 10^7 \text{ cm}^2$; release Lily contained 8 kg of 0.2 - 2 micron aluminum oxide with a cross section of $3 \times 10^7 \text{ cm}^2$; and release Hedy contained 18 kg of 0.5 - 5 micron specially prepared fluorescent cadmium sulfide with a cross section of $3 \times 10^7 \text{ cm}^2$. The gas was calculated to expand to 100 meters diameter on release at altitude. The gas and solids were released by a cutting charge placed

around the cylinder near one end. The total pressure-volume energy of the gas, if transferred to the solid as translational energy on release, would impart a velocity of about 50 m/sec to the mass of the solids.

Optical observation showed a surprisingly rapid growth of the released solids into an umbrella-shaped cloud. The maximum radial growth of 0.8 km in 0.25 sec, ¹⁰⁰⁶ or 3 km/sec, is about fifty times the rate (50 m/sec) expected from uniform energy transfer from gas to solid. This can only be the case if a relatively small amount of material is given a very high velocity, and a large bulk of the material a much lower average velocity. The observed parabolic shape did not point along the vehicle trajectory, and this is believed due to the aspect angle of the canister on release. At the instant the cutting charge opens the canister, a jet of gas pushes out radially through the cut, carrying solids with it, before the two parts of the canister can separate. As the parts of the canister separate, the gas stream is deflected, causing the umbrella (parabolic) shape.

The release Mavis occurred at 69 km, because of poor vehicle performance. At the time of release the solar horizon was at 100 km, or thirty km above the release point. The released solids, 3 kg of inert 0.03 micron aluminum oxide, were observed by light scatter for approximately one minute after release. This experiment conclusively proves that sufficient sunlight is scattered below the solar horizon to permit rescatter from inert solids 30 km below the solar horizon.

It may also be observed here that in all the Firefly vertical probe experiments, a second stage solid propellant engine was burned at an altitude

of 12-20 km leaving perhaps 20 kg of solid products of unknown particle size along the trajectory at that altitude. Those releases made "predawn" with a solar horizon of 60 - 150 km, consistently left a trail visible for several minutes after release. No nighttime launch left such a trail.

This confirms and extends the Mavis observation, that the solar scatter below the solar horizon is sufficient to observe inert solids 130 km below the solar horizon. This will not be independent of solar horizon, however, since the rapidly diminishing density above 150 km will not support rescatter. Thus a 300 km solar horizon will not permit rescatter from a 150 km altitude region.

Since the actual variation in optical cross section with wavelengths from 0.3 - 3 microns is still being evaluated;^{3001, 3027} it cannot be stated whether different particle sizes give sufficient differences for identification of particles of unknown size ejected from missiles.

The light emission from the cloud lasted for 1 - 2 minutes³⁰¹⁰ and then rapidly disappeared as the optical scatter density decreased further.

Motion of the entire cloud along a ballistic trajectory was observed.
²⁰⁰⁹ The cloud Hedy released at 108 km showed no significant variation over 90 seconds from a vacuum trajectory within a 0.2 km position accuracy as it proceeded through apogee at 130 km and then fell.²⁰²¹

11.3 Conclusions

- (1) Ejection of micron-sized particles can occur at very high velocities even with relatively low temperature, low pressure gas as the driving force.

- (2) Micron-sized particles are optically visible by solar scatter at a density of 10 kg per 100 cu km, and possibly below this value.
- (3) Inert solids can be observed well below the solar horizon, (at an altitude of 10 - 20 km when the solar horizon is at 150 km) by scatter of sunlight first by the atmosphere to regions below the solar horizon, then by rescatter from the inert solids to the observer.
- (4) Drag coefficients for micron size particles at 108 km altitude are sufficiently low that motion along a ballistic trajectory is not impeded.

11.4 Further data analysis is required to provide:

- (1) An accurate integration of scattered light intensity at various wavelengths and at various scattering angles for various particle sizes.
- (2) An accurate application of the drag equations for acceleration of particles first ejected in a gas stream and then slowed by the ambient, as a function of particle diameter.

11.5 Further experimental studies should include:

- (1) Ejection at a single defined velocity of a narrow particle size range of micron particles to give accurate measure of ambient density below 110 km.

GROWTH FROM PHOTOGRAPHY (0-10 seconds)

Howard D. Edwards

Engineering Experiment Station
Georgia Institute of Technology
Atlanta, Georgia

EQUIPMENT

The Eyzno 35 mm movie camera was used to record cloud growth during the first 10 seconds after burst. At least one of these cameras was located at each of the four optics sites.⁽¹⁾ The cameras were equipped with 50 mm focal length lenses at speeds of $f/1.1$ and $f/2$ and were operated at 4 frames per second. Royal X-Pan Recording film was used for most firings.

EXPERIMENTAL RESULTS

Usable data were recorded for twenty of the rockets fired during the 1960 series. In most cases simultaneous photographs were obtained from two or more stations. Due to high sky background and faint clouds, data were not obtained for Zelda, Anne, Norma, Arlene, Rena, Linda, and Mavis.

DISCUSSION⁽²⁾

In carrying out the analyses, each cloud has been assumed to consist of a bright dense center, called the main cloud, and a larger more or less concentric section of less intense radiation which is called the "particle wave." The main cloud continued to grow in size and was photographed by the K-24 still cameras⁽¹⁾ for periods up to 20-30 minutes or until sky background became too great for photographic recording.

The particle wave, however, was much less intense than the main cloud and was seldom recorded for more than a few frames or seconds on the movie cameras. The slower optics on the K-24 system ($f/2.5$ versus $f/1.1$) did not record the particle wave.

For both the main cloud and particle wave, the clouds were often elliptical and, hence, measurements were made for so-called major and minor axes.

Of the five night shots designed to create electron clouds (Cathy, Betsy, Amy, Ruth, and Gerta), data were obtained on all five and cloud growth as a function of time has been

(1) See article in this report entitled "Position, Drift and Growth from Photography," by H. D. Edwards.

(2) At the time of this report, film for Fireflies Frances, Carry, Cathy, Peggy, and Susan are being studied in Dr. Rosenberg's laboratory. Plots and photographs are not available for Frances, Carry and Cathy. Photographs are not available for Susan and Peggy.

measured for all but Cathy.⁽²⁾ For Amy and Gerta, only the main cloud was detected. For Betsey and Ruth, both the particle wave and the main cloud are present. The photographs and diameter versus time plots are shown in Figure 1 for Ruth which is typical of the night shots.

Of the nine dawn electron clouds, data were obtained on all shots except Zelda, which was fired during the daytime. Only the main cloud was observed on Marie, Peggy, Susan and Janet whereas both the main cloud and particle wave were observed on Lola, Olive, Jeannie, Dolly and Hilda. Atmospheric haze or film halation may be responsible for some of the large image sizes noted during the first few frames. Halation is probably responsible for the large image size noted for Lola during the first 1/4 second after burst. A haze effect or light ring, in addition to particle waves, was noted on Olive, Jeannie, and Dolly. Figure 2 for Olive is typical of the measurements which show the two conditions--main cloud and particle wave.

Peggy did not have a particle wave but the main cloud grew much faster than the other shots. Peggy had a diameter of 5 km at burst plus 5 seconds compared to less than 3 km size for the other clouds at the same time. The plot of diameter versus time is given for Peggy in Figure 3.

No data were obtained on the carbon arc shots--Teepee Anne and Norma.

For the high explosive shots (Carry and Arlene) data were obtained only for Carry and analysis has not been completed.⁽²⁾

For the three solar scatter shots (Mavis, Frances and Lily) data were obtained for Frances and Lily, and an analysis has been made for Lily only.⁽²⁾ The main cloud is the only one present and shows a growth rate similar to the average electron cloud. Growth versus time-after-burst is shown for Lily in Figure 4.

Growth rates for Hedy and Ida, the infrared scatter and chemiluminescent clouds respectively, are similar to those for the main clouds of the sodium-cesium releases.

Work is continuing in our laboratory on the "why" associated with the wide divergence of growth rates and presence or absence of particle waves.

Dr. John Paulson of the Geophysics Research Directorate has analyzed the shock-particle wave problem making use of our data as well as others. The results of his analyses are presented elsewhere in this publication.

Fig. 1. RUTH

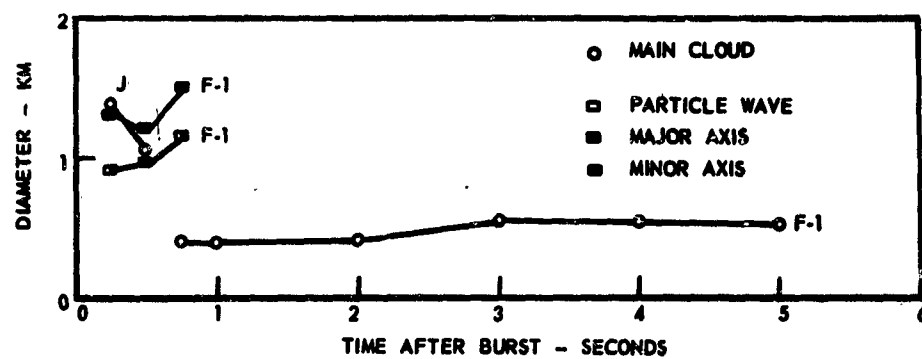
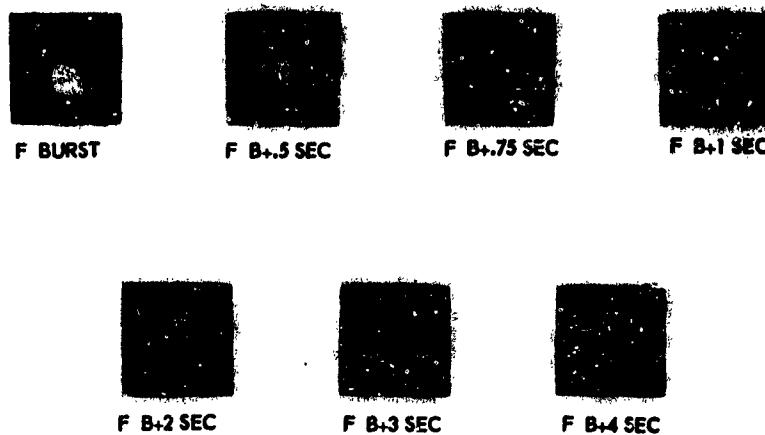
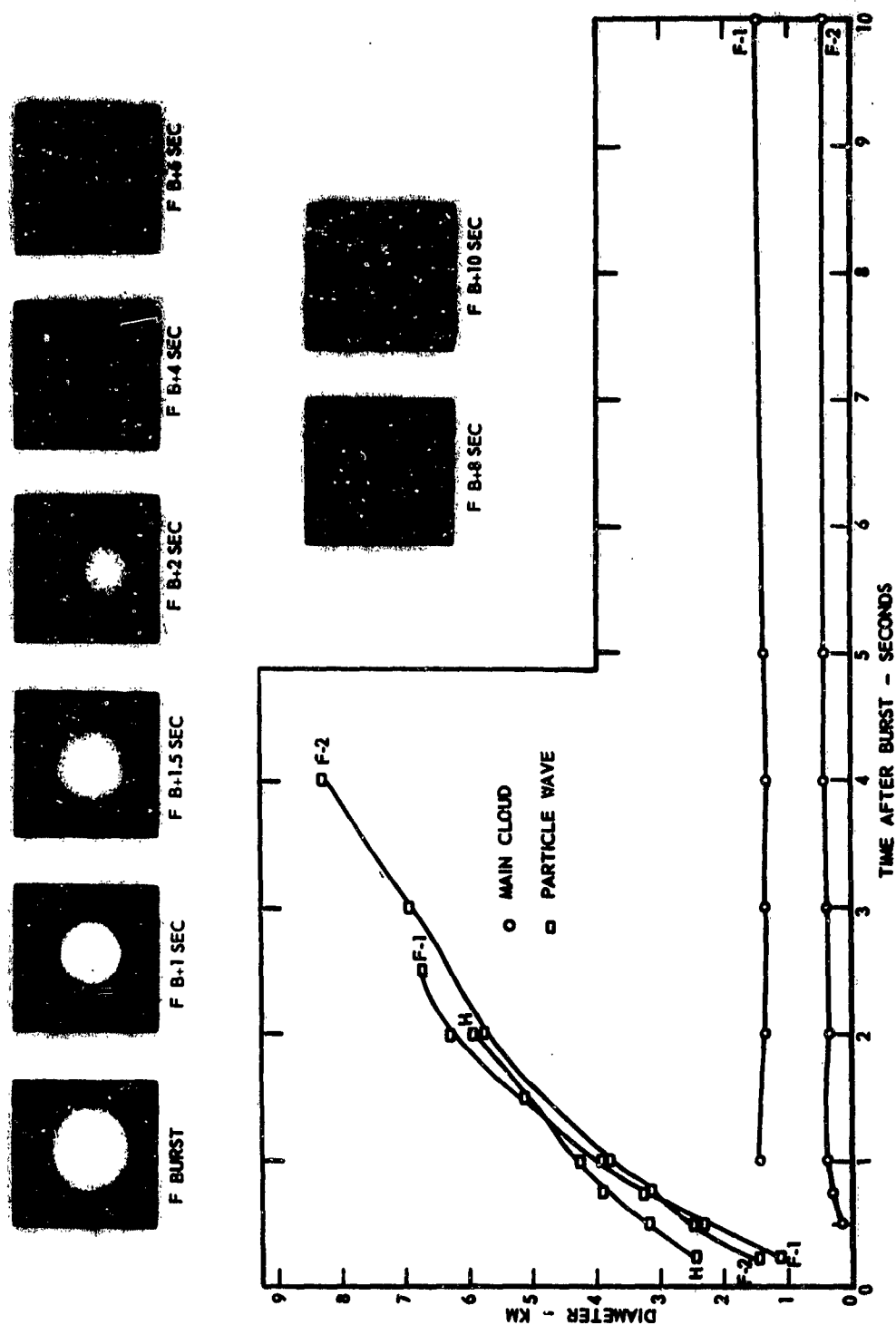


Fig. 2. OLIVE



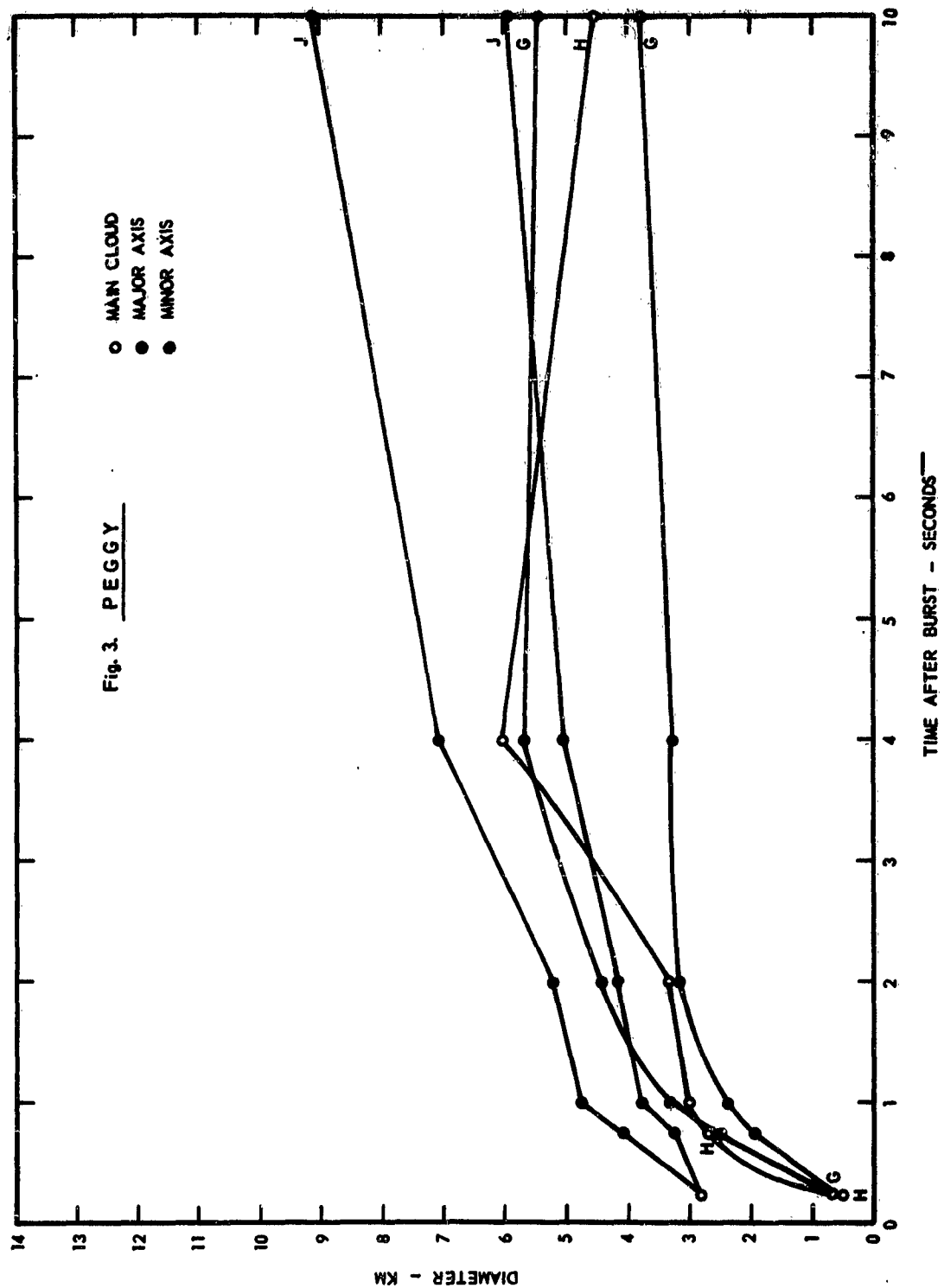
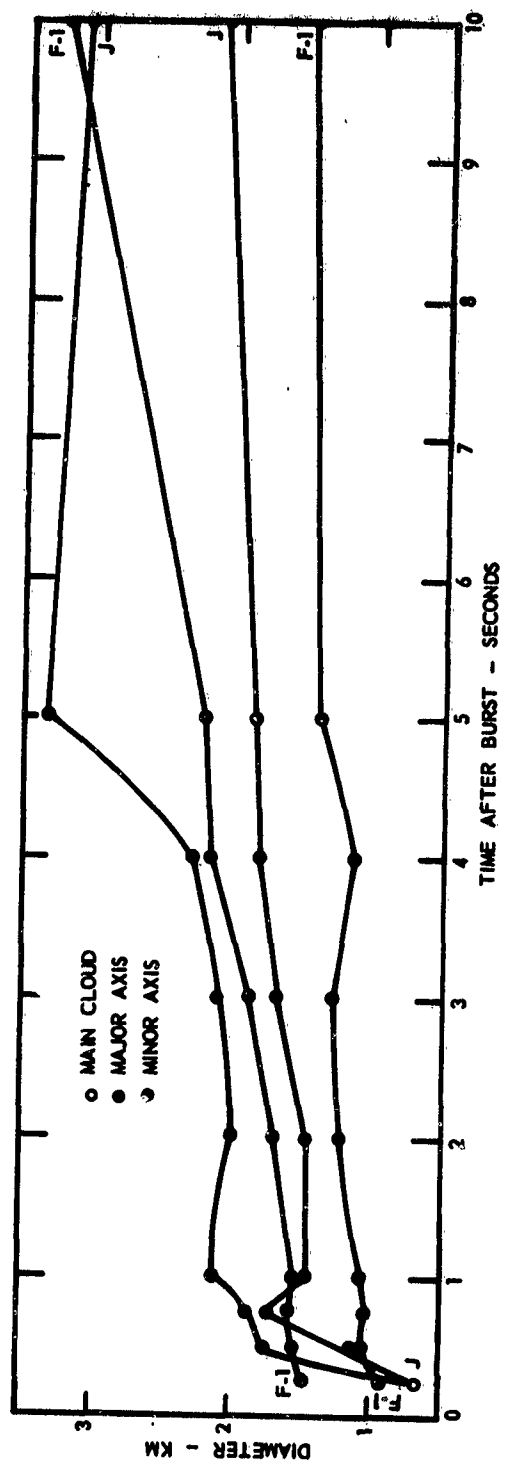
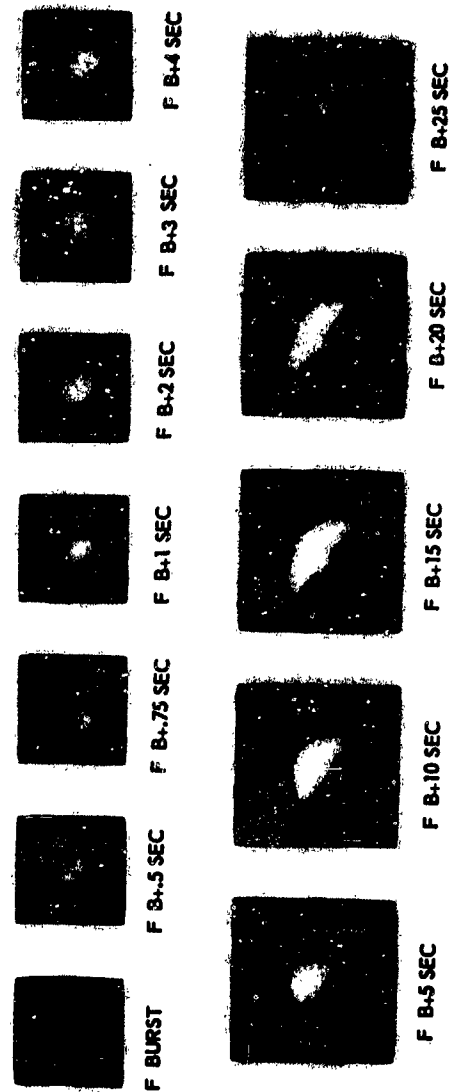


Fig. 4. LILY



SECRET TIME GROWTH AND PROPERTIES MEASUREMENTS

R. B. Molt

Device Development Corporation
Weston, Massachusetts

ABSTRACT

Our work during the last six months is described. To date, our program has consisted mainly of optical measurements in the field for Project Firefly 1960. General assistance is also being given to other groups in the project, and some laboratory work has been done. This report gives our program objectives, the scope of the work, a description of the equipment constructed and used during the past six months, and the observations made during the summer series of chemical releases.

1. PROGRAM OBJECTIVES

The observations which we have made in the field for Project Firefly were designed principally to study the effects listed in the following paragraphs. Although some of the work yields results of general geophysical interest, the emphasis is on measurements designed to obtain information for military application.

One of the objectives of our program was to study the possible existence of the shock wave which previous tests had indicated was present and might have behavior which was somewhat anomalous. For this purpose, we set up photomultiplier equipment which was provided with narrow acceptance angle optics and pointed slightly off the burst. This equipment should have detected the presence of such shock waves, but the results were negative. During the course of the test, a good portion of the photomultiplier equipment was diverted to the somewhat different purposes of attempting to observe spectral distribution of the light emitted from the cloud some seconds after the burst.

Another objective was the study of the early time behavior of the burst, with emphasis being placed on the study of possible particle waves emitted and on the spectral distribution and total light intensity emitted during the early development of the cloud. Both photographic and photomultiplier techniques were employed for this purpose, and the results are being correlated with RF reflection data in order to determine whether there is a

possibility of explaining some of the variations in RF performance of the clouds by examination of the early time development. Similarly, the same general techniques are being used to study electron removal and to study the possibility of simulation of nuclear blackout conditions. Spectrographic measurement seems to be one of the most fruitful means of analysis of the processes responsible for the various phenomena which occur on these upper atmosphere releases.

Polarization effects are of importance, particularly with respect to use of released light-scattering material for decoy purposes and for the possible detection of the use of such techniques by an enemy. Although the primary purpose of released material is the creation of infrared scattering, which is the problem of groups other than our own, we felt that making measurements in the visible region would add information as to the possible detection of decoy techniques. We therefore equipped some of our photometers and cameras with polarization attachments.

Our optical measurements on the trail releases which were planned were to have been applied to the dynamics of missile trail detection. The instrumentation problem connected with the analysis of the spectra emitted by the trail releases is quite similar to that applicable to missile trails in general, and could aid in the design of countermeasures equipment, and early warning equipment for the detection of missiles, and also in the detection of countermeasures being employed by an enemy.

We also assisted Dr. Sam Silverman at AFCL in the measurement of possible cesium flash phenomena which it was thought might occur a day or so following these releases. Although no positive result was obtained, this work has direct applications to the problems associated with spreading of materials in the upper atmosphere and to the computations which should be useful in predicting such effects as nuclear fall-out. Some of the work on the optical properties of cesium ions in the upper atmosphere may have application to ion propulsion engines for space vehicles.

2. SUMMARY OF PAST AND PROJECTED WORK

The work under this contract involves principally an optical

observation and interpretation program for Project Firefly. To date we have concentrated on measurements for the Firefly 1960 release series, and have about three-fourths completed the interpretation of the data obtained. In support of the same program, laboratory study of the properties of cesium ions has continued on a relatively low priority basis. Our observational work in the field has been concerned mainly with short-time phenomena of the chemical releases; but a variety of other optical work is also in progress, both within our own program and in support of other Project Firefly groups.

Generally speaking our measurements involve a combination of photographic and photomultiplier measurements, both types of techniques being used in combination with light filters covering a variety of wave length regions. This is an approximation to a spectroscopic method, in some cases well suited to the conditions existing in the chemical releases and in other cases merely supplementing measurements being taken by other groups. Although not enough experiments which were presumably identical insofar as external environment (altitude, degree of illumination by the sun, etc.) have been run to make a significant comparison, we believe that the reproducibility of the results obtained will depend largely upon the reproducibility of the initial release conditions. It is possible to study the reproducibility of the first few microseconds, at least, of the initial release conditions fairly independently of the altitude of release and other factors, since the interaction with the ambient does not occur until later times. Remarkably enough, one of the most disturbing results which we have obtained, and which our efforts are now being spent in trying to interpret, has been a puzzling lack of consistency in the initial behavior of supposedly very similar packages. We believe that the first few microseconds or milliseconds, which actually is the period in which the initial boundary conditions are set, may have a great deal to do with the subsequent performance of a particular package. Our high speed photomultipliers (for the microsecond and early millisecond range) plus our fast cameras (for times of a few milliseconds and longer) give the possibility of making a fairly complete study of this time range. Unfortunately, the data obtained so far by these techniques is only partially quantitative (although some very interesting qualitative information has been secured) and has not yet given very much in the way of

detailed spectral information. In the time range between the microsecond and millisecond range and the first few seconds, our slower motion picture cameras carry photographic coverage up to the beginning of the Georgia Tech coverage. For still longer times (as well as for short times), photomultipliers equipped with various filters can follow the burst and the developing cloud and give data which is superior to that obtained by films, or with image orthicons, on the actual total intensities being emitted. The signal to noise ratio in dealing with the low intensity, diffused burst in a substantial background of light is the principal problem in using such equipment, especially since the movement of the cloud and the development of daylight makes the determination of the noise or background level more difficult. Another serious problem in taking quantitative data is the fact that shots must frequently be made with partial cloud cover, and reflection from the clouds can easily confuse the readings which are obtained.

We have also assisted various other groups in their Project Firefly operations. Among these are Dr. Sam Silverman's search for cesium flashes (corresponding to the twilight sodium flashes regularly observed) from three locations, the University of Maryland's use of a Fabry-Perot interferometer in an attempt to measure the temperature of the release from the shape of certain spectral lines by providing pre-fogged film, Geophysics Corporation of America's interest in the observation of certain cesium recombination lines, and the provision to Bendix of certain photometers for possible missile trail observations.

Our activities other than observations in the field and interpretation of data have included the construction of a precision high voltage power supply for the laboratory work at Air Force Cambridge Research Laboratories, which is now in final test.

3. EQUIPMENT AND TECHNIQUES FOR FIELD OBSERVATIONS

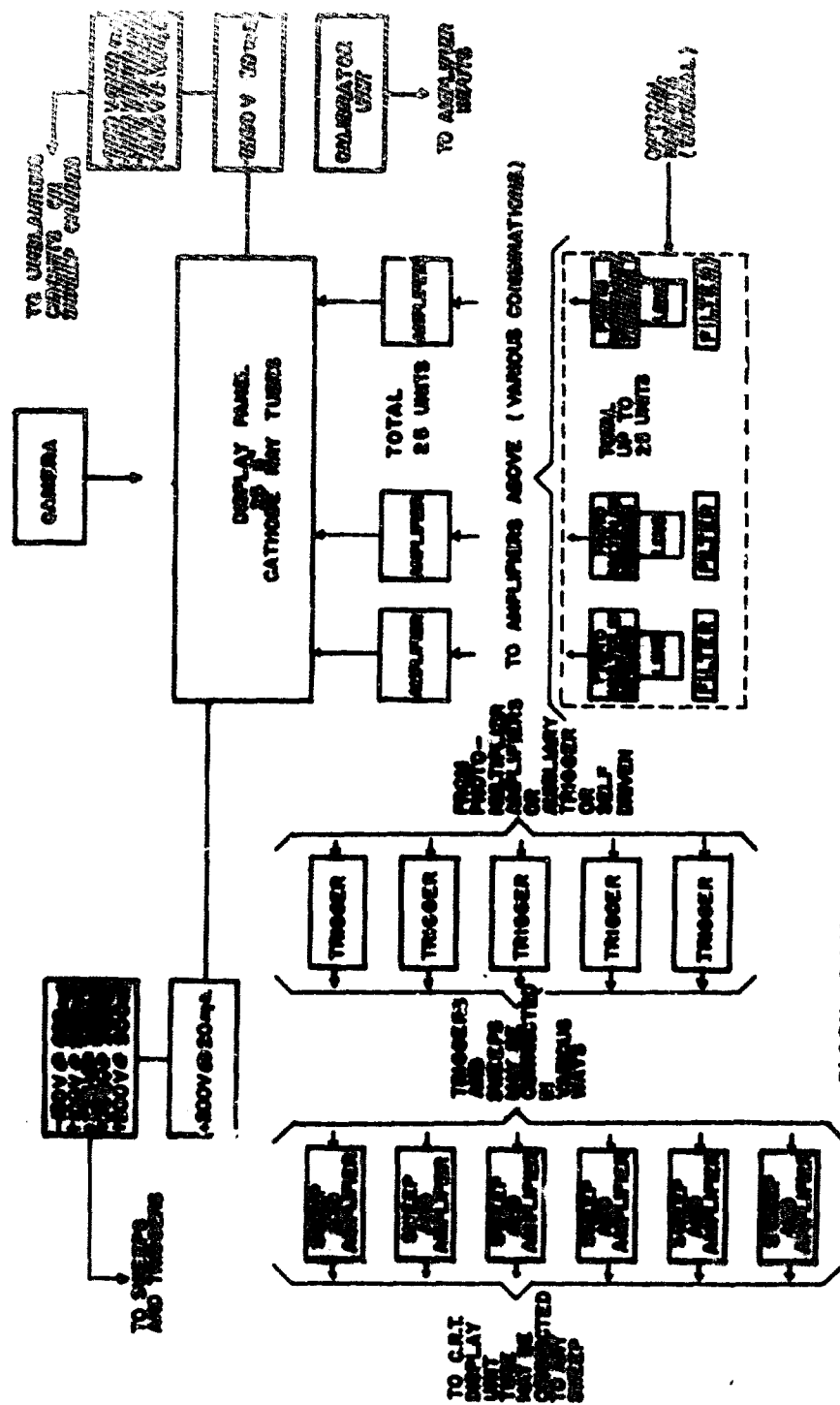
The equipment employed during these tests has been described in some detail in our last semiannual report (30 June 1960). There were a few modifications and changes, which will be mentioned here, and in addition, it is probably worth presenting a brief summary of the equipment actually used, even

though this will be partly a repetition of the previous report.

The equipment was installed in a house trailer which contained the electronic and other devices which we employed. This trailer included a photographic darkroom, a workspace, and a collection of spare parts and maintenance facilities. Also, the largest single piece of apparatus which we used was mounted in the trailer. This was a multiple unit cathode ray tube display used in conjunction with the photomultiplier detectors, diagrammed in the figure shown in the previous report and reproduced here. Briefly, it included 24 cathode ray tubes, arranged to give as wide as possible coverage of the initial phases of the release. Each of the 24 tubes was supplied with a separate amplifier, and 20 photomultipliers were provided with associated lens systems and various optical filters. Six different filter sweep choices were possible, any sweep being available for use on any of the cathode ray tubes. Any one of the sweeps could be triggered from any of the several available triggering sources which could be fed from the photomultipliers themselves or from any auxiliary trigger that might be supplied. Camera equipment for photographic single traces on these cathode ray tubes and for continuous photographic recording of the cathode ray tube which is allowed to "run free" was provided. This equipment was finished during the test and was available only for the later releases, so that unfortunately its full potential was not realized during this series. We still believe that its use will provide the very best available quantitative information on the early development of the burst.

The use of the equipment was somewhat different from that originally contemplated in that the absence of evidence for distinct shock waves on early shots caused us to plan more experiments for obtaining information on the spectrum of the developing clouds and less experiments for the initial shock wave evaluation. In view of this change in emphasis, we set up four recorders of the pen type (Varian Model G-2) for recording the DC outputs of some of our photomultipliers, equipped with various filters. A simple commutating arrangement was incorporated towards the end of the series to increase to eight the number of photomultipliers recorded on this type of instrument.

The mounts for aiming the photomultipliers and associated equipment were of two types. The first was a modified Navy gun director mount similar to



the ones used during the tests last year. These mounts were intended principally for use with tracking flares, which were attached to some of the rockets. Unfortunately, the failure of the flares in a large number of cases prevented these mounts from being very useful. Tracking mounts, of course, enable the use of our optical equipment with relatively narrow acceptance angles, which increases the probability of receiving sufficiently large signals (with respect to ambient light noise background) and which permits more accurate spectral distribution information due to this improved signal to noise ratio. Two of these mounts were employed, one carrying photomultipliers and the other carrying cameras and photomultipliers. The other type of mount used was a fixed mount (which was set pointing to the expected burst location before the firing) and which carried optical equipment of relatively wide acceptance angle. These fixed mounts could be rotated slowly, and were changed in position to follow the developing cloud in a number of tests. A primary difficulty in connection with the use of both the tracking and the fixed mounts was the lack of recording equipment for following the position of the mount, which made it difficult to determine whether certain signals obtained were actually due to changes of signal level or simply changes in background due to the movement of the mount which caused the photomultipliers to be seeing a different portion of the sky. The optical equipment mounted on the semi-fixed mounts included photomultipliers, streak cameras, and other relatively low speed cameras. One of the semi-fixed mounts also carried a snooperscope, for examination of the cloud visually by infrared, and was useful in tracking some of the clouds after they had become invisible to the eye.

We used a number of gelatin filters covering various regions of the spectrum, and also had available approximately a dozen interference filters for very narrow wave length bands. All of our lens mounts are equipped with provisions for standard filter holders, and the various filters could be interchanged between units of different acceptance angles and units having various types of detectors. While we did not have any such equipment available during this series, it would be very useful to have an iris diaphragm type of stop located at the focal point of the lens systems, to allow us to vary the acceptance angle during the development of the cloud.

Our lenses are mounted directly on the photomultiplier housings which we used. These housings are of two general types, one suited to end-on type photomultipliers, and the other suited to the 931 type of unit. Both are provided with some preamplification and cathode follower output to make possible the location of the photomultipliers at a considerable distance from the display unit.

Photographs of the mounts are included as figures as part of this report.

Any of the photomultipliers may be connected to any of the amplifiers, or a combination of them. It is possible to examine the difference in output of two photomultipliers, one of which can be directed toward the background, and the other which can be directed toward the cloud. The trigger units and sweep circuits provide sweep lengths from one microsecond to 1⁰ seconds in total length, and can be arranged for either self-triggering or for single sweep operation.

We also constructed a rotating polarization detection device, consisting of a three-inch clear polaroid disc which is rotated at a speed of thirty revolutions per second, and is placed in front of the lens and detector combination. Unfortunately, due to 60-cycle pick-up, which we were not able to remedy in sufficient time, this unit did not prove to be particularly useful. We therefore had to depend on hand operated polarizers during this series of tests.

Our photographic coverage was provided partly by our own group and partly by the photo-optics group at Eglin Air Force Base. Also, Fastax camera equipment was operated by the Vitro Corporation. We have undertaken to interpret all the films obtained, and the general photographic coverage of the early time after burst is described below.

We employed the same general type of streak photograph measurement which proved valuable in the 1959 Firefly tests, and had at least two of the modified Dumont streak cameras on all of the tests and were able to obtain four such cameras for about half of the tests. While we originally intended to have only one of the streak cameras equipped with Vitro time signals, we were able to have all of them so equipped before the series ended.



PHOTOMULTIPLIER UNITS ON FIXED
MOUNT. EQUIPMENT TRAILER IN
BACKGROUND.



DATA CAMERAS ON FIXED MOUNT.



TRACKING MOUNT WITH PHOTO-
MULTIPLIER UNITS. CAMERAS
CAN MOUNT ON CROSS MEMBER.



DUMONT STREAK CAMERAS ON
FIXED MOUNT

Fastax cameras operating at 500 frames per second (.001 second exposure) were used on most of the tests. Three of these were equipped with 2-inch lenses, giving an approximately 8° vertical field of view (and correspondingly larger horizontal fields) and were stationed on fixed mounts which were pointed to the expected burst angle. Two additional cameras with 4-inch lenses were used on a tracking mount, but the failure of flares made this type of coverage rather unsatisfactory, in that the rapid rate of film consumption and the low light intensity available combined to cause the operator to be out of film and to be dealing with too weak a source to photograph at the high speed employed by the time he could swing onto the burst.

We were able to obtain good intermediate speed coverage with Milliken 16 mm cameras, two of which were placed on a fixed mount and equipped with 1-inch lenses and 2 more of which were on a tracking mount equipped with 3-inch lenses. The 1-inch lenses employed were very fast (F1.1) which proved to be very useful with the relatively weak sources provided by the bursts. Here, the problem of using the cameras on a tracking mount was somewhat less than with the faster cameras in that the film lasted longer and the exposure was greater due to the slower speed. The operating speed of the Milliken cameras was 128 frames per second.

Four Mod IV cameras, two with 3-inch lenses on a fixed mount and two with 6-inch lenses on a tracking mount, were employed. These cameras operated at 20 frames per second, and excellent results were obtained with the tracking mount of some shots. The semi-telephoto type lenses and the 35 mm film on these cameras gave much more detail where they did obtain pictures than was obtained in other ways.

In all of the above cases Vitro time was included on the film and, except for instances where the time record was lost due to equipment failure or lack of proper exposure setting, it is possible to know the absolute time at which any particular frame was exposed with an accuracy of .01 second. This feature has proved invaluable in the interpretation of results in that many of the films which contained good information had to be examined with care near the portion of film corresponding to burst time in order to detect the images, since these are very small (on the order of a few thousandths of an inch in

diameter) in many cases. Furthermore, in cases only a few frames of information has been obtained, the coincidence in time of these frames with those from other cameras of the same or different types furnishes compelling evidence that artifacts are not being mistaken for bursts. Finally, the information on exact burst time is of value in the interpretation of magnetometer tests being made by other groups.

The solenoid operated 16 mm cameras mentioned briefly in the previous report were employed with good results on most of the tests. The method of using these cameras was to operate six of them with an exposure of $2/3$ second, an additional 6 with an exposure of $4/3$ second, and an additional 6 with an exposure of $8/3$ second. The switching operations of the solenoids were so synchronized that the dead time between exposures was out of phase on each succeeding step of exposure time, so that at every instant of time at least 12 cameras had open shutters. This precaution was necessary to prevent accidental missing of the original burst. Each of the six cameras in a particular exposure time group was equipped with different filters (chosen to suit the experiment at hand) and several types of film were employed (high speed infrared, royal X panchromatic, linagraph ortho, etc.) in order to obtain approximate spectral information on the bursts.

4. EXPERIMENTAL DATA AND RESULTS

In this report, we shall describe the experimental data obtained on the motion picture cameras in a qualitative way. For an examination of the general type of pictures obtained and clarification of comments made herein, the reader is referred to an atlas of photographs which we have prepared from the films obtained. This atlas contains over 500 photographs, only a few of which are reproduced here simply due to the difficulty of handling this bulk of material and also due to the fact that many of the exposures are sufficiently weak to give difficulty in reproduction.

As mentioned in our previous preliminary report of October 10, 1960, although field difficulties prevented obtaining as much data as we would have liked, particularly on the early tests, we did obtain approximately 8 miles of movie film, over 100 Varian recorder charts, and approximately 2 dozen rolls of

magnetic tape on which we recorded the results obtained and the comments made during the actual firings. At that time (October 10, 1960) approximately 500 man hours had been spent on the results, and it was estimated that we were approximately one-fourth of the way through with the evaluation of our data from Firefly 1960. At present, over 1000 additional man hours have been spent on these results, and we now estimate that we are between two-thirds and three-quarters of the way through with this evaluation procedure. We have completed the examination and printing of pertinent portions of the 35 mm and 16mm motion picture film, we have examined all of the Varian recorder charts and have located burst signals on a number of these, we have read the results off of all of the magnetic tapes, and have examined the Dumont streak photographs and the data camera photographs in a preliminary way. We still have the detailed evaluation of the Dumont and data camera pictures to do, as well as completion of the microphotometry of a number of the films.

FIREFLY MARGIE

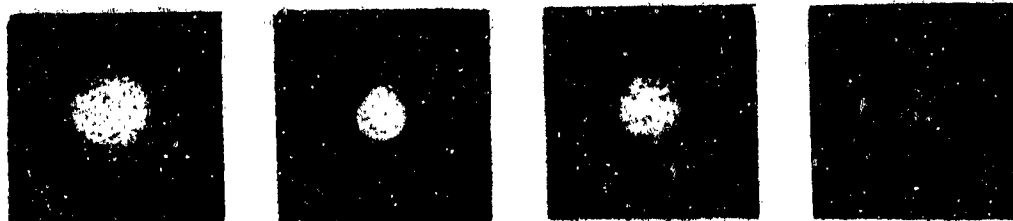
13 August 1960

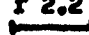
Good data was obtained on photometers, with the burst appearing as a pulse approximately 20 milliseconds long, with a rise time much less than 1 millisecond, and with a fast decay. The chart recorders also show the burst clearly, as well as a considerable period of following the intensity from the cloud. During this test, the persistence was long enough so that it was possible to try swinging on and off of the cloud several times, and the results of this work are being analyzed.

Photographic coverage was good, showing clearly both the initial burst and the later build-up of the cloud. Data was obtained until the end of our film. The exact time of burst was found to be 04:37:00.60.

Development of the cloud is shown on the accompanying photographs, and it can be seen that the apparent diameter is 1.1 kilometer at burst falling to a value of 0.7 kilometers at .05 seconds, and gradually building up (after 0.2 seconds) to approximately 1 kilometer. Photographs of this burst are also included from faster cameras, showing the difference in appearance which is obtained by the two different types of photographic coverage.

Good coverage was also obtained with the solenoid operated cameras,



BURST
 FIREFLY MARGIE, #607, MOD IV CAMERA, 20 FPS, 75MM LENS, f 2.2
 VITRO TIME AT BURST 37.00.62 \pm .05 1 KILOMETER = 



.208SEC

.458SEC


1.958SEC

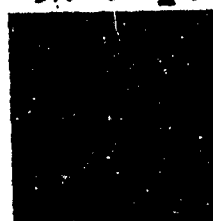
19.958SEC



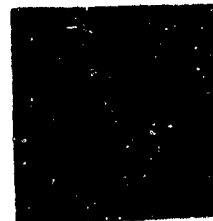
59.958SEC



BURST
 FIREFLY MARGIE, #611, MILLIKEN CAMERA, 128 FPS, 25MM LENS, f 1.1
 VITRO TIME AT BURST 37.00.62 \pm .05 1 KILOMETER = 



1.56 SEC



13.38SEC

with the drifting of the cloud showing up clearly. Some spectrographic data, not as yet reduced, will be available from these photographs.

FIREFLY MARIE

9 August 1960

The 15° difference between observed elevation and predicted elevation on this burst prevented any of our cameras from obtaining coverage of the initial phases of the explosion. However, by 04:38:28.3 (approximately 2 seconds after predicted burst) our tracking cameras were following the development of the cloud, and we have excellent pictures covering a long time (until the end of our films).

Due to the necessity of swinging the photomultiplier unit onto the burst, and due to the variation of background intensity with sky position, it is difficult to interpret the result of the chart recorders. While definite variations were observed, and we are attempting to correlate them with possible changes in intensities with time, more work will have to be done on this phase of the data before we can make any positive statements.

The fixed mount solenoid operated 16 mm cameras naturally did not obtain information on this burst, due to the difference in observed and predicted elevation.

FIREFLY LOLA

15 August 1960

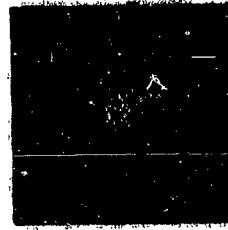
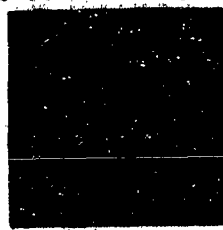
A good burst signal was observed, with a large amplitude and very fast rise. The build-up was certainly faster than 1 millisecond, and the decay of the initial signal faster than 10 milliseconds. Large photometer signals were obtained, which threw all units off scale initially. The chart recorders show the burst clearly with large intensities, and this data is being analyzed at the present time.

Good photographic coverage was also obtained. The exact time of burst was 04:38:00.12. The fixed cameras caught the initial portion of the burst and the tracking cameras were in position in approximately one and a half seconds, giving good coverage of the growth of the clouds from that time until the end of the film.

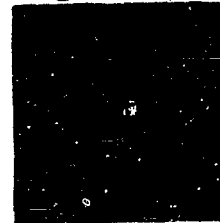
Photographs of the initial build-up of the burst are included from the



BURST .016SEC .078SEC
 FIREFLY JEANNIE, #36560, MILLIKEN CAMERA, 25MM LENS, f 1.1
 VITRO TIME AT BURST 36.40.90 ± .05 1 KILOMETER =

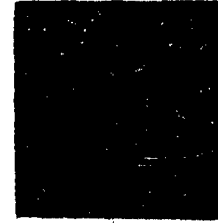


BURST .05SEC .20SEC .40SEC
 FIREFLY JEANNIE, #36554, MOD IV CAMERA, 75MM LENS, f 2.2
 VITRO TIME AT BURST 36.40.90 ± .05 1 KILOMETER =



.95SEC

1.70SEC



BURST .016SEC .30SEC 8.74SEC
 FIREFLY LOLA #12618, MILLIKEN CAMERA, 128FPS, 25MM, f 1.1.
 VITRO TIME AT BURST 38.00.18 1 KILOMETER =



41 SEC
 FIREFLY LOLA #12613
 MOD IV 20 FPS
 150MM, f 2.8
 1 KILOMETER =

23.5SEC

128 frames per second cameras showing a large initial apparent diameter (1.5 kilometers) with an apparent decrease to less than 1 kilometer at 0.31 seconds, followed by slow increase. One photograph from the 20 frame per second camera is included, at a 40 second time, to show the distinctive appearance of the burst as it develops.

FIREFLY ZEIDA

25 August 1960

Attempts were made, by the use of heavy filters, to photograph this shot. Preliminary examination of the film is disappointing, with no results seen. It will be necessary to re-evaluate this film, but we are of the present opinion that there will be little or nothing in the way of data.

Similarly, attempts to use photometers with heavy filters and with polarizers proved fruitless, in view of the daylight conditions prevailing during the launch.

FIREFLY PEGGY

16 August 1960

Failure to turn on the tape recorder during this test resulted in making our charts from the Varian recorders extremely difficult to interpret. Whether or not information that is useful can be rescued from the available charts is speculative. No effort to interpret the data has yet been made.

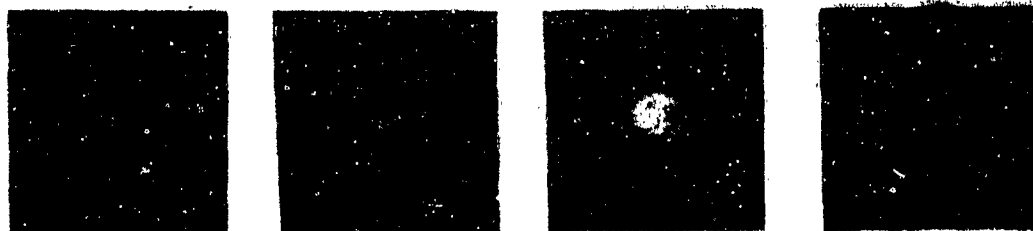
Very good photographic coverage was obtained, with time of burst established at $04:41:50.75 \pm .05$ seconds. The burst had a small initial diameter, and grew to over 1 kilometer in diameter in less than 0.2 seconds. Some asymmetry was noted in the appearance of the burst as the development proceeded.

FIREFLY OLIVE

18 August 1960

The very large background present on this test, due to the late firing, made setting of the photomultiplier units particularly difficult. Typically, we were operating with the units turned down to approximately one ten thousandth of their maximum sensitivity. Probably due to this cause, we did not notice any initial burst signal on the oscilloscopes.

The photometer traces do, however, yield signals over the first few seconds. For example, an infrared tube shows the signal building up within



BURST .05SEC .15SEC .30SEC
 FIREFLY OLIVE, #686, MOD IV CAMERA, 75MM LENS, f 2.2
 VITRO TIME AT BURST 41.50.16 \pm .05 SEC 1 KILOMETER = ———



.70SEC



BURST .015SEC .07SEC
 FIREFLY OLIVE, #686, MILLIKEN CAMERA, 25MM LENS, f 1.1
 VITRO TIME AT BURST 41.50.16 \pm .05 SEC 1 KILOMETER = ———

approximately 10 seconds after burst, gaining in amplitude for almost one minute, then starting to decay. An immediate signal on a photometer equipped only with a polarizer, decaying in approximately 15 seconds, was also observed. These data will be plotted on an absolute basis in the near future, and included with the next report.

Examination of the film shows the burst clearly visible at 04:41:50.16, with moderate persistence of the images on all cameras. The development of the cloud is shown on the accompanying photographs, some of which were taken on the 128 frame per second cameras, and the others on the 20 frame per second cameras. An initial size of .35 kilometers, even during the first .01 seconds, is observed, with very rapid increase of size to approximately 1 kilometer.

FIREFLY JEANNIE

10 August 1960

Excellent photographic coverage was obtained during this test. The tracking mount was directly on the burst, giving us semi-telephoto photographs of the initial development. The time was 04:36:40.80. The fast cameras had enough intensity to follow the burst for approximately 2 seconds, while the slower cameras (20 frames per second) followed for a few more seconds. The solenoid operated cameras obtained data for considerably longer period. Spectral information should be available from these films, after they have been photometered. Development of this burst on both the fast cameras (128 frames per second) and slower cameras is shown on the photographs which are reproduced herein.

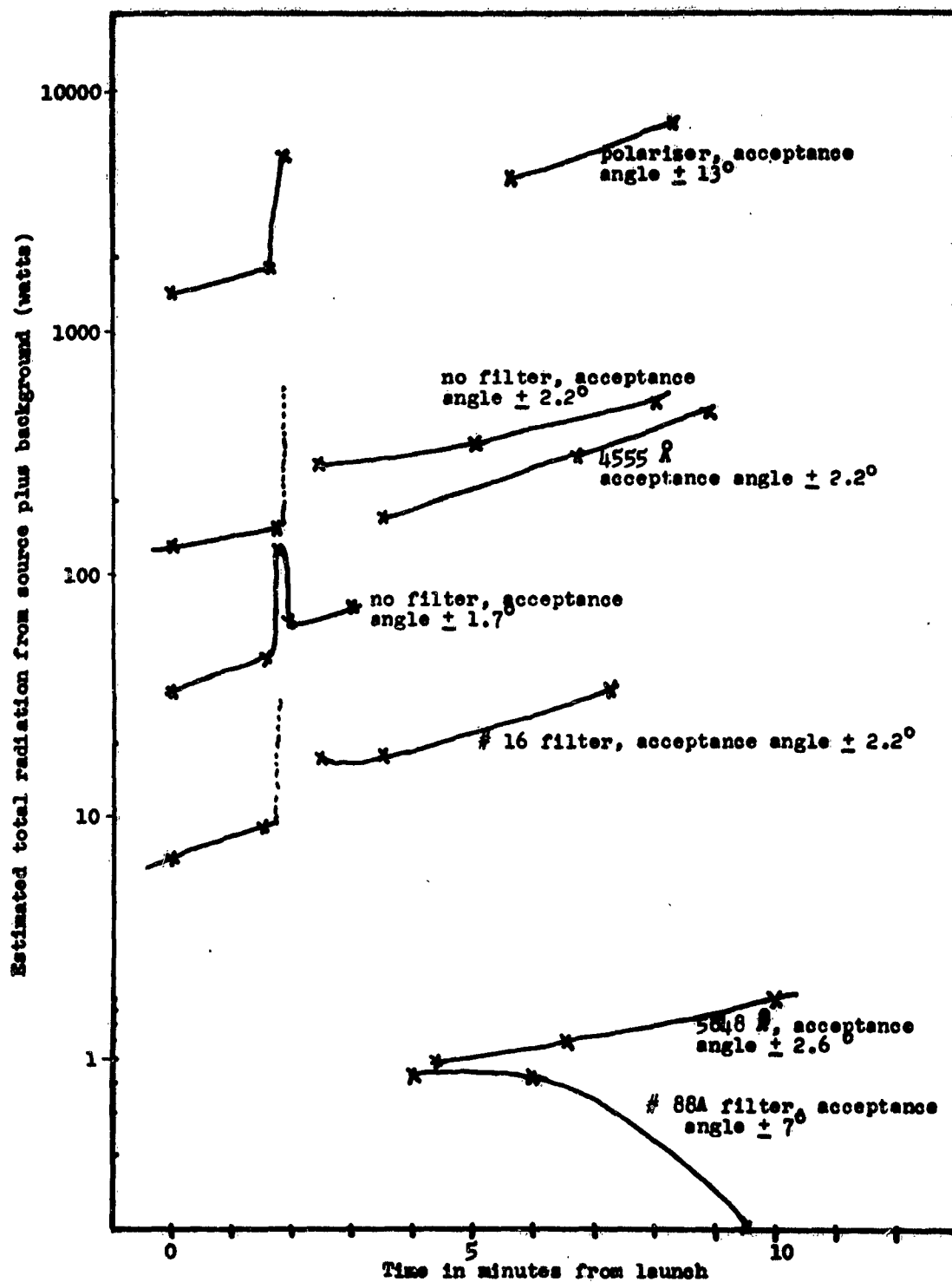
Large signals from the initial burst were obtained on the oscilloscopes, and on the chart recorders. The initial burst corresponded to a pulse with a total length of approximately 20 milliseconds, although it can be seen from analysis of the chart recorder data, which is included in the accompanying figure, that the signal persisted for considerably longer at a much lower level.

FIREFLY SUSAN

17 August 1960

Excellent photographic coverage of this shot was obtained on all cameras. Very rapid growth of the original cloud was observed, and the images persisted until the end of our film. The growth of the cloud seems to be

FIREFLY JEANNIE--PHOTOMETER RESULTS



completely normal and regular without the apparent very large size at the beginning typical of certain other bursts.

Burst time was 04:43:49.33, and good agreement was obtained between the various films examined insofar as burst time was concerned. Furthermore, the telephoto lens cameras were apparently directly on burst, giving us excellent photographs on a larger negative size for studying the early portions of the development of the cloud.

We observed the burst on the photometer traces, but the reduction of this data is not yet complete.

FIREFLY DOLLY

27 July 1960

We obtained approximately 10 seconds of data beginning at time 04:21:45.85, which agrees well with the time recorded by another group. This burst developed very rapidly, with the first frame on the 128 frame per second camera showing a diameter of 1 kilometer, developing to 2 kilometers in less than 0.25 seconds. Following the rapid initial increase in size at burst the growth was much slower. The intensity decreased relatively rapidly, apparently with a time constant of approximately 0.3 seconds.

We have satisfactory data on the solenoid operated 16 mm cameras for bridging the gap between the very fast and very slow regions, and have some spectral information available from this source.

Interference due to lightning flashes prevented certainty in determining whether signals were observed or not on the photometric equipment. While further analysis of the data will be attempted we noted that signals many times background were being caused by the lightning flashes, so that it is doubtful that we can definitely assign deflections on the instrument to the burst.

FIREFLY GATHY

29 July 1960

The burst was observed at 02:33:44.8 \pm .05 seconds. The initial flash of light decayed with a time constant on the order of a few hundredths of a second, and the build-up of the original light intensity was much faster than 10 milliseconds. Here again the full size was reached on the first frame of the 128 frame per second cameras, corresponding to approximately 1 kilometer.

The high intensity portion of the cloud decreased in size rapidly after the initial burst.

The photometers operated properly, and data was obtained for approximately 5 minutes after the initial burst. A small amount of spectral information was secured, which has not yet been analyzed.

On this test, observations were made more difficult by the fact that lenses were wet, due to condensation.

Data was obtained on the solenoid operated cameras for only a few seconds.

FIREFLY BETSEY

8 August 1960

The film on this test showed a burst time of 04:16:40.62. The intermediate speed cameras (128 frames per second) secured data for approximately 0.1 second before intensity decay prevented further results. The slower cameras (both 20 frames per second and 1 frame per second) obtained good coverage for longer times. Initial intensity was reached quite rapidly (within 10 milliseconds) and the decay constant seems to be (from the film) on the order of a few hundredths of a second.

Although the 128 frame per second cameras show full size (approximately 0.5 km) on the first frame with decreasing intensity thereafter, the 20 frame per second camera does show a growth of the cloud. This is undoubtedly due to the fact that the 20 frame per second cameras are picking up parts of the cloud that are not visible at the shorter effective exposures on the 128 frame per second cameras. A "particle wave" seems to appear quite clearly at approximately 0.15 seconds on the 20 frame per second cameras.

Dumont camera coverage obtained some results, but interpretation has been hampered by lack of good time marks on the film. This film will be studied further.

There were some lightning flashes during this test, which complicated the interpretation of photometer data. However, an unmistakable burst signal was seen on the oscilloscopes, with a very fast rise (much faster than 1 millisecond) and with a decay constant of approximately 30 milliseconds.

The burst is also clearly visible on the chart recorders, although

interpretation of the results at later times is complicated by the fact that the background is increasing rapidly and by the fact that the clouds seemed to be moving quite rapidly, making the tracking problem rather severe.

FIREFLY AMY

28 July 1960

We have determined the time of the burst on this test to be 02:32:45.26, in good agreement with the value reported by others. We were able to obtain initial burst data, showing full development of intensity within less than 0.01 seconds, with the cloud apparently at full size on the initial record. This appears to be approximately 1 kilometer, with only very slight expansion of the original cloud apparent as time went on.

Our solenoid operated 16 mm cameras were able to follow the burst for several seconds, but the intensity was quite low.

No photometer data was obtained, in spite of almost ideal background conditions, due to failure of the -1000 volt power supply serving the photomultiplier tubes.

FIREFLY RUTHY

1 August 1960

On this test we were able to establish the time of burst as 02:32:29.33 \pm .01 seconds. The data obtained on the fast cameras showed a very rapid rise of the initial pulse (faster than 10 milliseconds) and a decay constant of approximately .02 seconds. The size of the initial burst corresponded to approximately 0.5 kilometers with full intensity evident on the first frame and decreasing intensity thereafter.

Preliminary examination of the Dumont strip camera data shows no useful signal above background level, although the film is clear and the time marks are quite good.

Equipment difficulty (shorted high voltage cables) prevented obtaining photometer information on this test.

FIREFLY GERTA

6 August 1960

The photometers showed a large burst signal approximately 50 milliseconds wide, with a rise time of less than 1 millisecond. Also, the Varian

recorders showed the burst clearly, with several seconds of good data following the initial explosion. Very low background made the data very clear, and it should be possible to deduce some information on spectrum from these records.

Although faulty functioning of the Vitro time receiver made it necessary to examine the film frame by frame, the burst was located and the initial rise traced. From an initial diameter (at burst) of approximately 0.25 kilometers, the cloud grew to 0.4 kilometers at the end of .05 seconds, 0.6 kilometers at the end of 0.1 seconds and became very diffused and difficult to see by the end of 0.15 seconds. The appearance of the cloud is shown in the photographs included.

FIREFLY JANET

26 July 1960

Examination of the film from the 20 frame per second and the faster cameras failed to show any trace of burst on this test. We have obtained photographs with approximately 1 second exposure on the solenoid operated 16 mm cameras, and should have some data available here on relative spectral distribution of the emitted light for the first few seconds after the burst. Since we have not been able to locate the burst on the faster cameras we are not able to give an accurate time for this burst. The photographs which were obtained showed very little difference between the intensity of the burst and the sky background, at least in the blue region of the spectrum.

No photometer data was obtained, due to large background intensity and the small difference between background and signal levels.

FIREFLY HILDA

1 August 1960

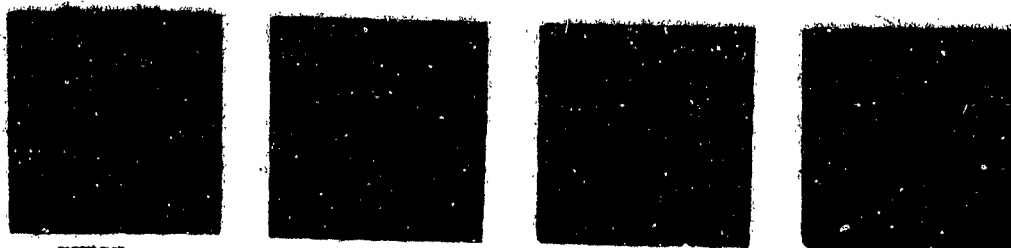
Poor recording of Vitro time on the film hampered interpretation of this data. The films have been examined frame by frame and no image has been found. Likewise, no burst was visible on the photometers.

Film from the solenoid operated 16 mm cameras has not yet been completely examined.

FIREFLY CARRY

18 July 1960

Analysis of the films obtained gave us a burst time of



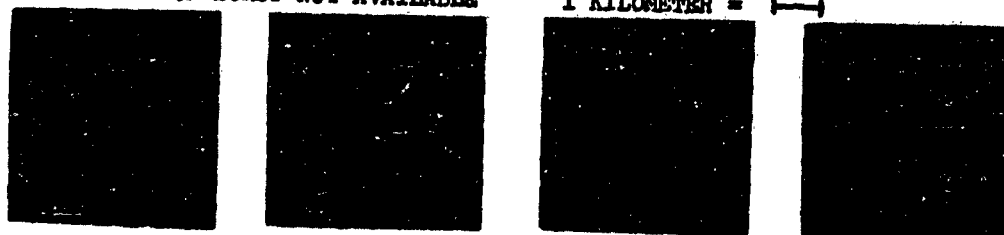
BURST .05SEC .45SEC .95SEC
 FIREFLY FRANCES, #2797, MOD IV CAMERA, 20 FPS, 75 MM LENS, f 2.2
 VITRO TIME AT BURST 08.20.925 ± .05 SEC, 1 KILOMETER =



2.05 SEC 4.15 SEC 10.60 SEC 22.10 SEC



BURST .05SEC .10SEC .15SEC
 FIREFLY GERTA, #07452, MOD IV CAMERA, 20 FPS, 75 MM LENS, f 2.2
 VITRO TIME OF BURST NOT AVAILABLE 1 KILOMETER =



BURST .05SEC .10SEC .95SEC
 FIREFLY HEDY, #60382, MOD IV CAMERA, 20 FPS, 75MM LENS, f 2.2
 VITRO TIME OF BURST 12.48.32 1 KILOMETER =



5.95SEC 22.95SEC.

04:03:28.14 \pm .05 seconds. This high explosive shot gave a very brief flash, showing up as 3 frames on the 20 frames per second cameras. An interesting feature was noted, in that the second frame of the three frames obtained seems to be in the shape of a doughnut. It is intended to photometer this film since the pictures are very clear and the film is well within its proper latitude, so that quantitative data can be obtained. Frame by frame examination of the higher speed camera film has not yielded any images, and, due to the fact that the Vitro time was not functioning properly on these cameras, it is not possible to locate exactly the portion of the film that corresponds to the burst time.

No signal above background was obtained on the photometric equipment, although two photomultipliers, one equipped with a polarizer and another with no filter, were trained on the expected burst location.

FIREFLY ARLENE

15 August 1960

Lack of Vitro time on the photographs for this shot made analysis difficult. However, no burst has been found and we do not believe that we have any data for this shot.

The photometers likewise show no data. Our tapes have the comment that there was a pinpoint of light approximately 8° off of our setting (which would have meant that neither our camera equipment nor our photometers would have been able to pick up the signal) and, although we swung the mount as rapidly as possible to this position, no further signal was observed.

FIREFLY TP ANNIE

13 August 1960

No data was obtained on this shot either by cameras or by photometers. The burst was not visible.

FIREFLY TP NORMA

13 August 1960

No data was obtained on this shot either by cameras or by photometers. The burst was not visible.

FIREFLY REMA

19 August 1960

Although an attempt was made to operate the photometers during the

daylight launch of this test, it was found that background was hopelessly high, so that no data was obtained. No cameras were operated during this test.

FIREFLY LINDA

17 August 1960

No data was obtained on this shot either by cameras or by photometers. The burst was not visible.

FIREFLY MAVIS

29 July 1960

Preliminary examination of the films from this test show no sign of burst in the vicinity of the predicted time, but it is intended that this finding will be reviewed carefully before being accepted. Likewise, the photometer data shows no apparent burst (no deflection on the meters was noted at the predicted time of burst) and the rapidly increasing background prevented possible differentiation of signals from the developing cloud from those of background. So far, therefore, we have absolutely no data on this test.

FIREFLY FRANCES

14 July 1960

We were able to establish the time of burst as 04:08:20.92 \pm .01 seconds. Examination of the 20 frame per second motion picture film shows that the cloud grew from an initial diameter of approximately 0.2 kilometers to 0.4 kilometers at the end of .05 seconds, 0.9 kilometers at the end of 0.5 seconds and 1.2 kilometers at the end of 1 second. Full brightness was achieved on the first frame, indicating a very rapid build-up of initial intensity. The various stages of the development of the cloud, including a later formation of the crescent shaped and nebulous form, is depicted in the photographs reproduced here.

Photometers were not operated during this test.

FIREFLY LILY

21 July 1960

We can establish the time of this burst at 04:05:17.33 \pm 0.01 seconds. The burst starts at a very small size (less than 0.1 km) and grows slowly, to a little over 1/2 kilometer at the end of one second. Our film records on this burst extend over several seconds, with the initial rise to maximum intensity

occurring in approximately 0.64 seconds. We also obtained good data on the Dumont strip film cameras on this shot, with a streak even on the fastest speed (400 inches per minute) extending over approximately two feet of film. Photometry of this strip will be done. Photographs on strip cameras were obtained with red and green filters.

Photometer signals were obtained on this burst with a persistence of several minutes. Intensity in the blue region was approximately ten times that in the red. We have not as yet reduced the photometer data to an absolute basis.

FIREFLY HEDY

22 July 1960

We have established the time on this burst as $04:12:48.4 \pm .05$ seconds. The rise of the intensity of the images on this film was rather slow. The initial size at burst was less than .05 kilometers, growing to 0.1 kilometers at 0.1 seconds, 0.25 kilometers at 1 second, and 0.4 kilometers after 6 seconds. Maximum intensity was not reached for almost 1 second and our data covers more than 20 seconds (until our film was exhausted). The development of the burst is shown on the photographs included herewith. Photometer data on this burst shows smaller signals than in Firefly Lily, with approximately the same spectral distribution. Reduction to absolute basis has not yet been completed.

FIREFLY IDA

20 July 1960

Examination of the films from this firing showed no trace of the burst on any of the cameras employed. Certainly one explanation for this was the fact that the burst was 6.5° off in elevation, and most of our equipment was set for a $\pm 5^\circ$ acceptance angle. On the basis of the results of this shot, we modified lens arrangements for future shots to enable us to accept a somewhat larger angle of view.

Although our photometer should have been operative during this shot, the same 5° field of view acceptance angle was employed as mentioned above, which prevented us from obtaining information on the initial burst. No signal above background was obtained on the photometric equipment.

FIREFLY KICKY

25 August 1960

Due to the large difference between observed and predicted elevation (approximately 48°) all of our equipment was pointed in the wrong direction on this launch.

We did not obtain any useful information upon swinging the mounts toward the observed burst.

We have no data whatsoever on this shot.

FIREFLY WENDY

18 August 1960

The 33° difference between observed and predicted elevation on this shot meant that all of our equipment was off of the burst when it occurred. Therefore, as might be expected, no photographs were obtained of the burst. Nevertheless, the amount of signal produced by the explosion was so large that we obtained a large deflection of the oscilloscope (completely off scale), probably because of reflections from the clouds that were in the field of view. We attempted to swing the photometer onto the burst, but again, due to variation of sky background with position, the results obtained are quite difficult to interpret. Although we shall continue trying to reduce this data (particularly attempting to estimate the total light emitted by this burst as compared to those at higher altitudes), we are dubious that very much useful information will result.

FIREFLY ETHEL

25 July 1960

No data was obtained on this shot either by cameras or by photometers. The burst was not visible.

FIREFLY DOTTY

15 July 1960

No data was obtained on this shot either by cameras or by photometers. The burst was not visible.

FIREFLY EDITH

12 July 1960

No data was obtained on this shot either by cameras or by photometers. The burst was not visible.

17 August 1960

The photometer records on this shot do not show any appreciable signals, except that a burst was noted at 182 seconds after launch. Discussion of this burst with the group present at the time showed the probability that this was a meteor, rather than the expected signal. The error of time of approximately two seconds is, we feel, significant here.

Thorough examination of these films has failed to reveal any images.

5. DISCUSSION OF RESULTS

Although some tentative comments have been made in the preceding text concerning various points, no really coordinated discussion of results has been possible to date because of the fact that our data must be coordinated with that of other groups. We are in the process of doing that at this time, and expect to include in the next report a thorough discussion of the meaning of our results as they are compared to data obtained by radio frequency reflection, by longer time photographic coverage, and by other methods. Also, it is expected that by the next report all of the remaining data will be evaluated, which will add approximately one-fourth additional information to that already presented.

It cannot be stressed too strongly that the photographs in the atlas which has been prepared are the best and really only satisfactory way of seeing the type of results obtained photographically.

Early-time Cloud Growth and Energy Distribution as Measured By Doppler Frequency Shift Methods

R. A. Barnes
Dr. P. B. Gallagher

Radioscience Lab
Stanford University

ABSTRACT

Procedures and results are presented for the measurement of early-time cloud growth. These are derived from velocities which are obtained from Doppler frequency shift records. The results suggest a predominant direction of growth for each release. Theoretical energy spectral distributions of Doppler shifts are compared to measured values for one case as a basis for determining initial cloud structure.

I. INTRODUCTION

Radio measurements of cloud growth during the first few seconds after release provide a means for observing shock wave phenomena, velocity and velocity decay of the expanding gas, and perhaps initial distribution of gaseous matter in the cloud. A bistatic CW transmitter-receiver system was employed in an effort to obtain some of the answers using frequency spectrum analysis. The velocity of growth is sufficient to generate a measureable Doppler frequency shift. This frequency shift, when integrated over the first few seconds, would give the early-time growth pattern. The resulting curves, when correlated with photographs, might give a basis for comparing electron-ion growth against the visible shock wave, gaseous, and particulate matter components of the expanding cloud. Spectrograms were obtained on all thirteen observed PEC releases (Zelda was not measured) and on the evening twilight Arlene HE release.

II. THEORY

A. Cloud Growth:

The expression relating maximum Doppler shift to uniform isotropic growth of a spherical reflecting surface is

$$v = \frac{(\Delta f) C}{2f_0} \sec \theta \quad (1)$$

when $v \ll C$

where

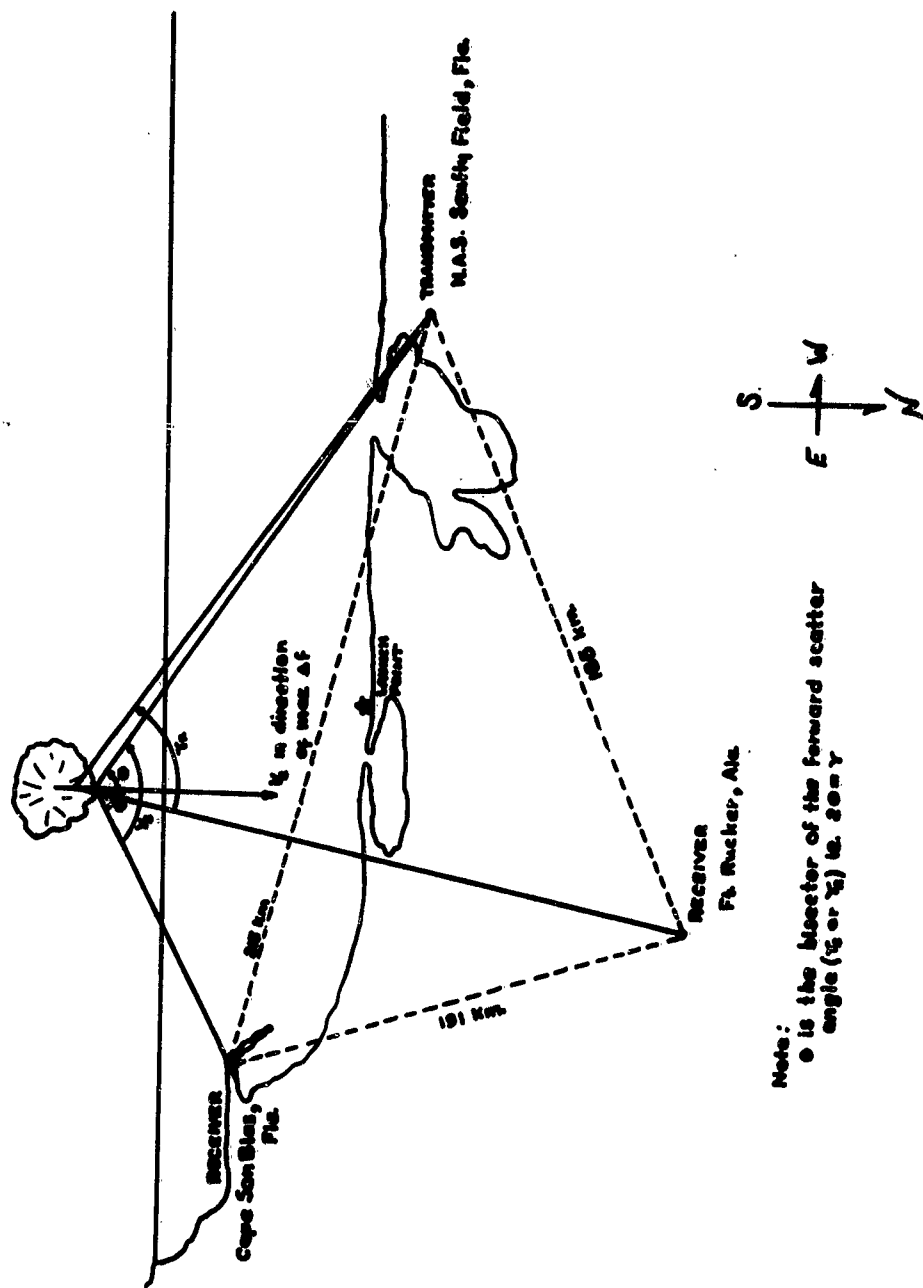
θ defines the bisector of the forward scatter angle γ_r or γ_s (Fig. 1)

v is the instantaneous growth velocity of the cloud in km/sec.

C is the velocity of propagation, $\approx 3 \times 10^5$ km/sec.

Δf is the maximum frequency shift from f_0 in cycles/sec.

f_0 is the radio frequency in cycles/sec.



Note:
 θ is the bisector of the forward scatter angle ($\frac{\theta}{2}$ or $\frac{\theta}{2}$) to 20m.

Fig. 1 Geometry of Coverage

Velocity v can be derived at any time T (if the cloud position is known) from the measured Doppler shift of the CW signal, which is transmitted via the cloud from Pensacola to San Blas or Rucker (Fig. 1). Integration of the Doppler shift curves over a period of time T yields a measure of the cloud growth, thus

$$\text{Growth} = \int_T v dt \quad (2)$$

B. Energy distribution of spectral components

Non-symmetrical cloud growth can be detected in the energy spectral distribution of measured Doppler shift components at the San Blas and Rucker sites. To approach this problem, a symmetrical growth model is first assumed for a spherically expanding surface with velocity v_c . From the geometry (Fig. 2) it can be shown that the velocity component v_s measured at either site is given by

$$v_s = 2v_c \sin \theta \sin \phi \quad (3)$$

We wish to determine how many (N) such velocity components are active in a constant bandwidth df (i.e., a velocity band $dv_s = \text{const.}$, since the analyzer filter is constant width), as contributors to measured spectral energy. The locus of constant v_s around the sphere is a circle of radius $k \cos \theta$ and length $l = k' \cos \theta$ (4)

The width $d\theta$ on the sphere of the band which contains all components between v_s and $v_s + dv_s$ is obtained from eq. (3)

$$d\theta = \frac{k' dv_s}{\cos \theta} \quad (5)$$

The total number of components is the product of equations (4) and (5), i.e.,

$$N = l d\theta = k dv_s = k df \quad (6)$$

and is independent of frequency. Therefore a flat spectral response is expected for the uniformly growing sphere.

If the sphere grows non uniformly this response is modulated, and spectral data must be matched in each case to a suitable distribution function for mass transport.

III. EQUIPMENT DESCRIPTION

A one kilowatt input CW transmitter was located at NAS Saufly Field, which is approximately 12 km N.W. of Pensacola, Florida and 80 km West of the launch area. Receiving sites were located at Cape San Blas, Florida (approx. 140 km East of launch) and Ft. Rucker, Ala., (approx. 135 km North of launch) to allow for growth measurements along two directions. For the geometry selected (Fig. 1) maximum Doppler shift at San Blas corresponds to growth approximately in the

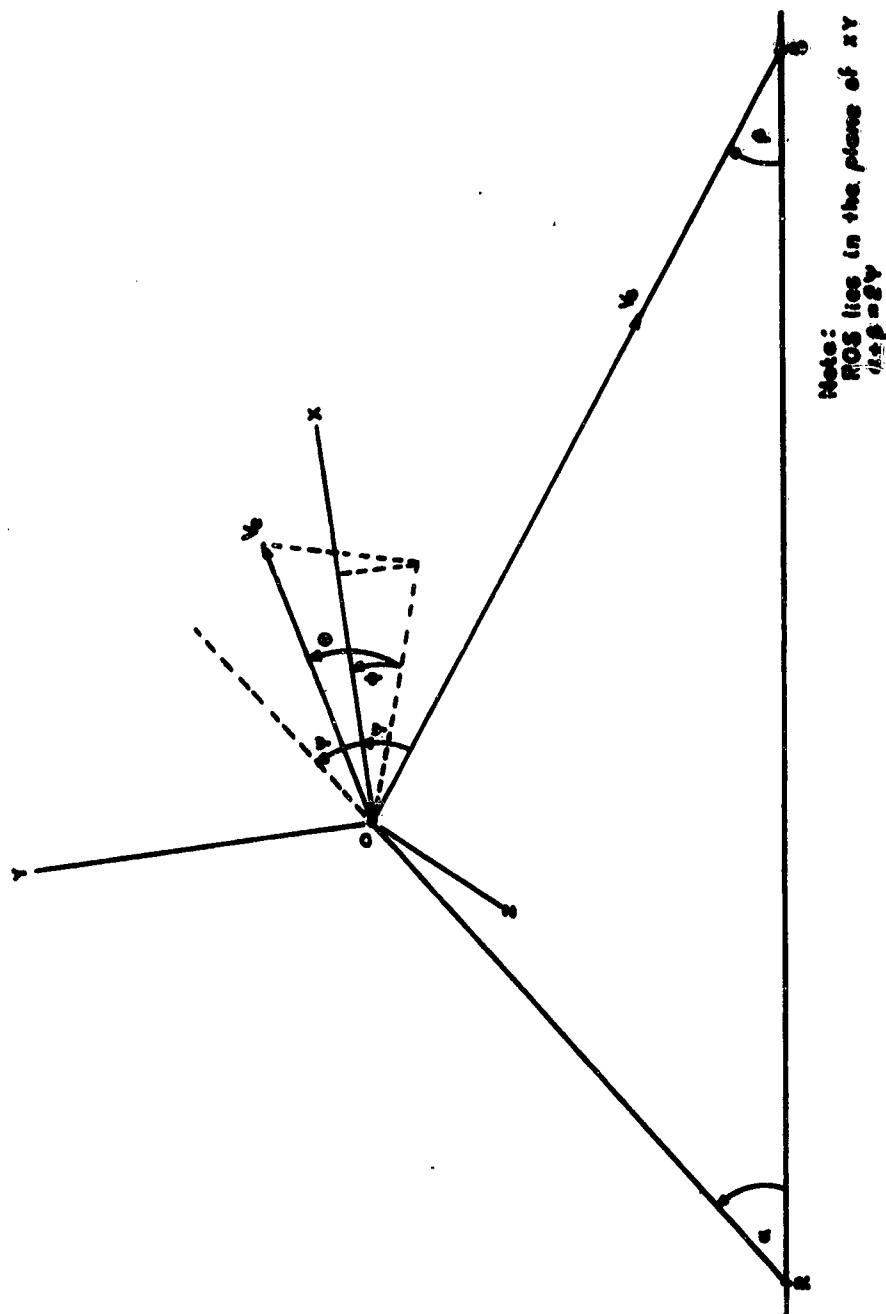


Fig. 2 Geometry For Spectral Distribution Model

vertical (up or down) direction; at Rucker, this direction is at approximately 30 degrees elevation angle along a nearly NW direction.

The transmitter had an output of approximately 600 watts at a carrier frequency near 25 Mc which fed a 3 element, 7 db gain, Yagi antenna. The beamwidth was sufficient to illuminate the expected region where releases were made without requiring reorientation of antennas.

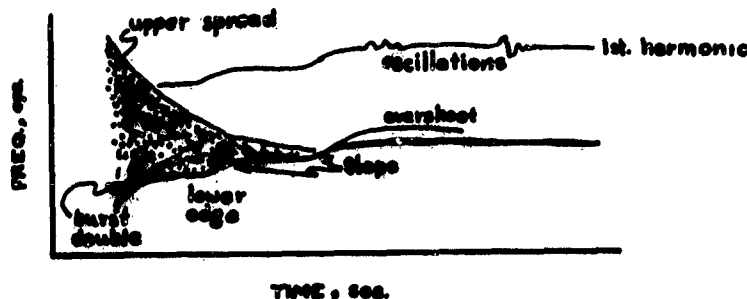
The receivers used a bandwidth of about 2 kc. and the HFO's were set for an output of about 400 c/s. Three element Yagi antennas were used at both receiving sites.

The outputs of the receivers were recorded on magnetic tape in order to facilitate data reduction at a later date.

IV. DISCUSSION

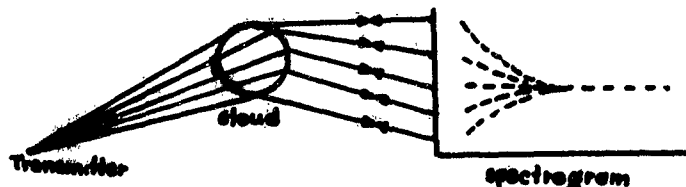
The spectrograms thus obtained (Fig. 3a, b, c, d) show many features that may lead us to obtain a better model for the releases. It appears from the spectrograms that on some of the shots the clouds appear to reflect as an overdense surface. However, a number of releases, especially at higher altitudes, produce a Doppler spread. This would arise from a generally underdense cloud composed of a number of high density scatter centers (Gerts, Ariane, Amy, Ruthy, etc.). This latter type of spectrum corresponds to cloud growth in many directions. From Cape San Blas the maximum Doppler shifts result from downward growth and an upward growth. From Ft. Rucker, however, such growth is along a NW-SE direction at 30 degrees elevation angle. The lower and upper boundaries are positions of maximum frequency shift and are used to measure cloud growth quantitatively. The heavy areas that lie between the outer boundaries of the spread traces represent other velocity components that arise from scatterers moving radially in the expanding sphere in other than these maximum directions. A close look at some of the spectrograms, show many cases of Doppler frequency shift steps. These steps may be associated with shock wave phenomena. It is possible that the first step may be the shock wave while succeeding steps are waves of gaseous (cesium) matter.

A brief discussion of each spectrogram follows. One must be careful not to misinterpret the multiples, which are produced from overloading the filters in the sonalyzer equipment. All possible features appearing on a burst sonogram are indicated in the following sketch:



1. Arlene

The diffusiveness indicates scattering from many regions of the growing bubble as shown in the sketch



The absence of a sharp trace corresponding to any one ray path is ascribed to the multiplicity of scatterers in the bubble. A strong upper trace appears in the San Blas but not Rucker record.

It is believed the Arlene pattern appears also in many of the Cesium releases at burst, obscuring the growth of the cesium cloud for the first one or two tenths of seconds.

2. Margie

The difference in apparent rest size observed from the two sites is over 3:1, possibly real, but maybe from a difference in sensitivities recorded on the sonogram. Both records show slight Doppler broadening on the downward growth, and no upper trace. (The latter for the same reasons as Lola below).

3. Marie

A record for Rucker only is available. The difference in payload is apparent in the intensity of returns. The lower growth trace appears clean; however a more sensitive sonogram may show otherwise. No upper trace is visible.

4. Lola

Growth at both sites is to a rest lower radius near 0.4 km. The suggestion of spectral broadening in the lower burst trace for S. B. may be overlapping of two, intense, clean traces; these are distinct at Rucker. The two traces must arise from growth of two major portions of the cloud in slightly different directions. The lack of an upper trace would be a consequence of the low release altitude, restrictive growth and resultant opaqueness to 25 Mc waves.

5. Cathy

Rest lower radius from both sites differ considerably. Georgia Tech photographs from site F also show desymmetry. A double trace on the lower side appears at S.B., but at Rucker the trace is rather spread. A very slight indication of step is seen by sighting endward on the record. Neither appears to show an initial rate of growth comparable to shock ionization.

6. Peggy

Initial growth size was somewhat less than Cathy at both sites; Rucker showed slightly larger lower radius. Unique in this record (and Olive) is the clean, smoothly varying trace with no steps, and no evidence of shock growth. There is very slight indication of a spread upper trace at San Blas; however the record is noisy. The clean features of the traces may signify a nearly uniform isotropic distribution of electrons in spherical growth; the fact that no Doppler spread appears outstanding suggests a smooth, opaque reflector during growth. Georgia Tech photographs for Burst to +3 seconds show good symmetry.

7. Olive

Initial growth size was even smaller than Peggy; a slight larger rest radius was observed at Rucker over San Blas. Similar to Peggy, the traces for both sites are clean, smoothly varying, with no steps, and no rapid initial Doppler decay corresponding to shock growth. Very slight suggestion of spectral broadening shows in the Rucker record, from the upper side. We are coming into altitudes where the cloud is not opaque. Photographs show good symmetry, but give indication of non uniform density.

8. Betsy

The difficulty in exacting rest sizes is compounded in Betsy where interference from noise, as well as differences in sensitivity at the two sites, raises uncertainty as to where the rate growth curve lies. The 2:1 difference in rest size indicated in the chart may not be meaningful. Growth rate for Betsy is essentially smooth, with a very slight step at San Blas at approximately +1 second. The very prominent spectral broadening is evident especially in the (cleaner) Rucker record, with an upper Doppler component. The cloud at this altitude begins to be transparent from the start. The spectral broadening appears to persist longer than did Arlene, and although it may initially arise from ionizing shock wave growth, it must in part be a result of scattering in the cloud.

9. Jeannie

Rest lower radius was nearly equal for both sites. The sonograms are marked by several peculiarities. Stepped growth was made fairly evident from the harmonics generated in the San Blas recordings; no harmonics appeared in the Rucker recording and only the one step was discernable there. There is no strong spectral spread in this release, but a strong convergent double trace appears at burst in the Rucker record. This may be ionizing shock growth, as it rapidly decays; however the absence of spread suggests more that the initial cloud growth was confined into two, probably opposite directions. A second peculiar effect is the overshoot at near 0.6 seconds, seen only at Rucker. A look at the second harmonic would help to determine whether the overshoot is real, corresponding to shrinkage of the cloud, or is spectral broadening due to signal overloading. No cloud photographs are available at this writing.

10. Amy

The larger rest size is possibly a result of altitude. Both Rucker and San Blas show nearly equal radii. A number of peculiarities appear in these records, as in Jeannie, including the overshoot at +.6 seconds, steps, and spectral broadening. Steps are especially noticed in the harmonics, as well as a peculiar set of oscillations in the second harmonic at Rucker near +1 second. (harmonics multiply amplitudes of frequency deviations). Spectral spread at burst is more than for any of the lower altitude releases. At burst, notably on the San Blas record, the sonograph record has the appearance of Arlene (shock growth). It would appear that this phenomena superimposes on the normal cesium growth to give the peculiar "reversed slope" of the growth curve, and that by removing this "shock" growth the burst portion of the record would appear more like Betsy; Doppler spread is still in the record. Shrinkage of the cloud is evident not only in the overshoot, but in also a slight droop of the second harmonic curve in the $\lambda \times$ plot at +3 seconds (this plot is not included in the figures). This may be a latent effect of modulation of cloud growth by rebounding shockwaves, which contribute also to the steps. Geo. Tech photographs show the cloud as a quite symmetrical donut.

11. Susan

Rest sizes are nearly equal at both sites. Little can be read from the SB record which is very noisy. There is no real evidence of stepped growth, neither is there evidence of a rapid decay shock front. In many respects this record is similar to Peggy and Olive, i.e., shock perturbation at release appeared minimal. The great difference is the appearance of upper and lower spectral broadening some 0.4 seconds after burst. Presumably this arises from increasing transparency of the cloud during growth, as it is quite weak.

12. Ruthy

The difference in rest size measured at the two sites is slight. The sonograms from these sites are, however, different in nearly all respects. The absence of significant spectral broadening at Rucker might be attributed to a weak signal, which must be an effect of a very unsymmetrical cloud as evidenced in the photographs. A Doppler "overshoot" also occurs at Rucker, but not at San Blas. The San Blas trace is stepped, and also has a familiar "shock" decay trace at burst, with up and down Doppler shifts. The cloud is very transparent from the start. It is of interest to note that the upper and lower "broadened" traces converge at a frequency offset on the low side from zero Doppler or rest. This may be a result of cloud dysymmetry.

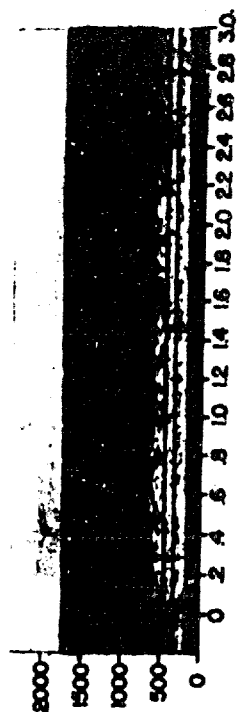
13. Dolly

The nearly 2:1 greater rest size at San Blas indicates a non-symmetrical release; this is also in evidence on Geo. Tech photos, but orientation is not certain on these. The S.B. record for Dolly is in all respects very similar to Ruthy, including steps, spectral spread, shock, etc. The Rucker record displays considerable upper Doppler spread as well as stepped growth, and clearly shows a Doppler "overshoot" as did Ruthy at Rucker. There is evidence also of oscillations at +1 second similar to those seen on Amy, also at Rucker.

14. Gerta

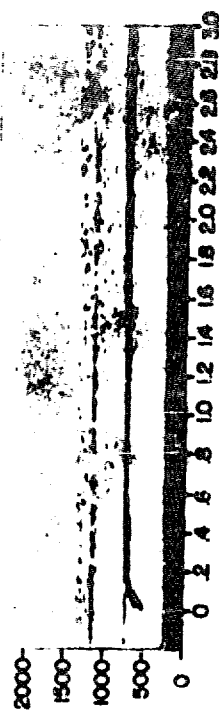
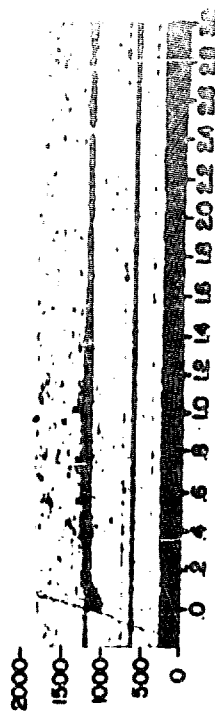
The rest size of the Gerta cloud is based only on the up and downward spread trace. This high altitude release is unique in the extreme broad spectral broadening that accompanies. There is no stepped growth apparent. Part of the difference in upper and lower spectral broadening is possibly due to atmospheric gradient; however it is probably that a good portion is due to the limited receiver bandwidth. The San Blas sonogram shows a down Doppler "scatter" component of lower intensity, but symmetrical to the upper component. This is believed the shock expansion, though not necessarily. A more firm descretetrace within would most likely be the expanding cesium cloud. The small rest size is a result of our inability to integrate these growth curves outside receiver bandwidth. The spectrums at SB and Rucker are quite similar in appearance. No photographs.

CAPE SAN BLAS, FLORIDA

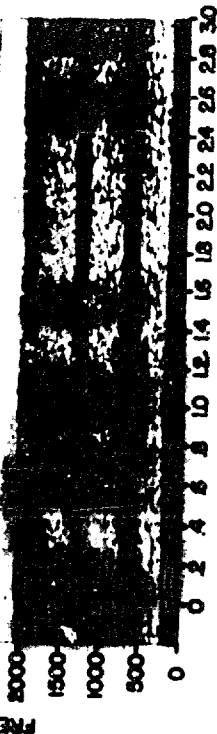


MARGIE, 8-13-60, 0435 CST, 74 Km. ALTITUDE

FT. RUCKER, ALABAMA



MARGIE, 8-9-60, 0437 CST, 82 Km. ALTITUDE



LOLA, 8-15-60, 0435 CST, 83 Km. ALTITUDE



CATNY, 7-29-60, 2030 CST, 84 Km. ALTITUDE

Fig. 3a Doppler Shift Spectrograms

CAPE SAN BLAS, FLORIDA

Fig. 3D Doppler Shift Spectrograms

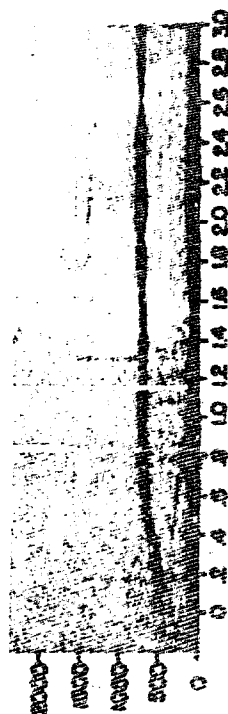
AT 0400 CST



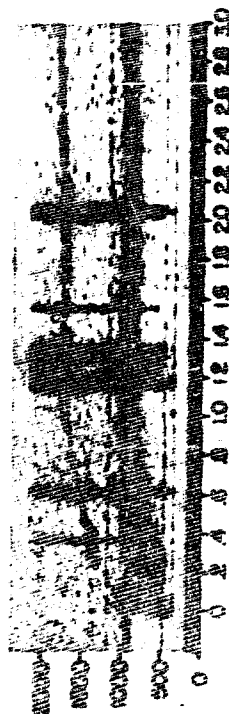
CAPE SAN BLAS, FLORIDA

Fig. 3c Doppler Shift Spectrograms

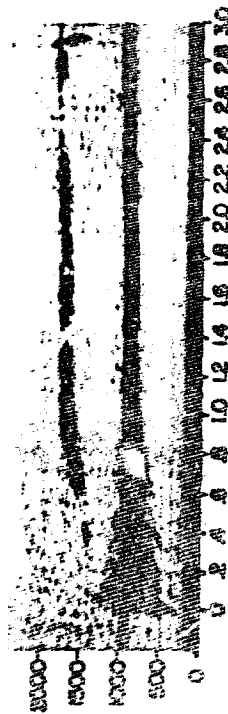
FL NUMBER, 44-22-24



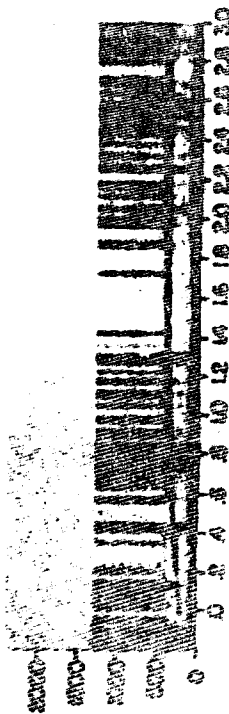
JEANNE, 8-10-60, 0436 CST, 109 Km. ALTITUDE.



AMY, 7-28-60, 0230 CST, 111 Km. ALTITUDE.



RUTHY, 8-1-60, 0230 CST, 113 Km. ALTITUDE.



SUSAN, 8-17-60, 0442 CST, 114 Km. ALTITUDE.

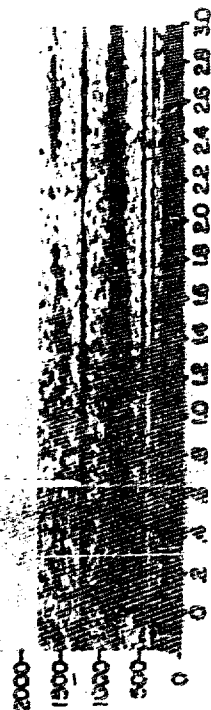
FREQUENCY (Hz)

TIME (sec)

Good Audio Copy

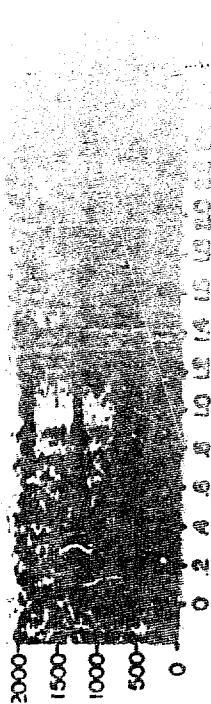
Fig. 3d Doppler Shift Spectrograms

CAPE SAN BLAS, FLORIDA

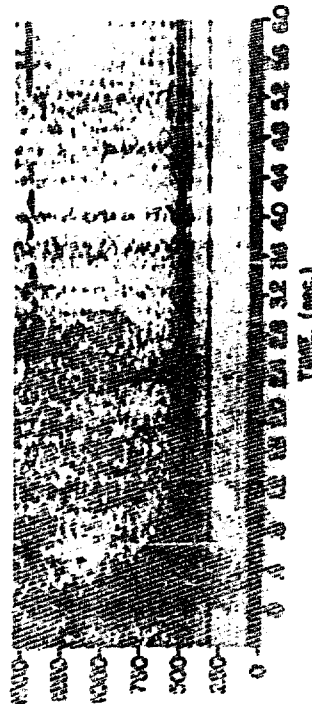


DOLLY, 7-27-60, 0419 CST, 115 Km. ALTITUDE

FT. RAINIER, MONTANA

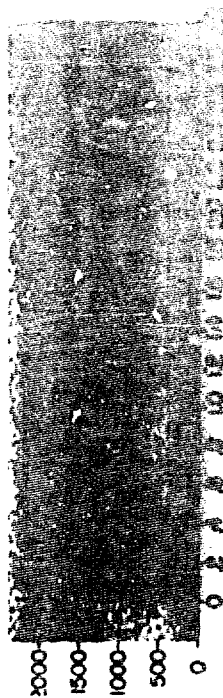


1000-1500 KHz



GERTIA, 8-6-60, 0300 CST, 138 Km. ALTITUDE

TIME, (sec.)



DO NOT WRITE IN GERTIA

Release	Upper Doppler Shift	Downward Doppler Shift	Spectral Broad ening	Doppler Steps
Margie		x		
Marie		x		
Lola		x	x	
Cathy		x	x	
Peggy		x		
Arlene	x	x	x	
Olive		x		
Betsy		x	x	x
Jeannie	x	x	x	x
Amy		x	x	x
Ruthy	x	x	x	x
Susan		x		x
Dolly	x	x	x	x
Gerta	x	x	x	x

Table 1. Category of observed phenomena on spectrograms

As Table I shows the spectrograph structure becomes much more complex as the shots increase in altitude. A possible reason lies in higher rates of expansion at higher altitudes giving rise to less dense clouds.

The growth curves (Fig. 4a,b,c) show the altitude effect on rest size. These curves are derived by graphically integrating the maximum Doppler shifts of the spectrograms. Growths were labelled in terms of down and up growth. (This is a misnomer for Rucker data - where growth curves are along the 30 degree elevation angle.) If the releases were truly spherical in shape then growths in both directions would be equal. But the spectrograms indicate that, at least for the electron-ion cloud, exactly spherical growth does not occur. The only apparent pattern set up by the growth curves is altitude dependence, shown in Fig. 5.

From sec. II, part B it is expected that the spectral distribution of Doppler shift energy, between the two extremes of shift frequency would be, for a particular time and assuming spherical shape, a square-well function. Amplitude response sections of the spectrogram for Gerta are given in Fig. 6, showing relative amplitude versus frequency. These indicate a predominant direction for gas transport at release, i.e., it is not a spherically uniform growth. A full analysis of this example is not yet completed; however, it appears from the San Blas record that little growth occurred in the horizontal direction (zero Doppler shift data). Amplitude sections of any spectrogram that appear to have information in them are being made but were not finished in time for publication of this report.

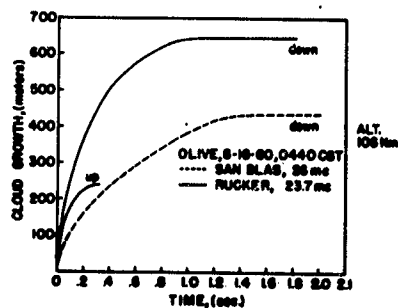
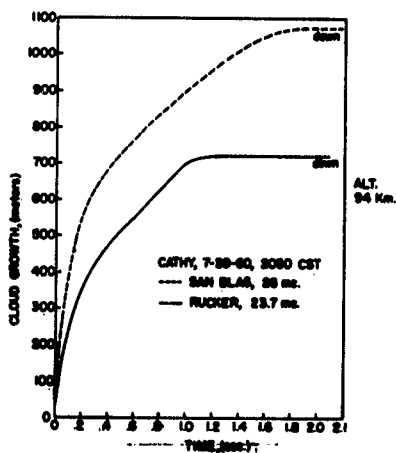
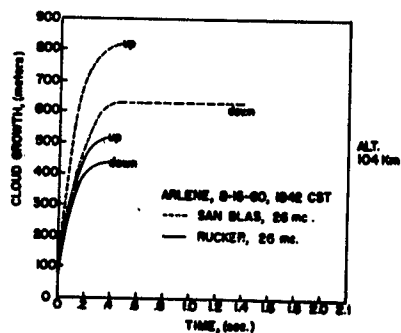
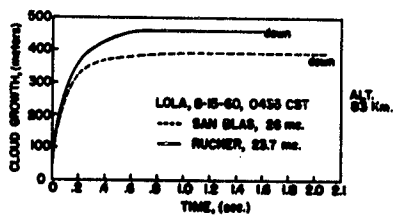
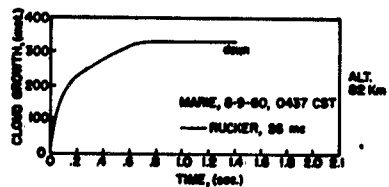
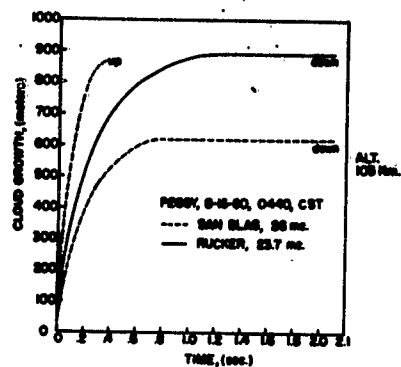
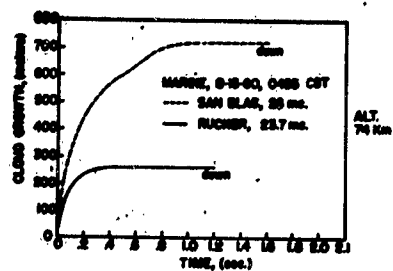


Fig. 4a Cloud Growth vs Time

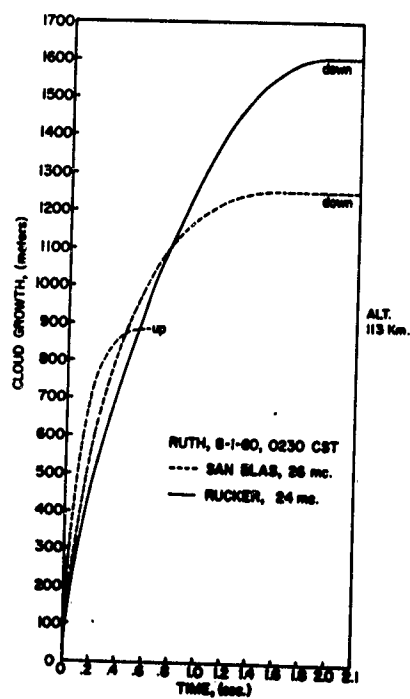
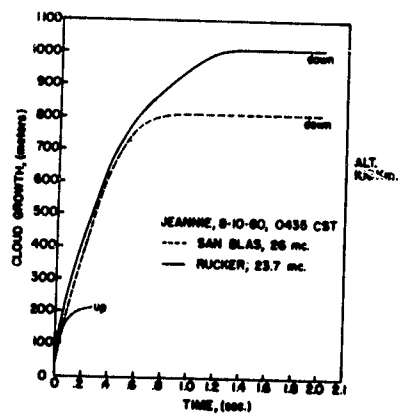
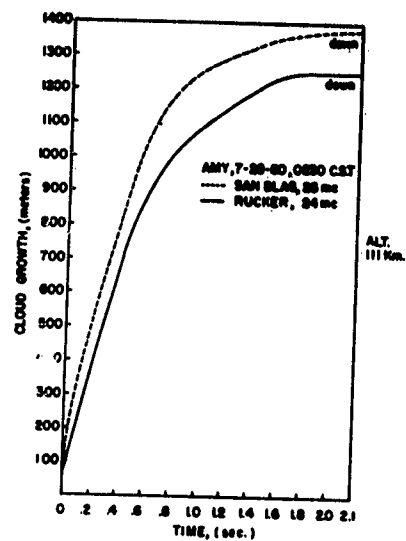
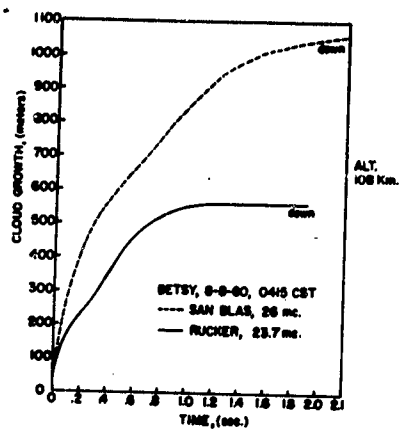


Fig. 4b Cloud Growth vs Time

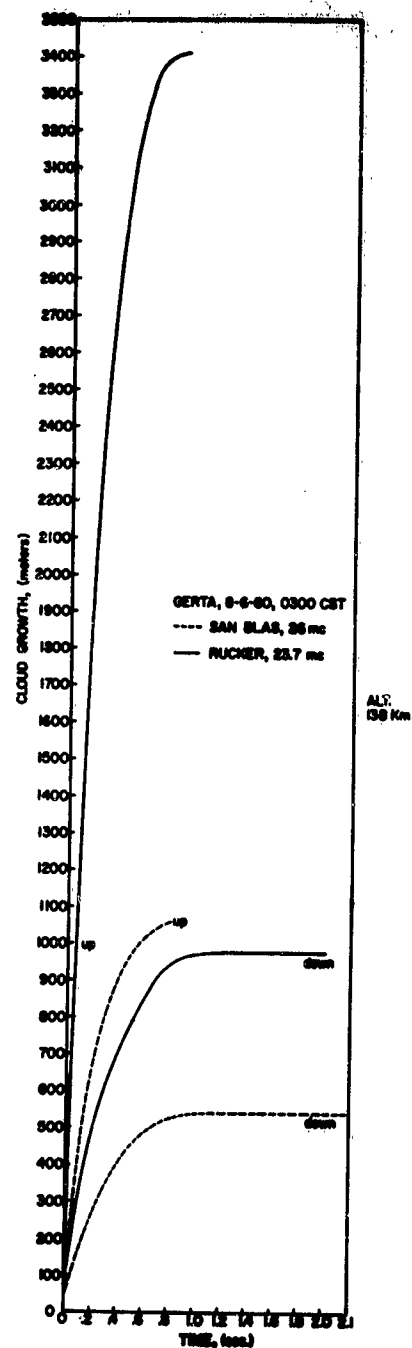
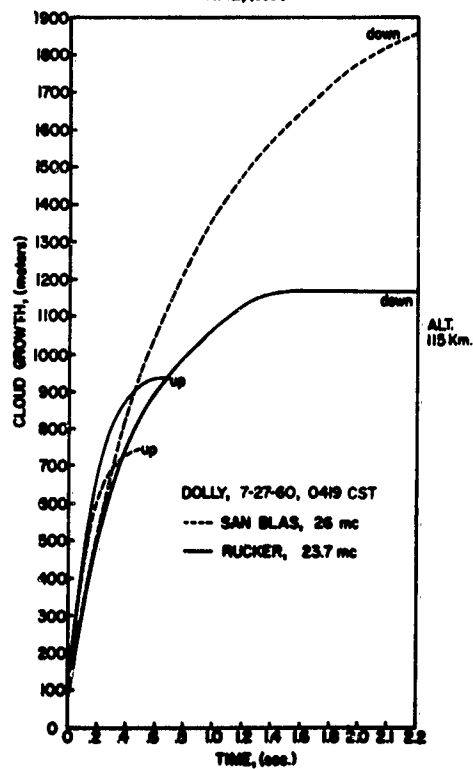
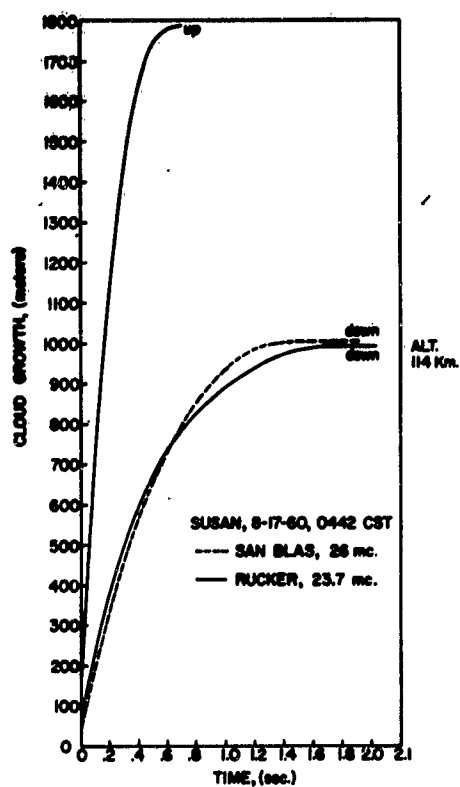


Fig. 4c Cloud Growth vs Time

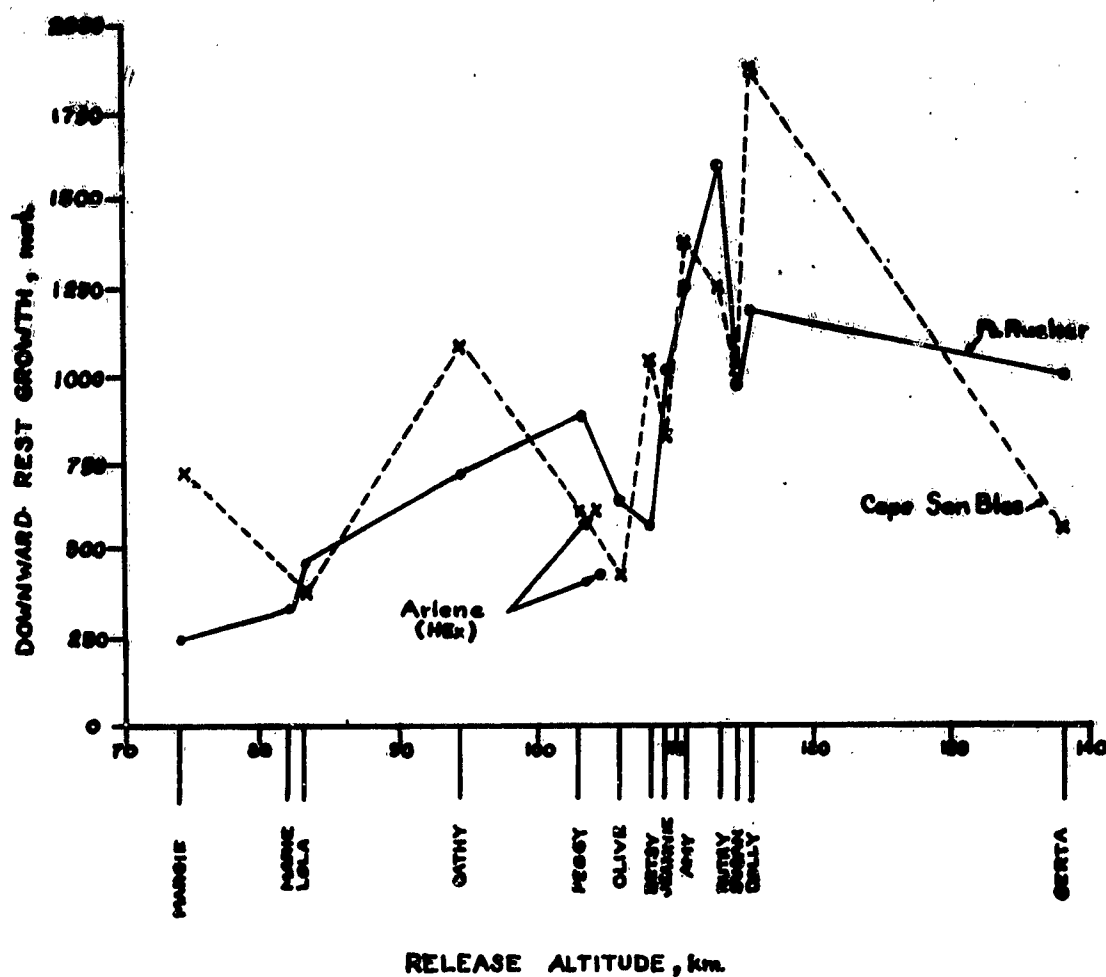
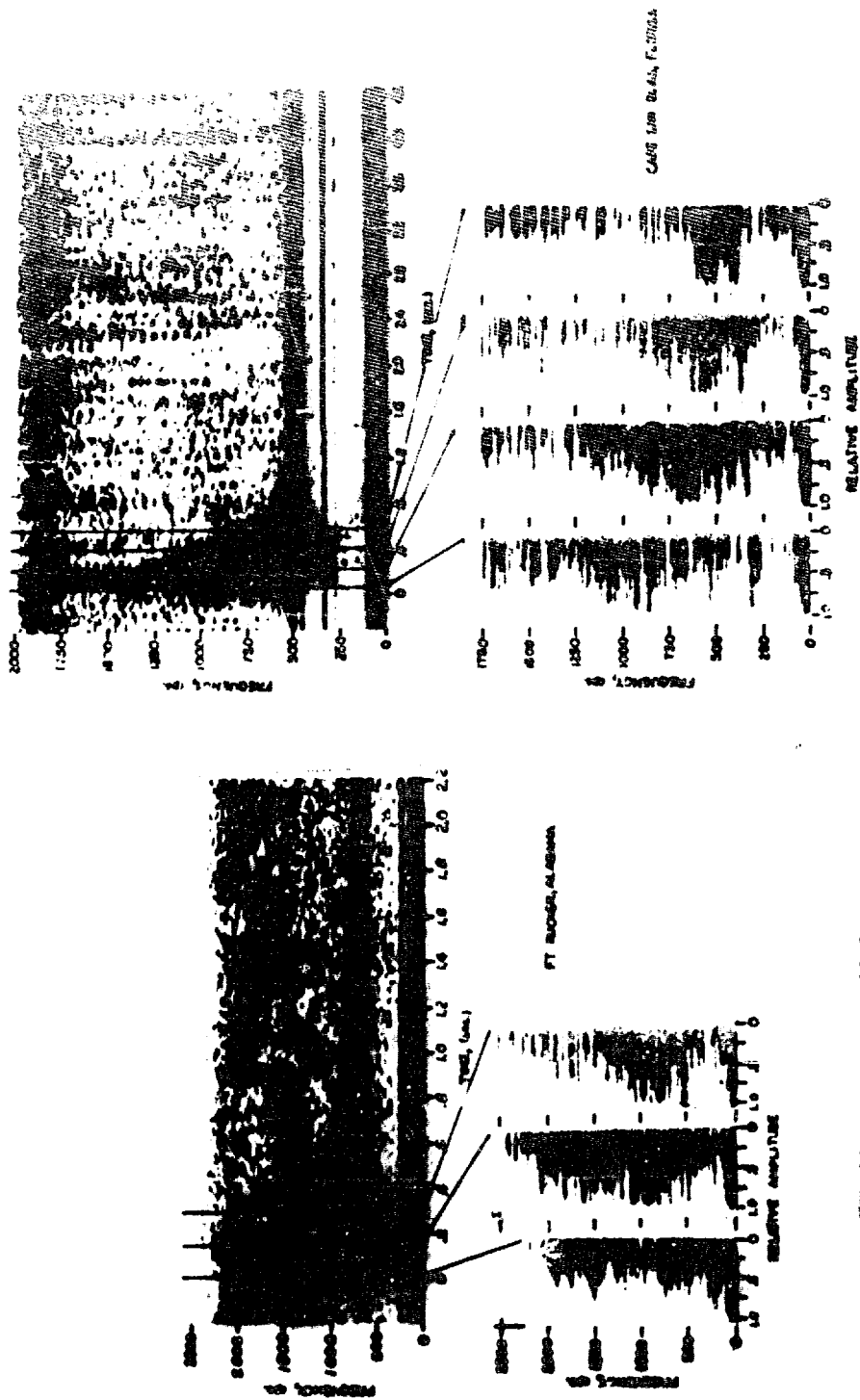


Fig. 5 Altitude Dependence For Downward Growth

V. SUMMARY

It is conjectured that

1. Shock wave ionization is detected in releases at altitudes of Betsy (108 km) and above, day or night.
2. Stepped growth is caused by multiple reflections of shock waves, and is observed only when shock waves are detected.
3. For most releases, especially above 106 km (Olive) the cloud is transparent or semi-transparent as evidenced by Doppler shifts in both directions.
4. Cloud growths are generally unsymmetrical with no preferred direction of growth.



SPECTRAL DISTRIBUTION OF ENERGY

Fig. 6 Spectral Amplitude Response For Gerta

EXPERIMENTAL AND THEORETICAL RESULTS ON ELECTRON CLOUD GROWTH 0 - 10 SECONDS AFTER RELEASE

John F. Paulson

Headquarters, Air Force Cambridge Research Laboratories,
Air Force Research Division (ARDC), Geophysics Research
Directorate, L.G. Hanscom Field, Bedford, Massachusetts

ABSTRACT

Two image orthicon television systems located at Site A-10 on Santa Rosa Island, 80 to 150 km from the release point, were used to obtain photographs of the chemical releases. Measurements taken from these photographs have given data on some of the early time low intensity visible phenomena accompanying point electron cloud releases. Cloud diameters so obtained have been compared with those obtained by other techniques, including conventional photography and Doppler shift, and with the results of the 1959 Firefly series. The results have also been compared with some theoretical predictions on the detonation of a spherical charge of TNT.

1. INTRODUCTION

The observations discussed in this report were made with two image orthicon television systems, located at Site A-10 on Santa Rosa Island and operated by personnel of Wright Air Development Division. The systems used either a General Electric Z5294 image orthicon tube, sensitive in the 3500 to 6000 Å spectral region, or a Z5395 tube, sensitive in the 6000 to 10,000 Å region. The viewing lens was a 150 mm f 0.75. The video signals were displayed on television monitors and photographed on 16 mm film at 24 frames per second and on 35 mm film at 20 frames per second. Appropriate spectral filters could be manually inserted in the optics system. A progressive neutral density scale and associated optics were used to produce images of progressive brightness levels on the monitors and the photographic record. Time was recorded on the film either as a clock image or by a timing signal.

2. RESULTS

Table I is a summary of the measured cloud diameters as a function of time. In several instances, diffuse radially growing waves appeared, in addition to the central chemical cloud; an example of this phenomenon is shown in Figure 1. Such waves grew rapidly e. g. 1 - 2 km/sec. radially, and usually disappeared within 10 secs. after the release. Their appearance suggests that they are analogous to those observed during the 1959 Firefly releases and designated "shock waves" in the Report on Project Firefly 1959. However, their growth rates are appreciably smaller and in fact agree more closely with the

TABLE I

Time-Seconds		0.1	0.3	0.5	0.7	1.0	3.0	5.0	7.0	10.0
Image										
Orthicon										
Tube Used										
Name		DIAMETER - KMS.								
Cathy										
Vis	No pictures obtained									
Betsy	IR	--	--	2.5 x 2.1	--	--	--	--	--	--
				0.7 x 0.7						
Amy	IR	1.6 x 1.4	2.2 x 1.0	2.5 x 1.9	2.5 x 1.9	0.8 x 0.6	--	--	--	--
						1.1 x 0.7	0.8 x 0.6	--	--	--
Ruthy	Vis	--	--	--	--	1.0 x 0.7	0.9 x 0.9	1.6 x 1.0	1.4 x 1.1	2.3 x 1.0
Gerta	Vis	--	--	--	--	1.7 x 1.4	2.0 x 1.7	2.3 x 2.2	2.8 x 2.6	--
Margie	IR	--	--	--	--	--	--	3.2 x 2.8	3.1 x 3.1	3.3 x 3.1
								0.9 x 0.7	0.8 x 0.7	0.9 x 0.9
Marie	IR	--	1.0 x 1.0	1.0 x 1.0	1.03 x 1.03	1.03 x 1.03	1.0 x 1.0	1.0 x 1.0	--	1.14 x 1.14
Lola	IR		1.6 x 1.7	2.3 x 2.4	3.0 x 3.2					
Zelda	IR	0.9 x 0.9	1.0 x 1.03	0.9 x 1.0	1.0 x 1.0	1.0 x 1.0	1.0 x 1.0	1.0 x 1.0	1.1 x 1.1	1.1 x 1.1
Peggy	IR	--	--	--	--	--	--	--	--	--
								3.6 x 6.0	3.6 x 6.0	3.5 x 5.6
	Vis	--	--	--	--	--	--	1.1 x 1.7	1.1 x 1.7	1.1 x 1.9
Olive	IR	1.36 x 1.36	2.2 x 2.0	2.95 x 2.95	4.0 x 4.0	4.8 x 4.8	8.3 x 8.3	8.9 x 8.9	9.8 x 9.8	2.8 x 6.1
						1.8 x 1.8	1.8 x 1.8	2.0 x 2.0	2.2 x 2.2	2.3 x 2.4
Jeanie	IR	2.7 x 1.4	2.8 x 2.7	--	5.4 x 5.0	7.1 x 6.3	12 x 12	12 x 12	12 x 12	12 x 12
		1.6 x 1.4	1.6 x 1.5	--	2.1 x 1.5	2.1 x 2.3	--	--	--	--
Susan	IR	--	--	--	--	1.5 x 1.3	1.9 x 1.3	2.1 x 1.5	2.0 x 1.3	2.1 x 1.3
						4	5 x 5	4.5	4.5	4.5
Dolly	IR	1.9 x 1.6	3.0 x 2.3	4.2 x 2.9	5.8 x 3.6	7.2 x 4.5	15 x 9	21 x 14	21 x 14	22
							3.3 x 1.8	3.3 x 2.2	3.5 x 2.2	3.3 x 2.2
Carry	Vis	1.3 x 1.0	2.8 x 2.8	3.4 x 3.4	--	--	--	--	--	--
Arlene	IR and Vis	No pictures obtained								
Mavis	Vis	No pictures obtained								
Frances	Vis	--	--	--	--	--	--	--	--	--
Lilly	Vis	--	--	--	--	--	--	4 x 8	--	6 x 16
Hedy	Vis	1.2 x 1.2	1.2 x 1.2	1.2 x 1.2	1.3 x 1.3	1.3 x 1.3	1.5 x 1.6	1.8 x 1.5	1.4 x 1.7	1.6 x 2.7



0.05



0.10



0.20



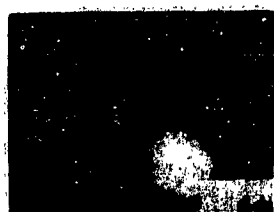
0.35



0.50



0.75



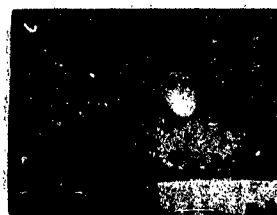
1



2



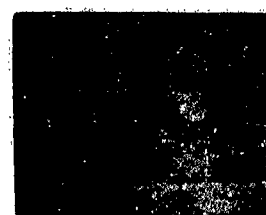
4



6



8



10

Fig. 1. Firefly Jeannie. Infrared Tube. Time in seconds.
Width of frame corresponds to 23 km.

growth rates of what were called the "particle waves" in the 1959 series. Of several explanations put forth to rationalize these observations, the most attractive is as follows. The TV equipment used in the 1959 series of releases was located at Biloxi, Mississippi, i. e., to the west of the burst, and therefore on what may be called a forward scatter path for dawn releases. During the 1960 series, the TV equipment was located at Site A-10, i. e., roughly north of the burst, and therefore on a side scatter path for either dawn or dusk releases. Examination of approximately simultaneous photographs taken using conventional techniques has shown that the radially growing waves are more persistent and produce denser images when photographed from sites on the forward scatter path compared with side scatter paths.

The observation of an anisotropic light intensity distribution suggests light scattering by small particles. A possible explanation of the greater wave velocities observed during the 1959 series of releases compared with the 1960 series is, then, that detection of particles at greater radial distances for a given time after release, i. e., corresponding to higher radial velocities (but lower particle number densities), would be favored at forward scatter sites. Another point of interest to this discussion is that the observations of radial waves in the 1959 series were made with the use of the relatively more sensitive Z5294 image orthicon tube, whereas the less sensitive Z5395 tube was used in observing most of the 1960 releases.

Particle waves were detected in two night releases, Amy and Betsy, with the aid of the TV cameras. Although scattered sunlight may have been responsible for their observation in Betsy, where the burst was about 15 km below the solar horizon, the only explanations for their observation in Amy are that they were lighted by the radiation from the burst or that the particles were hot enough to be self luminous for a fraction of a second. It is interesting that the observed wave lifetime and growth rate were considerably less than those observed in sunlit releases in the same altitude region. (See Figure 2)

Examination of several photographs taken with either TV or conventional methods has shown that the particle wave does not always dissipate at later times, i. e., beyond 20 secs., but, after losing most of its radial velocity, becomes the white "smokepuff" which appeared very clearly to the eye and on the K-24 photos as an entity distinct from the sodium-cesium gas cloud. This phenomenon was particularly evident in the low altitude releases, e. g., Margie, Marie, and Lola, but was also visible in Peggy.

Detonation of a high explosive package such as constitutes a point electron cloud (PEC) release produces roughly 400 moles of gases and 100 moles of solids. The rapidly expanding ball of gas will accelerate the solids by aerodynamic drag. Because of low ambient pressures and the large mass of the individual particles compared with that of the ambient air molecules, the solid particles will decelerate only slowly, as has been observed. Conventional explanations¹ of acceleration of solid particles in linear shock tubes state that the gas through which the shock has passed and which is moving at high velocity causes the initial acceleration of the solids. Subsequently the solids are overtaken by the contact surface and the expanding driver gas, which is moving at roughly the same velocity as the perturbed gas between the shock wave and the contact surface, and experience additional acceleration. In the experimental situation of interest in Project Firefly, the solids produced in the detonation reaction lie, at the instant of canister rupture, within the volume whose envelope is the shock wave. At times as short as those corresponding to rupture, the shock wave and contact surface are indistinguishable; at later times the radius of the shock always exceeds that of the contact surface. At the time of canister rupture, then, all solids, except those constituting the canister itself, lie inside the contact surface, and subsequent acceleration of the solids can be due only to motion of the gases produced in the detonation. The solids will of course retain their velocities to larger radial distances than will the gases.

Data obtained by Stanford University personnel using a Doppler shift technique have given size vs time measurements for times less than 2 secs. after release. Figure 3 shows a plot combining Doppler data, calculated shock wave and contact surface data (see below), and TV data for Firefly Jeannie. It appears, on the basis of this and similar graphs for other releases, that the Doppler shift technique gives a measure of cloud size comparable with that obtained by the TV camera at early times.

Brode² has carried out calculations on the blast wave from a spherical charge of TNT, without reliance on empirical values derived from explosion measurements. The only data pertinent to the actual chemical release which are necessary for calculating shock wave and contact surface radii from Brode's results are the energy of the release detonation,

1. See for example AVCO Technical Memorandum RAD-2-TM-57-7
2. H. L. Brode, Physics of Fluids 2 217 (1959)

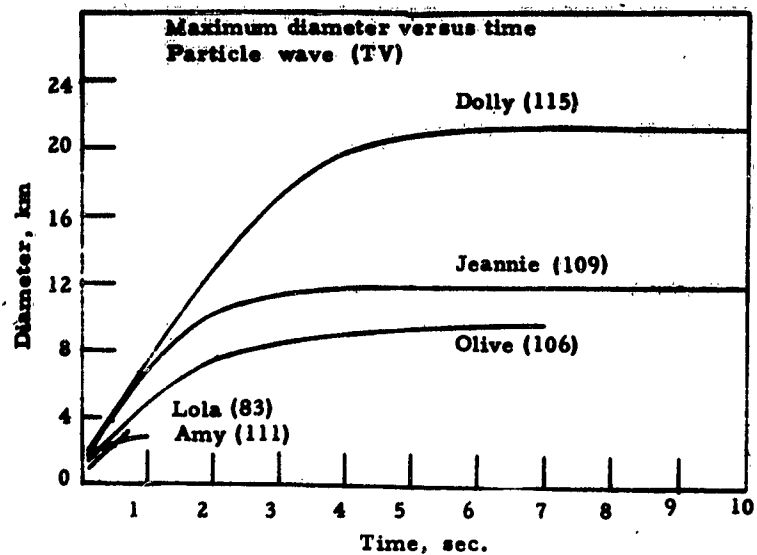


Fig. 2 Observed diameters of particle waves. Altitudes
Altitudes (km) in parentheses

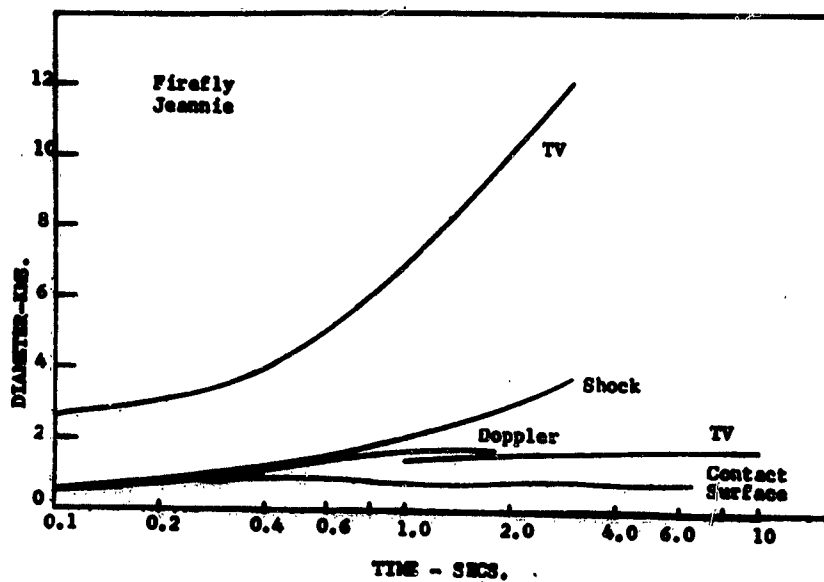


Fig. 3. Comparison of Theoretical and Observed Data
for Firefly Jeannie

ambient pressure and sonic velocity at the altitude considered, and time after release.

The curves shown in Figure 4, taken directly from Brode's paper, permit calculation of shock wave and contact surface radii. The following definitions apply:

$$\tau = \frac{t C_0}{\alpha}$$

$$\alpha^3 = \frac{\omega}{P_0}$$

$$R = \lambda \alpha$$

where t = time after the explosion, C_0 = sonic velocity in the ambient, ω = energy of the explosion, P_0 = ambient pressure, and R = radius. Figure 5 shows the results calculated from Brode's curves and those obtained from Doppler shift data. The energy used was that of the high explosive component i. e., RDX. The times used were those at which the Doppler shift data indicated no further increase in size. Except for Firefly Arlene, a high explosive release, these times were between about 0.5 and 1.6 secs. In order to have a clearly defined value for the time, a particular set of Doppler results was chosen; this set was the downward growth rates measured by the instrument at Rucker and was chosen simply because it was the most complete set and appeared to be the most reliable.

Although the experimental values are not duplicated by those calculated, the similarity in the curves is clear. However, agreement can hardly be expected, since the r. f. Doppler carrier signal is reflected, not from the shock wave, which at the radii of interest cannot thermally ionize the molecules of the ambient, but from regions of high electron density most probably produced in the detonation reactions. The fact that the radii obtained by Doppler shift measurements lie, on the average, within 25 percent of the calculated shock wave radii is then difficult to explain. Photoionization of the ambient by black body radiation from the detonation has been suggested. A more attractive hypothesis is implied by Brode's results, in which the temperature is seen to increase along the radial distance from the shock to the contact surface. Unfortunately, these temperature calculations have not been carried out to times and radii great enough for direct application to the present data. However, extrapolation of the curves to such times and radii suggests that temperatures in this region may still be several times those in the ambient. A third suggestion is that electrons produced in the detonation may diffuse to the radii of interest. Preliminary calculations on such phenomena are not favorable to this hypothesis. It is

Fig. 4.
Theoretical results
on detonation of TNT
calculated by Brode.

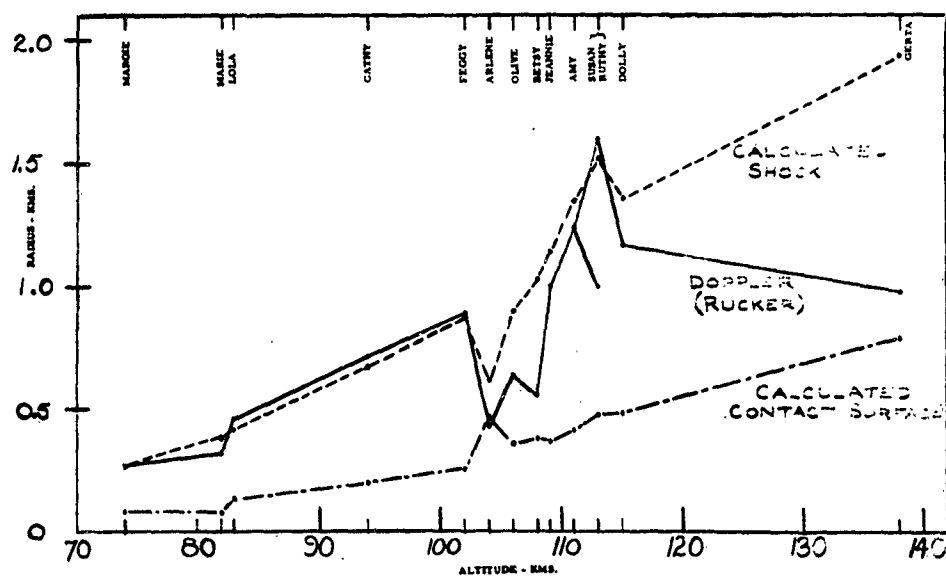
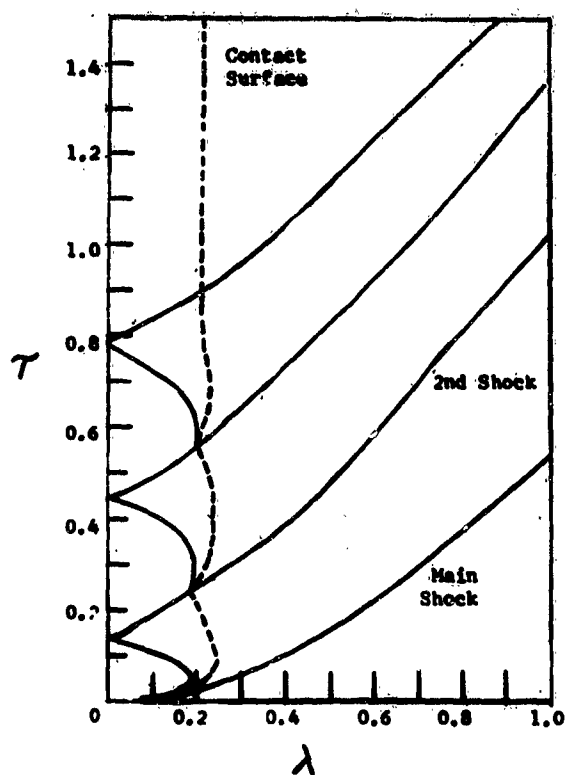


FIG. 5. COMPARISON OF OBSERVED AND CALCULATED RADAR. (NO DOPPLER SIGNAL WAS OBTAINED FOR ZELDA OR CARRY.)

important to recall that studies³ of the detonation of various PEC package compositions have shown that, although peak temperatures from a pure high explosive are greater than from those packages containing admixed alkali nitrate, the time at which the peak occurs increases with increasing percentage of alkali nitrate. The almost exact agreement between the measured radius and that calculated for the contact surface for Firefly Arlene is particularly interesting, since only for such a true high explosive release, in which the energy of the release detonation is known, can Brode's results be expected to apply with accuracy.

3. CONCLUSIONS

The results of this paper suggest that point electron cloud diameters, at times less than 2 secs. after release, can be predicted to within a factor of about 2 by the use of theoretical results. A mechanism for the acceleration of minute solid particles to high velocities has been proposed, and it is suggested that these particles are responsible for the rapidly growing radial waves observed in several PEC releases. Analysis of the deceleration rates of these particles may provide data on particle size, although preliminary calculations have shown that the decreasing particle number density must be taken into account. The question of visible shock waves in PEC and high explosive releases has been thoroughly discussed by Edwards⁴ in reporting on studies made by Young and McDowell at Georgia Tech. Although one or more shock waves are certainly produced, these studies have shown that they would not be observable with the equipment used. The observation of different radial growth rates, lifetimes, and densities from different sites, then, has led to the conclusion that the waves are composed of minute solid particles. The mechanism of production of such particles remains uncertain, although the production of aluminum oxide in the detonation is a possible explanation.

Because of the relatively small dynamic range of the TV equipment, total light output from a cloud is probably best calculated from films made with conventional photographic techniques rather than with the TV equipment. The small dynamic range of the TV equipment leads to another problem: the insertion of spectral filters in the optical path produced an effect like that of a neutral density filter, since the equipment operators had

3. W. E. Gordon, Project Firefly 1959, Semi-annual Report, July-December 1959, Geophysics Research Directorate, AFCRC (February 1960); Part II

4. H. D. Edwards, Project Firefly, Semi-annual Report, January-June 1960, Geophysics Research Directorate, AFCRL; Part I

insufficient time to adjust gain and contrast controls during the few seconds that the filters were in place.

It is suggested that, in the event of future upper atmosphere chemical release experiments, there be at least two sites used for the TV equipment and that one of these sites lie on the forward scatter path. Unless burst can be predicted with great accuracy, it would be desirable either to use a wide angle lens or to locate the equipment at a distance from the burst greater than that in the 1960 series of releases so that the events of the first few seconds following release will be recorded. If sufficient TV units are available, the use of one as a grating spectrograph would also be desirable.

PANEL ON MASS TRANSPORT (0 - 10 seconds)

PANEL:	K. W. Champion	AFGRL
	H. D. Edwards	Ga. Tech.
	R. H. Pennington	DASA
	B. Kivel	AVCO
	R. B. Holt	Device
	J. F. Paulson	AFGRL
	R. Barnes	Stanford
	N. W. Rosenberg	AFGRL
	P. Molmud	STL

Champion: If I could start with what might be said to be a provocative question, I would like to ask Dr. Holt if he could answer this one. His photographs of the various cloud bursts show some with a large diameter on the first frame which then appear to shrink with time. I would like to ask him whether he believes that the actual cloud does this or whether the initial size may be due to halation of the film.

Holt: We tried, of course, to determine whether the initial frame was halated or not. All of the film was provided with anti-halation backing, and it is a little doubtful (since the densities we obtained were not tremendously great) that there was halation on the film. However, it is conceivable that there might have been sufficient brightness at the very center of the burst to produce sort of a halo in the atmosphere, similar to the halo one sometime sees around the moon. This could have meant that as soon as the initial very, very bright burst was over, there would be insufficient intensity to continue producing this. We made some very high speed photomultiplier measurements that showed that the initial very intense flash was in general less than 50 milliseconds long, so that this would substantiate this thought.

Champion: Yes, I certainly agree with that. I think the initial flash is very brief in duration and extremely intense. Anyone else here want to have a comment on that? Dr. Edwards.

Edwards: We agree on the halation problem. I think in one case, I believe it is Lola, we did have a tremendous size at the beginning on the first frame and I think that may be due to halation. We did not

have the halation backing on our film, but we seemed to get the same kind of material, the ring, the particle waves that Dr. Holt showed on his pictures.

Kivel: One could introduce a wedge or step-down wedge so you get two images on some of these cameras so that you get one overexposed, the one that wouldn't overexpose would then be of better magnitude for the film.

Rosenberg: By the second or third frame isn't it the case, Dr. Holt, that you were at a density which could not cause halation, therefore if you dropped the first frame from your size consideration, you still have some rather high velocities to handle?

Holt: This is precisely right. On Susan, the slides that I showed this morning, although they do show an enormous first frame, show a second, third, fourth frame growth which is tremendously fast.

Rosenberg: And, not a halation because of the low density?

Holt: It can't be halation because this film is a long way from being saturated.

Rosenberg: The detonation velocity as given by Dr. Fisher this morning of 7 kilometers per second is in rather good agreement with the initial Doppler data of Mr. Barnes. Will you comment on that?

Barnes: The velocities that we got at a tenth of a second were typically $6\frac{1}{2}$, 6, and 9 kilometers/second. I believe the highest was 13 kilometers/second. There were a couple at about $3\frac{1}{2}$ kilometers/second also.

Rosenberg: Agreement with photographic data was then certainly within a factor of 2 and in several cases closer than that. It would appear that the initial growth of the material is continuing with the detonation velocity in the solid, which is perhaps not unexpected.

Champion: Could I ask Dr. Barnes a question? On most of these results the upward growth seemed to be more rapid than the downward growth, which is consistent with most of the optical data; however, on some of the shots including Ruthie and Dolly the cloud seems to grow more rapidly downward than upward. Was this because of the

angle that you were looking at it or was there some other reason?

Barnes: I don't know which site you are speaking of in particular, but it is possible that on measuring maximum velocity we are looking at a portion of the cloud of greater density than the photographic edge and we are reading a velocity component other than the maximum upward velocity; however, I would tend to say that because of the sharpness of the edges, we are probably reading close to the maximum upper growth velocity.

Kivel: I would like to make a comment on the comparison between shock waves and particle waves. The question that was asked last year was whether some of these waves were shock waves or were particle waves. There is a major difference between the two types of waves. The shock waves as they expand increase in area as the radius of the sphere squared, as a result of which is engulfed more and more air as the wave goes out. While air is tenuous at these high altitudes many tons of air are engulfed as the shock wave expands. At 1 kilometer radius at 120 kilometers of altitude you have engulfed about 40 kilograms of air, comparable to the weight of the high explosives. But at 2 kilometers, the amount is 320 kilograms, at 4 kilometers it is 2 tons, and at 8 kilometers it is 16 tons. It is very difficult for a shock to continue to go out and engulf this increasing amount of air from such a small explosion. On the other hand, the particles which go out have a constant area. A large number of little particles expands to make a large radius when you look at them, but their area remains the same. I made an estimate that 10 kilograms of material can produce about 10^{16} one micron size particles. The area of these particles is about 10^8 square centimeters, which is the same as the surface area of a 30 meter sphere. This is just another way of pointing out that the particles can go very large distances without slowing down, while the shock wave is slowed down very strongly after it is attenuated as it expands to large size.

Champion: I certainly would like to agree with Dr. Kivel. We have also been worrying about the problem of whether these waves that seem to go out very rapidly are solids or a shock wave, and my conclusion is that they are probably solids. More specifically, I have been looking at Brode's theory for the shock waves produced by explosions (such as Dr. Paulson discussed) and this theory has been calculated for one atmosphere pressure and other conditions on the ground. Brode states that his theory can be scaled to other conditions when the mass of air engulfed is ten times the mass of the explosive. This condition isn't quite satisfied in our clouds. Certainly in the first few seconds it is not satisfied, and this means that to get a suitable theory for the shock wave and the contact surfaces, Brode's theory needs to be recalculated putting in the appropriate initial conditions for the high altitude bursts. We hope to at least start on this problem in the next few months.

Kivel: I would like to find out the source of the radiation from these particle waves.

Rosenberg: Most of the releases in which the particle waves were observed were sunlit, although the observers were in the dark. However, a calculation can be made to determine the black body radiation from these particles assuming that they were at some high initial temperature. It turns out that a 10 micron particle will have dropped 300° Kelvin in approximately 1 second so certainly any luminosity seen at even 3/10 of a second is very hard to ascribe to black body radiation of hot particles. There is one shot in particular which we haven't completely evaluated yet, which is most difficult to explain. This is Dolly, where a very intense infrared emission of this solids wave (the wave that goes out to very far distances) is observed, yet low intensity is found in the visible. I believe Dr. Edwards will show us some photos of these later. This shot violates the picture that the sunlight must be the major mechanism for producing radiation, because sunlight won't give intense infrared and low intensity visible.

Kivel: I wonder if this isn't an opportunity to study upper atmosphere processes by enhancing the afterglow (the night glow or day glow) by working in conditions where there isn't any reflected sunlight and seeing if you get radiation from the particles enhancing radiation by catalysis. I am sure you are familiar with the work by Harteck & Reeves on placing elements in the afterglow which enhanced the radiation.

Champion: Well, this was actually tried, of course. Before the cobalt release we made a calculation of the amount of glow we expected. The calculation showed that it would probably be just below the sensitivity at which we could detect it. It was released and not detected.

Paulson: Yes, the answer to Dr. Kivel's question is one of the things that I tried to point out on one of my slides. We plotted size versus time for several shots. They were all damn shots except Amy, and the size versus time curve for Amy was of much shorter duration and showed much smaller slope than the others. I think that this means that the solid particles are lighted either by light from the burst or else they are hot so that at very short times they do radiate. Certainly at longer times what we are seeing is scattered sunlight. We believe this partly because we see different growth rates and different particle lifetimes from different sites. These sites give forward scatter paths or side scatter paths for sunlight, which can account for the difference.

Champion: Returning to Dr. Kivel's comment about enhancing the air glow, there has been another phenomena observed which hasn't been mentioned so far today. Following certain high explosive releases, about 110 to 160 kilometers in altitude, a persistent trail of whitish clouds have been observed, both by the French in the Sahara and the British in Australia. It has been suggested that this may involve an interaction between NO and atomic oxygen.

Paulson: Dr. Edward's Eymon pictures were taken from different sites. On the high explosive release pictures of the burst taken from site F (which was roughly at right angles to the line between the sun

and the burst) images were obtained for about 2 or 3 seconds. From site J (which was on the straight line path between the sun and the burst) apparent duration was about 15 seconds. Whether or not solids are doing the scattering I don't know, but apparent intensity varies strongly with the angle.

Rosenberg: Preoccupation with these high velocity solids is pertinent in certain other areas. In the missile trails we have observed, we have similarly distinguished between a gas and a solid. The solids motions are again at several kilometers/second and extend for extreme distances into the ambient, whereas the gases (similarly to the gases in the chemical release experiments) level out at approximately ambient pressure, depending upon the temperature of cooling. Dr. Holt, do any of your photographs indicate that we have to explain velocities of light-emitting species greater than 8 to 10 kilometers/second, which is our initiating velocity?

Holt: The great majority of velocities you do need to explain lie in this 8 to 10 kilometer/second range. There are a few cases where the size of the initial flash (which may be due to halation on the film, although we don't think so, or halation in the atmosphere, or something else) would mean that we had to assume larger velocities. For example, if you simply take the pictures to mean what they show rather than trying to find out what could be wrong, you get a velocity in excess of 100 kilometers/second, on at least two of the shots.

Molmud: I was asked by Ed Manring to explain an observed velocity of 5 times 10^5 centimeters per second. I said perhaps hydrogen could come out at this velocity, because this would correspond roughly to the thermal velocity of hydrogen at 5000° Kelvin. Has any thought been given to this possibility?

Champion: That is a question for chemists, who wants to volunteer? It might be hydrogen if it is produced in the explosion.

Molmud: I have another point to this. In the solid propellant now used on Polaris and Minute Man, which contains aluminum, one function of the

aluminum is to increase the available energy, another is to reduce the molecular weight of combustion products by reducing the various compounds present to produce a large amount of hydrogen. This tends to increase the specific impulse. You use an aluminumized explosive, don't you? In all probability you get a large amount of hydrogen released during the explosion. What happens to this hydrogen?

Rosenberg: None of the gaseous components seem to separate significantly from each other during the initial expansion. In other words, you have high pressure gas of mixed components: sodium, cesium, and others. In most cases we have very little separation of the sodium with weight 20 from the cesium with weight 130. Therefore, it would be difficult to picture how the hydrogen, despite its higher speed, could unmix from these others. Furthermore, the distances to which we would have to carry it to explain these initial velocities are far greater than those at which the gas cloud should come to ambient pressure. In other words, it isn't a problem of explaining expansion of 1 kilometer in a tenth of a second, but 10 kilometers in one second. The final gaseous products should never achieve more than a kilometer or so diameter in this initial expansion, so you would have to find a mechanism for separating the hydrogen from the other gaseous products.

Pennington: I wanted to ask Dr. Holt whether on Frances and on Hedy the orientation of these crescents are known?

Holt: Yes, we do know it. I don't recall offhand exactly what the orientation is but we can easily look it up for you.

Pennington: Is it correlated with anything specifically that you know of?

Champion: I think the orientation of those was correlated in the direction the rocket was pointing at the time that the canister was blown apart. I think we should discuss the solar scatter experiments further.

Rosenberg: The first release appeared to show growth along the vehicle trajectory and this made everybody happy since it appeared very

similar to missile trail phenomena. The second showed growth at right angles to the rocket trajectory. Both releases were at the same time of day so I don't think we can explain this by the direction of the sun, but it is quite probable that the vehicle is tumbling as it is moving along its trajectory, and the method of opening the canister at one end may be such as to create a crescent. The direction the crescent takes may be simply due to the random motion of the vehicle. We have several cases in which the electron cloud also appeared to have different orientations. In other words, the spin imparted to the vehicle was insufficient to keep it from tumbling during this vacuum phase of the trajectory.

Champion: We think we understand how these solids are released--it is a little bit like squeezing a tube of toothpaste or a water sprayer.

Dubin:
(NASA) Dr. Barnes made a statement that the ionization shown in his very nice measurements of velocity by Doppler methods was due to a shock wave, and in the discussion here we have heard a great deal about particles, but nothing about shock produced ionization. I would like to get an explanation of the movement of the ionization peak out from the center and the mechanism for the ionization. I will leave it open for the panel.

Champion: I believe that the shock wave is not producing any ionization, at least after very early times. There is just not enough energy in it. However, it may possibly be able to assist in transportation of some of the ionization which was produced at early times by thermal or chemi-ionization. I don't know if anyone wants to volunteer a different opinion.

Zimmerman:
(AFGRL) Dr. Paulson made the statement that in some region in the spherical shock phenomena, following the theory of Brode, there is a region having fairly high temperature some distance behind the shock. If this condition is maintained in a completely spherical phenomena with the contact center way behind the shock, then the ideas that the electrons will be migrating with the shock (where the temperature is fairly low) and that there will be a large

contact surface (where the temperature is fairly high) conflict. However, if you have a turbulent phenomena produced by the explosion, where the electrons can migrate behind the shock in this high temperature region by a turbulent mechanism, you can explain to some extent why the electrons are fairly close to the shock surface as Dr. Paulson has shown.

Wright: (NBS) I was wondering if there was any chance that any of the ionization observed in bursts like these can be photodetachment of electrons from negative ions in the ambient.

Champion: My feeling is that in the E region there are very few negative ions at this time of day but it is worth looking into.

Kivel: Could the size obtained from Doppler measurements be off by a factor of three? Then the correlation of increase in size with increasing altitude would fit---in other words electrons would stay behind the contact surface, as Dr. Paulson pointed out. The shock wave you mentioned is much too weak to make ionization, but the contact surface grows in the same way that the shock grows, and gets bigger with higher altitude.

Champion: I think it is more likely that there may be an error in the size assumed for the contact surface. In other words, if we recalculated Brode's theory for these conditions the contact surface might be quite a bit bigger.

Zimmerman: I think Dr. Paulson mentioned that Taylor presented the argument of a contact surface lying behind the shock and some distance behind it, but he made the statement that the idea of a spherical contact surface sitting behind the shock is purely conjecture. I might mention that the Ottawa people, who had exploded highly pressurized spheres in a container, have observed a marked degree of turbulence and no distinct spherical contact surface lying behind the shock.

Champion: This is true. There are laboratory photographs showing this.

Gallagher: (Stanford U) We did detect a shock phenomena in one of the evening twilight releases, since we did detect ionization from a pure high

explosive release; therefore, there must be at least enough energy perhaps for detachment at this time of day to account for that ionization that was observed. Another thing that we think we see on our records are the steps in growth. In most cases these appear to be correlated with cases where we see sort of a sharp tongue at the beginning of the growth period which presumably is, at least initially, a shock effect. Does anyone have any opinion as to whether these steps may not be due to shock waves which rebound at the boundaries of the growing cloud? Is there any evidence such as that presented a year or two ago on strip film showing initial growth followed by shrinkage of the cloud and then growth again?

Holt: We have some strip film that frankly hasn't been analyzed yet. We have gone through about 7 of our 8 miles of movie film, but the other mile still contains the strip film.

Dubin: The initial question I asked is still not really answered. Is the total ionization after the initial burst increasing or staying constant? Is there a mechanism for continued ionization from the shock or from some other cause?

Molmud: As far as continuous creation of electrons is concerned the cesium, or whatever is being ionized, will continue to produce electrons while the mechanisms which produce electrons (such as detachment) continue to operate. There are other mechanisms which haven't been discussed here, such as chemical reaction between cesium and whatever material is in the ambient atmosphere. Cesium can burn in oxygen and produce ionization. I would like to make a comment on the photo detachment of negative ions. Suppose initially you had a lot of photo detachment over a large region, and then you had recombination leading to production of a photon you would get an apparent large blob which will then shrink down very quickly.

Pennington: I would like to ask Dr. Holt about some of the pictures in the very early stages. It appeared that the regions were not truly spherical. One possible explanation I suppose is that they are

Taylor unstable. Are there other explanations for this?

Neil: That seems to be as good as any. Although I didn't show slides of Peggy, it was the most unsymmetrical of the bursts. It is interesting that Peggy has some other unique properties too. From the first few milliseconds on it had a sort of an oblong shape that was rather unusual.

Molund: I have a comment on the asymmetry of the crescent-like clouds. The axis might be lined up with the earth's magnetic field but I didn't know whether this was true or not. The radius of curvature of a singly ionized cesium atom is about 1 kilometer, so you might get asymmetry because of the magnetic field, as long as the collision frequency between the cesium and whatever particles are there is less than the cyclotron frequency.

POSITION, DRIFT AND GROWTH FROM PHOTOGRAPHY

Howard D. Edwards

Engineering Experiment Station
Georgia Institute of Technology
Atlanta, Georgia

ABSTRACT

A description is given of the photographic equipment used in the 1960 Firefly series and the location of the optics sites.

By means of triangulation techniques and electronic computers, height, shape and movement of the clouds have been calculated.

Cameras used for special assignments such as color recording, stereo, quick look altitude calculations, etc. are described and the results of the observations given.

A simple photometer was used to record burst time. The results of these observations are also given.

PURPOSE OF OPTICAL COVERAGE

The general purpose of optical coverage is to provide permanent records of the Firefly clouds which can then be analyzed in the laboratory. Due to the high resolution of the photographic images it is possible to record the altitude, shape, size, and movement of the clouds. By means of narrow band filters in front of the cameras, it is possible to isolate the various atomic species in the cloud and to independently study the interaction of each species with the ambient.

The optical observations are of assistance in the RF scatter analyses of cesium clouds since they provide height, position, and drift information as well as a picture of the "scattering antenna."

DESCRIPTION OF EQUIPMENT

The equipment provided for the 1960 series can in general be grouped into three categories:

- (1) Time exposure cameras were used to obtain photographs with exposure times from 1 sec to 22 seconds and for as long a period of time as the cloud was visible.
- (2) Movie cameras operating at 4 frames per second were used to record the cloud during the first few seconds of its life or in some cases out to 60 seconds.

(3) Other cameras were used either to record anomalous events or to operate in a special manner and were subject to change on a day-to-day basis.

A. Camera Mounts

Two types of camera mounts were used in obtaining the photographs.

The first, shown in Figure 1, is relatively simple and is capable of rapid assembly and disassembly and can be transported from site to site in a station wagon. The knock-down type base makes it possible to set up at remote sites with a minimum of preparation. The mount can be adjusted rapidly in azimuth and elevation and to an accuracy of 0.5 degrees and with care to 0.1 degree. The structure is capable of handling from 50-75 pounds of camera equipment. The arrangement in Figure 1 shows two K-24 time exposure cameras, one Eyemo movie camera, and an infrared sniperscope mounted on the equipment rack.

The second type used to mount cameras is shown in Figure 2 and was made from a 60-inch searchlight stand. The mount is capable of handling up to 1500 pounds of equipment with an accuracy of 0.1 degree or better in pointing. Due to the close tolerances and rugged construction of the searchlight unit, the reproducibility of azimuth and elevation settings from day to day is excellent.

As noted in Figure 2 the searchlight yoke assembly has been enclosed with an insulated metal cover and the unit air-conditioned to control temperature and humidity. This protection is necessary to insure equipment operation in the adverse weather conditions found on the beach. Another important feature which the enclosure provides is the ability to prepare for a firing on short notice. Equipment could be installed several days prior to a firing and then made ready within 30 minutes or less of the firing. Should rain showers occur shortly before firing, the equipment could be secured and then placed in operation in a few minutes.

The protective covers proved invaluable during the past summer's operation when a large number of rockets was fired on a close schedule.

The searchlight unit, while not portable in a station wagon, can be transported on a trailer or moving van to the vicinity of the observing site and then towed by hand, auto, or jeep to the final location.

B. Time Exposure Cameras

The standard K-24 aerial camera which has been modified for our needs is used to take time exposure photographs of the clouds.

This camera, which takes a 5" x 5" picture, is the largest type for which high speed lenses and a rapid cycling time are available.

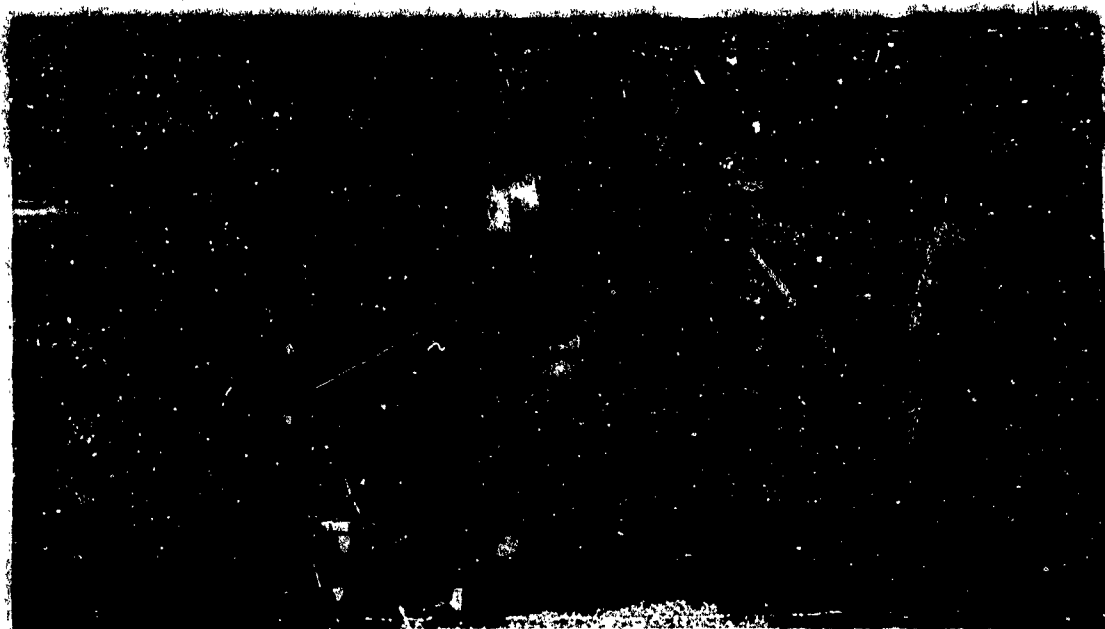


Figure 1



Figure 2

The K-24 is normally equipped with a 7" f/2.5 lens but other units of longer focal length are available as standard items. Due to the large diameter of the lens, star images which are used in position determinations are relatively easy to obtain. The camera utilizes a focal plane shutter which is operated by a pulse of 24 volts D.C. and is capable of exposure times as short as 1/900 sec and a frame rate of 3 per second. Filters can easily be installed in front of the lenses for spectral studies of the clouds. A data chamber is installed on the K-24 so that information relative to the firing can be permanently recorded on each film frame. The data chamber contains information on time, firefly shot, station number, filter type, date, camera number, and film type. These data are invaluable in analyzing the thousands of photographs which are taken.

The K-24 system is especially suited for field work due to ease of maintenance and availability of spare parts. For example, the complete working mechanism can be removed and a new unit installed by releasing one thumb screw.

The focal plane glass of the camera is precision ruled with a 1/2" grid which serves as the fiducial system for locating the center of the frame as well as subsequent cloud positions. Three small lights located behind the lens are pulsed by the timer and give sufficient light to record these grid lines on the film. The presence of the precision grid on the film permits correction for distortion due to film shrinkage and other effects. The small lights also effectively pre-sensitize the film with the result that the film speed is approximately doubled.

C. Movie Cameras

The Eyemo 35 mm movie camera was the other workhorse used on the Firefly operation and at least one was located at each optics site. The camera is described in another article in this report entitled "Growth from Photography (0-10 seconds)" by H. D. Edwards.

D. Special Cameras

(1) A Beattie-Coleman 35 mm camera was operated with 80270 color film at site F-2. The camera lens had a focal length of 50 mm and a speed of f/2.8. An exposure time of approximately 3 seconds was used.

(2) A Bolex 16 mm movie camera with color film and a lens focal length of 50 mm and speed of f/0.9 was in operation at site F-1.

(3) A bank of 5 each 16 mm pulse cameras was mounted at site F-1 and operated at 1 pulse/sec. Camera lenses varied from a focal length of 50 mm at speed of f/1.5 to 17 mm at f/2.5. The majority had a 17 mm focal length at a speed of f/2.5. For the solar scatter shots,

the five cameras were equipped with polaroid filters at successive $22\frac{1}{2}^\circ$ angles between the vertical and horizontal. For other shots the cameras had Wratten filters such as 58, 47, 35, 25, etc. mounted in front of the lens and were used to isolate selected regions of the visible spectrum.

(4) Polaroid land cameras and speed graphic type cameras with polaroid adapter backs were used at sites F-1, J and H to obtain a quick photograph of the cloud burst. Success at two or more of these sites enabled us to calculate burst height within 30 minutes to 1 hour after the rocket flight.

(5) A K-24 camera with 7" f/2.5 optics was operated at the Blue Horizon Motel to give possible stereo comparisons with other K-24 pictures from site F. Although the camera was operated manually, communications were good between the Blue Horizon and site F and photographs were taken simultaneously from the two sites.

(6) An Eyemo 35 mm movie camera with a 600 groove/mm transmission grating mounted in front of the 50 mm f/1.1 camera lens was in operation at site F-2. The camera operated at 4 fps and used Royal-X Pan Recording film.

(7) A simple photometer using a CBS 1002 photomultiplier was used to observe the exact time of burst on several of the firings. The instrumentation consisted of the photomultiplier with a simple condensing lens and coffee cup mount to limit the acceptance angle to 26° . Output of the photomultiplier was recorded on a visicorder through a logarithmic amplifier. Precise time was recorded from a Vitro time pulse which was fed to the visicorder.

E. Filters

The K-24 cameras and some of the special cameras were equipped with a variety of filters to isolate selected spectral regions.

For the solar scatter shots, the two K-24 cameras at each site were equipped with polaroid filters mounted at right angles to each other.

For the I fly shots which contained sodium and cesium, both Wratten gelatin filters and interference filters were used to isolate the resonant wavelengths. Each observing site had at least two K-24 cameras and would instrument one to photograph the sodium radiation at 5893 Angstroms and the other to photograph the cesium radiation at 8521 Angstroms.

LOCATION OF OPTICS OBSERVING SITES

All rockets during 1960 were fired from the Eglin Gulf Test Range on Santa Rosa Island, Florida. Optics sites G, H, and J were chosen to have approximately a 45° viewing angle for a cloud height of 120 km.

Cameras which were used primarily to gather spectral information and to record anomalous events were operated from site F. Hence, this site was chosen for convenience to the headquarters area where last minute changes and special arrangements could be made.

Camera installations were established at the following locations:

<u>Site Notation</u>	<u>Common Name</u>	<u>Latitude</u>	<u>Longitude</u>
F-1	A-10	30° 23' 58.66"	86° 41' 50.81"
F-2	A-10	30° 23' 58.66"	86° 41' 50.81"
G	Mexico Beach	29° 57' 03.938"	85° 25' 42.177"
H	Opp, Alabama	31° 16' 26.985"	86° 14' 50.312"
J	Mobile, Alabama	30° 13' 37.949"	88° 01' 26.605"

In addition a single K-24 camera was operated at the Blue Horizon Motel for stereo comparison with sites F-1 and F-2.

The map of Figure 3 shows the location of the camera sites.

DATA ANALYSIS

A. Photographs

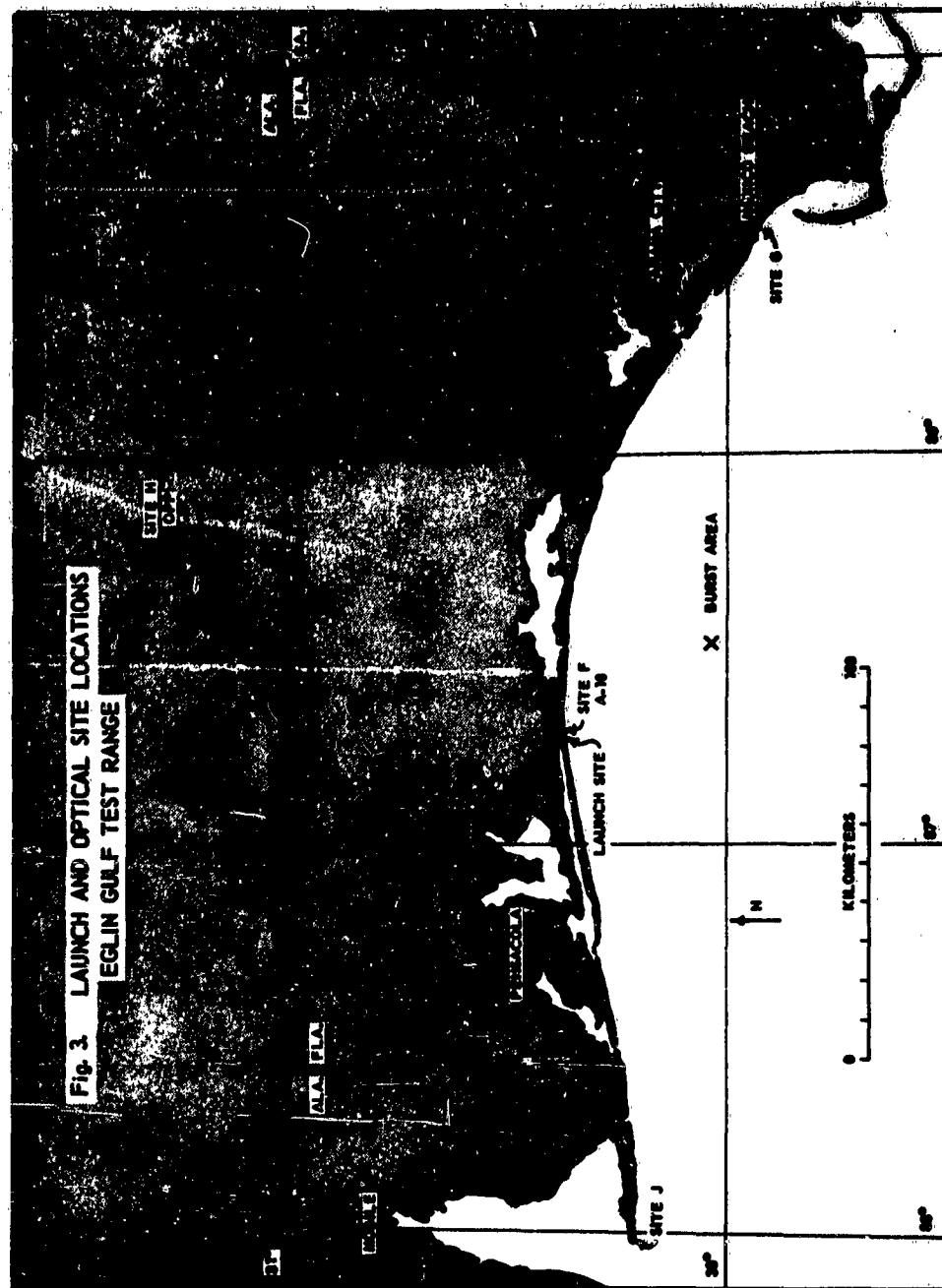
A large number of photographs were taken with the K-24 system and have been abstracted and compiled into a report by H. D. Edwards.⁽¹⁾ From this report, the reader can see at a glance the type, duration and quality of photographs which were taken of each firing. This report has been used frequently in subsequent analyses.

B. Position Calculations

Photographs were taken against a star background in all cases except where bright sunlight would render stars invisible. This was especially true in dawn shots where the sky background would increase during the later stages of the cloud formation and eliminate star images. In these cases, position data are calculated from azimuth and elevation settings of the apparatus rather than from star right ascension and declination.

Several points which were distributed over the length and width of the cloud and could be simultaneously identified from two or more stations were chosen and the corresponding calculations made for altitude and ground sub-point latitude and longitude as a function of time.

(1) "Photographic Coverage of Firefly 1960 (K-24 Cameras)," Technical Report No. 5, Contract No. AF 19(604)-5467, by Howard D. Edwards, January 15, 1961. (Due to the large number of photographs and resultant high cost only 10 copies were made. This limited supply has been exhausted.)



The number of points varied from one or two for some of the clouds to seventeen in the case of Jeannie. The length of time for which calculations could be made varied from a few minutes for many of the clouds to 20.5 minutes for Betsy. In most cases the duration of photographic coverage was limited either by fading of the clouds or by increase of sky background due to the approach of dawn.

Table 1 lists the parameters which were calculated for point 1 on the clouds. Similar data are available for other points on the clouds but for brevity are not published here.

Figures 4 through 14 show the latitude-longitude ground plots and altitude as a function of time for nine of the 1960 Firefly releases. Again for brevity, only a portion of the data which has been calculated is shown on the plots. Subsequent analyses are expected to produce similar plots for Frances, Ida, Janet, Hilda, Marie, and Lola. Other clouds were not of sufficient intensity and/or duration to produce drift and growth information.

Duration of the night shots (Cathy, Amy, Ruth, and Gerta) was about 1 minute or less and did not give sufficient data for drift analyses. Betsy was fired under night conditions and behaved similarly to the other night shots until about B + 5 minutes when the cloud became sunlit and reacted as a dawn cloud.

The altitude plots for the dawn shots studied so far (Betsy, Margie, Peggy, Olive, Jeannie, Susan, Dolly) show that many of the clouds disperse in both an upward and downward direction from the burst point. Accuracy of the calculated height positions is better than 0.5 km and hence the altitude deviations are a real effect and not due to experimental error. In similar manner the oscillations shown for many of the shots are real and not observational error.

For the dawn shots studied to date, the burst was at an altitude where high wind shears exist with the result that the clouds were torn into long lumpy filaments. These filaments would extend over an altitude range of up to 15 km within 10 minutes after burst.

Peggy, while having unusual radio frequency reflections, does not appear to be unlike several other shots with regards to dispersal by the wind, range of altitude, size of cloud, etc. The altitude range of 96 to 108 km for Peggy was somewhat different than for the other shots. Jeannie, Betsy, Susan, and Dolly were above this altitude range while Margie and Lola were at a lower altitude. Marie has not yet been studied.

Peggy was oriented East-West as shown by the ground plot whereas Jeannie, Susan, Betsy and Dolly had more of a North-South orientation. Perhaps the orientation of the Peggy antenna contributed to the long duration of the reflected signal.

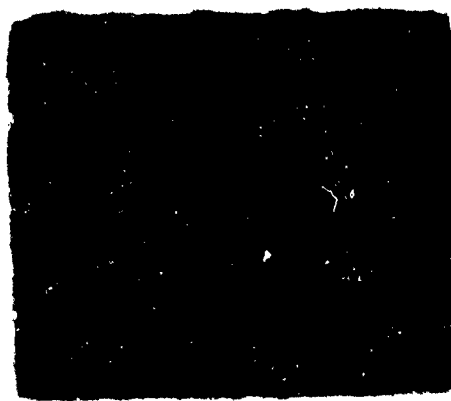
TABLE I

2007	TIME SECS.	AVERAGE LATITUDE	AVERAGE LONGITUDE	SLANT RANGE AT 2007	AVERAGE ALTITUDE 4000	PROB. ERR. ALT. 4000	N	AVZ. RES. 40	SHOT	TIME SECS.	AVERAGE LATITUDE	AVERAGE LONGITUDE	SLANT RANGE AT 2007	AVERAGE ALTITUDE 4000	PROB. ERR. ALT. 4000	N	AVZ. RES. 40
FRANCES																	
1	0	30.004	06.028	153.0	140.15	.05	6	.0016	WILDA	0	30.024	06.015	142.0	132.99	.08	4	.0004
1	15	30.001	06.047	149.2	140.00	.05	3	.0122	12	30	30.029	06.040	142.0	134.40	.42	3	.0000
1	30	30.024	06.067	144.4	136.77	.161	1	.0122	12	40	30.033	06.054	142.4	136.40	.22	3	.0000
1	45	30.007	06.066	142.6	134.15		1	.0109	12	150	30.014	06.099	140.2	130.00		1	.0002
CHERRY																	
2	0	30.031	06.052	134.3	129.86	.05	6	.0009	13	0	30.031	06.079	149.4	138.00	.15	4	.0010
104	0	30.025	06.045	140.4	139.40	.10	3	.0028	16	0	30.022	06.091	149.1	140.04	.20	4	.0002
3	2	29.925	06.059	140.6	129.69		1	.0011	15	0	30.126	06.056	97.9	01.49	.09	2	.0009
ALV									JEANIE								
0	0	30.148	06.049	153.6	130.44	.06	4	.0015	16	0	30.109	06.042	111.3	100.47	.15	2	.0016
4	15	30.180	06.046	152.8	149.32		1	.0020	16	30	30.185	06.070	112.0	116.00	.05	3	.0003
4	30	30.137	06.084	149.5	143.41		1	.0019	16	40	30.163	06.060	115.1	112.07	.13	3	.0003
4	45	30.119	06.091	144.4	139.49		1	.0034	16	90	30.141	06.099	113.4	113.40	.09	7	.0004
NEWY									16	150	30.054	06.092	113.4	110.72		1	.0009
5	0	30.151	06.047	112.0	104.93	.10	4	.0013	MARIE	0	30.129	06.044	00.0	74.70	.20	6	.0000
5	15	30.111	06.059	121.7	117.50	.31	3	.0040	17	40	30.120	06.042	03.5	77.37	.59	3	.0001
3	30	30.076	06.052	128.5	123.09	.06	3	.0029	17	100	30.132	06.043	02.0	76.07	.59	3	.0002
3	45	30.040	06.021	124.0	127.45	.28	3	.0043	17	300	30.139	06.000	01.3	75.43	.12	3	.0000
3	0	30.093	06.018	130.0	124.73	.50	3	.0000	17	420	30.137	06.073	01.5	75.02	.02	3	.0000
3	15	29.920	06.011	138.6	120.68	.27	3	.0125	17	540	30.146	06.049	00.5	75.11	.04	3	.0000
3	30	29.972	06.043	137.7	120.22	.19	3	.0119	17	660	30.152	06.062	00.3	75.04	.06	3	.0100
JANET									17								
0	0	29.042	06.217	135.6	110.90	.12	9	.0037	LOLA	0	30.004	06.013	04.0	03.22	.00	6	.0007
6	45	29.045	06.501	135.0	115.78	.24	3	.0145	20	30	30.196	06.023	07.4	04.02	.10	1	.0011
6	150	29.054	06.501	134.2	1												
6	300	29.062	06.418	137.1	115.19	.44	3	.0002	20	120	30.077	06.070	97.7	02.72	.19	1	.0012
6	450	29.094	06.313	140.9	120.47	.18	3	.0000	20	180	30.135	06.079	101.1	03.74		1	.0012
6	870	29.041	06.207	140.1	110.69	.41	3	.0100	ARLINE	0	30.115	06.000	111.0	104.19	.09	2	.0009
DOLLY									21	0	30.115	06.000	111.0	104.19	.09	2	.0009
7	0	29.031	06.407	143.5	115.20	.15	2	.0014	21	0	30.026	06.022	112.3	102.72	.04	12	.0011
7	30	29.039	06.407	143.5	115.25	.15	3	.0125	21	30	30.017	06.016	144.1	104.00	.00	3	.0000
7	45	29.053	06.412	144.6	116.00	.39	1	.0004	22	30	30.014	06.013	116.1	104.10	.19	3	.0003
7	0	29.046	06.419	140.3	115.03		3	.0153	22	40	30.039	06.034	115.0	107.00		1	.0001
7	15	29.045	06.424	144.6	117.03	.74	1	.0102	22	120	30.039	06.042	115.0	107.00		1	.0001
7	30	29.043	06.443	149.0	119.43		3	.0113	22	195	30.039	06.041	114.0	107.00	.25	3	.0004
7	45	29.052	06.443	149.0	119.43	.77	1	.0007	22	235	30.009	06.041	114.0	107.00	.25	3	.0004
7	0	29.053	06.473	140.3	117.44		1	.0115	22	315	30.001	06.040	114.0	107.00	.25	3	.0004
7	15	29.050	06.464	131.3	113.17		1	.0115	22	395	30.100	06.041	114.0	107.00	.25	3	.0004
7	30	29.049	06.464	120.0	110.00		1	.0004	22	475	30.111	06.044	114.0	107.00	.25	3	.0004
7	45	29.042	06.413	149.9	115.04		1	.0009	22	555	30.125	06.037	114.0	107.00	.25	3	.0004
087									22	555	30.134	06.034	100.03			1	.0009
0	0	29.027	06.032	142.0	110.99	.00	4	.0009	22	555	30.134	06.034	100.03			1	.0009
CHERRY									23	0	30.017	06.023	123.3	110.90	.00	6	.0000
0	0	29.720	06.046	122.0	93.90	.03	6	.0009	23	0	29.726	06.047	120.9	100.16	.00	6	.0000
10	0	30.013	06.093	67.9	67.20	.07	0	.0020	24	0	30.013	06.093	67.9	67.20	.07	0	.0020
JEANIE									24	0	30.013	06.093	67.9	67.20	.07	0	.0020
11	0	29.093	06.095	127.3	113.33	.04	3	.0016	24	0	29.093	06.095	127.3	113.33	.04	3	.0016

* NUMBER OF ESTIMATES WHICH HAVE BEEN ADOPTED.

A NUMBER OF ESTIMATES WHICH HAVE BEEN AVERAGED.
 APPROXIMATE NATIONAL INCREASE. THE NATIONALS FOR ANY PAIR OF STATIONS,
 IS THE ABLE BETWEEN THE PROJECTIONS OF THEIR LINES OF SIGHT ON A PLANE
 PERPENDICULAR TO THE ORIGIN LINE JOINING THE TWO STATIONS.

Fig. 4. BETSY



SITE H B+ 450 SEC



SITE J B+ 390 SEC

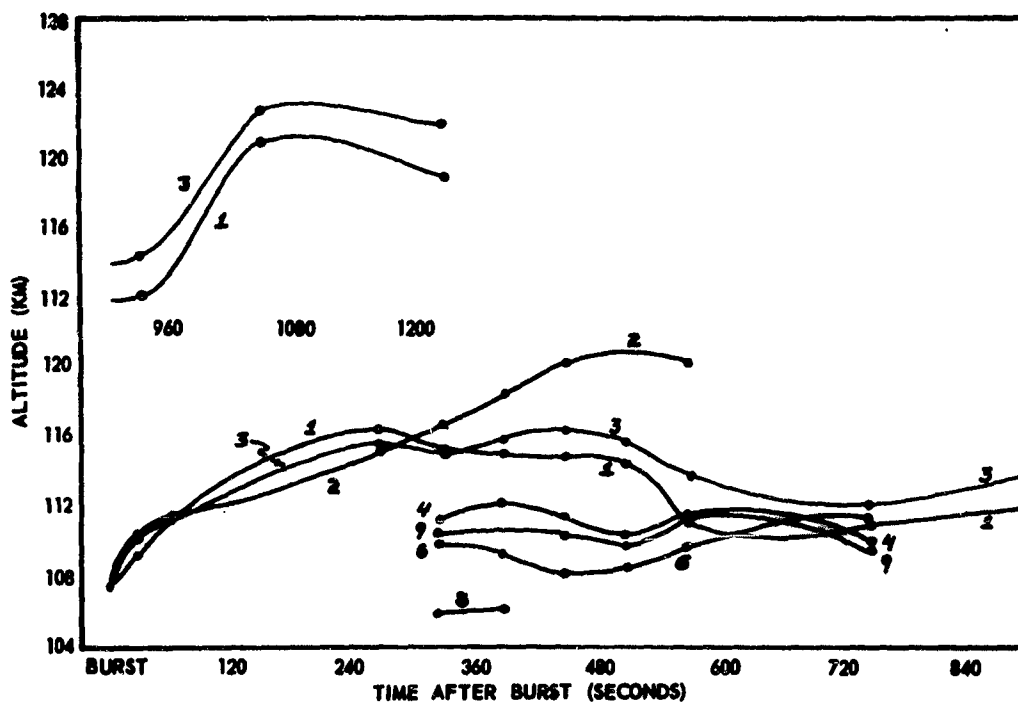


Fig. 5. BETSY

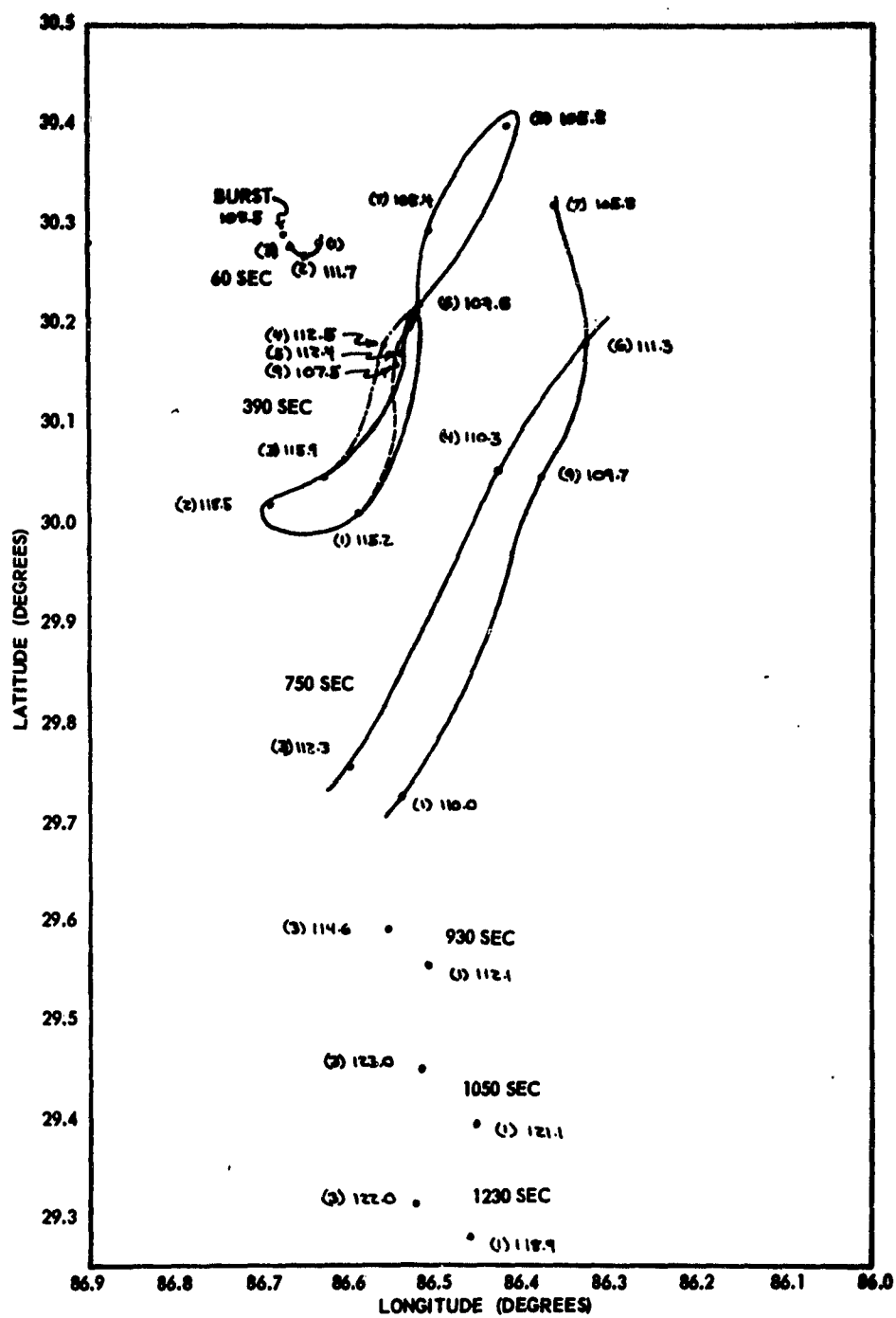


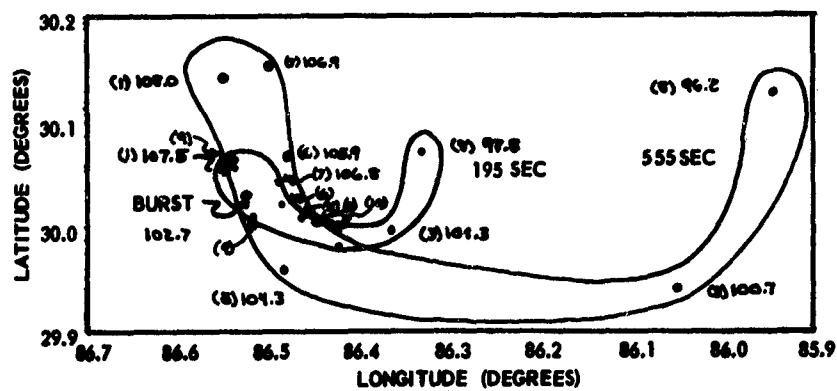
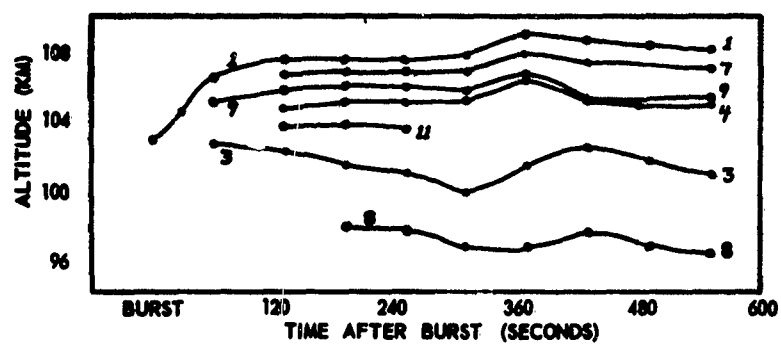
Fig. 7. PEGGY

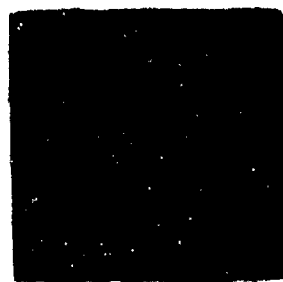


SITE F B+ 136 SEC



SITE F B+ 315 SEC





SITE H B+ 315 SEC

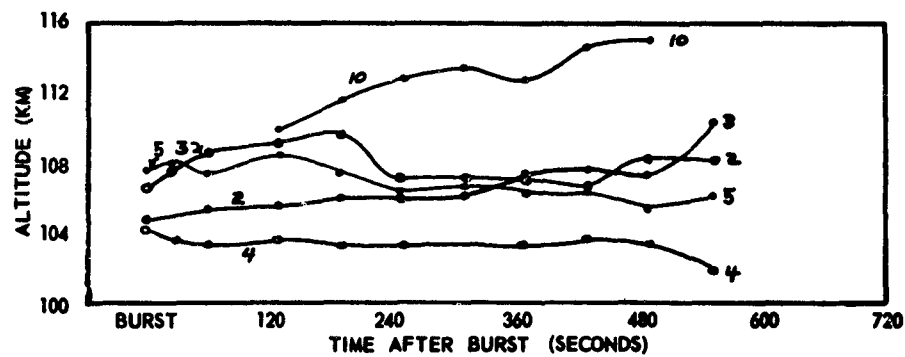
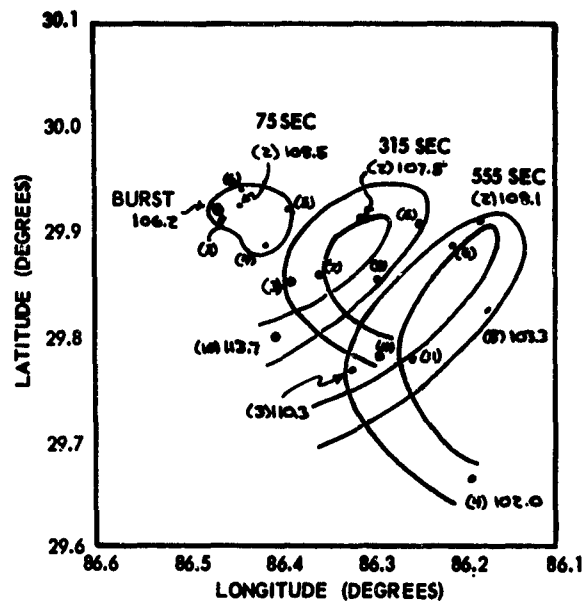


SITE H B+ 75 SEC

Fig. 8. OLIVE



SITE H B+ 555 SEC





SITE F B+ 210 SEC



SITE F B+ 630 SEC

Fig. 9. JEANNIE

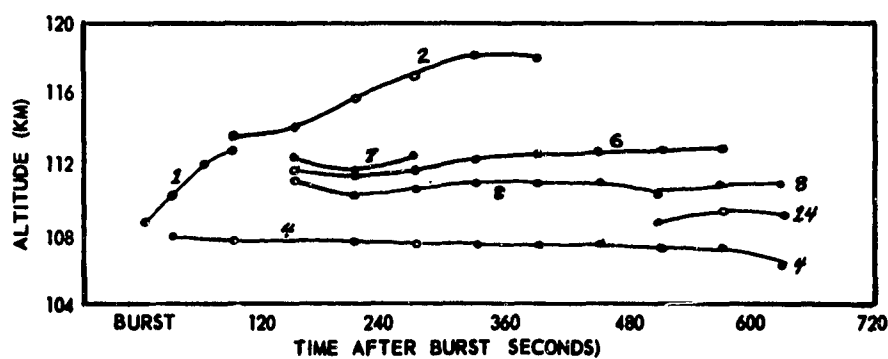
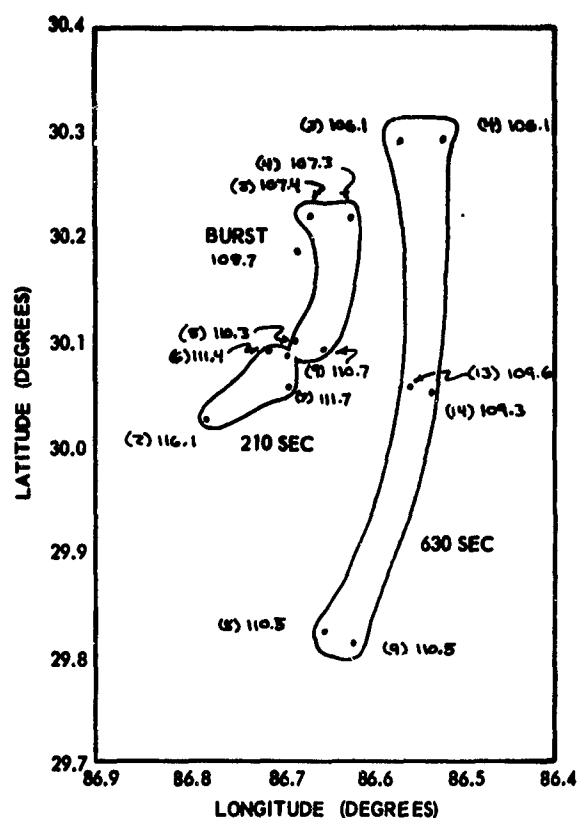


Fig. 10. SUSAN



SITE F B+ 540 SEC



SITE J B+ 540 SEC

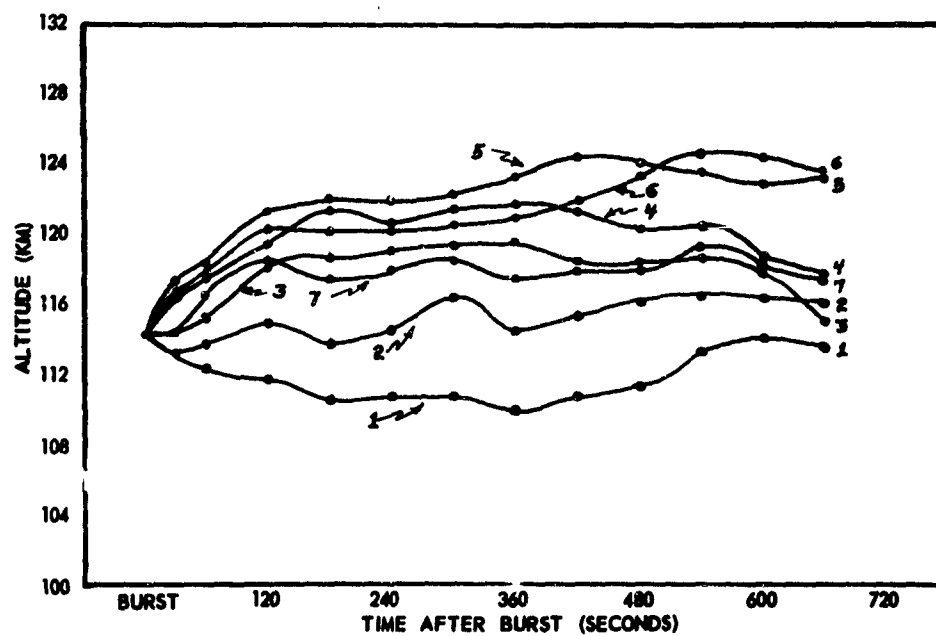
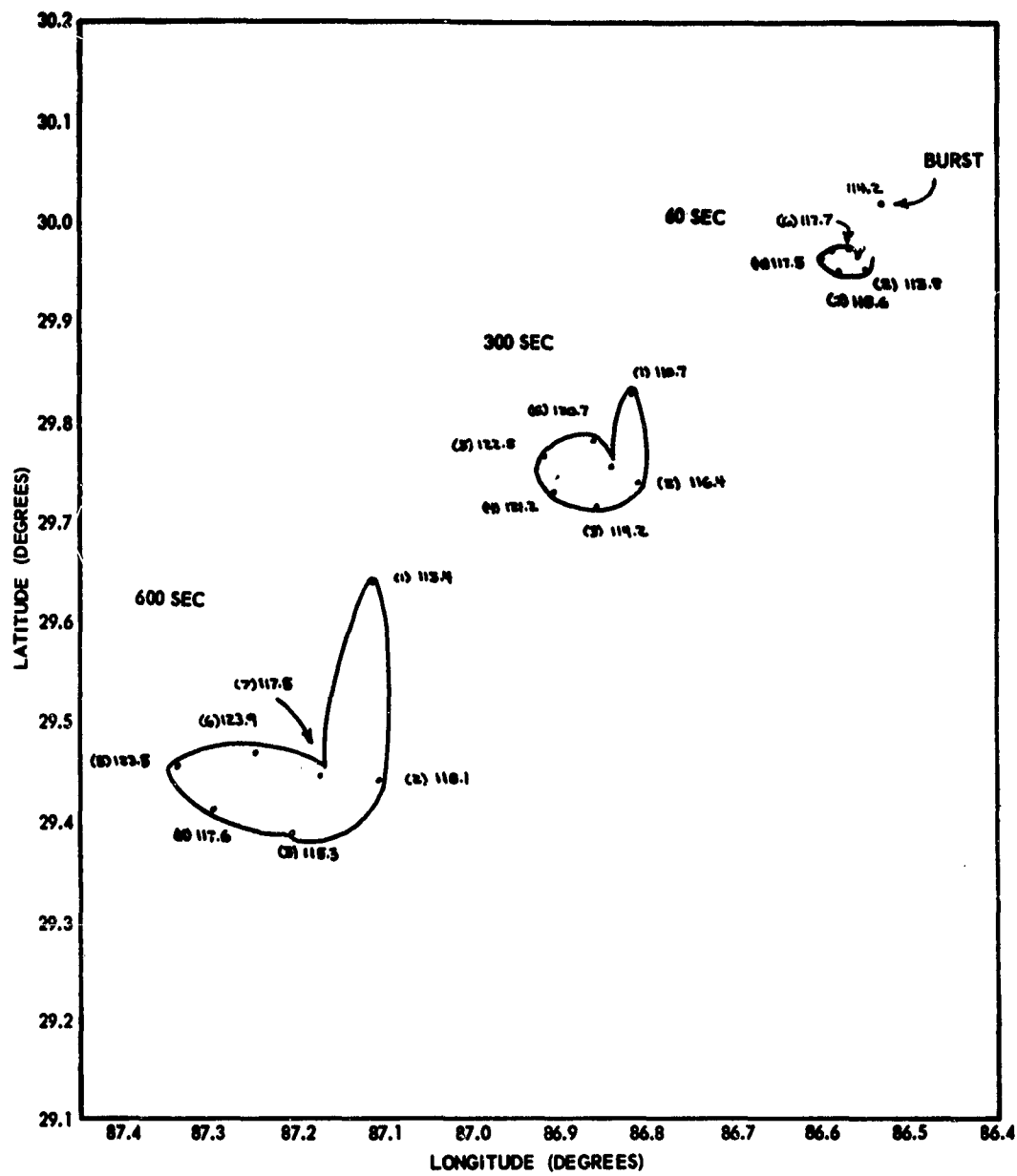


Fig. 11. SUSAN





SITE F B+ 330 SEC



SITE J B+ 60 SEC

Fig. 12. DOLLY



SITE F B+ 690 SEC

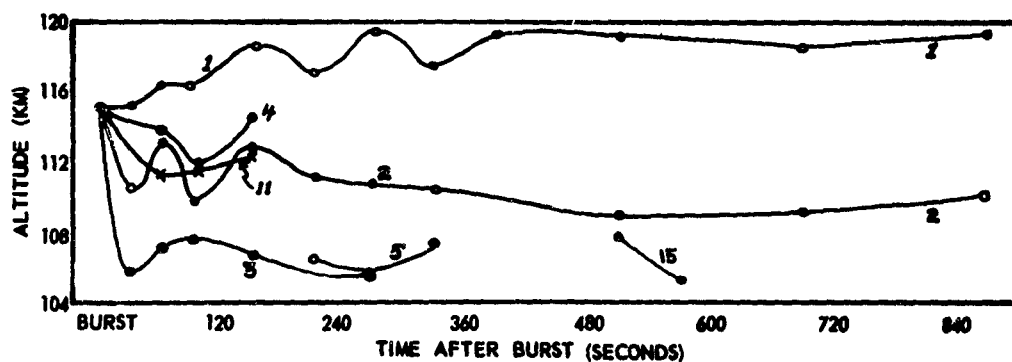
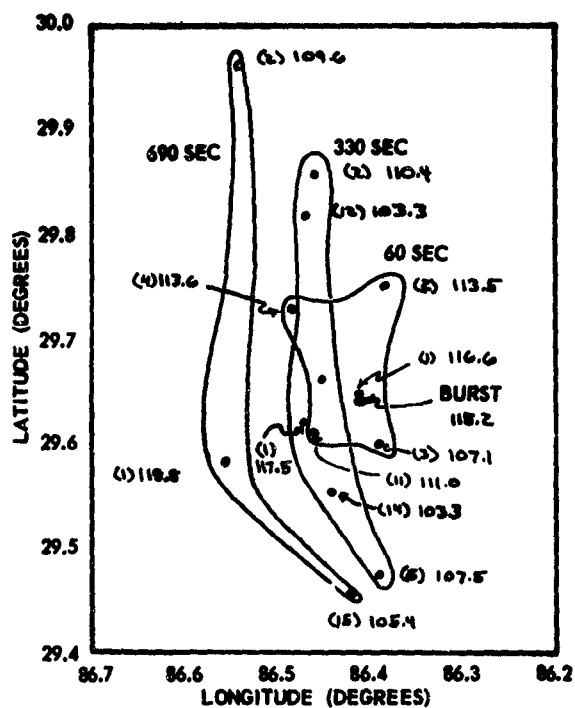


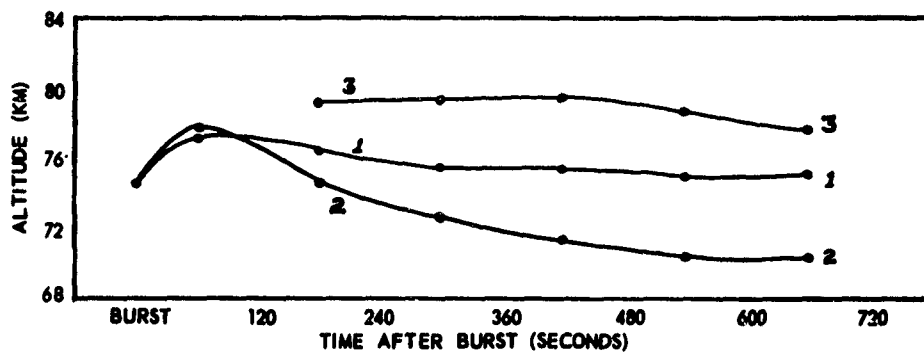
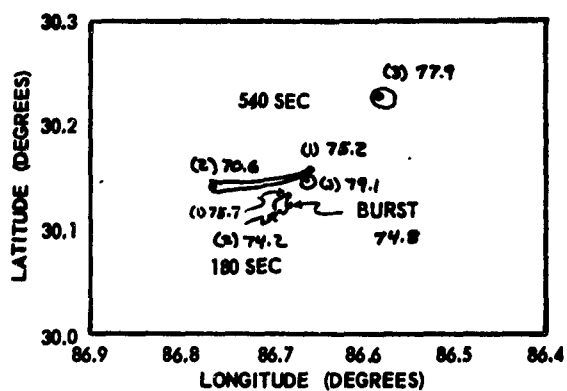
Fig. 6. MARGIE



SITE H B+ 120 SEC



SITE H B+ 600 SEC



Altitude and ground plots for Hedy and Lily are given in Figures 13 and 14. Lily was observed for 1 minute and then faded very rapidly. Hedy lasted for 1-1/2 minutes and then also faded rapidly from view. The three points identified in Hedy rose from 108 km to 130 in one minute and then dropped to a low of 124 km before it faded 30 seconds later. Lily, on the other hand, had its identifiable points fall from an altitude of 150 km to 139 km in less than 60 seconds. Five identifiable points were studied for Frances and a drop from 148 km to 132 km in 30 seconds was observed. These two extremes--rapid rise for Hedy and rapid fall for Lily and Frances--are due to vehicle velocity at release.

The two flights which used a carbon arc to create ionized and visible trails were Anne and Norma. Photographic observations were made on Norma only and the position data are given in Table 2.

Table 2: Norma*

<u>Time After Burst (sec)</u>	<u>Average Latitude (degrees)</u>	<u>Average Longitude (degrees)</u>	<u>Average Altitude (km)</u>
0	30.273	86.520	96.9
8	30.270	86.511	97.1
12	30.267	86.505	97.2
21	30.258	86.493	96.5
27	30.254	86.487	95.5
38	30.244	86.473	92.8
42	30.232	86.458	89.7

*The computations shown in this table result from a different computer program than the one used for the calculations given in Table 1. Hence residuals are not available. It is believed the data are good to better than 0.5 km in altitude.

It was previously understood that the carbon arc flights would trace out a path which included the peak of rocket trajectory. This trajectory was apparently achieved with a peak at 97 km and then the cloud moved down to about 90 km on the down leg. The burning time of 42 sec for the arc is approximately correct from what is known of the expected burn time.

In earlier preliminary studies it was concluded that the bright center of the clouds dropped very slightly during the first few seconds after burst and then rose again. Very careful measurements have now been made at few second intervals for several of the shots and

Fig. 13. LILY



SITE H B+ 30 SEC



SITE F B+ 30 SEC



SITE J B+ 30 SEC

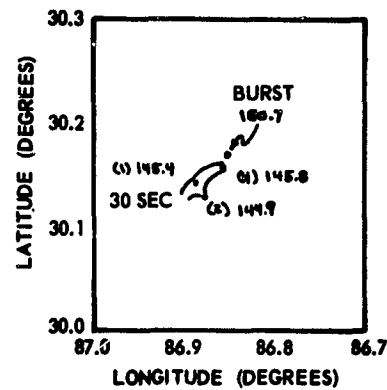
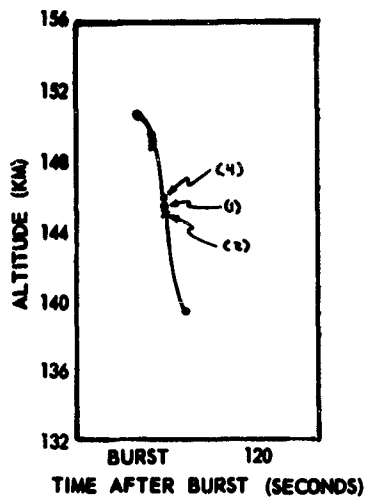


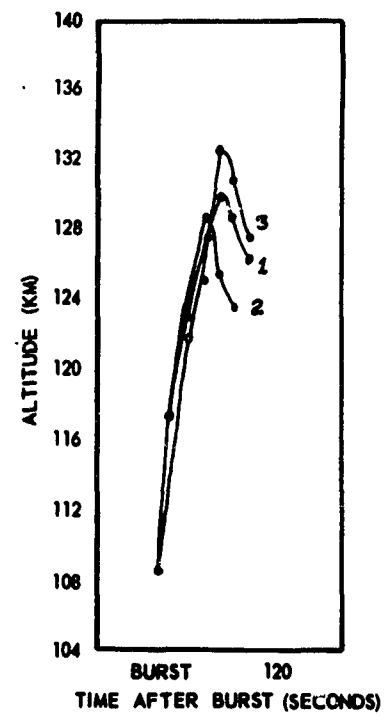
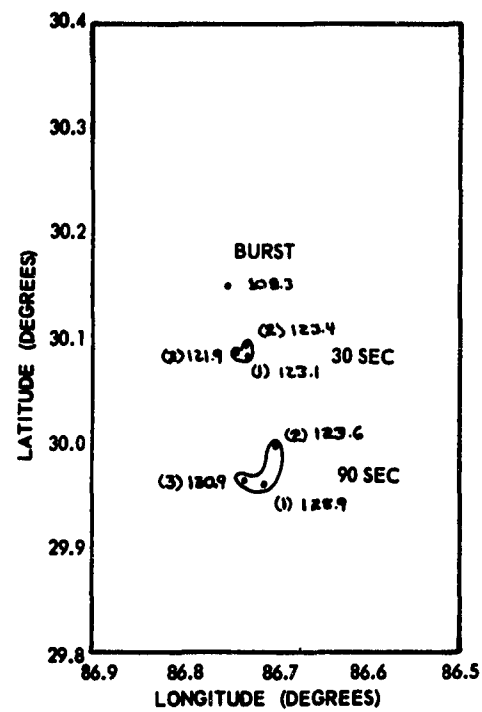
Fig. 14. HEDY



SITE H B+ 90 SEC



SITE F B+ 90 SEC



the data presented in Figure 15. In all of the cases studied the cloud "bright center" rose after burst. The rate of rise is proportional to altitude as indicated from the plot. The increase in rise rate with cloud release altitude may be partially explained by the decrease in ambient pressure with altitude. Rocket velocity at time of release is not immediately available and the contribution to cloud upward motion due to rocket motion is not calculable.

C. Special Cameras

(1) A Beattie-Coleman 35 mm camera was operated with SO270 color film at site F-2. A sequence of photographs at 5 second intervals was taken for the following shots:

Frances	Jeannie
Ida	Margie
Lily	Lola
Hedy	Peggy
Dolly	Susan

Slides have been made of many of the shots and are of general interest in studying the color of the clouds.

(2) A Bolex 16 mm movie camera with color film was in operation at F-1 and obtained movies of Hedy.

(3) The bank of 5 each 16 mm pulse cameras obtained data on most of the shots using either polaroid or Wratten filters. Much of the data was duplicated on K-24 film and hence no attempt will be made at analysis. In addition, inadequate marking of the film has made the analysis difficult.

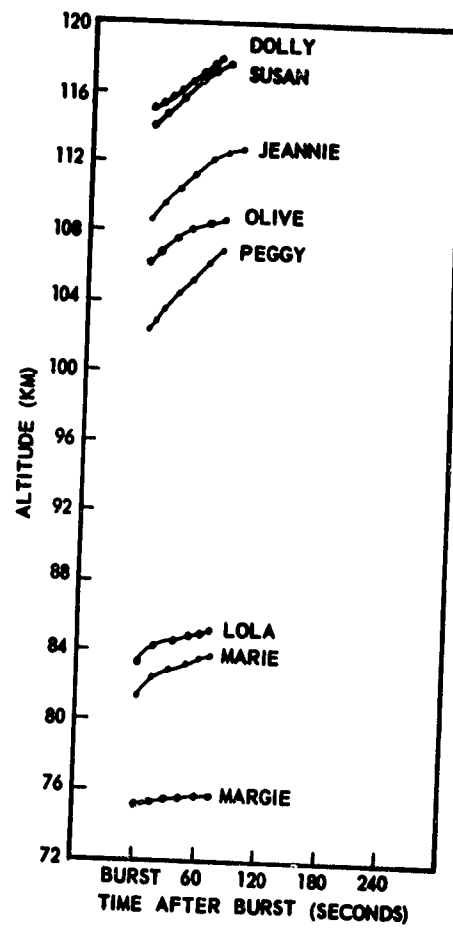
(4) The polaroid land cameras and speed graphic type cameras with polaroid adapter backs were used successfully to give quick results on burst altitude. These data were of value in planning the subsequent firings. The data are not presented here since the usefulness was limited to field planning and the data have now been superseded by more accurate calculations.

(5) The K-24 camera which was operated at the Blue Horizon Motel to give stereo pictures with the cameras at site A-10 obtained good photographs of most of the clouds.

A hurried but sufficiently thorough analysis of the film indicates that the clouds did not have enough structure to make practical the use of the stereo technique.

(6) The Eyemo 35 mm movie camera with a 600 groove/mm transmission grating mounted in front obtained spectrograms on Jeannie, Margie, Lola, Peggy, Susan and Olive. The analyses of this work have been prepared as a separate paper and will be presented in the section on spectrophotometry.

Fig. 15. "BRIGHT CENTER" ALTITUDE



(7) The simple photometer described in the instrumentation section was used to record the exact time of burst on several of the clouds. The data obtained are presented in Table 3.

Table 3: Release Times from Georgia Tech
"Eye in Sky" Photometric Observations

<u>Firefly</u>	<u>Burst Time CST</u>
Dolly	04:21:45.84
Amy	02:32:45.28
Cathy	02:32:44.95
Ruthy	02:32:29.37
Hilda	04:25:31.46 ⁽¹⁾
Betsy	04:16:40.72 ⁽²⁾
Marie	04:38:25.39 ⁽¹⁾
Jeannie	04:36:40.90 ⁽²⁾
Margie	04:37:00.60
Peggy	04:41:50.75
Susan	04:43:49.31
Olive	04:41:50.14
Wendy ⁽³⁾	04:18:40.62
Vicky ⁽³⁾	19:06:19.53

(1) Photometer did not record burst and the time recorded was obtained from a push button operated by an observer. Generally the time recorded was after burst due to observer reaction time of approximately 1/3 sec.

(2) It is noted that these measurements read 0.1 sec high compared to the results reported by Device Development Corporation in October 1960.

(3) Rocket failed.

CONCLUSIONS

A large amount of data was taken on the 1960 chemical releases. Much of these data has now been reduced and is included in this report.

Although additional studies will be made during the next few months sufficient data have been reduced to plan the 1961 series with confidence.

MOLECULAR AND TURBULENT DIFFUSION IN THE UPPER ATMOSPHERE

S. P. Zimmerman and K. S. W. Champion

Headquarters, Air Force Cambridge Research Laboratories,
Air Force Research Division (ARDC), Geophysics Research
Directorate, L. G. Hanscom Field, Bedford, Massachusetts

ABSTRACT

The diffusion of chemical clouds, which were created in the upper atmosphere by explosive release from a rocket, has been studied by visual and photographic means. These clouds for the most part are gaseous cesium with a trace of sodium added. However, gaseous and solid contaminants created in the explosion are also present. This study is concerned with that period after the initial explosive phase, when eddy or molecular diffusion controls the growth of the cloud.

1. THEORY

The problem is to determine the nature of the dispersion of a spherical cloud of material introduced into an ambient atmosphere at some arbitrary time, $t = 0$. The solutions obtained are based on three principle assumptions, viz:

(i) The cloud is spherical. This in essence ignores the effect of the wind shear elongating the cloud. Since the growth of the cloud is measured transverse to the direction of the shear, we may make this assumption.

(ii) The production and loss mechanisms for the diffusing particles are negligible. That is the total number of diffusing particles is constant.

(iii) The thermodynamic properties of the cloud (e. g. temperature and pressure) are the same as those of the ambient.

A consequence of the second assumption is that the cloud will disperse by purely diffusive properties.

Following the works of Kellogg,⁽¹⁾ Sutton,⁽²⁾ and Roberts⁽³⁾ we arrive at the following equation to explain the growth of a contaminant placed in same medium

$$r_0^2 = 2 \bar{r}^2 \left[1 + \ln \left(\frac{r_0^2 \text{ max.}}{2 a^2} \right) - \ln \left(\frac{\bar{r}^2}{a^2} \right) \right] \dots \dots \dots (1)$$

1. Kellogg, W. W., 1956, Journ. of Meteorology, 13, 241 - 250
2. Sutton, O. G., 1932, Proc. Roy. Soc., London, A, 135, 103 - 165
3. Roberts, O. F. T., 1923, Proc. Roy. Soc., London, A, 104, 604 - 654

where: r_0 is the visible radius

$\overline{r^2}$ is by definition the mean square deviation of a particle relative to the cloud center

a is the initial radius of the cloud controlled by diffusion (i.e. the radius when the cloud comes to equilibrium with the ambient at the termination of the explosive phase.

$r_{0 \text{ max}}$ is the maximum observable radius.

Applying the above equation hinges upon the derivation of $\overline{r^2}$. Kellogg has followed the works of Taylor, ^(4, 5) using the concept of a correlation coefficient to describe the mean deviation (cloud spread) of a particle from the center of the cloud. This defines $\overline{r^2}$ by

$$\overline{r^2} = 2 \left| \overline{v^2} \right| \int_0^t \int_0^\infty R_{\xi} d\xi d\tau \quad \dots \dots \dots (2)$$

where: $\overline{v^2}$ is the mean square turbulent velocity of the ambient

R_{ξ} is the LaGrangian correlation function

$$= \begin{cases} 1, & t \rightarrow 0 \\ 0, & t \rightarrow \infty \end{cases}$$

Thus:

$$\overline{r^2} = \begin{cases} \overline{v^2} t^2, & t \rightarrow 0 \\ 2 \overline{v^2} I t, & t \rightarrow \infty \end{cases} \quad \dots \dots \dots (3)$$

$$\text{where: } I = \lim_{t \rightarrow \infty} \int_0^t R_{\xi} d\xi$$

With this derivation Kellogg shows how the cloud growth, which he attributes to small scale eddies, follows equation (1) with $\overline{r^2} = \overline{v^2} t^2$. It is the feeling of the authors, that the above derivation while having the correct time dependence of $\overline{r_0^2}$ does not physically describe the parameters controlling diffusion. As an example, there is no method to distinguish the gross action of the cloud due to shear turbulence as differentiated from that due to isotropic turbulence. To correct this, a statistical mechanical argument advanced by Tchen ⁽⁶⁾ describes the diffusion of a source, where $\overline{r^2}$ is described by

$$\overline{r^2} = \text{Constant } t^2 \gamma^* \quad \dots \dots \dots (4)$$

4. Taylor, G.I., 1920, Proc. London Math. Soc., 2, 196 - 212
5. Taylor, G.I., 1935, Proc. Roy. Soc. London, A, 151, 421 - 478
6. Tchen, C.M., Advances in Geophysics, 6, 165 - 173 (1959)

* It should be emphasized here that Tchen only discusses the case for the small scale eddies, and does not cover diffusion due to large scale eddies.

where: $= \frac{3}{2}$ for isotropic turbulence
 $= 1$ for shear turbulence
 $= \frac{1}{2}$ for molecular diffusion

Since the region of the atmosphere that is being studied is a high shear region, we will assume that the turbulent growth will be due to a shear turbulence as hypothesized by Tchen,* and molecular when the atmosphere is not turbulent. Thus we can determine the appropriate constants by using the equations

$$r_0^2 = \overline{v^2} t^2 \left[1 + \ln (r_0^2 \text{ max} / 2 a^2) - \ln (\overline{v^2} t^2 / a^2) \right] \dots \dots \dots (5a)$$

for the turbulent growth, and

$$r_0^2 = 2 K t \left[1 + \ln (r_0^2 \text{ max} / 2 a^2) - \ln (2 K t / a^2) \right] \dots \dots \dots (5b)$$

for the molecular growth.

2. EXPERIMENTAL RESULTS

Figure 1 shows the results of the measurements of the cloud Echo (a 1959 experiment) and the fitting of equation 5 to the experimental plot. This gives us the values of $\overline{v^2}$ and K experimentally as shown in Figure 2. Also shown are the calculated values of molecular diffusion for sodium and cesium, based upon a simple kinetic theory, and the values, due to Booker,⁽⁷⁾ of the turbulent diffusion coefficient.

With the values of the molecular diffusion coefficient and the velocities of the small scale eddies, one may determine the rate of energy density in a region, and then the scale size for the small eddies. These are given by the simple relations⁽⁷⁾

$$w = \frac{\overline{v^2}}{K_{\text{mol}}} \dots \dots \dots (6)$$

$$L_2 = (K_{\text{mol}}^3 / w)^{\frac{1}{4}} \dots \dots \dots (7)$$

Simultaneously with this we may measure the scale sizes for the large eddies from the photographs directly. These results are shown in Figure 3, and also with the values for the small scale eddies measured by radio reflection from the clouds. That these measurements fit well the values predicted by Booker is fairly evident from the figure.

* This assumption is validated by the experimental curves which show both the $t^{\frac{1}{2}}$ dependence due to molecular diffusion and t^2 due to shear turbulence.
 7. Booker, H.G., J. Geophys. Res., 61, 1956, 673 - 705

With more data forthcoming, we hope to show the region in the atmosphere where one may expect turbulence, what manner of turbulence, and the time scales for observation.

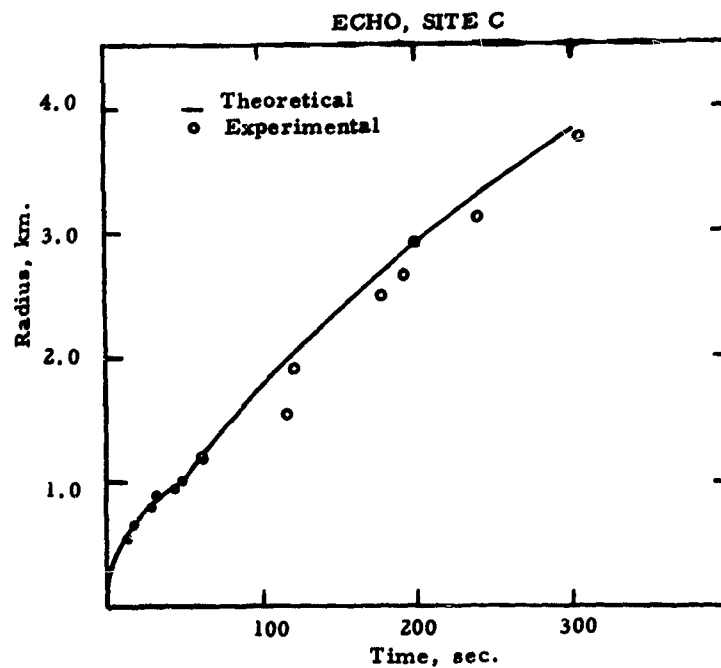


Figure 1

Radius of the cloud as a function of time showing the sudden shift in the expansion rate when turbulence is the major effect in the control of diffusion.

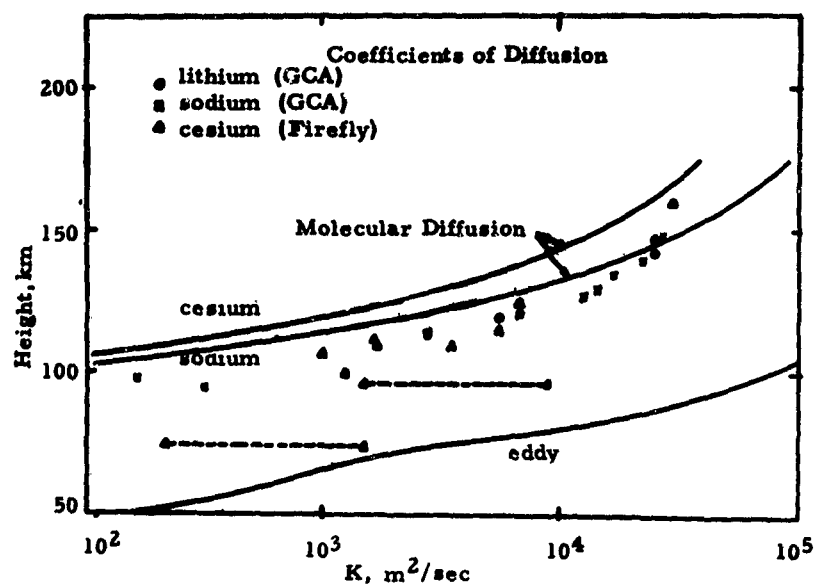


Figure 2

Diffusion coefficient K (both molecular and eddy) as a function of altitude. The dotted lines show the measured growth of the eddy diffusion coefficient over the period of observation. The solid line of the large scale eddy diffusion coefficient is due to Booker.

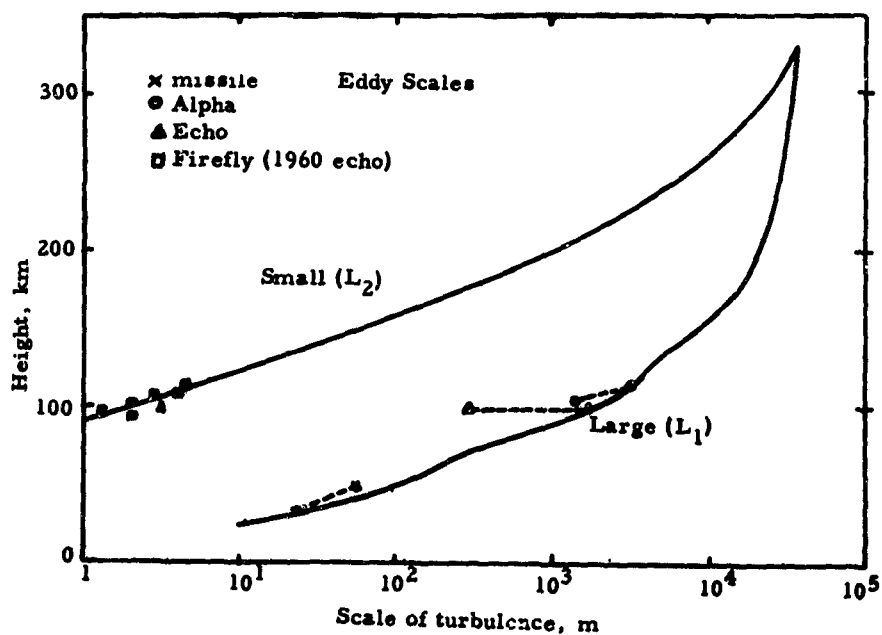


Figure 3

The scale sizes for the small and large eddies as a function of altitude. The solid lines are due to Booker.

PANEL DISCUSSION ON MASS TRANSPORT (10-3000 sec)

Panel Members:

H. D. Edwards	Ga. Tech	Chairman
E. R. Manring	GCA	
J. W. Wright	NBS	
C. G. Stergis	AFCRL	
M. W. Rosenberg	AFCRL	
S. Zimmerman	AFCRL	

Wright: Dr. Edwards, would you care to comment on the behavior of Betsy, which was observed to move in different directions by the radar and optics observations.

Edwards: I re-examined our photographs and we did photograph a portion of the cloud during the first few minutes which later fades out. I assume that this part which is no longer visible in the infrared after a few minutes, may be causing confusion. We were observing the cloud through the 87A Wratten filter and we continued to photograph the portion which moved in a southeasterly direction. The part that you tracked with radar moved more or less due east. I, too, think this phenomenon is very interesting since the cloud seemed to have two different components visible by different means.

Wright: These were at distinctly different altitudes, I believe, according to your data.

Edwards: Yes, that's right.

Rosenberg: The cloud rise generates the twisted shapes because of wind shears. Whether the cloud rise was due to an upward component of vehicle velocity or to the expanding gas volume (essentially a hydrodynamic rise because of the lower pressure above than below) is a problem. The two higher altitude shots were identical in rise rates, yet one of these was at a vehicle altitude where there was no longer an upward component to the velocity. Therefore, I think we can say that the rise is not associated with vehicle velocity upward but is a hydrodynamic push up--rather, a push down against the higher density ambient below. In any use of point releases it will be a problem to define the situation at a given altitude. The cloud will apparently always have an upward component unless, of course, we introduce a

downward vehicle component which causes other problems.

Zimmerman: Dr. Edwards, didn't you mention one cloud which had a drop in its trajectory? Was this release made when the rocket had reached its peak position?

Edwards: Yes, that was a solar scatter shot. Lily and Frances both showed this behavior, whereas Hedy was released before the rocket reached the peak and had an upward trajectory.

Zimmerman: None of the point electron clouds were released after the peak of the trajectory?

Edwards: I don't believe they were. The two high altitude releases that Dr. Rosenberg referred to, I believe, are Dolly and Susan. These were very close together and showed the same rise rate during the first minute.

Rosenberg: One of those had a 1 km per second upward vehicle velocity; the other one had a zero upward vehicle velocity.

Wright: I don't understand why the cloud should cease to rise after the first few seconds. Isn't it possible that the rise is caused by the explosive expansion of the cloud upwards for the first few seconds and that the cloud then remains at relatively constant altitude?

Zimmerman: The rise time, if I remember correctly from the photographs was quite long, with characteristic times of the order of 300 to 400 seconds, wasn't it?

Edwards: The clouds in many instances continued to rise for the three or four hundred seconds, as you say, before reaching the maximum altitude. Some altitude oscillations in a given portion of the cloud as a function of time were observed.

Manring: I've seen some of the data before. This time I noticed, if we're talking about the longer scale rise and drops rather than some of the very short ones, that from the same burst quite often you see some rises and some drops. Now I'm asking if you've looked at the data well enough to determine the material all starts at a single point and then gets dispersed up and down, perhaps through canister

explosion and continued reaction. I don't know what the mechanism is, but have you noticed that the parts in the uppermost region of the cloud continue expanding upward and those in the lower part downwards so that the center of mass of the clouds may remain at roughly the same height?

Edwards: Generally speaking, I think that the parts in the upper portion of the cloud do remain up--they don't cross over. We do have some parts that cross one another in altitude in the plot but this is the exception. However, the upward movement appears to be greater than the downward and will probably give a slight rise for the center of mass. I have not calculated the location of the center of mass but from studying points on the clouds which are distributed throughout the length and breadth of the cloud we do have a predominance of upward motion. As you speculate, the parts that start up continue up and the ones that start down continue down.

Manring: I wonder if the long term behavior can be explained in terms of localized gradients through the clouds and an apparent motion upward and apparent motion downward, depending upon how the material was laid out initially in the canister source.

Edwards: This might very well be so. On a slide which I plan to show in the next talk I'll show, for example, the separation of sodium and cesium for Peggy. The sodium appears at one end of the cloud and the cesium appears at the other end. From Dr. Fisher's talk this morning, this observation might very well be explained by the fact that sodium happened to be placed in a position in the canister from which it came out with higher density at a particular altitude and then did not appear during the later formation of the cesium clouds.

Stergis: Mr. Zimmerman, on your Echo results you show a smooth curve up to about 60 seconds and suddenly a nice break which seems to show turbulent diffusion. Why this sharp break? Physically, what does this mean?

Zimmerman: The observed initial rate of growth would correspond to a value of

diffusion coefficient almost three times as large as the expected molecular diffusion coefficient which Dr. Champion and I calculated. I infer from this that the phenomenon is partly turbulent and partly molecular and at some point, say at 60 seconds, the turbulence--really the eddies--gained control of the growth of the cloud and carried the material along.

Stergis: Could you differentiate between the turbulence introduced by the cloud itself and turbulence due to the ambient?

Zimmerman: Turbulence introduced by the cloud itself, I believe, is negligible in this case. Such turbulence wouldn't wait until 60 seconds to exhibit itself.

Stergis: That's true. You seem to indicate that between about 90 and 125 or 130 km primarily turbulent phenomena exist, and then on the last curve you show that, for a higher altitude, the result seemed to be pretty close to the molecular diffusion curve. How do you explain this?

Zimmerman: At about 140 km?

Stergis: Or even lower.

Zimmerman: The points on the curve are close, but this is a log plot and a small span on this log plot can be a factor of two. I have made some computations which show that the shear--and I believe Dr. Manring can support me in this--decreases rapidly above 120 km. Am I right, Dr. Manring?

Manring: We've observed turbulence in all of our filaments below about 97 km. In the region from about 97 to 115-120 km, the expansions that are molecular initially (in accordance with what Dr. Stergis said earlier) seem to be molecular for 5 minutes or so and then will suddenly break into a turbulent type of thing. These are very dramatic, particularly when you see them.

Stergis: They suddenly do this?

Manring: Yes, the expansion follows the molecular rule (with a diffusion coefficient for molecular expansion comparable to the computed value) until about 5 minutes, when the cloud suddenly breaks up and the expansion is much faster. There seems to be some sort of

instability there; perhaps the expansion is molecular until the cloud diameter becomes comparable to the eddy size and the expansion after that manifests itself as turbulent. We have observed this break-up up to about 117-120 km--I don't think we've ever observed anything that we could call turbulent about 120 km. We have probably two or three times the data now that we had at the time you looked at this. Most of our newer data shows a slightly smaller coefficient of diffusion and probably fits the curve a bit better, but I think all of it is within a factor of two of the curve, and I'm attributing the behavior essentially to molecular diffusion when we're that close. Some of this data that you have here was obtained on optically dense clouds which are hard to work with. So I think below 97 km our data indicates that there is always turbulence, and we have found the following: If you initially lay out a filament, turbulence manifests itself immediately below about 97 km and there is almost always a high shear in that region. This may just be fortuitous in the sense that there always are shears in this region and perhaps they are not associated with the turbulence, but we feel that some energy is being fed out of the shear region into the turbulent structure.

Zimmerman: In other words, if we assume that the turbulence below 97 km consists of small scale eddies initially, what is the smallest time constant that could be measured before the take over of this turbulent mechanism below 97 km?

Manring: We have a time resolution of about 2 to 3 seconds, and the turbulence shows up immediately.

Zimmerman: This checks pretty well with the numbers we have.

Stergis: Have you noticed any variations in the altitude at which turbulence sets in as a function of latitude? The reason I'm asking this is as follows: Some experiments made primarily by Meadows and Townsend indicate that at White Sands there is no molecular diffusion apparent up to about 137 km, but at Ft. Churchill, Canada, they seem to find molecular diffusion as low as 105 km, so there seems

to be some latitude variation. I wonder whether you have made enough firings at different latitudes to say anything about this.

Manring: We have not. We have observed expansion from New Mexico below this 105 km region. However, I certainly don't think there is enough data at the present time--the rocket program being what it is--to be called statistical.

Dubin:
(NASA) I'd like to ask Dr. Edwards about the early discussion with regard to the vertical motion. There should be a time at which equilibrium would set in for the different constituents as Zimmerman and Manring have shown. Whether the vertical motions could be said to be real or whether they would be temperature or rocket velocity affected is of interest. In particular, are these vertical motions real or not, based on the various analyses you've made so far on the various flights?

Edwards: As far as we know they're real. We have identified specific points in the cloud from two or more stations and have made the calculations with very low residuals from the computer programs and have plotted this as you saw in the diagrams.

Dubin: This is not the question. I certainly agree that your plots and computations are correct--your tracking and everything else is good. The question is, are the motions representative of atmospheric motions or do they represent a residual in the motion or expansion or heating of the cloud itself?

Zimmerman: I don't believe we have enough data to answer this question at the moment. You have to know more about the atmosphere--whether or not turbulence will carry mass upward at a greater rate than it would carry it downward, if you're referring to some mechanism other than the temperature expansion and bubble rise as Dr. Edwards hypothesizes.

Edwards: A more or less microscopic look at the atmosphere in those altitude regions in which we have clouds would be necessary if we are to know the effect which the ambient has on the upward and downward motion of the segments of our Firefly clouds. I'm not sure there is enough known about atmospheric conditions on this small a scale to

separate the atmospheric effects on the clouds from the effects on the cloud itself due to its temperature, the canister detonation and so on.

Dubin: I'd like to ask Mr. Zimmerman a question. In the last slide you showed some computations by Dr. Champion and yourself on molecular diffusion. At higher altitude there was a larger discrepancy between theory and the data than at lower. Can you say that your gas kinetics computation of turbulence using the diffusion equation is adequate for this pressure-density range in the atmosphere, since the gas kinetic computations do assume various conditions, such as the cross sections for scattering, the mean molecular velocity, and various interactions of this nature?

Zimmerman: Well, I don't know if I can answer this too well at the moment--insofar as I know Dr. Champion should answer the question. You asked whether or not the cross sections involved and similar quantities can be assumed to be those given by the simple kinetic theories for the molecular diffusion. I would say off-hand, yes. We have taken the data for the number density and the temperature at these altitudes from rocket flights and this in essence gives an average for the region in question. Hence, any variation over distances small with respect to the averaging length will be more or less smoothed out. In this case we can say our results show what would be, if this were a molecular type of diffusion rather than a turbulent mechanism.

Edwards: I believe Dr. Champion may have a comment on this subject.

Champion:
(AFCRL) Well, first of all I'd like to ask for a clarification of the question--it seems to me it wasn't clear whether the question was in connection with the calculations of molecular diffusion or turbulent diffusion. Could you clarify that, please?

Dubin: Basically what I'm asking is, can you assume that your classical diffusion--your molecular diffusion equations--are valid in this regime of gas kinetics?

Champion: Then the question is purely in connection with molecular diffusion?

Dubin: Yes

Champion: We're not absolutely sure, but I can tell you our feeling. We calculated the molecular diffusion by using theoretical expressions as given in Chapman and Cowling plus experimental values for cross sections for collisions between sodium and air. For cesium and air, I took the values for xenon and air because there were no cross sections given for cesium and air. Xenon has virtually the same mass. The temperatures at these altitudes are within the range in which these quantities were measured in the laboratory. The pressures, of course, are lower. I can only say that it's the best that we can do--we think that the values are reasonably good--it is quite possible if we had more information we would revise them a bit.

Dubin: Yes, but your viscosity problem comes in here too.

Champion: I don't see how.

Dubin: Well, one of the basic ways of measuring diffusion classically down to pressures of a few millimeters is by a viscous technique in the laboratory.

Champion: Yes.

Dubin: And you have a different regime of kinematic viscosity here than you have in any laboratory measurements.

Champion: No. This is not true at all. For example, you know in previous standard atmosphere studies values of diffusion coefficient in viscosity have been stopped at 90 km. The reason for this was that mean free paths then were becoming significant compared with dimensions of aircraft and missiles and so on. However, as far as the motions in the atmosphere we are concerned with are concerned, the mean free paths are small compared to the dimensions you are considering and this is really the only factor that comes in. If you're considering the motion of a missile through this atmosphere, you couldn't use that kind of viscosity coefficient. As far as motions in the atmosphere which involves kilometers and hundreds of kilometers are concerned, there is virtually no change.

Dubin: No. May we put it another way? I guess we can't go into this further, but your time between collisions in the gas differs considerably from what it would be down lower where you normally consider the Chapman-Cowling relationship.

Champion: Yes, but the time between collisions doesn't come into the theory.

Edwards: Perhaps we should go on to other questions. Dr. Marmo?

Marmo:
(GCA) Have you taken photographs of these rises and drops that you see with interference filters to see that you are looking at sodium-cesium? On what grounds can you just discount that the cloud might be just particulate matter. It would be very tempting, you know, to just say that the effects were from particulate matter going up and down and falling and so on.

Edwards: The photographs were taken through #87 Wratten filters which would cut out all radiation except the infrared. Of course, if the matter is particulate and is scattering sunlight in that region we wouldn't know the difference. However, I don't believe that we are looking at particulate matter; I think this is primarily the 8521 Å radiation.

Marmo: But you don't have narrow band interference filter photographs to show this?

Edwards: Yes, we have them. We have photographed these clouds through interference filters which are approximately 100 Å wide at the half power point.

Rosenberg: It is also the case that the optical density of the outer solids is considerably lower in most cases than that of the inner hot gas. The inner hot gas is approximately a kilometer in diameter--with the center located pretty well to one-half kilometer without much doubt.

Edwards: The particulate matter data that I was talking about this morning has not been used in the calculation of position. Position calculations were made from the bright center core, which grew much slower and lasted for 10 to 20 minutes.

Marmo: Dr. Wright, you had sporadic E, natural sporadic E, occurring at the time of the Betsy flight. You showed a slide in which you

indicated considerable electron density up to 5 minutes. How much longer does it go on? Did Betsy give you a longer lasting night-time cloud than other releases within the E-region?

Wright: When you asked about the duration, you were referring to the cloud, not the sporadic E?

Marmo: Yes.

Wright: Betsy lasted longer than a night-time cloud but Betsy was, of course, sunlit after the first five hundred seconds, so it was essentially a dawn cloud from then on. And it did last a long time. However, I don't believe that it lasted any longer than any of the other dawn clouds.

Marmo: How long did those last, roughly? Was it 5 minutes or 10 minutes?

Wright: We observed it to about 3,000 seconds.

Marmo: Probably 5 Mc. return, something like that?

Wright: Yes. Generally the dawn clouds tended to fade out of our antenna pattern.

Marmo: How about the truly night clouds--not ever lit by the sun?

Wright: The typical night cloud lasts approximately 1,000 seconds.

Marmo: And you had none of those occurring when you had a sporadic E of any kind, did you?

Wright: Quite the contrary. Nearly all of the night clouds were in the presence of strong sporadic E.

Marmo: We did some theoretical work on the night-time clouds at 105 and 103 km and it appears that durations should be 200 sec with no sporadic E. It's conceivable that whatever's causing the sporadic E might be enhancing this cloud.

Wright: There was only one night-time cloud in 1959--Oboe. So we don't have much to compare 1959 with 1960 so far as night-time clouds are concerned, but the amount of sporadic E was distinctly less in 1959 than in 1960 and yet there's no important difference between the persistence of Oboe and the other night-time shots.

Zimmerman: Have you tried correlating this with magnetic storms impinging upon the earth?

Wright: I have a slide that I am going to show tomorrow that will show the amount of magnetic activity and solar activity and so forth during both series. Over-all, one can say from the general level of magnetic and solar activity that the general level of ambient ionisation in the E-region was larger in 1960 than in 1959.

Gersen: (DOD) Has any thought been given toward coordinating one of these flights with the appearance of a surveillance-type satellite? For example, during daytime the backscatter for infrared or visible might be appreciably larger than the forward scatter and we may be able to better define the particulate volume from above than from below.

Wright: What is the advantage of observing it from above rather than from below?

Gersen: The backscatter cross section may be different than the cross section of sunlight through the cloud as we see it from the ground. There also may be additional absorption from the ground that we would not get from an observatory located well above the cloud.

Kofsky: (Tech.Op.) I really don't see how, if you're up above, you get anything different from what you get down below.

Eldridge: (Tech.Op.) If you look at the scattered flux coming from a cloud, being illuminated by the sun, and you're looking up at it, you're looking at essentially 90° from the direction the light is coming onto this cloud. If you get up on top and look down at it, you're still looking at 90° . The only advantage is that you don't have the extinction of an atmosphere, but the scattered flux alone is not going to be any different.

FILTER PHOTOGRAPHY AND PHOTOMETRY

Howard D. Edwards and John L. Brown

Engineering Experiment Station
Georgia Institute of Technology
Atlanta, Georgia

FILTER PHOTOGRAPHY

EQUIPMENT

For most of the firings, the K-24 cameras⁽¹⁾ were equipped with either Wratten or interference filters to isolate various spectral lines or regions.

EXPERIMENTAL RESULTS

In Table 1 a summary is given of the data obtained. The numbers 8521, 4555, 5893 refer to interference filters with a transmission of 70% and a pass band of approximately 100 Ångströms. The numbers 25, 15G, 58, 47, 35, and 87 refer to Wratten filters and the notation above the filter number is the color transmitted. Pol V and Pol H denote polaroid filters which are mounted vertically and horizontally in front of the cameras. The numbers in the body of the table indicate the approximate number of minutes for which photographs were taken. A dash in the table indicates that the filter was not used on that particular firing.

DISCUSSION

For those shots on which polaroid filters were used (notably Frances, Hedy and Lily), the duration and intensity of pictures indicated that the scattered light coming from the cloud was not polarized. Densitometric studies of Frances by the photographic technique⁽²⁾ (see Figure 1) show the same intensity for both vertical and horizontal arrangement of the polaroid filters.

Relative intensities for Peggy, Susan, Olive, Lola and Dolly as observed from 5893 Ångstrom sodium radiation and 8521 Ångstrom cesium radiation have been plotted by the photographic technique for times of burst, 30 seconds, 1 minute, 2 minutes and 4 minutes.

- - - - -

(1) These cameras are described in detail in another section of this report entitled "Position, Drift and Growth from Photography" by H. D. Edwards, Georgia Institute of Technology.

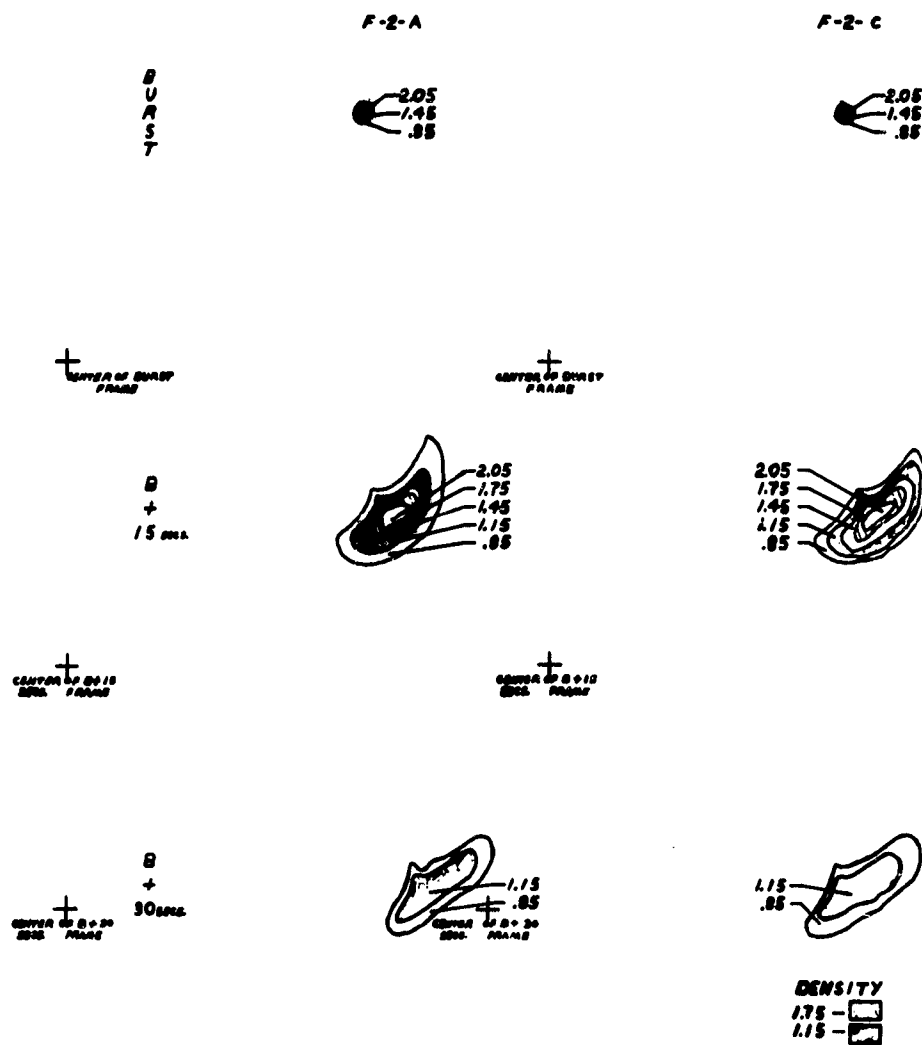
(2) This technique was perfected by Lt. Smith and Dr. Rosenberg of the Photochemistry Laboratory, GRD.

Table 1: Spectral Data (K-24 cameras)

No.	Firefly	Cs 8521	Cs 4555	Na 5893	Red 25	Yel 150	Green 58	Blue 47	Purple 35	IR 87	Pol V	Pol H	No Filter
1	Cathy	1	0	$\frac{1}{4}$	-	-	0	-	-	$1\frac{1}{4}$	-	-	$\frac{1}{2}$
2	Betsy*	-	20	-	-	20	2	-	-	20	-	-	-
3	Amy	$\frac{1}{4}$	0	$\frac{1}{4}$	-	-	0	-	-	2	-	-	2
4	Ruth	$\frac{1}{4}$	0	0	-	-	$\frac{1}{2}$	-	-	$\frac{1}{2}$	-	-	$1\frac{1}{4}$
5	Gerta	-	0	-	-	-	-	1	-	1	-	-	4
6	Margie	-	11	15	-	11	-	-	-	11	-	-	-
7	Marie	-	11	11	-	11	5	-	-	11	-	-	-
8	Lola	-	4	4	-	4	-	-	-	4	-	-	-
9	Zelda	No data; daytime firing											
10	Peggy	-	5	12	-	6	-	-	-	12	-	-	-
11	Olive	-	5	5	-	5	-	-	-	10	-	-	-
12	Jeannie	-	5	5	-	5	3	-	-	11	-	-	-
13	Susan	-	4	7	-	4	-	-	-	17	-	-	-
14	Dolly	15	10	8	-	-	5	$\frac{1}{4}$	-	15	-	-	6
15	Janet	-	$\frac{1}{60}$	0	-	-	0	$\frac{1}{4}$	-	15	-	-	1
16	Hilda	-	$\frac{1}{4}$	0	-	$\frac{1}{2}$	$\frac{1}{60}$	-	-	12	-	-	-
17	Teepee Anne	-	-	-	0	-	0	0	-	-	-	-	0
18	Teepee Norma	-	-	-	$\frac{1}{6}$	-	0	-	-	-	-	-	$\frac{1}{2}$
19	Carry	-	-	-	$\frac{1}{4}$	$\frac{1}{4}$	-	$\frac{1}{60}$	-	-	$\frac{1}{60}$	$\frac{1}{60}$	$\frac{1}{60}$
20	Arlene	-	-	-	-	$\frac{1}{60}$	-	-	-	-	-	-	$\frac{1}{4}$
21	Rena	No data; daytime firing											
22	Linda	No data; was not observed											
23	Mavis	-	-	-	-	-	$1\frac{1}{2}$	$1\frac{1}{2}$	-	0	$\frac{1}{2}$	$\frac{1}{2}$?	-
24	Frances	-	-	-	1	-	1	1	-	1	$1\frac{1}{4}$	$1\frac{1}{4}$	-
25	Lily	-	-	-	1	-	1	1	-	1	1	1	-
26	Hedy	-	-	-	$1\frac{1}{2}$	-	$1\frac{1}{2}$	$1\frac{1}{2}$	$1\frac{1}{2}$	$1\frac{1}{2}$	$1\frac{1}{2}$	$1\frac{1}{2}$	$1\frac{1}{2}$
27	Ida	-	-	-	$\frac{1}{2}$	-	$\frac{1}{4}$	$\frac{1}{4}$	$\frac{1}{4}$	$\frac{1}{2}$	$\frac{1}{4}$	$\frac{1}{4}$	$\frac{1}{2}$

* Betsy was visible for approximately 2 minutes. It then faded and built up at the B + 4 to 6 min point when the solar horizon reached the Cs-Na.

Fig. 1. **FRANCES**
 F-2-A V-POL
 F-2-C H-POL



The intensity plots for Olive are presented in Figures 2 and 3 and show that the more intense centers of 5893 Angstrom radiation coincide with the bright centers for 8521 Angstrom radiation. Lola and Susan are similar to Olive.

Peggy, shown in Figures 4 and 5, is somewhat different since the location of the most intense sodium radiation is at the opposite end of the cloud from the intense cesium radiation.

PHOTOMETRY

GENERAL

Some encouraging results were obtained from photometric studies of clouds and shockwaves of the Firefly series in the fall of 1959 using the GRD 20" photometer. The primary drawback to the instrumentation was slow response time and inability to rapidly interchange filters for spectral measurements.

The entire photometer system was modified for the Firefly 1960 series to eliminate these drawbacks.

DESCRIPTION OF EQUIPMENT

The mounting and mirror system of the GRD 20" photometer form essentially a reflecting telescope on an altazimuth mounting with a photomultiplier tube at the prime focus. The mechanical modifications to the system provided a rotating filter wheel driven by a synchronous motor at 600 rpm. The wheel contained 5 equally spaced openings near the periphery which would accept 2" x 2" filters. Provisions were included for balancing the wheel to allow for different types of filters. A magnetic pickup recorded the wheel position on the final data chart to allow correlation of filter and signal peak on the data chart.

Optical modification consisted of a simple telecentric lens system to provide a plane wave front for nearly parallel transmission through interference filters. The constants were such that the relative aperture of the photometer was not lowered, and maximum deviation from parallelism of wave front and filter surface was only 7° for a 1 degree photometer field.

Electronic modifications included the use of photomultiplier amplifiers with logarithmic amplitude response and better than 10 millisecond rise time. The output was fed into a model 1108 visicorder.

Both the Dumont 6363 and CBS 1002 photomultiplier tubes were used. These tubes have the S-11 spectral response.

Fig2. OLIVE

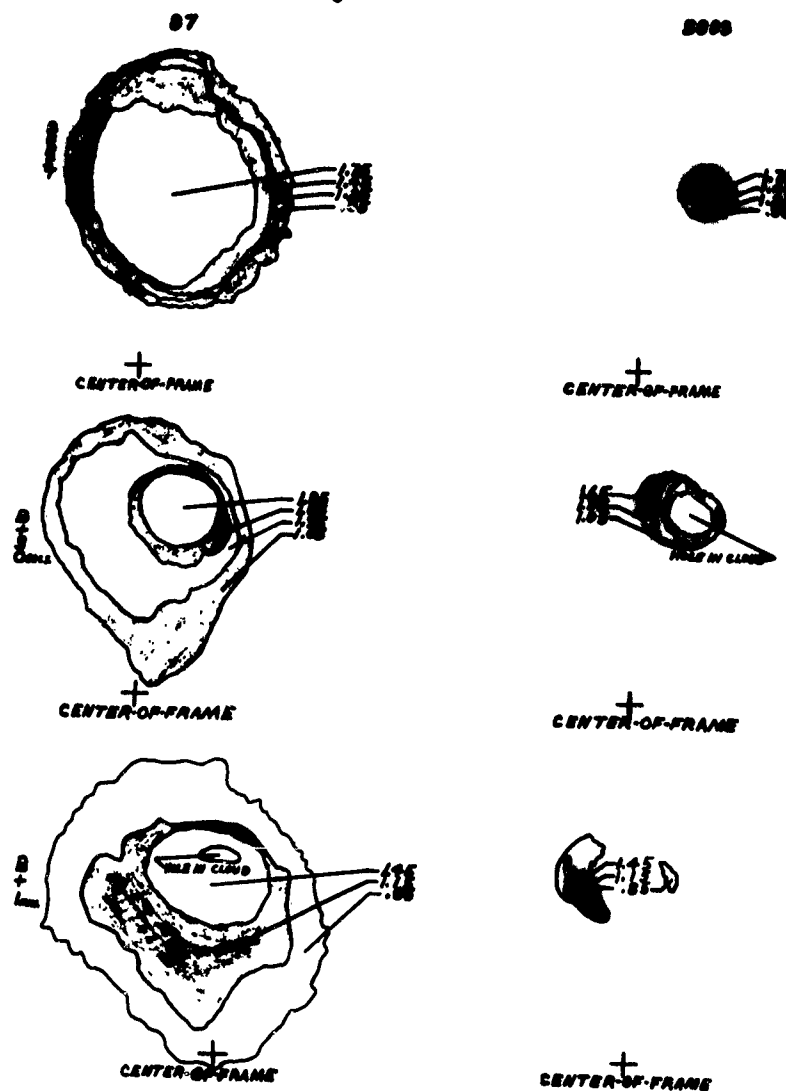
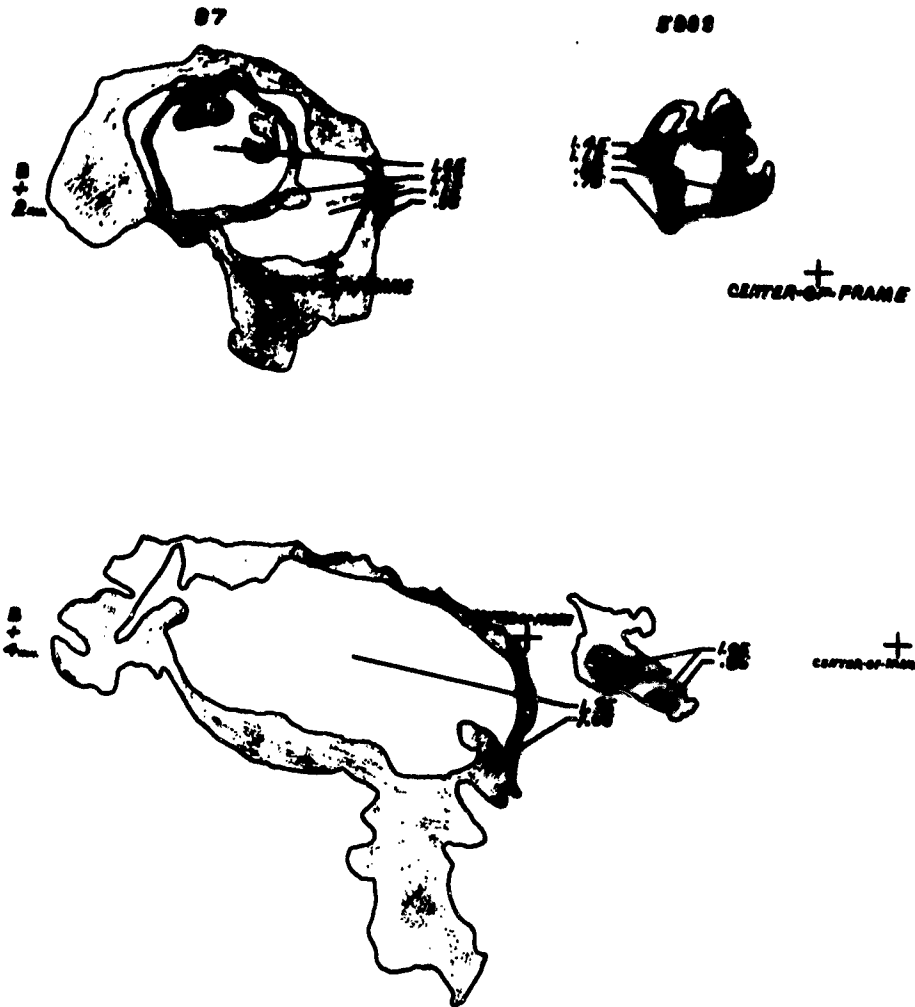


Fig 3. OLIVE



3024

Fig 4. PEGGY

87



CENTER OF FRAME

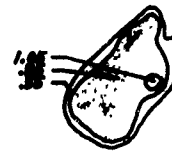
5883



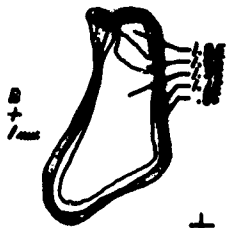
CENTER OF FRAME



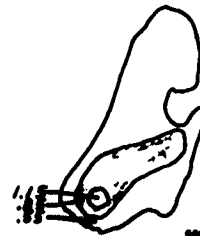
CENTER OF FRAME



CENTER OF FRAME



CENTER OF FRAME

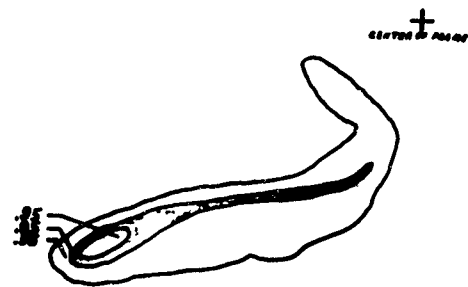
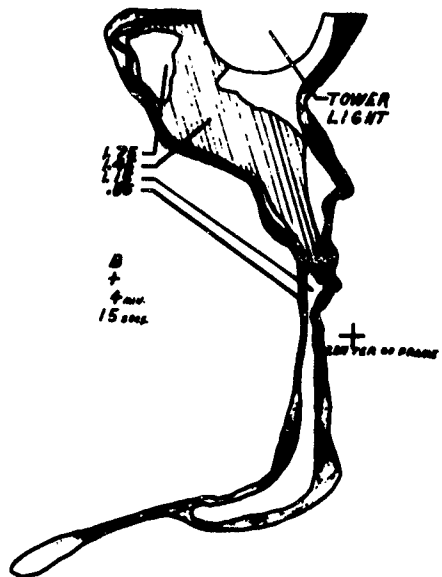
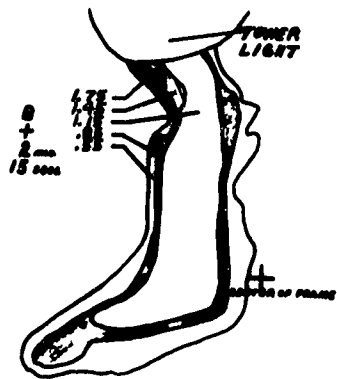


CENTER OF FRAME

Fig 5. PEGGY

87

5000



3008

OPERATING TECHNIQUES

For shockwave studies the photometer was aimed in accordance with predicted azimuth-elevation figures by means of graduated circles on the mount. Using a $1/2$ degree field it was considered unlikely that the release would ever occur in the field of view. This proved to be true. As the shockwave moved through the field of view its emission would be rapidly sampled by the rotating filter wheel containing interference filters.

For solar scatter measurements the photometer was aimed by a sighting telescope at the brightest visible part of the cloud. The filter wheel was equipped with Wratten filters to sample various regions of the spectrum.

SOLAR SCATTER RESULTS

Each shot will be discussed separately.

(1) Francesa. For this shot no filters were used; the filter wheel was stationary in the open position. Amplitude response versus time from burst are shown in Figure 6.

(2) Lily. Wratten filters nos. 25, 35, 47, and 58 were used on this shot. Relative amplitudes in the various spectral regions are shown in Figure 7. No response was recorded from filter no. 25 since the photomultiplier tube has very low red sensitivity.

Lily was observed at an elevation corresponding to an optical air mass $m = 1$. From the solar spectral irradiance curves the ratio of 4400 \AA to 5300 \AA for $m = 1$ is approximately 0.8. These wavelengths correspond to the transmission peaks of Wratten filters nos. 47 and 58. The initial amplitude ratio of these filter responses is about 1.06. This indicates a higher blue response than the solar curve. A particle size analysis of the SS 2 material shows that approximately 50% of the particles are less than 1500 \AA in size and therefore effective in scattering at the blue end of the spectrum. This may account for the high blue response.

(3) Hedy. Wratten filters nos. 25, 35, 47 and 58 were again used and the results are shown in Figure 8.

The ratio of 47 to 58 filter response is 0.56 indicating a higher amplitude in the 5300 \AA region than that of the solar curve. The particle size analysis for the ODS material shows the size of greatest frequency to be around 2500 \AA with 62% of the particles below 5600 \AA . This size would be more effective in scattering in the range covered by the Wratten 58 filter.

Fig. 6 FRANKS SS 1

Solar Scatter

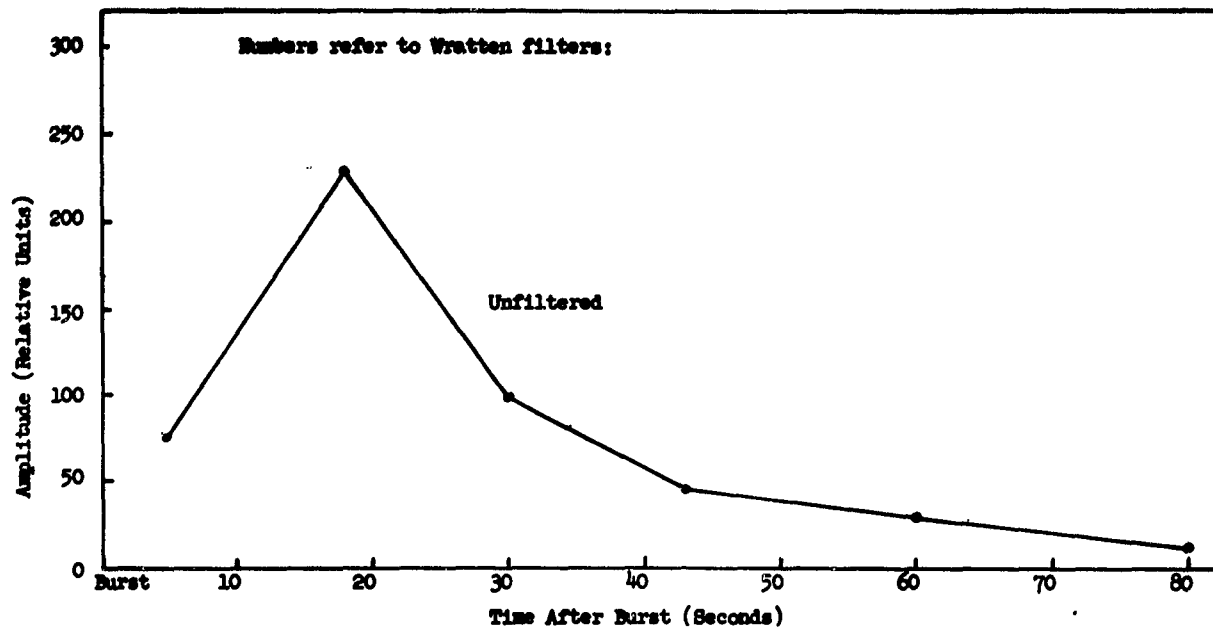


Fig. 7 LILY SS 2

Solar Scatter

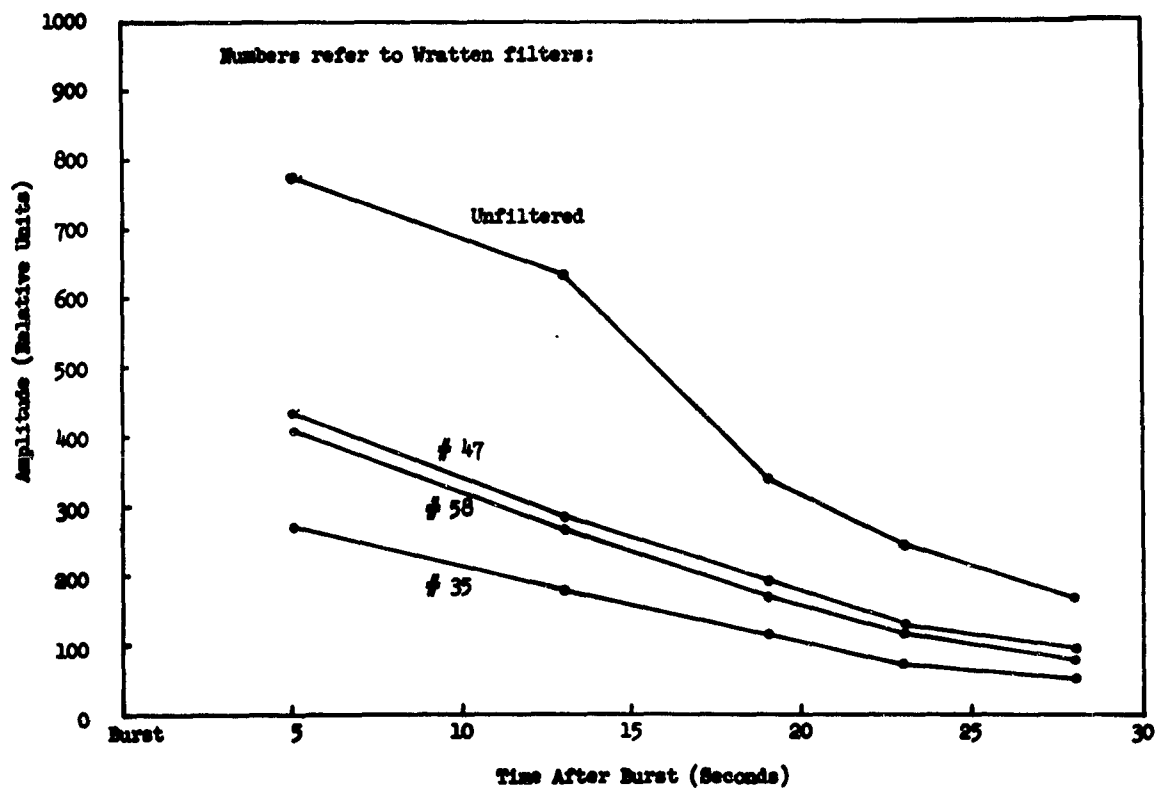
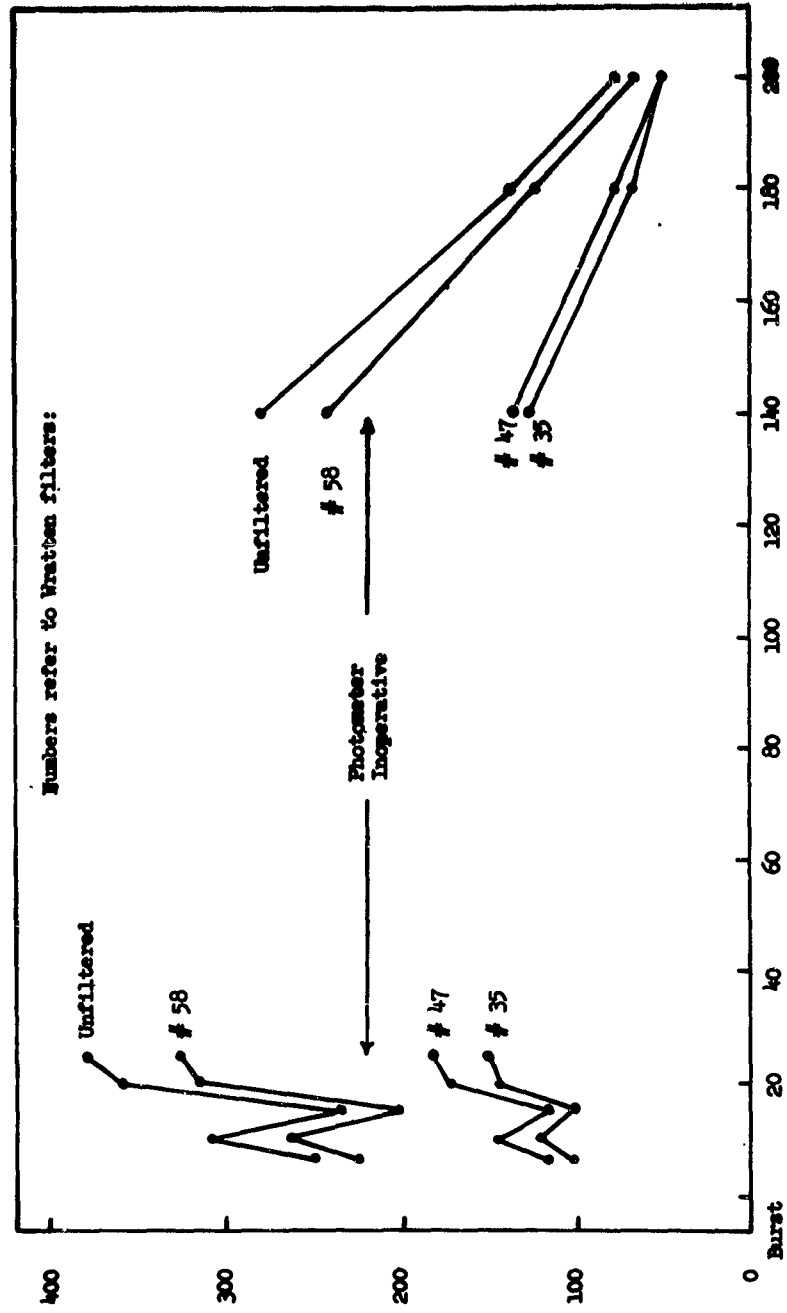


Fig. 6 MEV CAS
Solar Scatter



SHOCKWAVE OBSERVATIONS

1960 releases were disappointing from the viewpoint of shockwave observations when compared to the 1959 series. We did not observe a single clear distinct shock ring such as was observed on several of the 1959 releases.

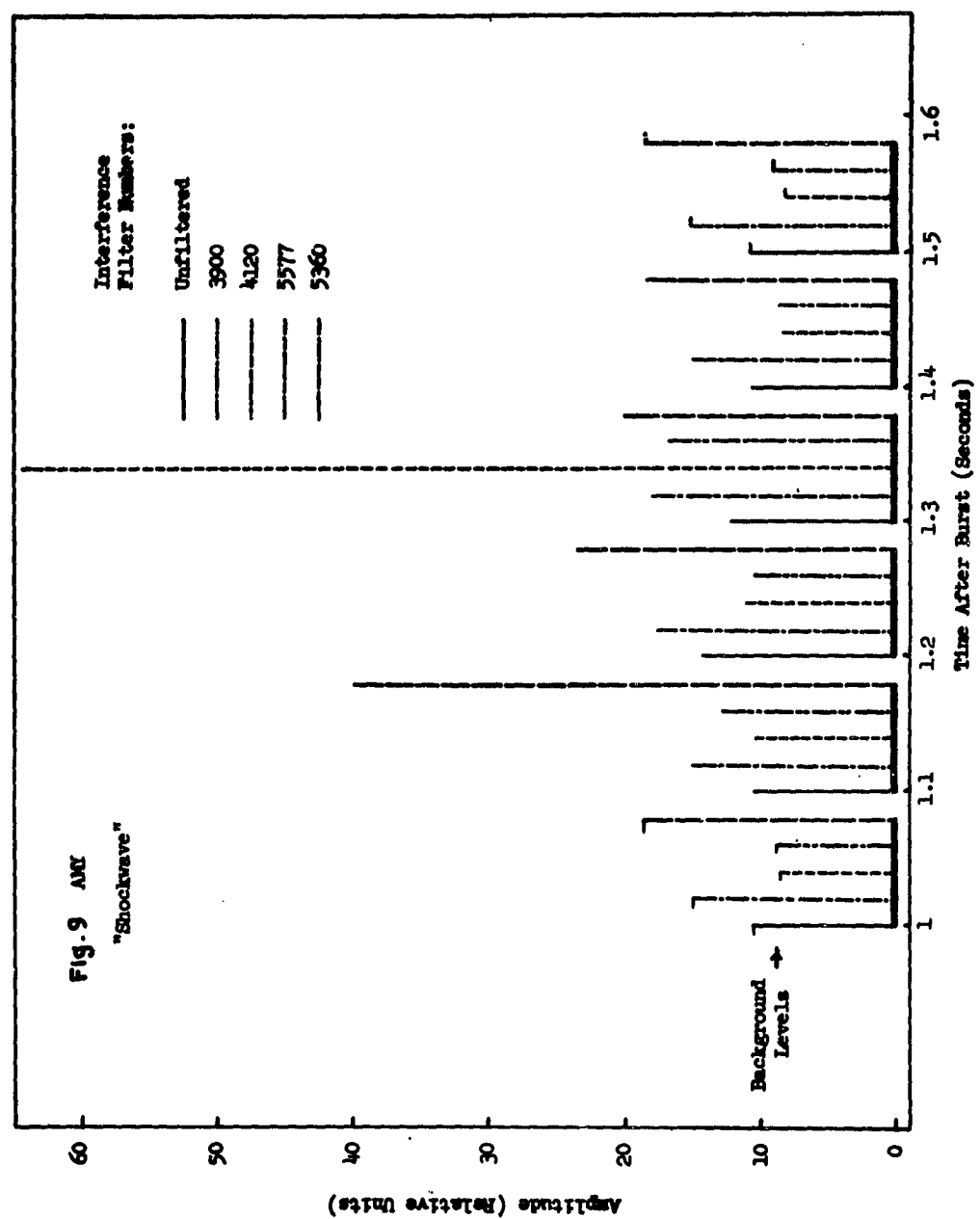
Hence the photometer with its narrow field of view and interference filters did not have an opportunity to record much in the way of shockwaves. The only shot on which a possible shockwave was observed was Amy and for it the observations are strange. The shockwave velocity is approximately 10 km/sec which is twice as fast as those observed in 1959. For the Amy firing the filter wheel was equipped with a filter at 3900 Ångstroms to isolate the H_2^+ first negative band and another at 4120 Ångstroms to measure sky background near the 3900 band. Two additional filters, one peaked for the oxygen green line at 5577 Ångstroms, the other for background observations at 5360 Ångstroms, were installed in the filter wheel.

All filters were recording steady signals due to background prior to the shockwave transit as shown in the first series of bars in Figure 9. During the shockwave transit the amplified output from the filters varied considerably. Between $B + 1.1$ sec and $B + 1.2$ sec the output from the 5577 filter almost doubled as did that for the 5360 Ångstrom region. The output from the 4120 filter and the unfiltered channel also increased. Between $B + 1.2$ sec and $B + 1.3$ sec there was a decline in output from the 5360 and 5577 filters as well as the open hole. However, output from the 4120 and 3900 regions showed a rise. Between $B + 1.3$ sec and $B + 1.4$ sec the output from the 4120 Ångstrom filter increased by 6 fold and the 5577 by 50% over its previous value. The opening without filter showed a decrease in output. Obviously the open hole could see more radiation than the 4120 filter, hence it is concluded that the 4120 and 5570 signals were either spurious or of such short duration that the change in intensity took place in less than $1/100$ sec. After $B + 1.5$ sec all filters returned to normal background reading.

A wide angle unfiltered photometer was adjacent to the filter wheel photometer and observed the same two strong peaks at approximately $B + 1.16$ sec and $B + 1.35$ sec.

Calculations⁽³⁾ have shown that the oxygen forbidden transition at 5577 Å would likely occur in the shockwave. In spite of the apparent agreement with theory, it is unwise to conclude that the 5577 radiation was present in the Amy release. It is hoped that 1961 releases will clear some of the mysteries which now exist in shockwave spectral characteristics.

(3) "Position, Growth and Spectral Distribution from Photography of Firefly 1959 Chemical Clouds," Technical Report No. 4, Contract No. AF 19(604)-5467, 15 June 1960. H. D. Edwards.



SPECTROGRAPHIC DATA

H. D. Edwards

Engineering Experiment Station
Georgia Institute of Technology
Atlanta, Georgia

EQUIPMENT

A Bausch and Lomb plane transmission grating with 600 grooves/mm and blazed for a first order wavelength of 5500 \AA was mounted in front of a 35 mm Eyma movie camera. The camera was equipped with an f/1.1 50 mm Nikon lens and used Royal-X Recording film. The grating and movie camera were used without a slit and hence the full image of the firefly cloud was focused on the film.

The equipment was installed on the searchlight camera mount at site F-2 and the camera operated for about 60 seconds per firing at 4 frames per second.

EXPERIMENTAL RESULTS

Spectrographic coverage was provided for all Firefly shots beginning with Gerta and extending through Olive. Spectra were recorded for Jeannie, Margie, Lola, Peggy, Susan and Olive.

The spectrograms taken of Peggy, Susan and Jeannie show only a continuum while those for Margie, Lola and Olive show several lines in addition to the continuum.

Identification of the lines is in doubt due to misalignment of the grating.

No attempt has been made to include prints of the spectrograms since the lines are faint and reproduction would undoubtedly be ineffective.

A detailed description of the spectrum as a function of time will be given for each shot.

(1) Peggy. The spectrum recorded for the burst frame ($1/4 \text{ sec} > \text{time} > 0$) shows a continuum of medium intensity but no evidence of lines.

By the second frame ($1/2 \text{ sec} > \text{time} > 1/4 \text{ sec}$), the spectrum became fainter. This fading continues until the spectrum is very faint at 3 seconds after release but is still visible for the duration of camera operation or 60 seconds.

(2) Susan. The spectrum of the burst frame shows a faint continuum with no lines. The spectrum rapidly fades and is no longer visible 1 second after burst.

(3) Jeannie. The spectrum of the burst frame shows a bright continuum with no lines.

The spectrum grows fainter with time and has disappeared by 5 seconds after burst.

(4) Margie. The spectrum of the burst frame shows a bright continuum as well as 3-6 bands or lines. The line spectrum has disappeared by the second frame or within the first 1/4 second after burst. The continuous spectrum remained for the duration of movie camera operation or 60 seconds.

(5) Lola. The spectrum of the burst frame has a bright continuum as well as 10-15 bands or lines. For the 2nd frame ($1/2 \text{ sec} > \text{time} > 1/4 \text{ sec}$), the spectrogram shows the same continuum and lines as for the first frame. By burst plus 1 second, the lines have disappeared but the continuum remained throughout the observing time or 60 seconds.

(6) Olive. The burst frame contains a continuum as well as two bright lines. By the second frame, or within the first 1/4 second after burst, the lines have disappeared and only the continuum remains. The continuum diminishes in intensity and disappears by burst plus 2 seconds.

DISCUSSION

In comparing our crude but short exposure time spectra with the more refined but long exposure time measurements made by Dr. C. D. Cooper of the University of Georgia⁽¹⁾ and reported to the Firefly group in October 1960, a number of interesting differences are observed.

The exposure time for our spectrograms was less than 1/4 second and the camera operated at 4 frames per second whereas Dr. Cooper's spectra were obtained with exposure times greater than 10 seconds.

On the six firings for which we have comparable data, the two sets of data are not in complete agreement.

For Margie we observed a bright line spectrum as well as a continuum for the first 1/4 second. Thereafter, we observed only the continuum, or solar scatter. Dr. Cooper observed only the continuum.

For Lola we observed line spectra for the first 1/2 second and thereafter only the continuum. Again Dr. Cooper observed only the continuum or solar scatter.

For Peggy, Susan and Jeannie we observed only continuum whereas Dr. Cooper reports lines due to Na and Cs and bands due to AlO.

For Olive we observed two bright lines during the first 1/4 second and thereafter only

(1) See report by Dr. Cooper in this publication.

the continuum. Dr. Cooper found lines from Cs and Ba as well as bands of AlO but very little solar scatter.

Further attempts will be made to identify our spectral lines and the results compared to Dr. Cooper's and other spectral data.

FINELY 1960 SPECTROGRAPHIC DATA

C. Dewey Cooper

Physics Department
University of Georgia

ABSTRACT

Spectrograms of the PEC and TEC releases show the resonant lines of sodium, cesium and in some cases lithium. AlO is detected in some of the releases and the bands are assigned to the $A^2\Sigma \rightarrow X^2\Sigma$ transition. Relative intensity measurements of the cesium 4555A and 4593A lines indicate that the excitation of these lines is not entirely due to resonant scattering.

1. EQUIPMENT

Releases of chemicals in the upper atmosphere may be studied by the light which they emit or scatter. Spectrograms of the observed light can provide information relative to the composition of the ambient and the products resulting from the releases. Spectrographs which use slits provide the maximum spectral information, but their total light gathering power is limited by the entrance slit. The following spectrographs were used in the stated spectral regions: visible - f/1.8 camera lens with a fixed 50 micron slit; visible, auroral type, f/0.8 Schmidt type camera lens with an adjustable slit; and in the ultraviolet - f/2.5 camera lens with a fixed 50 micron slit. Telescopic lenses were used to image the light on the slit and the field of view was about one-half of a degree. For the earlier experiments an attempt to use the auroral spectrograph as a spectrometer failed to record the desired spectra.

2. EXPERIMENTAL RESULTS

A. Spectra of Rocket Releases.

Spectrographic coverage was provided for all of the night or twilight releases. Spectra were recorded for PEC or TEC releases only. All other releases failed to produce a detectable exposure on the spectrographic film. From a visual observation, the glow which persisted for about two minutes for Amy should have been recorded by our spectrograph if line or band emissions were predominate. The failure to detect a spectrum indicates that the glow represents a continuum. The observed spectral lines for each rocket are shown in Table I.

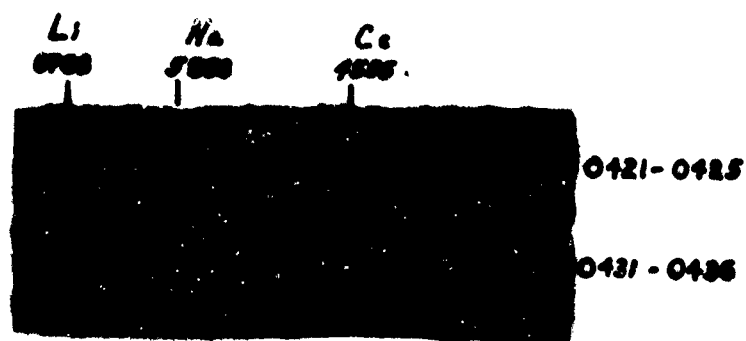
TABLE I
OBSERVED SPECTRA FIREFLY 1960

Rocket Code Name	Na 5890	Cs 4593	Cs 4555	Cs 3876	Cs 3611	A10 Bands 4648 4842 5079	Solar Scatter	Other Lines		
Margie							x			
Marie							x			
Lola							x			
Peggy	x	x	x				x	5845 6150	6180? 6220	6305 6360
Olive	x	x	x				x			
Jeannie	x	x	x	x	x	x	x	5845	6200	6280 6360
Susan	x	x	x			x	x			
Dolly	x	x	x	x			x		Li 6708	
Betsy	x	x	x				x			

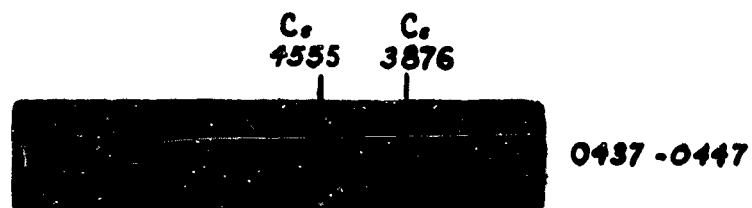
The resonant lines of cesium, sodium, and lithium were to be expected from preceding experiments if the atoms were present in the release. The appearance of the A10 bands confirms an earlier observation¹ of a band at 4850A which was tentatively assigned to A10. The use of 1 and 2 mm slits on the auroral spectrograph favored the recording of bands or continua and produced three groups of the A10 bands as shown in Fig. 2. Eight different vibrational bands are observed. The A10 4842 band as observed with the 50 micron slit spectrograph is shown in Fig. 1 for the Susan release. A10 radiation was observed for a period of 3.5 minutes following the burst.

Generally the $f/1.8$ visible spectrograph with the 50 micron slit was used to provide relative intensity data for various atomic lines. For Jeannie, a Kodak Type 103A-D film was used and the results show the 4555A, 4593A, and 3876A cesium lines to have the relative intensities 15, 5, and 1, respectively. Usually, Type 103A-F film was employed and the first exposure of 5 minutes was followed by successive exposures of 2 minutes each. The intensities, on an arbitrary scale, of the observed lines are presented in Table II for

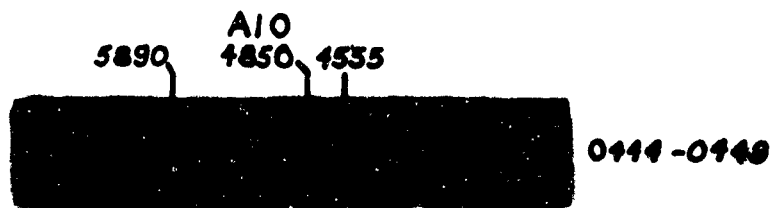
¹Project Firefly 1959, Part I: Optical Studies. Geophysics Research Directorate, AFMRC, ARDC, Bedford, Mass., Page F1.



DOLLY



JEANNIE



SUSAN

Fig. 1 Representative spectra of PEC releases using a 50 micron slit.

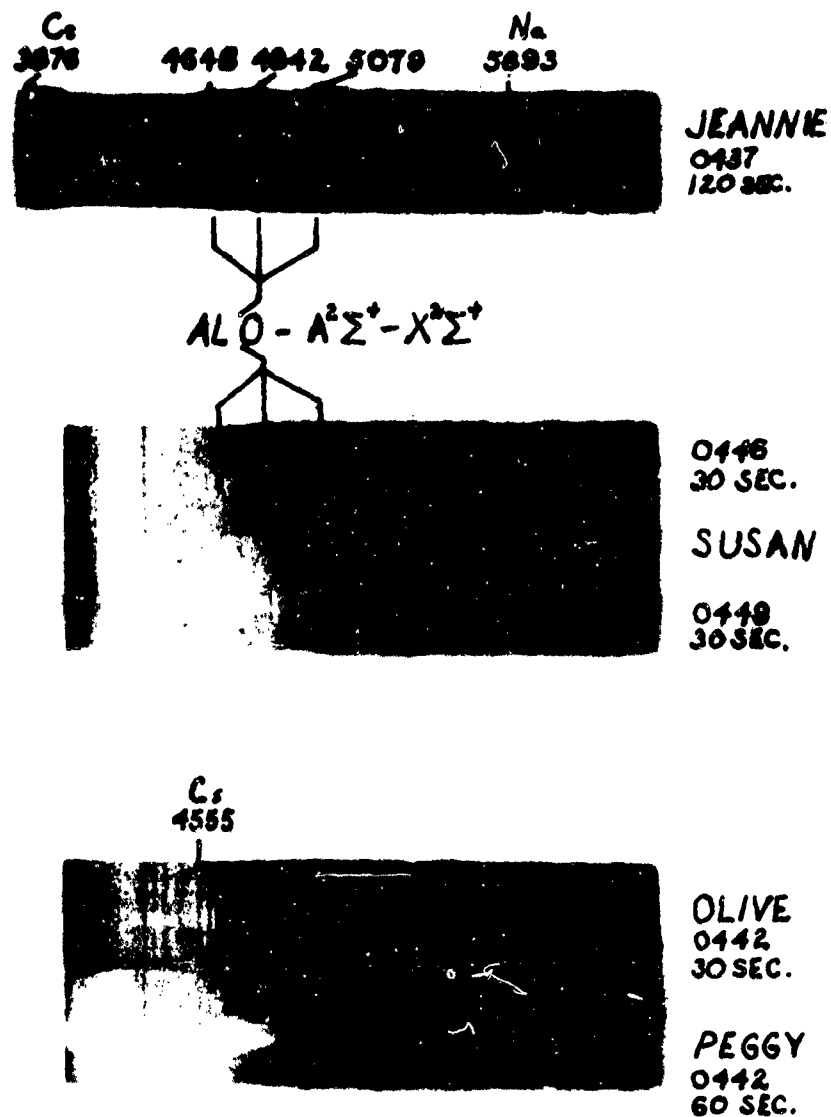


Fig. 2 Representative spectra of PEC releases using a 1 mm slit and the f/0.8 camera.

several releases. These intensities have been corrected for different exposure times and background intensities.

TABLE II
INTENSITIES OF EMISSION LINES OPERATION FIREFLY 1960

Rocket Code Name & Time	Intensity Na 5893A	Intensity Cs 4553A	Intensity Cs 4593A	$\frac{I \text{ Na } 5893}{I \text{ Cs } 4553}$	$\frac{I \text{ Cs } 4553}{I \text{ Cs } 4593}$
PEGGY					
0442-0447	4	5	2	0.8	2.5
0447-0449		15	5		3.0
0449-0451		25	5		5.0
0451-0453		37?	8		4.6
OLIVE					
0442-0447	6	4	2	1.5	2.0
SUSAN					
0442-0447	22	9	7.1	2.4	2.0
0447-0449	18	9	4	2.0	2.2
0449-0451	16	10	3	1.6	3.0
0451-0453	10	13?		0.8	
DOLLY					
0422-0426	10	14	4	0.7	3.5
0426-0431	7	19	4	0.4	4.7
0431-0436	4	27		0.2	

Intensity data cannot be obtained from the spectrograms taken with the auroral spectrograph because the lines of interest are strongly overexposed. However, it can be said that for the first 30 seconds on Susan the total radiation from the A10 bands is greater than that from either of the visible cesium or sodium lines.

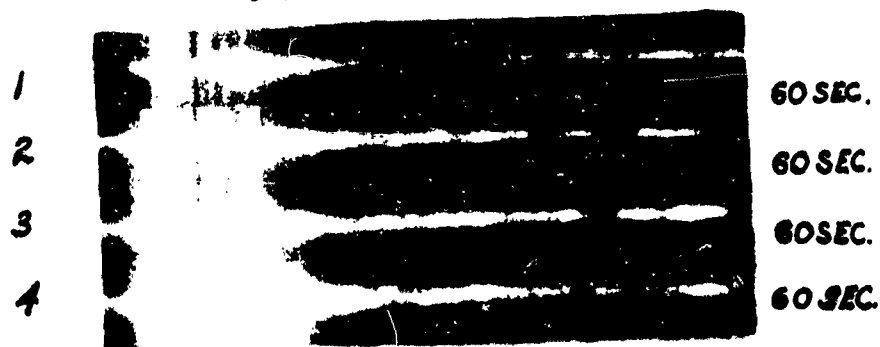
The three low altitude releases, Margie, Marie, and Lola show only continua which appear to be solar scatter. Definitely, Lola acted primarily as a solar scatterer as is indicated by the strong Fraunhofer lines in the properly exposed spectrogram. Over exposure on both Marie and Margie prevents the distinguishing between a continuum and solar scatter during the first two or three minutes. It is of interest to note that considerable solar scatter was observed from Peggy along with resonance radiation from Na and Cs. However, Olive which was only 4 km higher shows very little solar scatter, see Fig. 2.

Referring again to Table I, we see that additional spectra lines or bands were

C. 3004



LOLA
3900 - 6550 A



MARGIE
3900 - 6550 A



MARIE
3350 - 6000 A

Fig. 3 Spectra showing intense continua or solar scatter for the low altitude rocket.

observed for Peggy and Joannie. Of the lines recorded, the 5845, 6210, and 6355A lines are observed on both spectrograms. The error in the wavelengths of these lines does not exceed 210Å.

B. Spectra of Ground Test Releases of RDX, Al and CsNO_3 .

Mr. John Brown of Georgia Tech obtained spectra of various explosive Al + CsNO_3 test-type releases during the experimental ground testing program. We aided in the analysis of these spectra. Our combined efforts show that the test release did not produce a spectrum of ionized cesium as reported earlier by Arthur D. Little². Arthur D. Little has rechecked their spectra and found that their original spectra assignments were incorrect and only CaI lines were obtained. In the earlier report, they had noted that there was insufficient energy available from the chemical reaction to produce the excited cesium ions.

The spectra obtained in the tests show that levels within 0.2 e.v. of the ionization level of cesium are excited; therefore, we can conclude that cesium ions would be formed in the explosion, but there is no evidence for the existence of excited cesium ions.

3. DISCUSSION

The recorded resonant lines of sodium, cesium, and lithium serve to show whether these substances were present in their atomic states. Relative intensity measurements of various atomic lines can be used to check on the type of excitation mechanism involved. According to the known f values the intensity ratio of the 4555Å and 4593Å lines should be 4 to 1. Successive exposures for the same rocket show that the relative intensity of these two lines is about 2 to 1 for the first five minutes and gradually increases with time to about 5 to 1. For Dolly and Susan the 4555Å line increases in intensity for the last exposure (see Table II) and the 4593Å line is barely detectable. At first sight it would seem that the data on the first exposures could be interpreted to mean that the cloud is dense enough to absorb and scatter all of the 4555Å radiation which enters it. This hypothesis breaks down whenever we note that the intensity of the 4555Å line is not as great as that of the sodium 5893 line. If all of the available 4555Å radiation was scattered, the intensity of this wavelength should be much greater than that of the 5893Å line because about 95% of the 5893Å solar radiation is absorbed by the sun's atmosphere and a Cs 4555Å Fraunhofer absorption line has not been ob-

²Project Firefly 1969, Part II, Geophysics Research Directorate, AFCEC, ARDC, Bedford, Massachusetts.

served in solar radiation. A satisfactory explanation of the recorded variation in relative intensities with time is not readily available, but the data indicate that the excitation mechanism for the blue lines of cesium is only partly due to resonant scattering.

The appearance of AlO bands shows that AlO is often a by-product of the RDX, aluminum, cesium nitrate reaction. The persistence of this radiation for 3 or 4 minutes indicates that it results from a resonant scattering of sunlight. The observed bands are the 0,0; 1,0; 0,1; 1,1; 2,2; 2,1; 3,2; and 2,3 bands of the $A^2 \Sigma \rightarrow X^2 \Sigma$ transition. If chemical releases can be planned which will release primarily AlO, then its spectrum can be used to determine the temperature of the upper atmosphere. A spectrograph with sufficient dispersion to resolve the rotation lines can be used to determine rotational line intensities. These data can be used to determine the temperature for the release altitude.

From a practical point of view, the trail of solid fuel rockets which use aluminum should be checked for the presence of AlO.

Most of the red lines which were observed for Peggy and Jeannie are still unassigned. Two of the lines, 6305A and 6360A, are assigned as the oxygen red lines which are usually observed in the night air glow.

Near Infrared Photometry of Artificial Clouds

Radiation Effects Branch
Thermal Radiation Laboratory
Air Force Cambridge Research Laboratories

Summary Prepared by:

Ralph G. Eldridge*
Technical Operations, Inc.
Burlington, Mass.

John D. Armitage, Jr.**
Radiation Effects Branch
Thermal Radiation Laboratory
AFCRL, Bedford, Mass.

and

J. H. Taylor†
J. J. Freymouth
J. L. Streete
Southwestern at Memphis
Memphis, Tenn.

The brightness of solar illuminated artificial clouds as a function of time is presented. The spectral region of observation is 0.8 to 2.3 microns wavelength. The attempt to infer a spectral change with time results in approximating that which would result with or from a rising sun.

* Supported by Contract AF 19(604)-6140, Thermal Radiation Laboratory, AFCRL.

** A more complete technical report on this data is being prepared by Project 7674, "Thermal Radiation from Nuclear Weapons", for submission to the Defense Atomic Support Agency (DASA).

† This research was supported by Contract AF 19(604)-4953, Thermal Radiation Laboratory, AFCRL, funded by the DASA through Project 7674, "Thermal Radiation from Nuclear Weapons". A comprehensive report is available in the Quarterly Status Report dated 1 January 1961.

Introduction

Measurements of the near infrared radiation from artificial clouds above 100 Km altitude were made during Project Firefly by Project 7674, "Thermal Radiation from Nuclear Weapons and Environmental Effects." Data were obtained by two groups: the Radiation Effects Branch of the Geophysics Research Directorate (John Armitage**) and Southwestern at Memphis (Dr. John Taylor†).

The Geophysics Research Directorate team used a radiometer built by Technical Operations, Inc. This instrument employed a PbS detector which viewed the artificial cloud through a 60-in "Search Light" optical system. The collecting optics and the 1-in square detector were so configured that the field of view was 2.4 degrees. Provision was made for rotating a series of transmission filters between the detector and the 90 cps chopper assembly.

The radiometer operated by Southwestern at Memphis used a 10 by 10 mm PbS detector, and a 60-inch focal length mirror system resulting in a square field of view of 0.372 degrees on a side. Transmission filters were also introduced in front of the PbS detector.

Figure 1 shows the detector-filter spectral response of the Geophysics Research Directorate radiometer. Figure 2 shows the response of the Southwestern at Memphis radiometer with 2.2 precipitable centimeters of water considered as an additional filter.

Observed Brightness Data

The observed near infrared radiation data are plotted as brightness ($\text{watts cm}^{-2} \text{ster}^{-1}$) as a function of time (in seconds) from release of the cloud material. The reduction of the energy to a brightness represents an approximation because no consideration has been given for the extinction of the radiation by the intervening atmosphere or the fact that most of the "clouds" did not fill the instrumental field of view of 2.4° for at least the first 50 seconds of existence; and in some cases not until 200 seconds had elapsed after release. This situation is not true in the case of the data observed by Southwestern at Memphis since their radiometer had a smaller field of view. Jack Taylor approximated the atmospheric path by assuming the presence of 2.2 cm of precipitable water and applied this to his filter factor corrections.

FIGURE 1

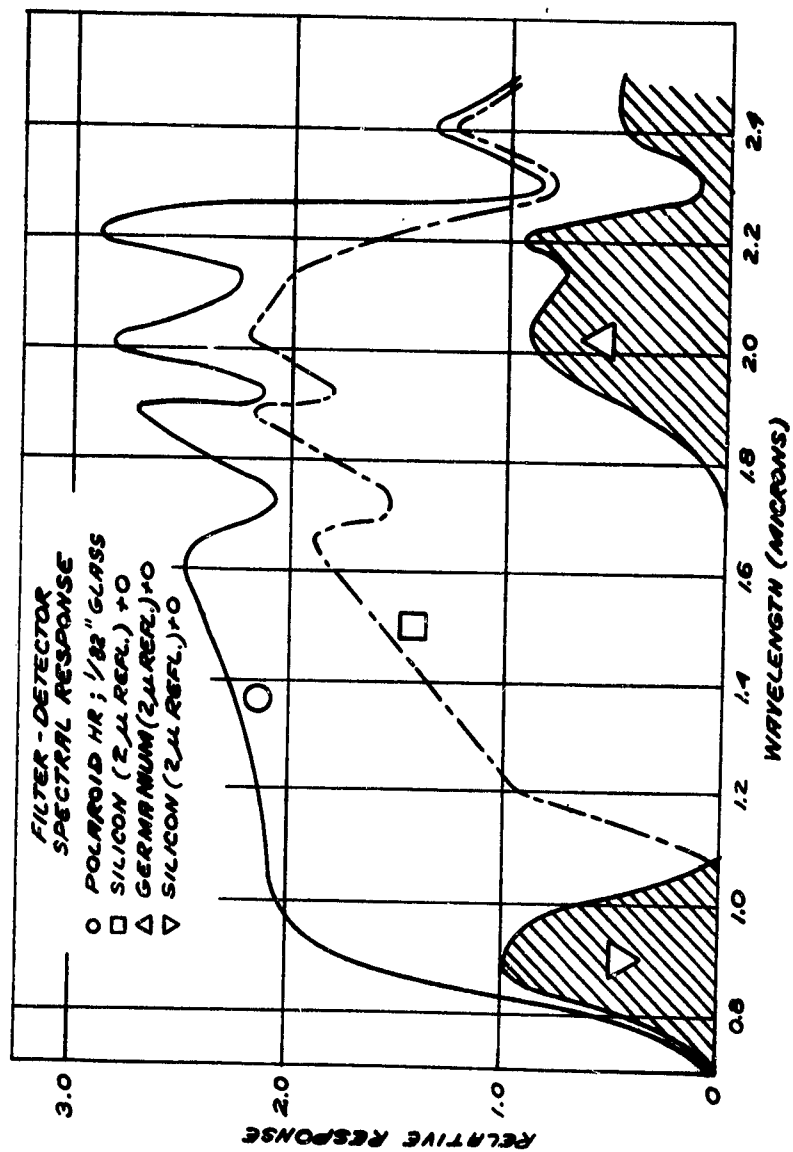
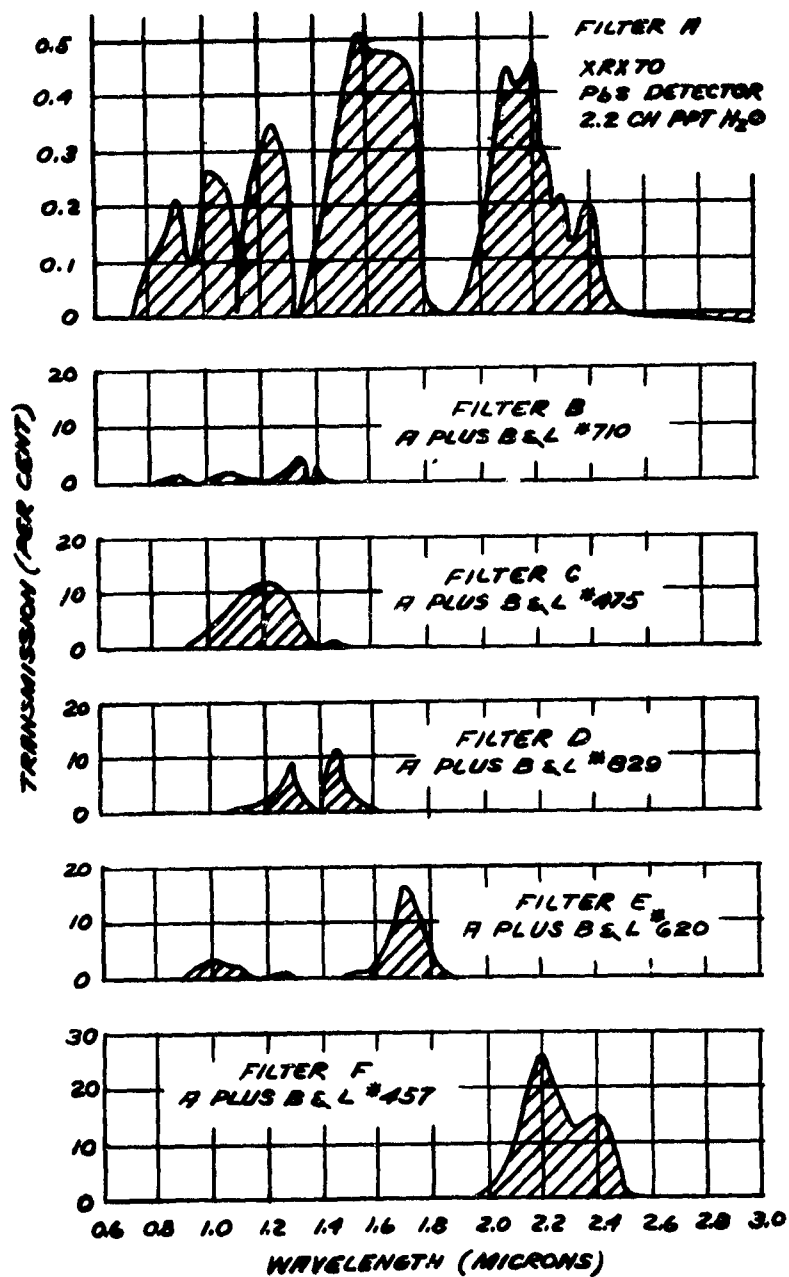


FIGURE 2



The brightness measurements for point electron clouds BETSY and DOLLY are presented in Figure 3. It has been indicated that BETSY became sunlit after about 500 seconds. The physical parameters of both clouds are similar and it appears that their brightness will approach similar values at about 1000 seconds. The brightness of HILDA, a "trail electron cloud" is also included for visual comparison.

The separation of an artificial cloud into distinct parts is illustrated by the brightness measurements of PEGGY, Figure 4. Inspection of some photographs indicate this is not an uncommon occurrence. The definition of the "head" of this cloud as distinct from its "tail" is more obvious in infrared photographs. The brightness of the tail appears to decay at a regular rate, whereas the head appears to grow in brightness after 250 seconds. The photographs show the "head and tail" become distinct after about 45 seconds and the head grown in brightness after some 100 seconds. The "Tail" section fills the field of view of the instrument after the first 60 seconds. It is only after about 200 seconds that the "head" approaches a size that will fill the field of view. This is considered the reason for the rather abnormal changes in brightness of the "head" section of the cloud.

In the next Figures, 5 and 6, the brightness observation of MARGIE by the radio-meters operated by GRD and Southwestern are presented in that order. Referring now to Figure 5, a rather interesting phenomena results as the cloud passed nearly between the moon and the observing point. The artificial cloud appears to separate into two parts after about 250 seconds, and after a lapse of 300 seconds, one section drifted into close proximity to the moon. This cloud exhibits an increase in brightness which can be attributed to the forward scattered flux from the moon. Inspection of the change in brightness with time indicates that the contribution of the forward scattered flux is becoming evident at least at a time of about 200 seconds.

The brightness measured by Southwestern while observing MARGIE is shown in Figure 6. Without formal knowledge of the precise portion of the cloud which was being observed, it appears that this instrument was viewing the brighter portion which passed near the moon.

FIGURE 3

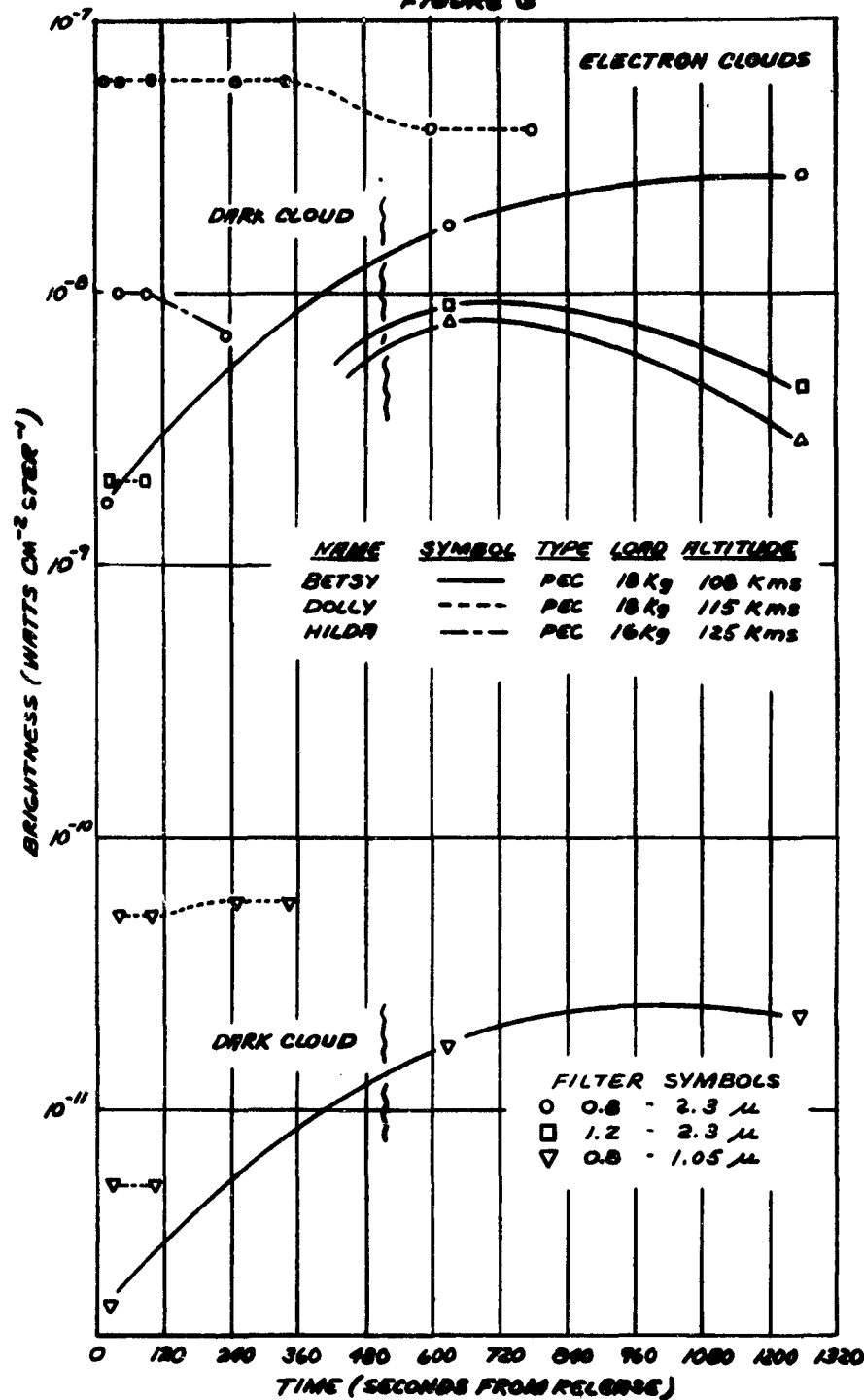
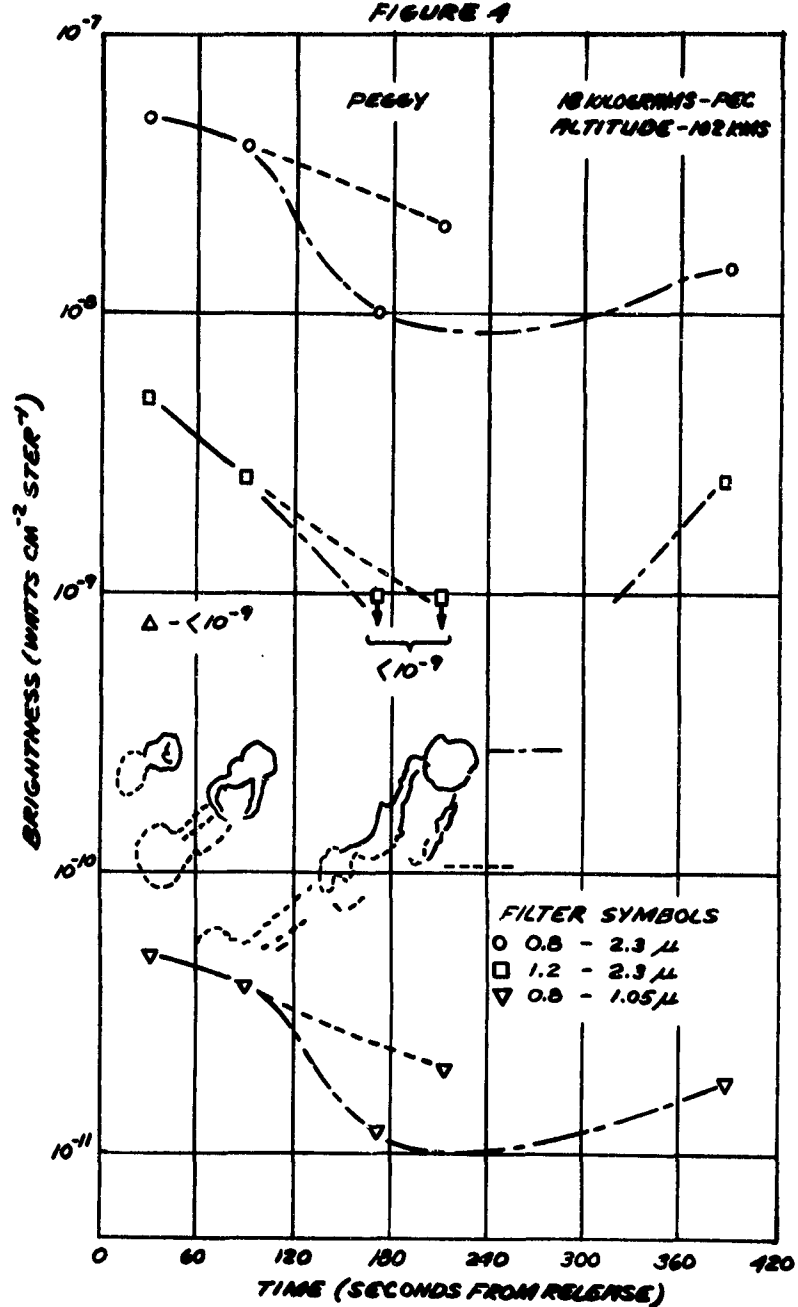


FIGURE 4



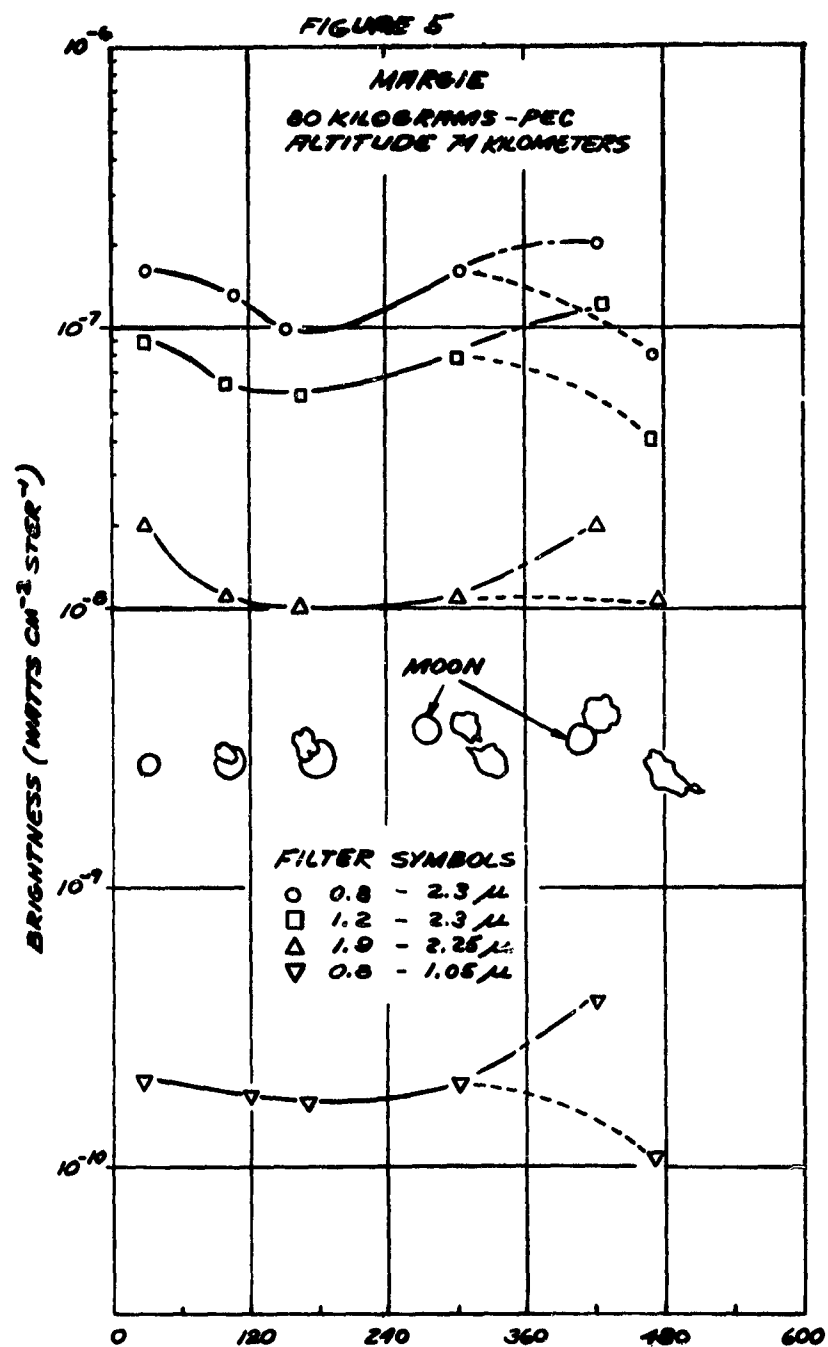
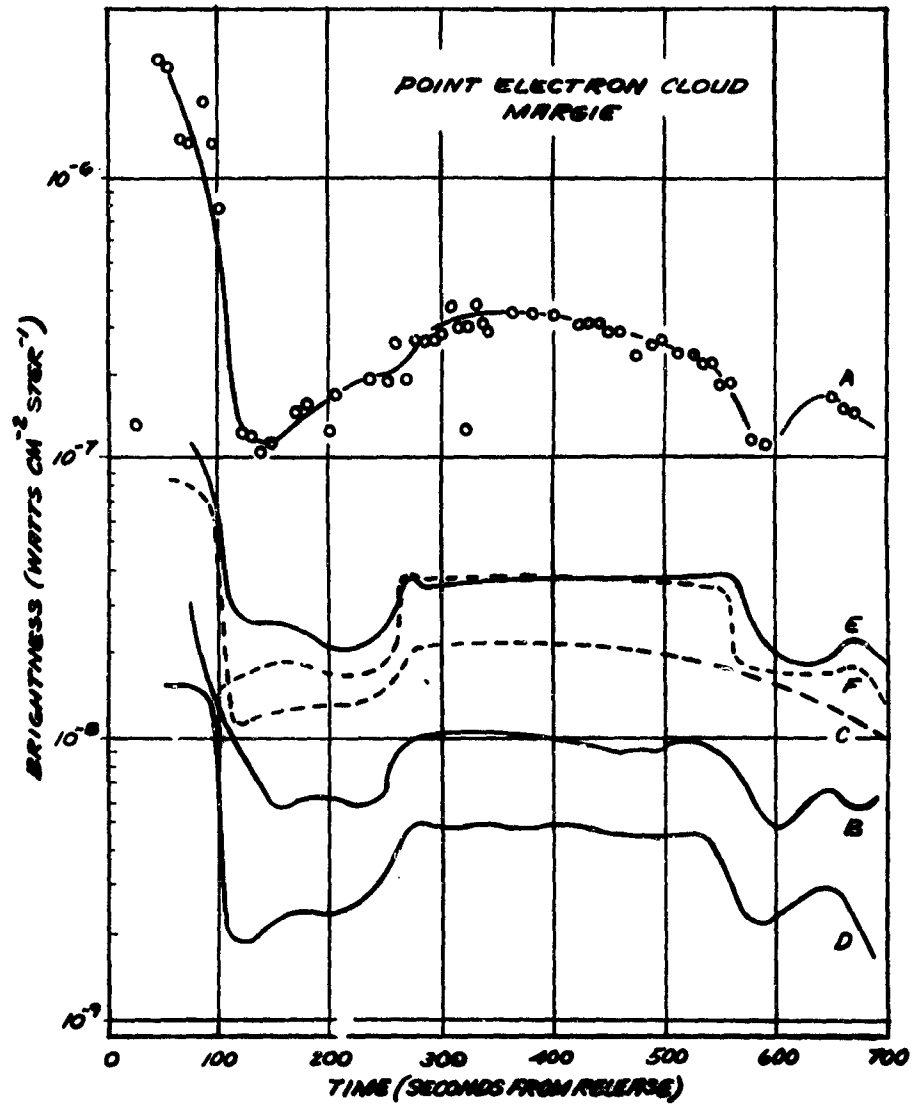


FIGURE 6



The brightness of several types of artificial particulate clouds are plotted in Figure 7. Of particular interest is HEDY, a cloud composed of Cadmium Sulphide (CdS) material. It was hoped that it would exhibit a solar -luminence phenomena at about 1 micron wavelength. LILY, composed of 2 micron Al_2O_3 particles, was to be used as a comparison. It is true that in the near infrared they exhibit a different brightness and decay rate. However, because of the difference in altitude of the release of the particulate matter and the decay rate, of the brightness, any comparison is tenuous. The brightness of FRANCIS and LILY are reasonably similar. IDA is also included for visual reference because of its uniqueness. The spectral relationship between LILY and HEDY is discussed later.

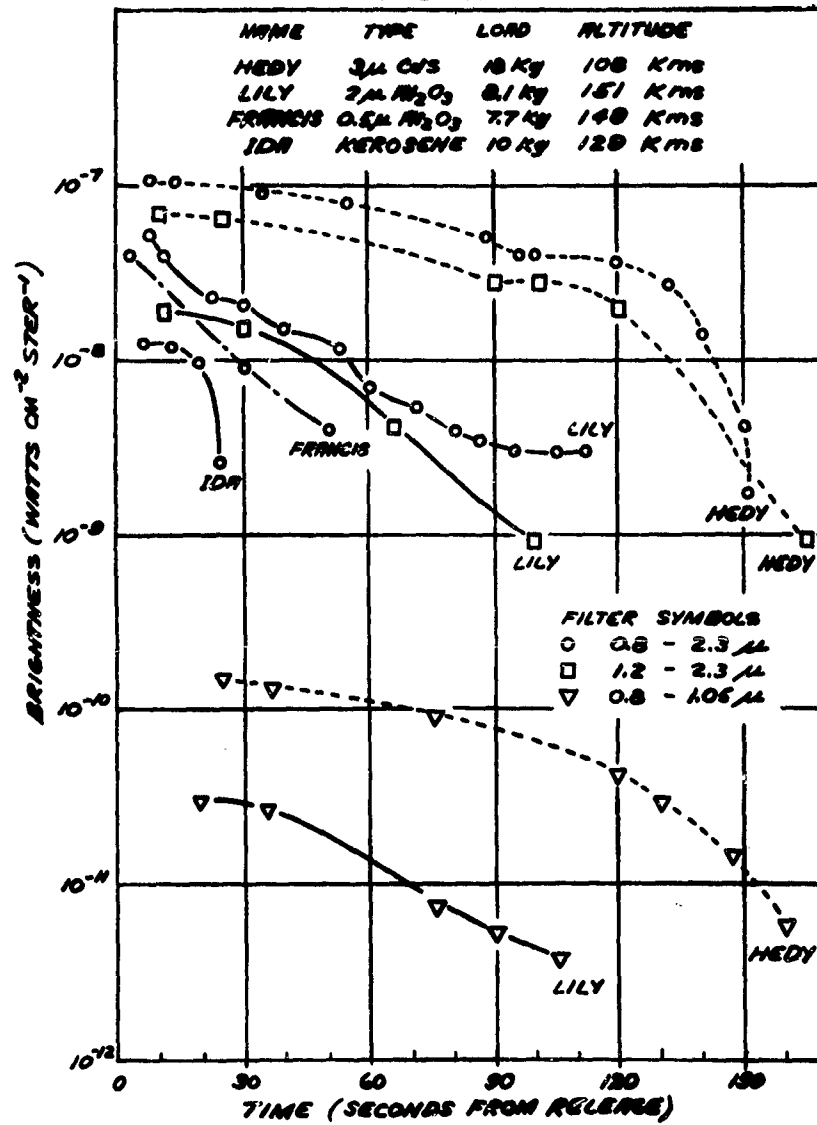
Again the difference in instrumentation and observation techniques is obvious when one compares the data obtained by Southwestern at Memphis in Figure 8 with the previous Figure. The rapid decay in the first 30 seconds seems characteristic of much of the data observed by Southwestern during the initial stages. With a field of view looking at about 1/25th the area of the GRD radiometer, the Southwestern instrument probably observed different portions of the cloud which may account for the appearance of noisy datum about the smooth curve.

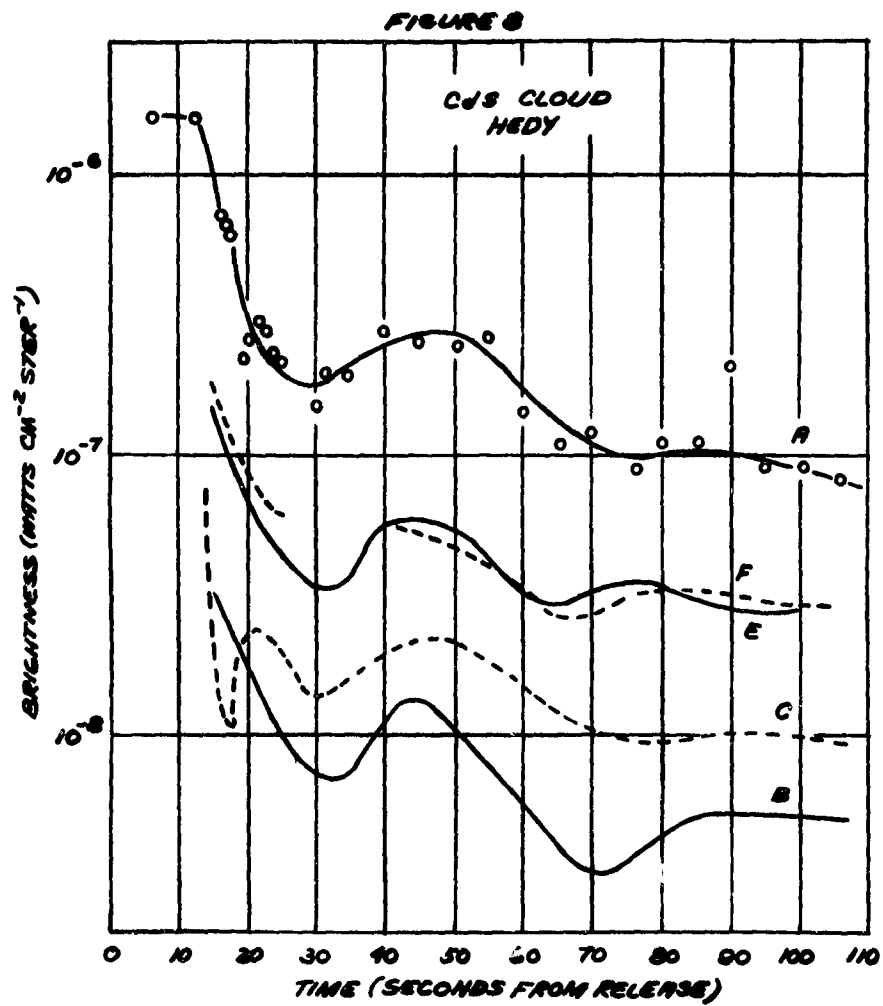
The Symposium directive requested the determination of the fading rate. Figure 9 depicts some fading rates for a variety of artificial clouds. These cover about two decades and any one curve is approximate only within a factor of about ± 2 . If the cloud is dissipating fast, it is located near the top of the chart. HEDY undergoes quite a change. For the first 100 seconds, its fading rate decreases until suddenly the cloud starts to fade quite rapidly.

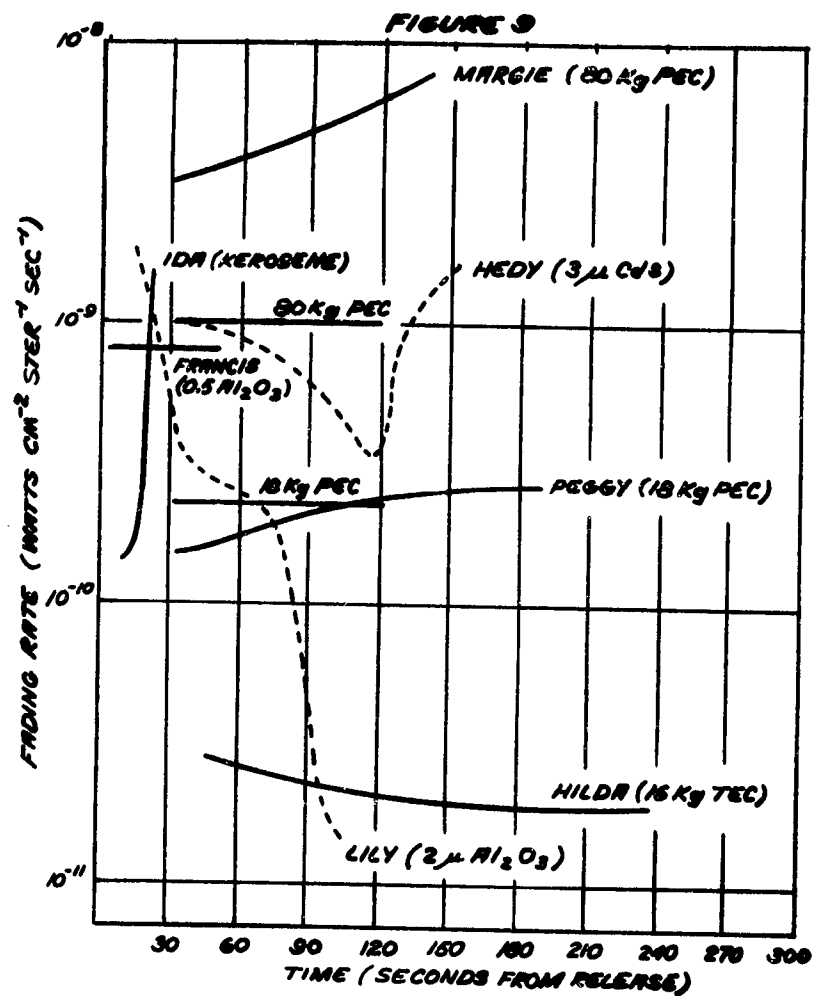
Analysis

As was mentioned earlier, an attempt to discover any spectral changes with time would be made. The relative change in the ratio of the infrared (1.2-2.3 μ wavelength) to the red (0.8-1.05 μ wavelength) is used as an indicator. The brightness for all spectral regions was reduced by a filter factor derived from two measurements of the moon's reflected sunlight. These filter factors are considered the best for this purpose because the detector is looking at a source of reflected light, that is from the sun, which is transmitted through a similar atmospheric path. It is appreciated that the albedo of the moon and the artificial cloud may not be identical, but the difference is considered a second order effect compared to using a non-sunlight source without a realistic atmospheric path.

FIGURE 7







The ratio of IR/RED is plotted for the last 600 seconds of BETSY on the bottom of Figure 10. As it can be seen, the radiant energy becomes more red with time. The dash curve following the same trend is the relative spectral change for the same filters observing the sky background. The three curves at the top of the Figure show the change in brightness of the sky background for LOLA. The five sky background measurements made before and after an observation of artificial clouds show a remarkable consistency which lends confidence to using an average sky background and thus a relative spectral change for sky background.

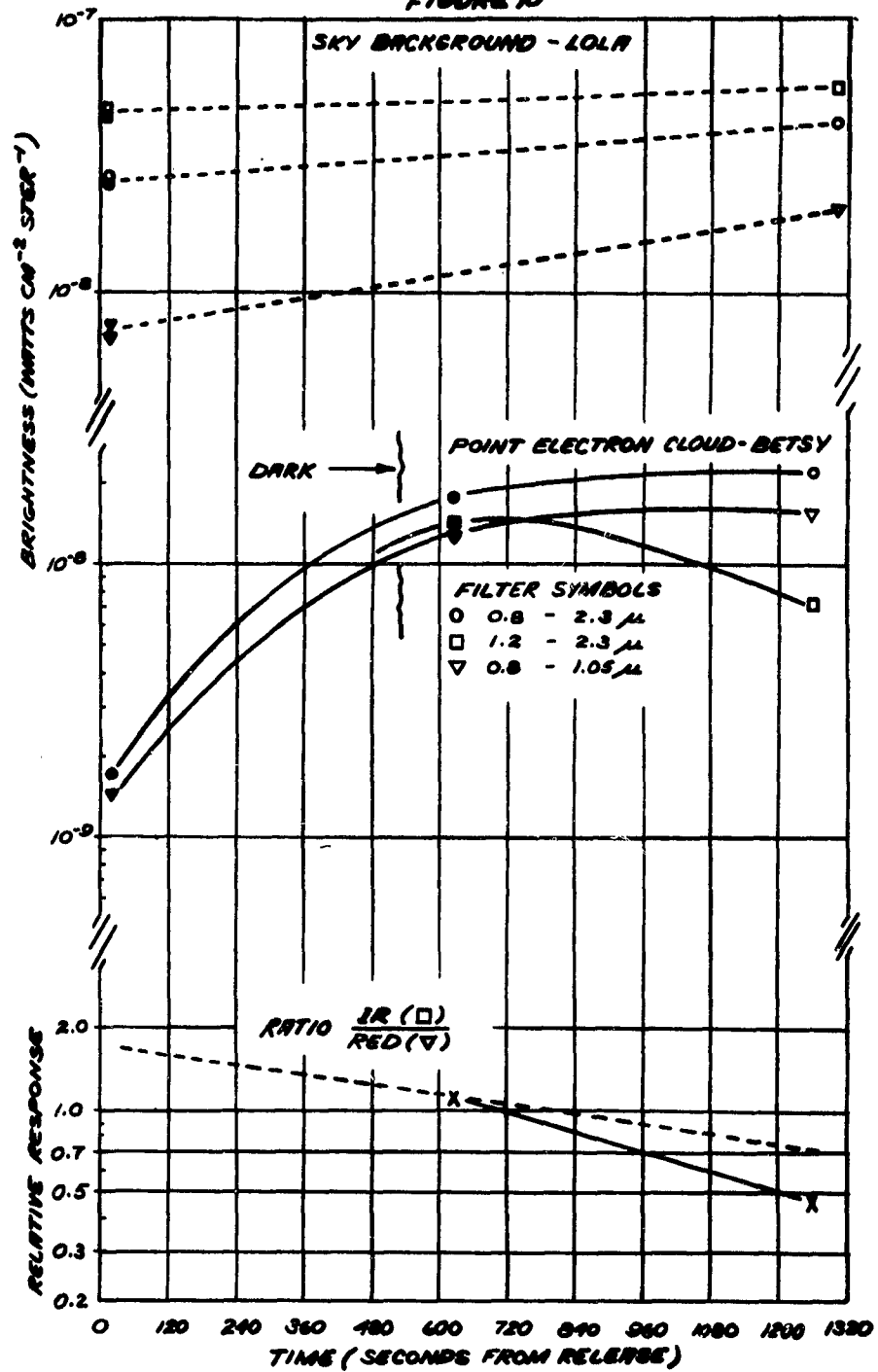
The difference between the ratio of IR/RED for BETSY is not considered significant.

Figure 11 shows the brightness measurements observed for various "clouds" at various times which have been subjected to the same filter factor corrections as previously described. Measurements of the sky brightness before each of the cloud observations are plotted on the left ordinate. Two conclusions may be inferred from these data: (1) the brightness of point electron clouds formed from 80 kilogram load exhibit about 2-3 times the brightness of a cloud formed from 18 kilogram load; and (2) that the gross spectral change in time conforms with the sky background.

In spite of a full moon during MARGIE, the sky background is within the normal referred to above. The cloud brightnesses have also been modified with the moon filter factors with the results shown in Figure 12. Here is the only consistent (though not true significant) deviation in the relative spectral change between the IR and RED. It may be interesting to speculate that the forward scattered light from the moon by the "head" cloud indicates a shift toward longer wavelengths, whereas the "tail" assumes characteristics of the sky background.

In Figure 13 the brightness for MARGIE as measured by both radiometers in the near infrared spectral region is plotted as a function of time. The ratio of IR/RED is also included for visual comparison. The agreement is quite good considering the Southwestern at Memphis data has been corrected with an assumed representative atmospheric absorption, and the difference in the instrumental fields of view. If an equivalent atmospheric absorption was applied to the GRD data, it would be moved upward by a factor of 3 or 4.

FIGURE 10



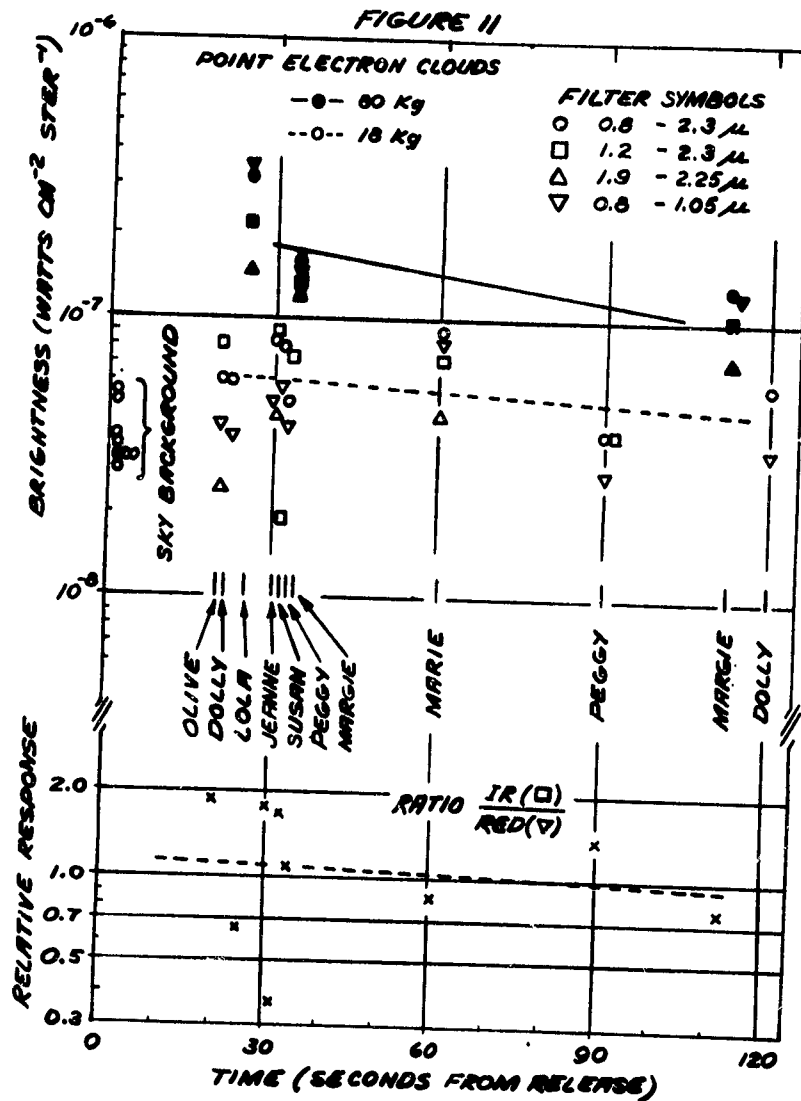


FIGURE 12

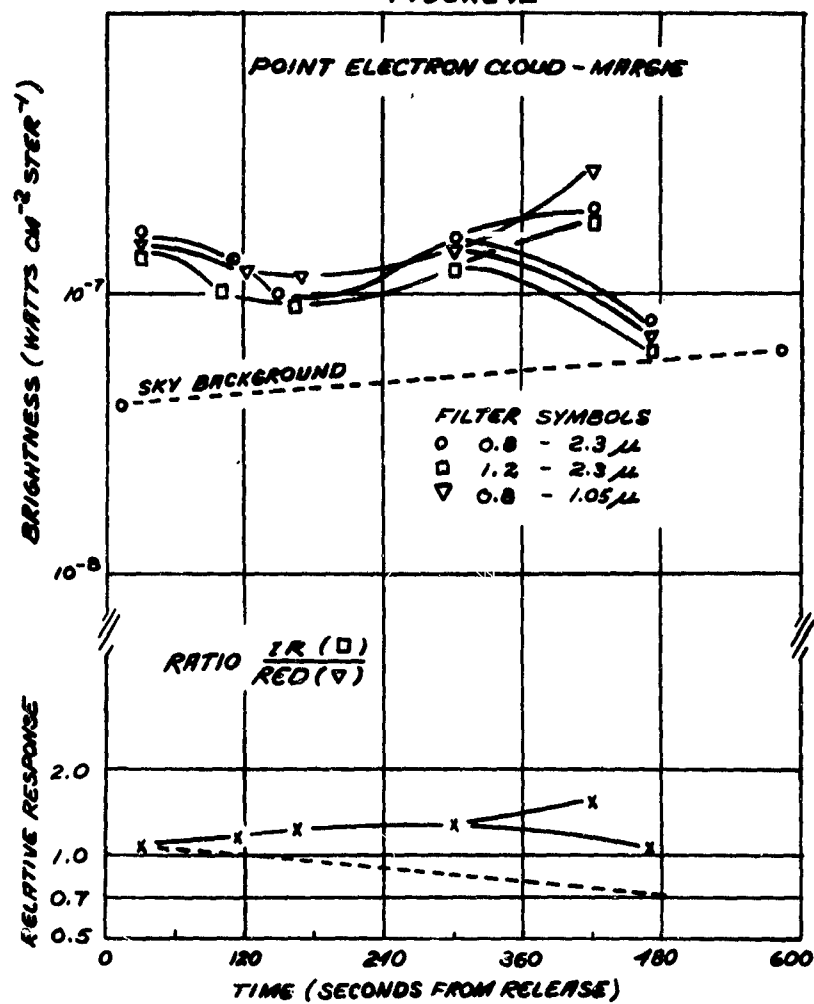
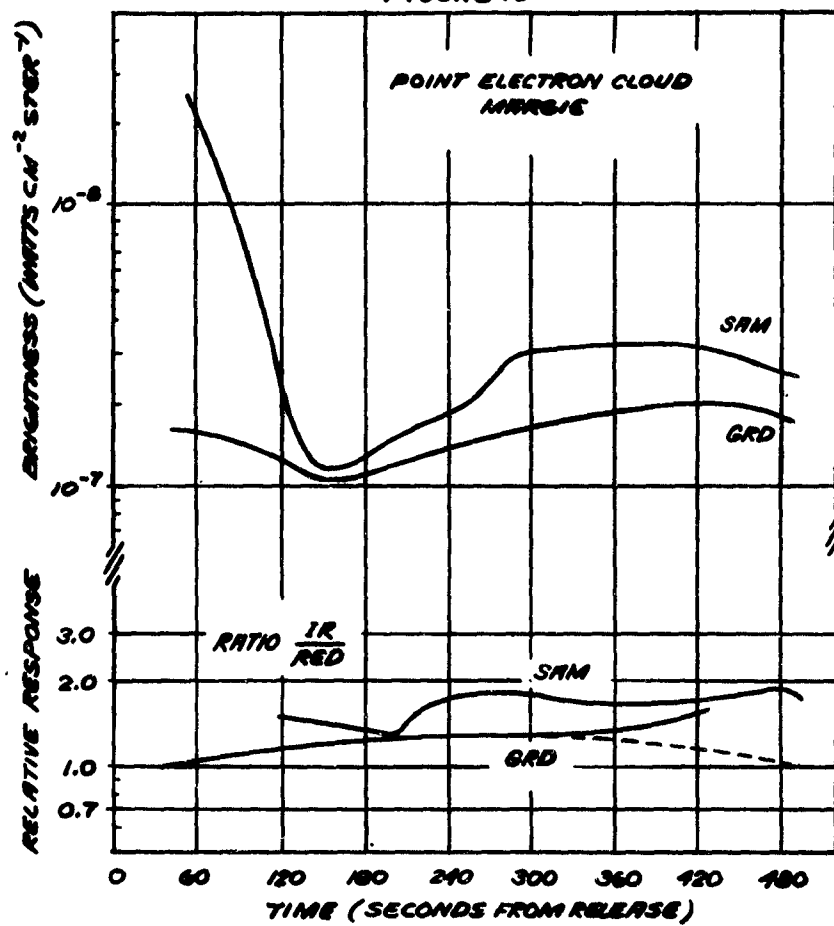


FIGURE 13



The brightnesses for HEDY and LILY, Figure 14, have been subjected to the same filter factor as previously mentioned. These data show a rather good internal consistence. The ratio of IR/RED also appears to be consistent with the change in sky background.

Again the brightness data of HEDY observed by GRD with the Tech/Ops built radiometer and the radiometer operated by Southwestern at Memphis is shown for visual comparison in Figure 15. The correlation is reasonable when consideration is given to the difference in observation techniques and the uncertainty attendant the evaluation of the effect of the atmospheric path.

Conclusions

Any conclusions which might be drawn from this preliminary analysis of the data must be tempered with caution or be considered speculative. However, a few points seem obvious. The brightness measured in the near infrared spectral region is primarily solar scattered energy. Also because these artificial clouds are quite nebulous, the effect of sky background cannot be discounted, even when the field of view of the radiometer is filled. Finally, any examination of spectral changes can only be inferred because of the wide spectral regions observed by the bandwidth of the filters.

Addendum

Just prior to presentation of the data at the Symposium, I was informed that the data observed by Southwestern at Memphis required a correction of a factor of π . Therefore the brightness curves in Figures 6 and 8, and those labeled SAM in Figures 13 and 15 should be raised by this value.

FIGURE 14

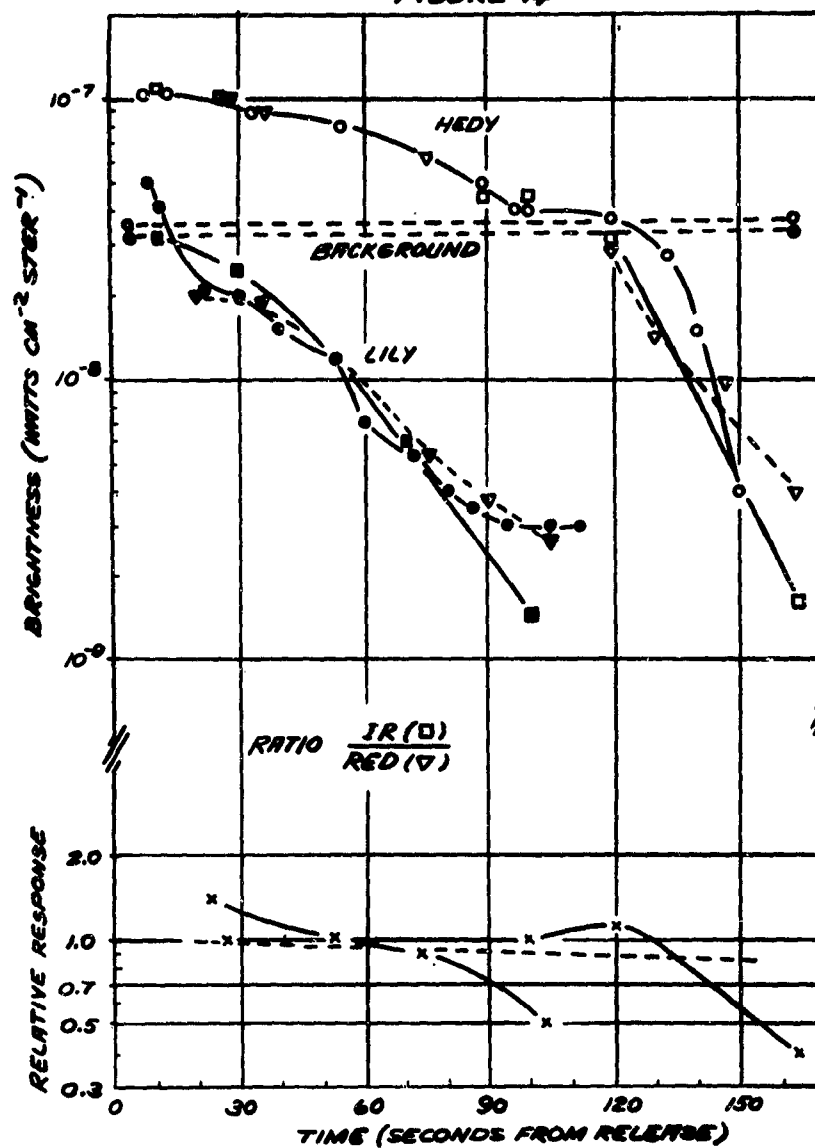
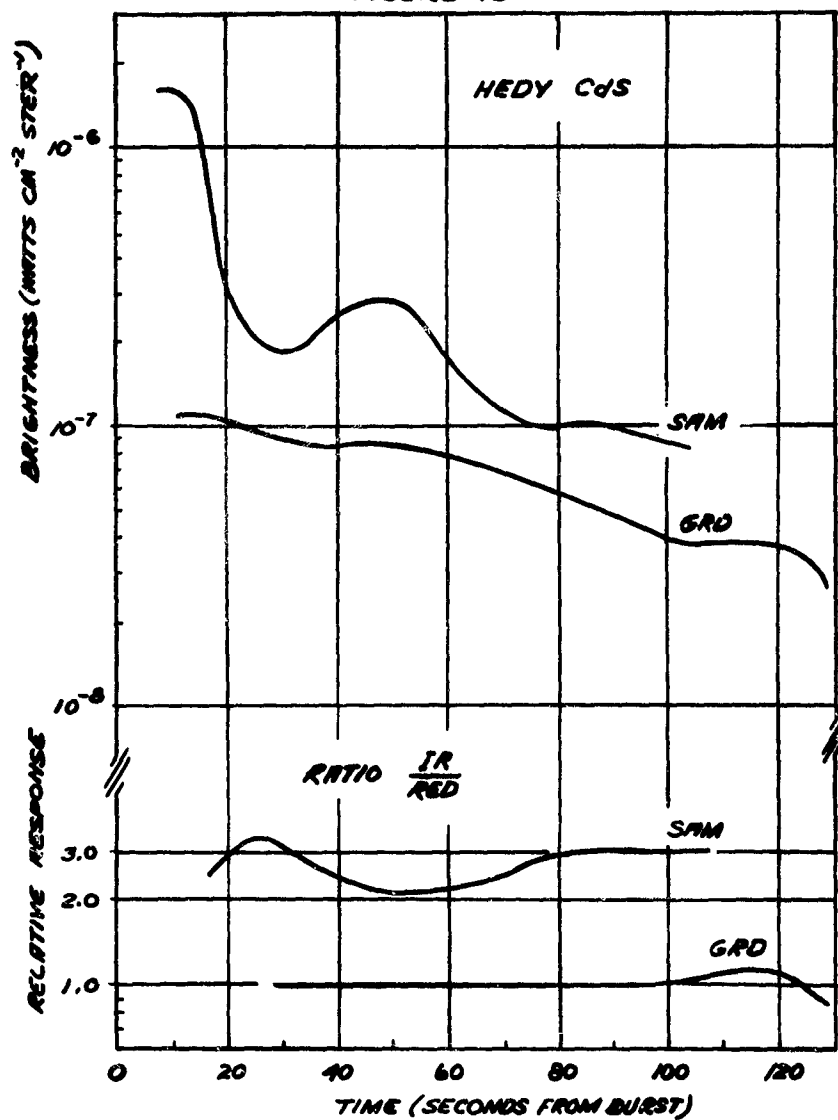


FIGURE 15



SPECTROPHOTOMETRY PANEL DISCUSSION

Panel Members:

R. B. Holt	Device
O. Oldenberg	APCRL
C. D. Cooper	Univ. of Ga.
S. Silverman	APCRL
H. Schiff	McGill
H. D. Edwards	Ga. Tech.
M. W. Rosenberg	APCRL
T. P. Markham	APCRL
J. Street	S. W. Memphis
R. Eldridge	Tech. Op.

Holt: I should like to ask Street whether he got any signals corresponding to burst itself on any of these releases? Were you ever directly enough on the burst to pick up anything?

Street: At first, before we decided to stay off the cloud and look for a shock wave, we did obtain some data of the burst itself. However, for the later shots we did not obtain data at burst.

Holt: How about the other IR group? Did you get anything on burst itself? Your acceptance angle was wider, so you might have been on burst some of the time. Nothing corresponding to burst signal?

Eldridge: We did not.

Holt: Did you feel that your sensitivity in the infrared at the resonance line of cesium was sufficient so that you would pick up a great deal of the 8521 \AA radiation from the point releases? You had one filter that passed this wavelength, I believe.

Eldridge: At 8521 \AA the sensitivity is down; actually, there was no way of telling because the filter band was too wide.

Holt: I see. Would you have any comment as to what your ultimate sensitivity was in that wavelength range? We do not have a lot of data from other measurements in that range.

Eldridge: The radiometer built by Technical Operations, Inc., and operated by GRD has a measured sensitivity of about 1.5×10^{-7} watts to a black body at 270°K . However, the important point to remember is that both radiometers were background limited. The data which I presented (Figures 10, 11 and 12 in the written version of the report) gives the measured brightness of the background before and

after the obscuration of the particulate clouds.

Holt: We might ask Professor Oldenberg if he has some comment concerning the general kind of observations we are making. I personally am a little concerned about the ones we do ourselves, and I suppose most of the people here are similarly concerned, because we have available a huge number of quanta coming from these various releases and so far we have not been very successful in obtaining records on them. Do you have any suggestions on techniques or procedures?

Oldenberg: We have seen in this meeting quite a few photographs of spectra and quite a few direct images through interference filters. I would like to know what the spectrum taken at the ground from a sample explosion with a good spectrograph looks like; in other words, I would like to know whether the lines are very persistent and whether they could be separated by interference filters, or whether these lines are more or less covered by a molecular background.

Holt: Perhaps Dr. Fisher would have some comment on that.

Fisher:
(Aerojet) John Paulson and John Brown came out to Downey and a lot of charges were fired. We only prepared these charges and I haven't seen the data so I think Dr. Paulson ought to answer the question.

Paulson:
(AFORL) Dr. Cooper has the data.

Cooper: The spectra are grossly overexposed generally. Where there are no bands showing up there is a background continuum and the spectral lines are definitely those of cesium neutral.

Edwards: The shots were made in sunlight so the spectrograph was looking out through a hole in the wall into sunlight and then superimposed on the resulting continuum was the burst itself. We obtained a very dark spectrum, as Cooper indicated, but on the edges you could see enough of the lines to match up with the neutral cesium spectrum as found in the cesium lamp.

Cooper: Yes, that's true, but there was no evidence of any molecular spectra actually showing up.

Rosenberg: Does that include last year's spectra which were perhaps made in the dark rather than in sunlight?

Cooper: I have only seen the general report from last year's spectra. I can comment that there seemed to be continuous background but not any band spectra.

Holt: The ones from the previous year were actually made during daylight conditions, but not in terribly bright sunlight.

Rosenberg: In the clouds which broke in two or which had two very different looking segments (one rather fuzzy in outline, one rather clear cut in outline) is there any way of distinguishing whether one of these is largely cesium radiation and the other one continuum from solar scatter from solids? Specifically, Peggy had one section with a rather sharp edge, another section fuzzy edged, and Margie broke into two, again with a fuzzy edged unit and a sharp edged unit. There are 20 kilograms of aluminum oxide around somewhere. Where is it? Would any of the panel want to comment on this?

Cooper: I might comment on Peggy. Immediately following the burst our spectrograph was looking at the white section of the cloud that I believe is the section that the sodium was in. We observed sodium absorption for 20 seconds, then we get weak emission for another exposure on the spectrograph. Then we switched with the spectrograph and tried to follow the cloud which had the strong cesium in it (using the snooperscope which was picking up the infrared radiation to guide on), but with the spectrometer we stayed on the white cloud because there was no snooperscope tracking provided for it. The spectrometer then would show the sodium and aluminum oxide. On Margie we tracked both clouds with the spectrometers, switching after about 30 or 40 seconds to the weaker cloud, and there was no indication of aluminum oxide. However, there is some erratic behavior which I believe may have come from an overloading of the electrometer. This data has not been completely reduced, but there was no indication on Margie of the sodium, cesium, or aluminum oxide.

Holt: Now, to discuss further Professor Oldenberg's question, I think that Dr. Rosenberg had in mind when talking to me the other day doing

some more experiments along the line that you mentioned, with the idea of trying to determine what the spectrum on the ground for some of these cases is like, as soon as we have the proper equipment set up for doing it. It is quite difficult to interpret the spectroscopic information obtained in Firefly releases because you are usually taking spectra in the presence of background which is larger than the signal you want to measure. This complicates things a good deal, because if you widen out your acceptance angle so you get the whole cloud you more than proportionately increase your background. If you narrow it down you will be looking only at a small portion of the cloud and the question arises as to which portion are you looking at and how are you going to track all your equipment. Some work was tried using filters on TV units but it is a difficult experimental problem.

I wonder if we could turn to one other thing. Dr. Silverman might have some estimates as to what happened to all the cesium we have been letting go based on his evaluation of negative results from field stations.

Silverman: Really, I haven't got the estimates of how little the field measurements would detect. At Sacramento Peak there were a good many of the twilight spectra taken with the 4555 filter and these were all negative, but I have not calculated what the concentration corresponding to a negative result would be. In Mexico results were also negative but there were only two or three spectra taken at twilight there. Peru again was negative, so I can't really give you an estimate at this point on minimum quantities that would have been there.

Holt: Levels were certainly lower than naturally present sodium, though?

Silverman: Yes.

Oldenberg: Doesn't this experiment depend upon the wind? Thus it would be necessary to check the same observations over and over again and occasionally one may get a strong effect.

Holt: Yes, that is what we had hoped. We had about a dozen cesium releases and we had hoped that at least one time there would be the proper wind going in the right direction to take some of it over one of the observing stations, which were fairly widely spread geographically. Of course, it is not only the direction of the wind, but how fast the wind is that is important, because if it blew the cloud by at some time other than sunrise or sunset the flash doesn't appear.

Silverman: On the photometric filter results which Dr. Holt showed, there was a 4555 \AA filter and a #87A filter (which passed up 8521 \AA probably). As I remember, if prior to the burst you have a given level of 4555 \AA , then past burst a new level established which is above the extrapolation of the preburst level.

Holt: At most wavelengths the enhancement occurs. At 4555 \AA on the particular shot discussed, we did not have a preburst reading, unfortunately. We didn't have the recorder on the 4555 \AA photometer. The ones that we did record the burst on were the #16 filter (which is a deep yellow) and a couple of units with no filters.

Silverman: On the records of Jeannie that you showed, didn't you have data of this sort?

Holt: Yes, but not the wavelength 4555 \AA .

Silverman: Can't you measure the difference above the level, for example, that the #87A filter showed us as compared to normal twilight results, and thus estimate the additional level due to the cloud?

Holt: We do have some data from which we can estimate it.

Silverman: If the #87A filter is measuring 8521 \AA radiation, the oscillator strength for this transition is greater by a factor of approximately 50 or more than for 4555 \AA , so I would like to ask you if this would be enough to then make the cloud optically black at 8521 \AA but not at 4555 \AA ? If so, when the cloud moves into the sunlight your decrease in 8521 \AA intensity might be equivalent to the resonance absorption effect that you get in sodium. If it is, then possibly you can use this to get some information on number density

from the data taken together with the increased level of 4555 \AA .

Melt: This is a very good suggestion; we will try to do this. One reason that the infrared end of the curve goes down rather than up (all the others for visible wavelengths go up) is simply that there is a delay in the build-up of the infrared background as daylight comes on. We were measuring at the intermediate time during which the blue background is already built up or is building up very, very rapidly, and just before the infrared section starts building up. I think your suggestion that the cloud may have been optically black at 8521 \AA is certainly possible.

Schiff: I would like to ask Dr. Edwards whether on any of the nighttime PEO tests he has data on the sodium and cesium relative intensities.

Edwards: On the nighttime releases we had very short exposure time. We haven't run the densitometric studies on the one or two bursts we have, but there is not much data.

Schiff: I think that would be very interesting information to have if we could get it. One other question to Dr. Cooper. In the case of the A10, where you had three vibrational levels, is there any sense to asking what is a vibrational temperature here?

Cooper: I think not on vibrational temperature, since this is resonant scattering of sunlight in this case. I think there is good possibility of probably setting up and getting rotational temperature in another shot. On one of these releases the A10 radiation is initially ten times stronger than cesium and towards dawn I think you could get enough intensity to use sufficient dispersion to get a temperature determination.

Schiff: In the nighttime shots there was no continuum at all, I gather.

Rosenberg: This is one of the saddest features of the series this year, in that on all of the nighttime shots there was between 3 and 5 minutes persistence at a low intensity level and some sort of continuum. As Cooper points out it was not sufficiently intense to show up on the spectrographs, but the fact that it didn't show implies that it was a continuum or bands rather than a line structure. We will have to

go after this with more sensitive equipment, but it was very frustrating standing there and pointing equipment at something that an eyeball could see and have these very expensive instruments ignore it completely.

Holt: That comment really strikes home to all of us, I think. I believe that all that we can say in our own defense is that if we can have more shots we can probably do better.

Edwards: I also say that an eyeball may be cheap, but it is still one of the best optical instruments that I know of. We stuck a transmission grating in our pocket and put it in front of an Eyemo movie camera without slits and ran the thing at 4 frames per second during some of these shots. As I described it, we did this in rather hurried fashion so we have some problems mainly in identifying the bands and lines that we saw. But we have some data that perhaps supplements that which Cooper has mentioned. His spectra were taken at about burst plus 10 seconds, and beyond. I'm talking about spectra during the first one-fourth to one-half second. On Margie we have some three to six lines or bands unidentified at the present time, but I feel fairly certain that a couple of them are the blue lines of cesium at 4555 \AA and 4593 \AA . These occurred for the first one-quarter second of the cloud's life. Thereafter we have only the continuum which Cooper found on his spectra. On Lola we have some 10 or 15 bands or lines during the first one-half second. Thereafter we have just the continuum. Peggy, Susan and Jeannie show only the continuum from the beginning until sixty seconds or so whereas Cooper found sodium, cesium, and aluminum oxide. On Olive we find two rather sharp lines during the first one-quarter second and a continuum thereafter. I think these are again the cesium blue lines. Cooper found cesium, sodium and aluminum oxide. I believe that our grating mounting probably made the sodium D line fall off scale. I think that we probably also have the blue lines of cesium and some of the aluminum oxide bands in these shots on which we saw spectra.

Fisher: I wanted to point out that the sodium was in the forward end of the charge, and it would have been enveloped in the reaction products about 70 microseconds after the time of initiation, that it would have been dropped in an axial direction and probably thrown in the direction that the nose cone was pointing. Also some of the time this sodium nitrate was alone and sometimes it had a reducing atmosphere of aluminum with it, and I wanted to know if this made any difference to anybody.

Edwards: Sounds to me like on Peggy that it was in the wrong end. We had sodium at the bottom end of the cloud and according to the way I understood you it would have been the top end. Is that right?

Fisher: If the orientation were such that the nose cone were pointed up. It didn't go back the other way having been hit on the bottom, I can assure you.

Edwards: I don't know where the rocket was, I assume it was going up.

Holt: Another question here?

Dodd: In light of Dr. Edward's report I have been thinking that the possibility of using an objective prism or grating at the very instant of burst might give some information on the initial spectra and help Dr. Oldenberg in his comments. At the very beginning even with a larger instrument when the cloud has a size of some fraction of a kilometer I think you should be able to get fairly good resolution.

Holt: I might simply comment here that we tried a similar technique last year on Firefly 59 with a prism and I think a grating was tried by Millman last year. We always do try to take care of this possibility of getting spectra while the cloud is still behaving more or less as a point source. It seems like our greatest weaknesses come later in the cloud development, because then we are dealing with a very tenuous cloud in tremendous background and so the problems are much more severe. We need both kinds of data, you are absolutely right. We are following up the suggestion of using the source itself as a point.

Zimmerman: Would it be possible to pick up excitation caused by the passage of a shock wave of any of the constituents or even the particulate oxides?

Edwards: What we identified as or call the shock waves we saw only on Amy. Our filter wheel was running at 600 revolutions per minute, and we had about one hundredth of a second between filters. We had some strange phenomena which I showed on the last slide, it wasn't too clear, and perhaps you didn't see what we had there. We did get some increase in radiation through some of the filters. These filters were about 80 to 100 Angstroms wide. That is the only one that we identified as a shock wave, to be differentiated from the particle waves and the main cloud. This one was traveling at 10 kilometers per second, and we had an increase at the region 4120 \AA (which was picked to be away from any of the expected bands which might otherwise be expected from atmospheric molecules and atoms). We also saw a small increase in 5577 which we had thought might be excited by the shock wave in passing through the atmosphere. Since we have all of this on one firing, I hesitate to draw too many conclusions from it. If we could have had this repeated on several other shots, I would feel much more comfortable about it.

Zimmerman: This is again to Dr. Edwards, in line with his last reply. Can you differentiate between the shock and the solid particle waves in this case?

Edwards: We do in this way. The particle waves that I have talked about we were able to photograph with the Eyemo movie cameras. We can see this on the film. We did not see similar effects for Amy on our film. We picked this response up on the photometer, which is much more sensitive than the film, and maybe it was just a fainter particle wave. We certainly wouldn't argue that point.

Rosenberg: May I make a comment on that shock wave. You saw it at one and one-half seconds after burst and it had a speed of about 10 kilometers per second. I assume that it was 15 kilometers from the burst point. I don't believe that the energy in the initial

detonation is sufficient to excite appreciably a volume 15 kilometers in radius at this altitude. Too much energy would be required.

Edwards: Perhaps we measured a flashlight.

Rosenberg: Or, the other possibility is that has created the ring but the time delay is embarrassing. A 15 kilometer radius sphere contains tons of material, as Dr. Kivel pointed out. We just don't have that much energy.

Paulson: I would just like to point out that we did see this so-called particle wave on Amy with the image orthicon equipment, so it is definitely there.

**"RESEARCH DIRECTED TOWARD A THEORETICAL STUDY OF PHYSICAL PROCESSES
ASSOCIATED WITH CHEMICAL RELEASES"***

**GEOPHYSICS CORPORATION OF AMERICA
Bedford, Massachusetts**

ABSTRACT

This report reviews the contributions of GCA in examining the fundamental, physico-chemical processes involved in the "Firefly" contamination program. The objective here has been to put on as firm a basis as possible our understanding of these processes. As part of this program, there has been critically examined the mathematics and physics of the diffusion process with associated loss and production processes for single and multiple species. The chemistry involved in upper atmosphere releases has been investigated as well as the nature of the recombination during the radial free expansion of a plasma sphere. With a view toward the diagnosis of the chemical release and the geophysical interactions, work has been pursued on the optical behavior of resonant and chemiluminescent clouds under a variety of initial and physical conditions. Devices for determining the nature of the diffusion mechanism such as paired resonant tracers have been studied. Concisely stated then, the two principal objectives of the program were the development of methods of measuring upper atmospheric geophysical parameters and a detailed investigation of the applicability of the techniques to existing and future Air Force systems requirements.

*This work has been conducted under Contract No. AF 19(604)-7269 (sponsored by ARPA) and this report has been prepared by F. F. Marmo, Project Director and principal investigator.

1. INTRODUCTION

The program of rocket experiments wherein various chemical contaminants are released into the upper atmosphere are specifically designed to test the feasibility of utilizing such techniques to determine atmospheric parameters as well as investigating practical applications to the military system technology. Since the experimentalist is confronted with an exceedingly complex, non-laboratory controlled experiment, great care must be taken to develop a firm theoretical understanding of the phenomenology including mathematical models, physical-chemical reactions, etc. so as not to derive purely qualitative results from a series of flights. It has been a primary objective of this study to identify those areas requiring further theoretical effort and as a consequence generate appropriate study programs. A test of this philosophy of operation may be found in the successful application of many previous recommendations in the areas of planning, performance and data analysis. A further function of this program is to indicate and develop ideas and areas in which practical application to current and future Air Force requirements seem appropriate.

The most efficient method of illustrating the types of problems investigated thus far is simply to list the titles of the various technical AFCL publications that have been prepared by GCA to date under this contract.

The Technical Reports and Memos include the following:

- 1) Chemical Release Studies I: Time Varying Concentration Field Equations of a Single Substance With an Initial Arbitrary Configuration in Free Space.
H.K. Brown, F.F. Marmo, J. Pressman AFCL 222
- 2) Chemical Release Studies II: Coupled Time Varying Concentration Field Equations of Two Substances With Initial Arbitrary Configurations in Free Space.
H.K. Brown, F.F. Marmo, J. Pressman AFCL 223
- 3) Chemical Release Studies III: Some Theoretical Considerations Relating to Radiative Recombinations.
A.M. Naqvi AFCL 210
- 4) Chemical Release Studies IV: Chemistry of Upper Altitude Releases.
D. Colomb, A.W. Berger AFCL 229
- 5) Chemical Release Studies V: Recombination During Radial Free Expansion of a Plasma Sphere.
D. Colomb, A.W. Berger AFCL 202
- 6) Chemical Release Studies VI: Optical Properties of Chemiluminescent Clouds for Two-Body Chemical Reactions Without Diffusion.
J. Pressman, H.K. Brown, F.F. Marmo AFCL 201

- 7) Chemical Release Studies VII: Optical Properties of Resonance Clouds With Diffusion, for Various Initial Release Geometries.
J. Pressman, F.F. Marmo, H.K. Brown AFORL 207
- 8) Chemical Release Studies VIII: Some Comments on Shklovsky and Kurt's Measurement of the Density at 430 KMc by Sodium Resonance Cloud Techniques.
J. Pressman, F.F. Marmo AFORL 218
- 9) A Memo on the Use of Resonant Tracers for the Determination of Diffusion Mechanisms.
F.F. Marmo, R. Berendsen Technical Memo No. 61-1-AFM
- 10) Feasibility Study: Generation of Artificial Electron Clouds by Radioactive Species.
P.J. Nawrocki Technical Memo No. 60-5-G

From an inspection of the above titles it can be seen that a wide gamut of associated technical areas have been investigated. The choice of topics, however, was very methodical and represents what it is felt to be present outstanding gaps in the fundamental understanding and appreciation of some of the more basic aspects of the technology. Integral to each of the above-cited technical reports are recommendations for application, experimental implementation or logical continuation of the reported technique or investigation. It is the purpose of this document to summarize the more important results and conclusions reached during the program and expressed in more detail in the several technical reports. Included in this integration an attempt will simultaneously be made to indicate the utility and application of the results and data thus reported.

Four distinct areas can be naturally subdivided for the purposes of discussion herein and represent the bulk of the GCA effort under this program:

Chemistry of Upper Atmosphere Releases
Mathematical Models for Chemical Release Studies
Optical Properties of Chemical Releases
RF Propagation Studies

Finally, a brief summary is given including plans for future efforts in this area.

2. CHEMISTRY OF UPPER ATMOSPHERE RELEASES

A. General

For purpose of artificial (ionized or unionized) cloud generation, vapors are released from rocket-borne canisters. These releases are analyzed in terms of two successive processes: first, formation of the initial reaction products and second, evaluation of the non-equilibrium kinetic processes during expansion. Application of various models and comparison with experimental results provides the basis for recommendations for optimization for various types of releases.

Initial reaction product compositions and flame temperatures can be calculated on the basis of equilibrium processes with the aid of thermodynamical data. Details are given in AFGL Report No. 229 entitled "Chemical Release Studies IV: Chemistry of Upper Altitude Releases" by D. Golomb and A. W. Berger.

In the aluminum-alkali nitrate reaction maximum ionization is obtained with the stoichiometric reactant ratio. However, this reaction is relatively slow and therefore the reaction may be extinguished at burst of the canister, i.e. when the equilibrium pressure above the reacting mixture reaches the burst pressure of the canister.

Addition of a high explosive may speed up the reaction so that it is complete before disintegration of the canister. This was actually done in some releases of the Firefly series. It is difficult to predict the flame composition and ionization yield in a multi-component detonation system. It is probably also difficult to assure reproducibility in a series of releases based upon detonating mixtures, unless the packaging, grain size, canister strength, etc. are completely equal. Furthermore, recombination losses of the ionized species (and neutral atoms) is increased in a high pressure release.

Propellant-type constant pressure releases have been shown to have potentially greater ionization efficiency than detonation systems. Optimum propellant systems contain contaminants of low ionization potential in flame product gases of maximum thermodynamic stability. The Cs doped carbon monoxide-nitrogen carrier provides an optimum for chemical reaction. Solid propellant formulations yielding such optimum products are suggested in the above-mentioned AFGL Report No. 229.

The disadvantage inherent in constant pressure (propellant-type) releases of having a long, narrow trail of relatively dilute plasma may be overcome by using a cluster of nozzles, or a large number of nozzles mounted on a spherical container (hedgehop bomb).

Since the recombination equations relating to a nozzle-type, steady-state release are well established yield predictions and correlations between experiments are much easier and better reproducibility may be ensured.

B. Initial Expansion

Although an accurate evaluation of the initial stages of an explosion is very complicated, simplified models may be set up to approximate the expected yield of chemical species (primarily electrons) which survive the recombination during expansion.

In an earlier report an elementary model was assumed in which the plasma ball obtained in the detonation expanded with a constant velocity and with uniform density, and there was no additional ionization at $t > 0$.

In a more sophisticated model (cf. AFCEL 202, "Chemical Release Studies V: Recombination During Radial Free Expansion of a Plasma Sphere" by D. Golomb and A. W. Berger), the time dependence of the expansion rate, density and reaction rate is included.

Correlation of the calculated number of electrons quenched in the cloud after expansion with ground observations indicates that the models are a useful approximation. Furthermore, the models suggest the following important conclusions:

1. The final degree of ionization in the expanded cloud is a direct function of initial energy and an inverse function of initial radius.
2. The initial expanded cloud distribution (neglecting turbulence) is non-homogeneous. The electron density is expected to decrease monotonically from the center point to the outer boundary.
3. The final degree of ionization is inversely proportional to the average specific heat ratio of the expanding gas.

C. Special Releases

1. The Aluminum-Barium Nitrate Reaction and the "India" Release

The failure to observe elementary barium in the "India" release may be traced to a lower temperature than reported for some of the "Firefly" releases (4500°K), and/or recombination of the products during initial expansion. In Technical Report No. AFCEL 229 we have shown that if thermodynamic equilibrium is maintained up to a temperature drop to 3000°K , then practically all of the elementary barium is recombined to BaO .

Two approaches may be used to improve the barium releases. First, reductants such as carbon, germanium or zirconium yielding oxides of higher thermodynamic stability may be employed instead of aluminum. Second, low pressure (trail) releases will quench Ba recombination at higher temperatures, thus increasing the atomic barium yield.

2. Releases of NH_3 , CCl_2F_2 , N_2H_4 , $\text{n-C}_7\text{H}_{16}$ and SF_6

The amount of liquid vaporized in the releases of the above chemicals was calculated with the aid of a simple equilibrium model. Details are given in a Technical Memo OCA 61-2-APM. Here we attach only the final results (Table 1). Within the limitations of the calculations, the releases all appear feasible.

TABLE 1

FLASH VAPORIZATION

Substance	Final State	T_f °C	P_f mm Hg	Initial State		Vaporized		Remarks
				Temp °C	Pressure psia	%	lbs/cu ft	
NH_3	Triple point	-77.8	45	50	295	50.7	17.8	
				25	145	44.9	16.9	
CCl_2F_2	liquid	-100	5	100	520	79.9	44.8	
				25	95	50.3	41.1	
N_2H_4	triple point	0	3	25	0.28	30.9	19.5	single step expansion correction estimated from NH_3 data
$\text{n-C}_7\text{H}_{16}$	liquid	-50	-	100	20	71.9	27.9	single step expansion uncorrected
				25	0.7	26.4	11.2	
SF_6	triple point	-50	1700	100	1500	100.0	100.0	critical temperature 45.5°C
				25	360	73.3	68.8	

3. MATHEMATICAL MODELS FOR CHEMICAL RELEASE STUDIES

A. General

In the systematic analysis of chemical releases an area of prime importance is the generation and proper utilization of appropriate theoretical models to compare to the experimental data. The various physical and chemical processes involved are numerous; in addition the situation is further complicated by the interdependence of the many processes which in turn depend upon ill-defined or poorly known parameters. For example, the processes of generation of electrons can include thermochemical, photoionization, shock phenomena and photodetachment. Electron decay processes involve recombination, electron attachment and ion-electron kinetics among others. Further, these many processes are intimately related and vary in a complex manner and degree with such parameters as altitude of release, ambient or contaminant temperature, available solar flux, atmospheric composition, etc. This interplay of processes is further complicated by dynamic phenomena such as diffusion, shear and atmospheric turbulence which continually alter the problem with time. Chemical production of the contaminant (alkali metals for this study), the method of ejection and subsequent chemical consumption of contaminant by the active ambient species introduce other problems. Finally, the very practical consideration of engineering and cloud detection methods involve problems of still another nature.

The concentration field of the cloud, produced by the released contaminant can be used to measure rates, provided one knows the initial and boundary conditions which are associated with the continuity equations of the concentration fields of both the contaminant and any atmospheric reactant. The continuity equation for a particular substance can be viewed as a specification of the physico-chemical processes, assumed to be in action, controlling the time rate of change of density of the particular substance whereas the initial and boundary conditions assumed for the substance specify the constraints on the concentration field. In short, these specifications of continuity equation and initial and boundary conditions specify a model for the artificial cloud. Additionally, for each plausible artificial cloud model one can associate the experimental data with the parameters of the model.

The objective of the current effort is to generate a number of such models for a single substance (AFCRL-222) and two substances (AFCRL-223) and to derive the concentration field equation for each proposed model.

1. Single Substance

For the single substance treatment the most complicated model investigated (with respect to the chemi-physical processes assumed to be in action) is characterized by the partial differential equation (1):

$$\frac{\partial n}{\partial t} = D \nabla^2 n - \alpha n^2 + \beta n + F(R, t) \quad t > 0 \quad (1)$$

where the characteristic physical or chemical processes associated with the various terms of Equation (1) are respectively: (a) diffusion, $D \nabla^2 n$; (b) recombination, αn^2 ; (c) linear growth (or decay), βn ; and (d) some arbitrary generation (or decay) process at point R in space for $t \geq 0$, $F(R, t)$.

Equation (1) defines the continuity equation of a concentration field, $n = n(R, t)$, generated by the instantaneous release of an amount $N(0)$ of a single substance into all space, at the instant $t = 0$, with the initial density distribution

$$n(x, y, z, 0) = n(R, 0) = f(x, y, z) = f(R) \quad (2)$$

where

$$N(0) = \iiint_{-\infty}^{\infty} n(x', y', z', 0) dx' dy' dz' \quad (3)$$

2. Two Substances

For the case of two substances (coupled and/or mutually coupled) an analogous treatment has been generated with appropriate mathematical compromises in view of the more complex physical situation. The details are treated extensively in AFCEL-222 and AFCEL-223 and will not even be sketched out here. Rather for completeness here is included the Table of Contents and Summaries as they appear in these two reports. These are self-explanatory and serve well to indicate the breadth and scope of the theoretical development of models thus far accomplished.

It is noted that the several entries in the Tables and Summaries below retain their respective equation and page designations as they appear in the original documents. This was done to afford a ready, accurate reference for the interested reader.

The following is the Table of Contents as reproduced from the Technical Report No. AFCEM 222 entitled "Chemical Release Studies I: Time Variation Concentration Field Equations of a Single Substance With an Initial Arbitrary Configuration in Free Space" by H.K. Brown, F.F. Marmo and J. Pressman. It provides in a uniform manner the scope of the work, the diversity of the problems plus the various models and their boundary conditions which were considered.

TABLE OF CONTENTS

<u>Section</u>	<u>Title</u>	<u>Page</u>
	INTRODUCTION.....	1
	CHAPTER I	
	CONCENTRATION FIELDS: RECOMBINATION WITHOUT DIFFUSION.....	7
1.	Simple Recombination.....	7
2.	Simple Recombination with a Constant Generation Rate at Each Point of the Cloud.....	8
3.	Simple Recombination with Linear Growth.....	10
4.	Simple Recombination with an Exponentially Decaying Source at Each Point of the Cloud.....	11
	a. Riccati's equation and the Bessel function solution.....	12
	b. Asymptotic formulas.....	15
	CHAPTER II	
	CONCENTRATION FIELDS: DIFFUSION WITHOUT RECOMBINATION.....	21
	PRELIMINARY REMARKS.....	21
5.	Diffusion with Linear Growth.....	24
	a. Arbitrary free space cloud model.....	24
	b. Spherically symmetric cloud models.....	27
	c. Axially symmetric cloud models.....	37
	d. Cylindrically symmetric cloud models.....	44
6.	Diffusion, Linear Growth, and an Arbitrary Generation Rate at Each Point of the Cloud.....	57
	Example 1: $F(R,t) = \gamma n_0$, $f(r) = n(0,0)\exp(-\frac{r^2}{2})$, $r^2 = x^2+y^2+z^2$	64
	Example 2: $F(R,t) = \gamma n_0 e^{-bt}$, $f(r) = n(0,0)\exp(-\frac{r^2}{2})$, $r^2 = x^2+y^2+z^2$	67
	Example 3: $F(R,t) = F(t)$, $f(R)$ arbitrary.....	68

TABLE OF CONTENTS (continued)

<u>Section</u>	<u>Title</u>	<u>Page</u>
CHAPTER III		
	CONCENTRATION FIELDS WITH BOTH DIFFUSION AND RECOMBINATION.....	71
7.	Diffusion with Recombination.....	76
8.	Diffusion, Linear Growth, and Recombination.....	83
9.	Diffusion, Recombination, and an Arbitrary Generation Rate at Each Point of the Cloud.....	89
10.	Diffusion, Recombination, Linear Growth, and an Arbitrary Generation Rate at Each Point of the Cloud.....	95
11.	Recapitulation and Estimation of the Errors of Approximation.....	99
	CONCLUDING REMARKS.....	103
	SUMMARY OF CLOUD MODEL FORMULAS.....	104

The following Summary is taken from Technical Report No. AFCEL 222 entitled "Chemical Release Studies I: Time Variation Concentration Field Equations of a Single Substance With an Initial Arbitrary Configuration in Free Space" by H. K. Brown, F. F. Marne, and J. Pressman. The format and equations are retained for quick reference and are reproduced as they appear in the original document.

CHAPTER I

CONCENTRATION FIELDS: RECOMBINATION WITHOUT DIFFUSION

Section 1

$$\frac{\partial n}{\partial x} = -\alpha n^2, \quad n(R,0) = f(R) \quad (12)$$

$$1. \quad n(R,x) = \frac{f(R)}{1 + \alpha x f(R)} \quad (15)$$

Section 2

$$\frac{\partial n}{\partial x} = -\alpha n^2 + \gamma n_0, \quad n(R,0) = f(R) \quad (18)$$

$$2. \quad n(R,x) = \left[\frac{\gamma n_0}{\alpha} \right]^{1/2} \tanh \left[x (\alpha \gamma n_0)^{1/2} + \tanh^{-1} \mu \right] \quad \mu < 1 \quad (23)$$

$$n(R,x) = \left[\frac{\gamma n_0}{\alpha} \right]^{1/2} \coth \left[x (\alpha \gamma n_0)^{1/2} + \coth^{-1} \mu \right] \quad \mu > 1$$

where

$$\mu = f(R) \left[\frac{\alpha}{\gamma n_0} \right]^{1/2}$$

Section 3

$$\frac{\partial n}{\partial x} = -\alpha n^2 + \beta n, \quad n(R,0) = f(R) \quad (24)$$

$$3. \quad n(R,x) = \frac{\beta \mathcal{H}(\beta x) f(R)}{\beta - [1 - \mathcal{H}(\beta x) \alpha f(R)]} \quad (25)$$

Section 4

$$\frac{\partial n}{\partial x} = -\alpha n^2 + \gamma n_0 \mathcal{H}(-bx), \quad n(R,0) = f(R) \quad (27)$$

$$4. \quad n(R, x) = \left[\frac{\delta n_0}{\alpha} \right]^{1/2} \operatorname{sh} \left(-\frac{1}{2} b x \right) \frac{\Delta \psi_1 + \psi_2}{\mu \psi_3 + \psi_4} \quad (44)$$

where

$$\begin{aligned} \psi_1 &= I_0(\lambda) K_1(\lambda \xi) + I_1(\lambda \xi) K_0(\lambda) \\ \psi_2 &= I_1(\lambda) K_1(\lambda \xi) - I_1(\lambda \xi) K_1(\lambda) \\ \psi_3 &= I_0(\lambda) K_0(\lambda \xi) - I_0(\lambda \xi) K_0(\lambda) \\ \psi_4 &= I_1(\lambda) K_0(\lambda \xi) + I_0(\lambda \xi) K_1(\lambda) \end{aligned} \quad (45)$$

where

$$\mu = f(R) \left[\frac{\alpha}{\delta n_0} \right]^{1/2} \quad \xi = \operatorname{sh} \left(-\frac{1}{2} b x \right) \quad \lambda = \frac{2}{b} [\alpha \delta n_0]^{1/2} \quad (43)$$

CHAPTER II

CONCENTRATION FIELDS: DIFFUSION WITHOUT RECOMBINATION

Section 3

(a) Arbitrary free space cloud models

$$\frac{\partial n}{\partial t} = -D \nabla^2 n + \beta n \quad n(R, 0) = f(R) \quad (70)$$

$$5a. \quad n(R, t) = \frac{\exp(\beta t)}{[2(\pi D t)^{3/2}]} \iiint_{-\infty}^{\infty} \frac{f(R')}{[2(\pi D t)^{3/2}]^3} \exp\left[-\frac{(x-x')^2 + (y-y')^2 + (z-z')^2}{4Dt}\right] dx' dy' dz'$$

(b) Spherically symmetric cloud models

$$\frac{\partial n}{\partial t} = \frac{D}{r^2} \frac{\partial}{\partial r} \left(r^2 \frac{\partial n}{\partial r} \right) + \beta n$$

(1) Delta Gaussian release

$$5b(1) \quad n(r, t) = \frac{\exp(\beta t)}{[2(\pi D t)^{3/2}]^3} \exp\left(-\frac{r^2}{4Dt}\right) \quad (79)$$

(2) Standard Gaussian release

$$5b(2) \quad n(r, t) = n(0, 0) \frac{r_0^3}{r_g^3} \exp(\beta t) \exp\left(-\frac{r^2}{r_g^2}\right) \quad (81)$$

where

$$r_g^2 = r_0^2 + 4Dt \quad (82)$$

$$n(r, 0) = f(r) = n(0, 0) \exp\left(-\frac{r^2}{r_0^2}\right)$$

(3) Arbitrary release

$$5b(3) \quad n(r, t) = \frac{\exp(\beta t)}{r[\pi D t]^{1/2}} \int_0^\infty \xi f(\xi) \sinh\left(\frac{r\xi}{2Dt}\right) \exp\left(-\frac{r^2 + \xi^2}{4Dt}\right) d\xi \quad (90)$$

where

$$n(r, 0) = f(r)$$

(c) Axially symmetric cloud models

$$\frac{\partial n}{\partial x} = \frac{\partial}{\partial r} \left(r \frac{\partial n}{\partial r} \right) + \beta n$$

(1) Delta Gaussian release

$$5c(1) \quad n(r, x) = \frac{\exp(\beta x)}{4\pi \beta x} \exp\left(-\frac{r^2}{4\beta x}\right) \quad (100)$$

(2) Standard Gaussian release

$$5c(2) \quad n(r, x) = n(0, 0) \exp(\beta x) \frac{r_0^2}{r_g^2} \exp\left(-\frac{r^2}{r_g^2}\right) \quad (102)$$

where

$$r_g^2 = r_0^2 + 4\beta x$$

$$n(r, 0) = n(0, 0) \exp\left(-\frac{r^2}{r_0^2}\right)$$

(3) Arbitrary release

$$5c(3) \quad n(r, x) = \frac{\exp(\beta x)}{2\beta x} \int_0^\infty \xi f(\xi) I_0\left(\frac{r\xi}{2\beta x}\right) \exp\left(-\frac{r^2 + \xi^2}{4\beta x}\right) d\xi \quad (107)$$

where

$$n(r, 0) = f(r)$$

(d) Cylindrically symmetric cloud models

$$\frac{\partial n}{\partial x} = \frac{\partial}{\partial r} \left(r \frac{\partial n}{\partial r} \right) + \frac{\partial^2 n}{\partial z^2} + \beta n$$

(1) Delta Gaussian release in the finite interval

$$-b < z < b$$

$$5d(1) \quad n(r, z, x) = \frac{N(0) \exp(\beta x)}{(4\pi \beta x)(2b)} \exp\left(-\frac{r^2}{4\beta x}\right) Q(z, x) \quad (140)$$

where

$$= \frac{1}{2} \left[\operatorname{erf} \left(\frac{b-z}{2[\mathcal{D}x]^{1/2}} \right) + \operatorname{erf} \left(\frac{b+z}{2[\mathcal{D}x]^{1/2}} \right) \right] \quad |z| < b \quad (132)$$

$Q(z, t)$

$$= \frac{1}{2} \left[\operatorname{erf} \left(\frac{z+b}{2[\mathcal{D}x]^{1/2}} \right) - \operatorname{erf} \left(\frac{z-b}{2[\mathcal{D}x]^{1/2}} \right) \right] \quad |z| > b \quad (133)$$

where

$$\begin{aligned} n(r, z, 0^+) &= \lim_{x \rightarrow 0} \frac{N(0)}{(4\pi\mathcal{D}x)(2b)} \operatorname{erf} \left(-\frac{r^2}{4\mathcal{D}x} \right) \quad |z| < b \\ &= 0 \quad |z| > b \end{aligned}$$

(2) Standard Gaussian release in the finite interval

$$5d(2) \quad n(r, z, t) = n(0, 0, 0) \operatorname{erf}(\beta x) \frac{r_0^2}{r_g^2} Q(z, t) \quad (143)$$

where $Q(z, t)$ is defined by (132) and (133) and where

$$r_g^2 = r_0^2 + 4\mathcal{D}x \quad (82)$$

and

$$\begin{aligned} n(r, z, 0) &= n(0, 0, 0) \operatorname{erf} \left(-\frac{r^2}{r_0^2} \right) \quad |z| < b \\ &= 0 \quad |z| > b \end{aligned} \quad (144)$$

$$N(0) = 2\pi r_0^2 b n(0, 0, 0)$$

(d) Cylindrically symmetric cloud models

(3) Arbitrary release

$$5d(3) \quad n(r, z, t) = \operatorname{erf}(\beta x) \int_0^\infty 2\pi \xi f(\xi, \mathcal{D}) d\xi \int_{-\infty}^\infty \psi(r, z, \xi, \mathcal{D}, t) d\mathcal{D} \quad (149)$$

where

$$\begin{aligned} \psi(r, z, \xi, \mathcal{D}, t) &= \frac{1}{[2(\pi\mathcal{D}x)^{1/2}]^3} I_0 \left(\frac{r\xi}{2\mathcal{D}x} \right) \operatorname{erfc} \left(\frac{z\xi}{2\mathcal{D}x} \right) \operatorname{erf} \left(-\frac{R^2 + \xi^2 + \mathcal{D}^2}{4\mathcal{D}x} \right) \\ R^2 &= r^2 + z^2 = x^2 + y^2 + z^2 \end{aligned} \quad (148)$$

and where

$$n(r, z, 0^+) = f(r, z)$$

Section 6

$$\frac{\partial n}{\partial x} = D \nabla^2 n + \beta n + F(R, z) \quad (151)$$

$$\begin{aligned} 6. \quad n(R, z) = & \frac{\mathcal{H}(\beta z)}{[2(\pi D x)^{1/2}]^3} \iiint_{-\infty}^{\infty} f(R') \mathcal{H}\left(-\frac{R^2}{4Dx}\right) dV' \\ & + \mathcal{H}(\beta z) \int_0^x \frac{\mathcal{H}(-\beta \gamma)}{[2(\pi D(x-\gamma))^{1/2}]^3} \iiint_{-\infty}^{\infty} F(R', \gamma) \mathcal{H}\left(-\frac{R^2}{4D(x-\gamma)}\right) dV' \end{aligned} \quad (168)$$

where

$$R^2 = (x-x')^2 + (y-y')^2 + (z-z')^2$$

$$R = R(x, y, z) \quad R' = R'(x', y', z')$$

and where

$$n(R, 0) = f(R)$$

Example 1:

$$F(R, z) = \gamma n_0 \quad f(r) = n(0, 0) \mathcal{H}\left(-\frac{r^2}{r_0^2}\right) \quad r^2 = x^2 + y^2 + z^2$$

$$6(1) \quad n(r, z) = n(0, 0) \mathcal{H}(\beta z) \frac{r_0^3}{r_0^3} \mathcal{H}\left(-\frac{r^2}{r_0^2}\right) + \frac{\gamma n_0}{\beta} [\mathcal{H}(\beta z) - 1] \quad (171)$$

where

$$r_0^2 = r_0^2 + 4Dx$$

Example 2:

$$F(R, z) = \gamma n_0 \mathcal{H}(-bx) \quad f(r) = n(0, 0) \mathcal{H}\left(-\frac{r^2}{r_0^2}\right) \quad r^2 = x^2 + y^2 + z^2$$

$$6(2) \quad n(r, z) = n(0, 0) \mathcal{H}(\beta z) \frac{r_0^3}{r_0^3} \mathcal{H}\left(-\frac{r^2}{r_0^2}\right) \quad (176)$$

$$+ \frac{\gamma n_0 \mathcal{H}(\beta z)}{\beta + b} [1 - \mathcal{H}(-\beta + b)x]$$

where

$$r_0^2 = r_0^2 + 4Dx$$

Example 3: $\nabla(R,t) = \nabla(t)$, $f(R)$ arbitrary

$$6(3) \quad \nabla(R,t) = \mathcal{H}_p(\beta t) U(R,t) + \mathcal{H}_p(\beta t) \int_0^t \mathcal{H}_p(-\beta \tau) F(\tau) d\tau \quad (182)$$

where

$$U(R,t) = \frac{1}{[2(\pi \beta t)^{3/2}]^3} \iiint_{-\infty}^{\infty} f(R') \mathcal{H}_p\left(-\frac{R^2}{4\beta t}\right) dV'$$

$$R^2 = (x-x')^2 + (y-y')^2 + (z-z')^2$$

$$R = R(x, y, z) \quad R' = R'(x', y', z')$$

CHAPTER III

CONCENTRATION FIELDS WITH BOTH DIFFUSION AND RECOMBINATION

Section 7

$$\frac{\partial n}{\partial t} = D \nabla^2 n - \alpha n^2 \quad n(R, 0) = f(R) \quad (203)$$

$$7. \quad n(R, t) \cong y(R, t) = \frac{\mu(R, t)}{1 + \alpha t \mu(R, t)} \quad (217)$$

where

$$\mu(R, t) = \frac{1}{[2(\pi Dt)^{1/2}]^3} \iiint_{-\infty}^{\infty} f(R') \exp\left(-\frac{R^2}{4Dt}\right) dV' \quad (209)$$

and where

$$\frac{\partial y}{\partial t} = D \nabla^2 y - \alpha(R, t) y^2 \quad y(R, 0) = f(R)$$

and

$$\alpha(R, t) = [1 - \phi(R, t)] \alpha \quad (213)$$

$$\phi(R, t) = \frac{2Dt}{1 + \alpha t \mu} \left(\frac{\bar{\nabla} \mu \cdot \bar{\nabla} \mu}{\mu^2} \right) \quad (222)$$

Section 8

$$\frac{\partial n}{\partial t} = D \nabla^2 n - \alpha n^2 + \beta n \quad n(R, 0) = f(R) \quad (229)$$

$$8. \quad n(R, t) \cong y(R, t) = \frac{\beta \exp(\beta t) \mu(R, t)}{\beta + [\exp(\beta t) - 1] \alpha \mu(R, t)} \quad (237c)$$

where

$$\mu(R, t) = \frac{1}{[2(\pi Dt)^{1/2}]^3} \iiint_{-\infty}^{\infty} f(R') \exp\left(-\frac{R^2}{4Dt}\right) dV'$$

and where

$$\frac{\partial y}{\partial t} = D \nabla^2 y - \alpha(R, t) y^2 + \beta y \quad y(R, 0) = f(R) \quad (230)$$

and

$$\alpha(R, t) = [1 - \phi(R, t)] \alpha \quad (213)$$

$$\phi(R, t) = \frac{2D[1 - \exp(-\beta t)]}{\beta + [\exp(\beta t) - 1] \alpha \mu(R, t)} \left(\frac{\bar{\nabla} \mu \cdot \bar{\nabla} \mu}{\mu^2} \right) \quad (240)$$

Section 9

$$\frac{\partial n}{\partial x} = \mathcal{D} \nabla^2 n - \alpha n^2 + F(R, x) \quad n(R, 0) = f(R) \quad (246)$$

$$9. \quad n(R, x) \cong y(R, x) = \frac{v(R, x)}{1 + \alpha x v(R, x)} \quad (248)$$

where

$$v(R, x) = v'(R, x) + v''(R, x) \quad (256)$$

$$v'(R, x) = \frac{1}{[2(\pi \mathcal{D} x)^{1/2}]^3} \iiint_{-\infty}^{\infty} f(R') \mathcal{H} \left(-\frac{R^2}{4 \mathcal{D} x} \right) dV' \quad (259)$$

$$v''(R, x) = \int_0^x \frac{d\gamma}{[2(\pi \mathcal{D}(x-\gamma))^{1/2}]^3} \iiint_{-\infty}^{\infty} \left[1 + \alpha x v'(R', \gamma) \right]^2 F(R', \gamma) \mathcal{H} \left(-\frac{R^2}{4 \mathcal{D}(x-\gamma)} \right) dV' \quad (260)$$

and where

$$\frac{\partial y}{\partial x} = \mathcal{D} \nabla^2 y - \alpha(R, x) y + h(R, x) F(R, x) \quad (247)$$

$$\alpha(R, x) = [1 - \phi(R, x)] \alpha \quad (213)$$

$$\phi(R, x) = \frac{2 \mathcal{D} x}{1 + \alpha x v(R, x)} \left(\frac{\bar{\nabla} v \cdot \bar{\nabla} v}{v^2} \right) \quad (251)$$

and

$$h(R, x) = \left[\frac{1 + \alpha x v'(R, x)}{1 + \alpha x v(R, x)} \right]^2 \quad (254)$$

Section 10

$$\frac{\partial n}{\partial x} = \mathcal{D} \nabla^2 n - \alpha n^2 + \beta n + F(R, x) \quad n(R, 0) = f(R) \quad (262)$$

$$10. \quad n(R, x) \cong y(R, x) = \frac{\beta \mathcal{H}(\beta x) z(R, x)}{\beta + [\mathcal{H}(\beta x) - 1] \alpha z(R, x)} \quad (264)$$

where

$$z(R, x) = z'(R, x) + z''(R, x)$$

$$z'(R, x) = \frac{1}{[2(\pi \mathcal{D} x)^{1/2}]^3} \iiint_{-\infty}^{\infty} f(R') \mathcal{H} \left(-\frac{R^2}{4 \mathcal{D} x} \right) dV' \quad (273)$$

$$z''(R, x) = \int_0^x d\gamma \iiint_{-\infty}^{\infty} f(R', \gamma) \psi(R, R', x, \gamma) dV' \quad (274)$$

where

$$\psi(R, R', x, \gamma) = \frac{1}{[2(\pi D(x-\gamma))^{1/2}]^3} \exp\left(-\frac{R^2}{4\pi D(x-\gamma)}\right)$$

and

$$f(R, x) = \frac{1}{\beta^2} \exp(-\beta x) [\beta + \alpha(\exp(\beta x) - 1) z'(R, x)]^2 F(R, x) \quad (275)$$

and where

$$\frac{\partial y}{\partial x} = D \nabla^2 y - \alpha(R, x) y^2 + \beta y + h(R, x) F(R, x) \quad (263)$$

$$\alpha(R, x) = [1 - \phi(R, x)] \alpha \quad (213)$$

$$\phi(R, x) = \frac{2D[1 - \exp(-\beta x)]}{\beta + [\exp(\beta x) - 1] \alpha z(R, x)} \left(\frac{\bar{\nabla} z \cdot \bar{\nabla} z}{z^2} \right) \quad (267)$$

and

$$h(R, x) = \left[\frac{\beta + [\exp(\beta x) - 1] \alpha z'(R, x)}{\beta + [\exp(\beta x) - 1] \alpha z(R, x)} \right]^2 \quad (272)$$

The Table of Contents from Technical Report No. AFCEP 223 entitled "Chemical Release Studies II: Coupled Time Varying Concentration Field Equations of Two Substances With Initial Arbitrary Configurations in Free Space" by H.K. Brown, F.F. Marmo and J. Pressman is as follows:

TABLE OF CONTENTS

<u>Section</u>	<u>Title</u>	<u>Page</u>
	INTRODUCTION.....	1
	CHAPTER I	
	CLOUD MODELS WITH DIFFUSION BUT NO RECOMBINATION: IDENTICAL DIFFUSION COEFFICIENTS FOR BOTH SUBSTANCES.....	4
1.	Identical Linear Coefficients.....	4
2.	Distinct Linear Coefficients.....	9
	CHAPTER II	
	CLOUD MODELS WITH DIFFUSION BUT NO RECOMBINATION: DISTINCT DIFFUSION AND LINEAR COEFFICIENTS FOR BOTH SUBSTANCES.....	15
3.	Definition of the Generalized Unit Source Function $\Psi(R, R', t, \tau)$	15
4.	Derivation of the Concentration Field Equations for Arbitrary Initial Density Distributions of Both Substances.....	21
5.	Spherically Symmetric Cloud Models.....	27
	a. Standard Gaussian release.....	27
	b. Arbitrary release.....	32
6.	Axially Symmetric Cloud Models.....	36
	a. Standard Gaussian release.....	36
	b. Arbitrary release.....	39
7.	Cylindrically Symmetric Cloud Models.....	41
	a. Arbitrary release.....	41
	b. Finite length axially symmetric Gaussian release.....	44
8.	General Integral Formula for the Concentration Field Equation of the Second Substance.....	52
	CHAPTER III	
	CLOUD MODELS WITH RECOMBINATION BUT NO DIFFUSION.....	58
9.	Identical Coefficients for Both Substances.....	58

TABLE OF CONTENTS (continued)

<u>Section</u>	<u>Title</u>	<u>Page</u>
CHAPTER IV		
	CLOUD MODELS WITH DIFFUSION, PSEUDO-NON-LINEAR PROCESSES, AND LINEAR PROCESSES.....	64
10.	Identical Coefficients for Both Substances.....	69
11.	Distinct Coefficients for Both Substances.....	73
	a. Diffusion coefficients distinct.....	73
	b. Diffusion coefficients identical.....	79
CHAPTER V		
	CLOUD MODELS GENERATED BY THE COUPLED ACTION OF DIFFUSION AND OF NON-LINEAR AND LINEAR PROCESSES.....	81
12.	Identical Diffusion, Non-Linear, and Linear Coefficients for Both Substances.....	87
13.	Distinct Coefficients for Both Substances (Without a Non-Linear Growth Process for the First Substance).....	96
	CONCLUDING REMARKS.....	100
	SUMMARY OF CLOUD MODEL FORMULAS.....	103

The Summary taken from Technical Report No. AFCEC 223 entitled "Chemical Release Studies II: Coupled Time Varying Concentration Field Equations of Two Substances With Initial Arbitrary Configurations in Free Space" by H. K. Brown, F. F. Harms, and J. Pressman is as follows.

CHAPTER I

CLOUD MODELS WITH DIFFUSION BUT NO RECOMBINATION: IDENTICAL DIFFUSION COEFFICIENTS FOR BOTH SUBSTANCES

Section 1

$$\begin{aligned} (a) \quad \frac{\partial n_1}{\partial t} &= D \nabla^2 n_1 - k n_1, & n_1(R, 0) &= f_1(R) \\ (b) \quad \frac{\partial n_2}{\partial t} &= D \nabla^2 n_2 + k n_1, & n_2(R, 0) &= 0 \end{aligned} \quad (1)$$

$$\begin{aligned} (a) \quad n_1(R, t) &= \mathcal{H}(-kt) U(R, t) \\ (b) \quad n_2(R, t) &= [1 - \mathcal{H}(-kt)] U(R, t) \end{aligned} \quad (11)$$

where $U(R, t)$ is defined as the solution of the boundary value problem

$$(a) \quad \frac{\partial U}{\partial t} = D \nabla^2 U, \quad U(R, 0) = f_1(R) \quad (12)$$

or by the integral formula

$$(b) \quad U(R, t) = \iiint_{-\infty}^{\infty} f_1(R') \psi(R, R', t) dV'$$

where $\psi(R, R', t)$ is a unit source function in a form corresponding to the symmetry of $f_1(R)$; otherwise it is defined as

$$\psi(R, R', t) = \frac{1}{[2(\pi Dt)^{3/2}]^3} \mathcal{H}\left(-\frac{R^2}{4Dt}\right) \quad t > 0 \quad (3)$$

where

$$R^2 = (x - x')^2 + (y - y')^2 + (z - z')^2$$

and

$$R = R: (x, y, z) \quad R' = R': (x', y', z')$$

Section 2

$$\begin{aligned} (a) \quad \frac{\partial n_1}{\partial x} &= \mathcal{D} \nabla^2 n_1 - k_1 n_1, & n_1(R, 0) &= f_1(R) \\ (b) \quad \frac{\partial n_2}{\partial x} &= \mathcal{D} \nabla^2 n_2 + k_2 n_1, & n_2(R, 0) &= 0 \end{aligned} \quad (14)$$

$$(a) \quad n_1(R, x) = \exp(-k_1 x) U(R, x)$$

2.

$$(b) \quad n_2(R, x) = \frac{k_2}{k_1} [1 - \exp(-k_1 x)] U(R, x)$$

where $U(R, x)$ is defined by equation (12b).

CHAPTER II

CLOUD MODELS WITH DIFFUSION BUT NO RECOMBINATION: DISTINCT DIFFUSION AND LINEAR COEFFICIENTS FOR BOTH SUBSTANCES

Section 3

$$\begin{aligned} \text{(a)} \quad \frac{\partial n}{\partial t} &= D \nabla^2 n + F(R, t) \\ \text{(b)} \quad n(R, 0) &= 0 \end{aligned} \tag{26}$$

$$3. \quad n(R, t) = \int_0^t d\gamma \iiint_{-\infty}^{\infty} F(R', \gamma) \psi(R, R', t, \gamma) dV' \tag{32}$$

where $\psi(R, R', t, \gamma)$ is a unit source function in a form corresponding to the symmetry of $F(R, t)$; otherwise it is defined as

$$\psi(R, R', t, \gamma) = \frac{1}{[2(\pi D(t-\gamma))^{3/2}]^3} \exp\left(-\frac{R^2}{4\pi D(t-\gamma)}\right) \tag{30}$$

where

$$t > \gamma \quad R \equiv R: (x, y, z) \quad R' \equiv R': (x', y', z')$$

and

$$R^2 = (x-x')^2 + (y-y')^2 + (z-z')^2$$

Section 4

$$\begin{aligned} \text{(a)} \quad \frac{\partial n_1}{\partial t} &= D_1 \nabla^2 n_1 - k_1 n_1 & n_1(R, 0) &= f_1(R) \\ \text{(b)} \quad \frac{\partial n_2}{\partial t} &= D_2 \nabla^2 n_2 + k_2 n_1 & n_2(R, 0) &= f_2(R) \end{aligned} \tag{51}$$

$$\begin{aligned} \text{(a)} \quad n_1(R, t) &= \exp(-k_1 t) U_1(R, t) \\ 4. \quad \text{(b)} \quad n_2(R, t) &= U_2(R, t) + k_2 \int_0^t d\gamma \iiint_{-\infty}^{\infty} n_1(R', \gamma) \psi_2(R, R', t, \gamma) dV' \end{aligned} \tag{52}$$

where $U_i(R, t)$ is defined as the solution of the boundary value problem

$$(a) \quad \frac{\partial U_i}{\partial t} = D_i \nabla^2 U_i \quad U_i(R, 0) = f_i(R) \quad i = 1, 2,$$

or by the integral formula

$$(b) \quad U_i(R, t) = \int \int \int_{-\infty}^{\infty} f_i(R') \psi_i(R, R', t) dV' \quad (52)$$

and where $\psi_i(R, R', t)$ is a unit source function in a form corresponding to the symmetry of $f_i(R)$; otherwise it is defined as

$$\psi_i(R, R', t) = \frac{1}{[2(\pi D_i t)^{3/2}]^3} \exp\left(-\frac{R^2}{4D_i t}\right) \quad t > 0 \quad (52)$$

furthermore, $\psi_2(R, R', t, \tau)$ is a unit source function which is defined by the formula

$$\psi_2(R, R', t, \tau) \equiv \psi_2(R, R', t - \tau) \quad t > \tau \quad (52)$$

Section 5(a)

$$(a) \quad \frac{\partial n_1}{\partial t} = D_1 \nabla^2 n_1 - k_1 n_1 \quad n_1(r, 0) = n_1(0, 0) \exp\left(-\frac{r^2}{t_0^2}\right) \quad (53)$$

$$(b) \quad \frac{\partial n_2}{\partial t} = D_2 \nabla^2 n_2 + k_2 n_1 \quad n_2(r, 0) = 0$$

where $r^2 = x^2 + y^2 + z^2$ and the Laplacian $\nabla^2 n$ is in the spherically symmetric form:

$$\nabla^2 n = \frac{1}{r^2} \frac{\partial}{\partial r} \left(r^2 \frac{\partial n}{\partial r} \right)$$

$$(a) \quad n_1(r, t) = \exp(-k_1 t) U_1(r, t) \quad (55)$$

5a.

$$(b) \quad n_2(r, t) = k_2 \int_0^t \exp(-k_1 \tau) U_1(r, \tau) d\tau \quad (55)$$

where

$$(a) \quad U_1(r, t) = n_1(0, 0) \frac{r_0^3}{r_{g,1}^3} \exp\left(-\frac{r^2}{t_{g,1}^2}\right) \quad (55)$$

$$(b) \quad r_{g,1}^2 = r_0^2 + 4D_1 t$$

and where

$$\begin{aligned}
 (a) \quad U_1(r, \gamma) &= n_1(0, 0) \frac{r_0^3}{r^3} \exp\left(-\frac{r^2}{r_0^2}\right) \\
 (b) \quad r_\sigma^2 &= r_0^2 + 4\sigma(x, \gamma) \\
 (c) \quad \gamma &= \frac{\sigma(x, \gamma)}{D_1} = \gamma + \frac{D_2}{D_1}(x - \gamma) \quad x > \gamma
 \end{aligned}
 \tag{69}$$

Section 5(b)

$$\begin{aligned}
 (a) \quad \frac{\partial n_1}{\partial x} &= D_1 \nabla^2 n_1 - k_1 n_1, & n_1(r, 0) &= f_1(r) \\
 (b) \quad \frac{\partial n_2}{\partial x} &= D_2 \nabla^2 n_2 + k_2 n_1, & n_2(r, 0) &= f_2(r)
 \end{aligned}$$

where the Laplacian $\nabla^2 n$ is in spherically symmetric form and the $f_i(r)$ are spherically symmetric.

$$(a) \quad n_1(r, x) = \exp(-k_1 x) U_1(r, x)$$

5b.

$$(b) \quad n_2(r, x) = U_2(r, x) + k_2 \int_0^x \exp(-k_1 \gamma) d\gamma \int_0^\infty 4\pi \xi^2 U_1(\xi, \gamma) \psi_2(r, \xi, x, \gamma) d\xi \tag{72}$$

where

$$\begin{aligned}
 (a) \quad U_i(r, x) &= \int_0^\infty f_i(\xi) \psi_i(r, \xi, x) 4\pi \xi^2 d\xi \quad i=1, 2, \\
 (b) \quad \psi_i(r, \xi, x) &= \frac{1}{4\pi r \xi [\pi D_i x]^{1/2}} \sinh\left(\frac{r\xi}{2D_i x}\right) \exp\left(-\frac{r^2 + \xi^2}{4D_i x}\right) \\
 (c) \quad \psi_2(r, \xi, x, \gamma) &\equiv \psi_2(r, \xi, x - \gamma) \quad x > \gamma
 \end{aligned}
 \tag{73}$$

Section 6(a)

$$\begin{aligned}
 (a) \quad \frac{\partial n_1}{\partial x} &= D_1 \nabla^2 n_1 - k_1 n_1, & n_1(r, 0) &= n_1(0, 0) \exp\left(-\frac{r^2}{r_0^2}\right) \\
 (b) \quad \frac{\partial n_2}{\partial x} &= D_2 \nabla^2 n_2 + k_2 n_1, & n_2(r, 0) &= 0
 \end{aligned}
 \tag{75}$$

where $r^2 = x^2 + y^2$ and the Laplacian $\nabla^2 n$ is in the axially symmetric form

$$\nabla^2 n = \frac{1}{r} \frac{\partial}{\partial r} \left(r \frac{\partial n}{\partial r} \right)$$

$$(a) \quad n_1(r, x) = \mathcal{H}_p(-k, x) U_1(r, x) \quad (77)$$

6a.

$$(b) \quad n_2(r, x) = k_2 \int_0^x \mathcal{H}_p(-k, \gamma) U_1(r, \gamma) d\gamma \quad (86)$$

where

$$(a) \quad U_1(r, x) = n_1(0, 0) \frac{r_0^2}{r_{g_1}^2} \mathcal{H}_p\left(-\frac{r^2}{r_{g_1}^2}\right) \quad (77)$$

$$(b) \quad r_{g_1}^2 = r_0^2 + 4D_1 x$$

and where

$$(a) \quad U_1(r, \gamma) = n_1(0, 0) \frac{r_0^2}{r_0^2} \mathcal{H}_p\left(-\frac{r^2}{r_0^2}\right)$$

$$(b) \quad r_0^2 = r_0^2 + 4D(x, \gamma) \quad (85)$$

$$(c) \quad \mathcal{F} = \frac{\sigma(x, \gamma)}{D_1} = \gamma + \frac{D_2}{D_1} (x - \gamma) \quad x > \gamma$$

Section 6(b)

$$(a) \quad \frac{\partial n_1}{\partial x} = D_1 \nabla^2 n_1 - k_1 n_1, \quad n_1(r, 0) = f_1(r) \quad (87)$$

$$(b) \quad \frac{\partial n_2}{\partial x} = D_2 \nabla^2 n_2 + k_2 n_2, \quad n_2(r, 0) = f_2(r)$$

where the Laplacian $\nabla^2 n$ is in axially symmetric form and the $f_1(r)$ are axially symmetric.

$$(a) \quad n_1(r, x) = \mathcal{H}_p(-k, x) U_1(r, x)$$

6b.

$$(b) \quad n_2(r, x) = U_2(r, x) + k_2 \int_0^x \mathcal{H}_p(-k, \gamma) d\gamma \int_0^\infty 2\pi \xi U_1(\xi, \gamma) \psi_2(r, \xi, x, \gamma) d\xi \quad (88)$$

where

$$\begin{aligned}
 (a) \quad U_i(r, x) &= \int_0^\infty f_i(\xi) \psi_i(r, \xi, x) 2\pi \xi d\xi \\
 (b) \quad \psi_i(r, \xi, x) &= \frac{1}{4\pi D_i x} I_0\left(\frac{r\xi}{2D_i x}\right) \exp\left(-\frac{r^2 + \xi^2}{4D_i x}\right) \\
 (c) \quad \psi_i(r, \xi, x, \gamma) &\equiv \psi_i(r, \xi, x - \gamma) \quad x > \gamma
 \end{aligned} \tag{89}$$

Section 7(a)

$$\begin{aligned}
 (a) \quad \frac{\partial n_1}{\partial x} &= D_1 \nabla^2 n_1 - k_1 n_1 \quad n_1(r, z, 0) = f_1(r, z) \\
 (b) \quad \frac{\partial n_2}{\partial x} &= D_2 \nabla^2 n_2 + k_2 n_1 \quad n_2(r, z, 0) = f_2(r, z)
 \end{aligned} \tag{92}$$

where the Laplacian $\nabla^2 n$ is in the cylindrically symmetric form

$$\nabla^2 n = \frac{1}{r} \frac{\partial}{\partial r} \left(r \frac{\partial n}{\partial r} \right) + \frac{\partial^2 n}{\partial z^2} \quad r^2 = x^2 + y^2$$

and the $f_1(r, z)$ are axially symmetric.

$$(a) \quad n_1(r, z, x) = \exp(-k_1 x) U_1(r, z, x)$$

7a.

$$(b) \quad n_2(r, z, x) = U_2(r, z, x) + k_2 \int_0^x \exp(-k_1 \gamma) U_1(r, z, \gamma) d\gamma$$

where

$$\begin{aligned}
 (a) \quad U_i(r, z, x) &= \int_0^\infty 2\pi \xi d\xi \int_{-\infty}^\infty f_i(\xi, \eta) \psi_i(r, z, \xi, \eta, x) d\eta \\
 (b) \quad \psi_i(r, z, \xi, \eta, x) &= \frac{1}{[2(\pi D_i x)^{1/2}]^3} I_0\left(\frac{r\xi}{2D_i x}\right) \cosh\left(\frac{z\eta}{2D_i x}\right) \exp\left(-\frac{R^2 + R'^2}{4D_i x}\right) \\
 (c) \quad \gamma = \frac{\sigma(x, \gamma)}{D_i} &= \gamma + \frac{D_2}{D_i} (x - \gamma) \quad x > \gamma
 \end{aligned}$$

Section 7(b)

$$\begin{aligned}
 (a) \quad \frac{\partial n_1}{\partial x} &= D_1 \nabla^2 n_1 - k_1 n_1 \\
 &= n_1(0,0,0) \exp\left(-\frac{r^2}{r_0^2}\right) & |z| < b \\
 n_1(r,z,0) &= 0 & |z| > b
 \end{aligned} \tag{102}$$

(b)

where the Laplacian $\nabla^2 n$ is in cylindrically symmetric form.

$$(a) \quad n_1(r, z, x) = \exp(-k_1 x) U_1(r, z, x) \tag{93}$$

7b.

$$(b) \quad n_2(r, z, x) = k_2 \int_0^x \exp(-k_1 \gamma) U_1(r, z, \gamma) d\gamma \tag{129}$$

where

$$(a) \quad U_1(r, z, x) = P_1(r, x) Q_1(z, x)$$

$$(b) \quad P_1(r, x) = n_1(0,0,0) \frac{r_0^2}{r_g^2} \exp\left(-\frac{r^2}{r_g^2}\right) \quad r \geq 0$$

$$(c) \quad Q_1(z, x) = \frac{1}{2} \left[\exp\left(\frac{b+z}{2[D_1 x]^{1/2}}\right) + \exp\left(\frac{b-z}{2[D_1 x]^{1/2}}\right) \right] \quad |z| < b \tag{122b}$$

$$(d) \quad Q_1(z, x) = \frac{1}{2} \left[\exp\left(\frac{z+b}{2[D_1 x]^{1/2}}\right) - \exp\left(\frac{z-b}{2[D_1 x]^{1/2}}\right) \right] \quad |z| > b$$

$$r_g^2 = r_0^2 + 4D_1 x$$

$$(e) \quad \xi = \frac{\sigma(x, \gamma)}{D_1} = \gamma + \frac{D_2}{D_1} (x - \gamma) = \frac{\sigma}{D_1}$$

In particular,

$$(a) \quad U_1(r, z, \xi) = P_1(r, \xi) Q(z, \xi)$$

$$(b) \quad P_1(r, \xi) = n_1(0,0,0) \frac{r_0^2}{r_\sigma^2} \exp\left(-\frac{r^2}{r_\sigma^2}\right) \tag{126}$$

$$\begin{aligned}
 (c) \quad Q_1(z, \xi) &= \frac{1}{2} \left[\exp\left(\frac{b+z}{2\sigma^{1/2}}\right) + \exp\left(\frac{b-z}{2\sigma^{1/2}}\right) \right] & |z| < b \\
 &= \frac{1}{2} \left[\exp\left(\frac{z+b}{2\sigma^{1/2}}\right) - \exp\left(\frac{z-b}{2\sigma^{1/2}}\right) \right] & |z| > b
 \end{aligned}$$

Section 8

$$(a) \quad \frac{\partial n_1}{\partial t} = D_1 \nabla^2 n_1 - k_1 n_1, \quad n_1(R, 0) = f_1(R) \quad (26)$$

$$(b) \quad \frac{\partial n_2}{\partial t} = D_2 \nabla^2 n_2 + k_2 n_1, \quad n_2(R, 0) = 0 \quad (28)$$

where the Laplacian $\nabla^2 n$ is in the generalized form

$$\nabla^2 n = \bar{\nabla} \cdot \bar{\nabla} n$$

$$(a) \quad n_1(R, t) = \mathcal{H}_p(-k_1, t) U_1(R, t) \quad (29)$$

8.

$$(b) \quad n_2(R, t) = k_2 \int_0^t \mathcal{H}_p(-k_1, \tau) U_1(R, \tau) d\tau$$

where $U_1(R, t)$ is defined as the solution of the boundary value problem

$$\frac{\partial U_1}{\partial t} = D_1 \nabla^2 U_1, \quad U_1(R, 0) = f_1(R) \quad (36)$$

otherwise, it is defined by the integral formula

$$U_1(R, t) = \iiint_{-\infty}^{\infty} f_1(R') \psi_1(R, R', t) dV$$

where $\psi_1(R, R', t)$ is an appropriate unit source function corresponding to the symmetry of $f_1(R)$.

The variable ξ is defined as

$$\xi = \frac{\sigma(x, \gamma)}{D_1} = \frac{\sigma}{D_1} = \gamma + \frac{D_2}{D_1} (t - \gamma) \quad (133)$$

An alternate definition of $U_1(R, \xi)$ is

$$U_1(R, \xi) \equiv \iiint_{-\infty}^{\infty} U_1(R', \gamma) \psi_2(R, R', t, \gamma) dV' \quad (136)$$

where

$$\psi_2(R, R', t, \gamma) = \frac{1}{[2(\pi D_2(t - \gamma))^{3/2}]^3} \mathcal{H}_p\left(-\frac{R^2}{4D_2(t - \gamma)}\right)$$

with

$$R^2 = (x - x')^2 + (y - y')^2 + (z - z')^2$$

CHAPTER III

CLOUD MODELS WITH RECOMBINATION BUT NO DIFFUSION

Section 9

$$\begin{aligned} (a) \quad \frac{\partial n_1}{\partial x} &= \alpha n_2^2 - k n_1, & n_1(R, 0) &= f_1(R) \\ (b) \quad \frac{\partial n_2}{\partial x} &= -\alpha n_2^2 + k n_1, & n_2(R, 0) &= 0 \end{aligned} \quad (137)$$

$$(a) \quad n_1(R, x) = f_1(R) - V_2(R) \left[1 - \frac{2+3\gamma}{1+\gamma+(1+2\gamma)\exp\left(\frac{(2+\gamma)\gamma x}{1+\gamma}\right)} \right] \quad (157)$$

$$(b) \quad n_2(R, x) = V_2(R) \left[1 - \frac{2+3\gamma}{1+\gamma+(1+2\gamma)\exp\left(\frac{(2+\gamma)\gamma x}{1+\gamma}\right)} \right]$$

where

$$\begin{aligned} (a) \quad \gamma &= V_2(R) / f_1(R) \\ (b) \quad V_2(R) &= \frac{1}{2\alpha} \left[(R^2 + 4R\alpha f_1(R))^{1/2} - R \right] \end{aligned} \quad (156)$$

Note that $V_2(R)$ is the steady state value of $n_2(R, t)$

$$\lim_{x \rightarrow T} n_2(R, x) = V_2(R) \quad T > M$$

CHAPTER IV

CLOUD MODELS WITH DIFFUSION, PSEUDO-NON-LINEAR PROCESSES, AND LINEAR PROCESSES

Section 10

$$\begin{aligned} (a) \quad \frac{\partial n_1}{\partial x} &= \nabla^2 n_1 + \gamma n_1 - k n_1, & n_1(R, 0) &= f(R) \\ (b) \quad \frac{\partial n_2}{\partial x} &= \nabla^2 n_2 - \gamma n_2 + k n_1, & n_2(R, 0) &= 0 \end{aligned} \quad (162)$$

$$(a) \quad n_1(R, x) = \left[\frac{\gamma}{\gamma + k} + \frac{k}{\gamma + k} \operatorname{erfc}(-(\gamma + k)x) \right] U(R, x) \quad (174)$$

10.

$$(b) \quad n_2(R, x) = \left[\frac{k}{\gamma + k} + \frac{k}{\gamma + k} \operatorname{erfc}(-(\gamma + k)x) \right] U(R, x) \quad (175)$$

where $U(R, t)$ is the solution of the boundary value problem

$$(a) \quad \frac{\partial U}{\partial x} = \nabla^2 U \quad U(R, 0) = f(R) \quad (165)$$

and is defined by the integral formula

$$(b) \quad U(R, x) = \iiint_{-\infty}^{\infty} f(R') \psi(R, R', x) dV' \quad (166)$$

where $\psi(R, R', t)$ is a unit source function expressed in a form corresponding to the symmetry of $f(R)$; otherwise, it is defined as

$$\psi(R, R', x) = \frac{1}{[2(\pi D x)^{3/2}]^3} \operatorname{erfc}\left(-\frac{R^2}{4 D x}\right) \quad (166)$$

where

$$R^2 = (x - x')^2 + (y - y')^2 + (z - z')^2$$

and

$$R = R : (x, y, z) \quad R' = R' : (x', y', z')$$

Section 11(a)

$$\begin{aligned} (a) \quad \frac{\partial n_1}{\partial x} &= D_1 \nabla^2 n_1 - k_1 n_1, & n_1(R, 0) &= f_1(R) \\ (b) \quad \frac{\partial n_2}{\partial x} &= D_2 \nabla^2 n_2 - \gamma_2 n_2 + k_2 n_1, & n_2(R, 0) &= 0 \end{aligned} \quad (163)$$

$$(a) \quad n_1(R, x) = \mathcal{H}(-k_1 x) U_1(R, x)$$

11a.

$$(b) \quad n_2(R, x) = k_2 \mathcal{H}(-\gamma_2 x) \int_0^x \mathcal{H}((\gamma_2 - k_1)\gamma) U_1(R, \gamma) d\gamma \quad (164)$$

where

$$\gamma = \frac{\sigma(x, \gamma)}{D_1} = \gamma + \frac{D_2}{D_1} (x - \gamma)$$

and where $U_1(R, t)$ is defined either as the solution of the boundary value problem

$$\frac{\partial U_1}{\partial x} = D_1 \nabla^2 U_1, \quad U_1(R, 0) = f_1(R)$$

or by the integral formula

$$U_1(R, x) = \iiint_{-\infty}^{\infty} f_1(R') \psi_1(R, R', x) dV'$$

where $\psi(R, R', t)$ is a unit source function expressed in a form corresponding to the symmetry of $f_1(R)$; otherwise, it is defined as

$$\psi_1(R, R', x) = \frac{1}{[2(\pi D_1 x)^{1/2}]^3} \mathcal{H}\left(-\frac{R^2}{4D_1 x}\right)$$

where

$$R^2 = (x - x')^2 + (y - y')^2 + (z - z')^2$$

Section 11(b)

$$\begin{aligned} (a) \quad \frac{\partial n_1}{\partial x} &= D \nabla^2 n_1 - k_1 n_1, & n_1(R, 0) &= f_1(R) \\ (b) \quad \frac{\partial n_2}{\partial x} &= D \nabla^2 n_2 - \gamma_2 n_2 + k_2 n_1, & n_2(R, 0) &= 0 \end{aligned}$$

$$(a) \quad \eta_1(R, t) = \exp(-k_1 t) U_1(R, t)$$

11b.

$$(b) \quad \eta_2(R, t) = \frac{k_2}{\delta_2 - k_1} [\exp(-k_1 t) - \exp(-\delta_2 t)] U_1(R, t)$$

where $U_1(R, t)$ is defined as in Section 11(b).

CHAPTER V

CLOUD MODELS GENERATED BY THE COUPLED ACTION OF DIFFUSION AND OF NON-LINEAR AND LINEAR PROCESSES

Section 12

$$(a) \quad \frac{\partial n_1}{\partial x} = D \nabla^2 n_1 + \alpha n_1^2 - k n_1, \quad n_1(R, 0) = f_1(R) \quad (204)$$

$$(b) \quad \frac{\partial n_2}{\partial x} = D \nabla^2 n_2 - \alpha n_1^2 + k n_1, \quad n_2(R, 0) = 0$$

$$(a) \quad n_1(R, t) = U(R, t) - n_2(R, t)$$

$$12. \quad (b) \quad U(R, t) = \iiint_{-\infty}^{\infty} f(R') \psi(R, R', t) dV' \quad (207)$$

$$(c) \quad n_2(R, t) \cong y(R, t) = \frac{k \operatorname{erf}(-kt) z(R, t)}{k + [1 - \operatorname{erf}(-kt)] \alpha z(R, t)}$$

where $y(R, t)$ is the solution of the problem

$$(a) \quad \frac{\partial y}{\partial t} = D \nabla^2 y - \alpha(r, t) y^2 - k y + h(R, t) k U(R, t) \quad (212)$$

$$(b) \quad k(R, t) = \left[\frac{k}{k + 4\alpha U(R, t) \operatorname{sinh}^2(\frac{1}{2} kt)} \right]^2 \quad (225)$$

$$(c) \quad \alpha(R, t) = [1 - \phi(R, t)] \alpha$$

where

$$(d) \quad \phi(R, t) = \frac{2D [\operatorname{erf}(kt) - 1]}{k + 4\alpha U(R, t) \operatorname{sinh}^2(\frac{1}{2} kt)} \left(\frac{\bar{\nabla} U \cdot \bar{\nabla} U}{U^2} \right) \quad (226)$$

in particular

$$(a) \quad z(R, t) = [\operatorname{erf}(kt) - 1] U(R, t)$$

$$(b) \quad y(R, t) = \frac{k [1 - \operatorname{erf}(-kt)] U(R, t)}{k + 4\alpha U(R, t) \operatorname{sinh}^2(\frac{1}{2} kt)} \quad (224)$$

furthermore, $z = z(R, t)$ satisfies the boundary value problem conditions

$$\frac{\partial z}{\partial t} = \mathcal{D} \nabla^2 z + k_1 \exp(k_1 t) U(R, t) \quad z(R, 0) = 0 \quad (222)$$

When $f_1(R)$ is spherically symmetric Gaussian

$$f_1(R) = n_1(0, 0) \exp\left(-\frac{r^2}{r_0^2}\right) \quad r^2 = x^2 + y^2 + z^2$$

then

$$U(R, t) = n_1(0, 0) \frac{r_0^3}{r_g^3} \exp\left(-\frac{r^2}{r_g^2}\right)$$

with

$$r_g^2 = r_0^2 + 4 \mathcal{D} t$$

The corresponding values of $y(R, t) \approx n_2(R, t)$, $\phi(R, t)$ and $h(R, t)$ are found by using this function of $U(R, t)$ in formulas for $y(R, t)$, $\phi(R, t)$ and $h(R, t)$, respectively.

Section 13

$$\begin{aligned} (a) \quad \frac{\partial n_1}{\partial t} &= \mathcal{D}_1 \nabla^2 n_1 - k_1 n_1 & n_1(r, 0) &= f_1(r) \\ (b) \quad \frac{\partial n_2}{\partial t} &= \mathcal{D}_2 \nabla^2 n_2 - \alpha_2 n_2^2 + k_2 n_1 & n_2(R, 0) &= f_2(R) \end{aligned} \quad (234)$$

$$(a) \quad n_1(R, t) = \exp(-k_1 t) U_1(R, t) \quad (236)$$

$$13. \quad (b) \quad U_1(R, t) = \iiint_{-\infty}^{\infty} f_1(R') \psi(R, R', t) dV' \quad (235)$$

$$(c) \quad n_2(R, t) \approx y(R, t) = \frac{v(R, t)}{1 + \alpha_2 t v(R, t)} \quad (239)$$

where $y(R, t)$ is the solution of the boundary value problem

$$(a) \quad \frac{\partial y}{\partial t} = \mathcal{D}_2 \nabla^2 y - \alpha_2(R, t) y^2 + k_2 \exp(-k_1 t) U_1(R, t) h(R, t)$$

where

$$(b) \quad \alpha(R, t) = [1 - \phi(R, t)] \alpha_2 \quad (240)$$

$$(c) \quad \phi(R, t) = \frac{2 \mathcal{D}_2 t}{1 + \alpha_2 t v(R, t)} \left(\frac{\bar{\nabla} v \cdot \bar{\nabla} v}{v^2} \right)$$

$$(d) \quad h(R, x) = \left[\frac{1 + \alpha_2 x v'(R, x)}{1 + \alpha_2 x v(R, x)} \right]^2 \quad (241)$$

and where

$$(e) \quad v'(R, x) = \iiint_{-\infty}^{\infty} f_2(R') \psi_2(R, R', x) dV' \quad (244)$$

$$(f) \quad v''(R, x) = k_2 \int_0^x \exp(-k_1 \gamma) d\gamma \iiint_{-\infty}^{\infty} (1 + \alpha_2 \gamma v'(R', \gamma))^2 \times U_1(R', \gamma) \psi_2(R, R', x, \gamma) dV' \quad (245)$$

where

$$(g) \quad v(R, x) = v'(R, x) + v''(R, x)$$

4. OPTICAL PROPERTIES OF CHEMICAL RELEASES

The value of an understanding of the optical behavior of planned experiments has been discussed in previous reports. This phase represents a continuing effort for the understanding of the several pertinent areas including resonance, chemiluminescence and particulate scattering. Some aspects of the case of resonance scattering have been treated previously. However, in this quarter additional input to resonance scattering has been generated and is given below along with brief references to some previously reported material. The latter is included for continuity and completeness. In addition, chemiluminescence studies have been initiated; the current status of this effort is indicated in this section. The cases of resonance scattering and chemiluminescence are discussed in turn. The case of particulate scattering is left as a future effort.

A. Resonance Scattering

Optical properties of resonance clouds with diffusion has been discussed in some detail in AFCL 207; therefore, no details are given here. However, Tables 2a through 2d reproduced here from AFCL 207 serve as a convenient condensation of the technical area covered. The Tables identify the physical problems investigated, the corresponding defining equations, the derived concentration functions, and the pertinent solutions for the preceding cases. Tables 3a through 3d present a summary of the techniques to employ for reducing and analyzing the data. For an extended theoretical treatment see "Chemical Release Studies VII".

However, aside from theoretical approach, considerable parameterization was accomplished in order to better appreciate some of the practical implications of the theory as to proper experimental design related to the determination of geophysical constant and/or practical utility in systems. Only a few examples of this type of parameterization are included here.

1. Parameterization

Table 4 gives the values of the parameters used as well as the governing equations. In Figs. 1 and 2 are plotted the variation of isophote distance with time. Fig. 3 shows the time required for an isophote to reach its maximum size and to collapse to zero. The graphs shown are computed for the specific case of the release of 0.5 mole sodium and then represent the behavior of the isophote corresponding to $S = 10^{11}$ atms/cm². Note that the "minimum size cloud" refers to the case when the initial contaminant

SUMMARY OF OPTICAL PROPERTIES		
TABLE 2a. DESCRIPTION OF PHYSICAL PROBLEM		
Type	Continuity Equation Initial Release Function	Concentration Function $n(r,t)$
I. Spherically Symmetric Diffusion, Initial Gaussian Release	$\frac{\partial n}{\partial t} = D \nabla^2 n \quad n = n(r,t)$ $n(r,0) = n_0 \exp\left(-\frac{r^2}{r_0^2}\right)$	$\frac{N}{\pi^{3/2} r_0^3} \exp\left(-\frac{r^2}{r_g^2}\right)$ $r_g^2 = r_0^2 + 4Dt$
II. Expansion of a Rarefied Gas into a Vacuum, Initial Delta Gaussian Release	$\lim_{t \rightarrow 0} \frac{N}{\pi^{3/2} v^3 t^3} \exp\left(-\frac{r^2}{v^2 t^2}\right)$	$\frac{N}{\pi^{3/2} v^3 t^3} \exp\left(-\frac{r^2}{v^2 t^2}\right)$
III. Spherically Symmetric Diffusion with Consumption, Initial Gaussian Release	$\frac{\partial n}{\partial t} = D \nabla^2 n - kn \quad n = n(r,t)$ $n(r,0) = n_0 \exp\left(-\frac{r^2}{r_0^2}\right)$	$\frac{N}{\pi^{3/2} r_0^3} \exp(-kt) \exp\left(-\frac{r^2}{r_g^2}\right)$
IV. Spherically Symmetric Diffusion with Production of Resonant Species, Initial Gaussian Release	$\frac{\partial n}{\partial t} = D \nabla^2 n + kn_1$ $\frac{\partial n_1}{\partial t} = D \nabla^2 n_1 - kn_1$ $n(r,0) = 0, n_1(r,0) = n_{10} \exp\left(-\frac{r^2}{r_0^2}\right)$	$\frac{N}{\pi^{3/2}} \frac{[1 - \exp(-kt)]}{r_0^3} \exp\left(-\frac{r^2}{r_g^2}\right)$ $N = \pi^{3/2} n_{10} r_0^3$
V. Cylindrically Symmetric Diffusion, Finite Length Initial Gaussian Release	$\frac{\partial n}{\partial t} = D \frac{\partial}{\partial r} \left(r \frac{\partial n}{\partial r} \right) + D \frac{\partial^2 n}{\partial z^2}$ $n(r,0) = n_0 \exp\left(-\frac{r^2}{r_0^2}\right), z < b$ $= 0, z > b$	$n(r,z,t) = n_0 \frac{r_0^2}{r_g^2} \exp\left(-\frac{r^2}{r_g^2}\right) Q(z,b,t)$ $= \frac{1}{2} \left[\exp\left(\frac{b+z}{2[Dt]^{1/2}}\right) + \exp\left(\frac{b-z}{2[Dt]^{1/2}}\right) \right], z < b$ $Q(z,b,t)$ $= \frac{1}{2} \left[\exp\left(\frac{z+b}{2[Dt]^{1/2}}\right) - \exp\left(\frac{z-b}{2[Dt]^{1/2}}\right) \right], z > b$

SUMMARY OF OPTICAL PROPERTIES

TABLE 2b. OPTICAL BEHAVIOR OF ISOPHOTE

Type	$S = S(d, t)$ Number of Particles in Integrated Line of Sight	d^2 Distance to Isophote Corresponding To $S=S(d, t)$ (Squared)
I.	$\frac{N}{\pi r_g^2} \exp\left(-\frac{d^2}{r_g^2}\right)$	$r_g^2 \ln\left(\frac{N}{\pi S r_g^2}\right)$
II.	$\frac{N}{\pi v^2 x^2} \exp\left(-\frac{d^2}{v^2 x^2}\right)$	$v^2 x^2 \ln\left(\frac{N}{\pi S r_g^2}\right)$
III.	$\frac{N \exp(-kx)}{\pi r_g^2} \exp\left(-\frac{d^2}{r_g^2}\right)$	$r_g^2 \ln \frac{N \exp(-kx)}{\pi S r_g^2}$
IV.	$\frac{N}{\pi r_g^2} [1 - \exp(-kx)] \exp\left(-\frac{d^2}{r_g^2}\right)$	$r_g^2 \ln\left(\frac{N}{\pi S r_g^2} [1 - \exp(-kx)]\right)$
V.	$S(\xi, 0, \alpha, x) = \frac{\pi^{1/2} n_0 r_g^2}{r_g} Y \sec \alpha \exp\left(-\frac{\xi^2}{r_g^2}\right)$ $Y = \exp\left[\frac{b \cos \alpha}{(r_g^2 - r_0^2 \cos^2 \alpha)^{1/2}}\right]$	$r_g^2 \ln \left[\frac{N Y \sec \alpha}{2 \pi^{1/2} b r_g S} \right]$

SUMMARY OF OPTICAL PROPERTIES			
TABLE 2c. PARAMETERS OF TURNING POINT AND DISAPPEARANCE POINT			
Type	d_{\max}^2	$t_{d=\max}$	$t_{d=0}$
I.	$\frac{N}{e\pi s}$	$\frac{1}{4D} \left(\frac{N}{e\pi s} - r_0^2 \right)$	$\frac{1}{4D} \left(\frac{N}{\pi s} - r_0^2 \right)$
II.	$\frac{N}{e\pi s}$	$\frac{1}{v} \left(\frac{N}{e\pi s} \right)^{1/2}$	$\frac{1}{v} \left(\frac{N}{\pi s} \right)^{1/2}$
III.	$r_g^2 \left(1 + \frac{C}{4D} r_g^2 \right)$ $r_g^2 = r_0^2 + 4D t_{d=\max}$	$t_{d=\max} = \frac{1}{4D} \left[\frac{N}{e\pi s} \operatorname{erf} \left(-2 \left(t_{d=\max} - \frac{C r_0^2}{4D} \right) \right) - r_0^2 \right]$	$t_{d=0} = \frac{1}{4D} \left[\frac{N}{\pi s} \operatorname{erf} \left(- \left(t_{d=0} \right) \right) - r_0^2 \right]$
IV.	$r_g^2 \left(1 - \frac{r_g^2 k \operatorname{erf}(-kt)}{4D [1 - \operatorname{erf}(-kt)]} \right)$ $t = t_{d=\max} \quad r_g^2 = r_0^2 + 4D t_{d=\max}$	$\frac{r_g^2 k \operatorname{erf}(-kt)}{4D [1 - \operatorname{erf}(-kt)]} =$ $\ln \left[\frac{e\pi s r_g^2}{N [1 - \operatorname{erf}(-kt)]} \right]$ $t = t_{d=\max} \quad r_g^2 = r_0^2 + 4D t_{d=\max}$	$t_{d=0} = \frac{1}{4D} \left[\frac{N}{\pi s} [1 - \operatorname{erf}(-kt)] - r_0^2 \right]$
V.	$\frac{r_g^2}{2} \left[1 + \frac{2b r_g^2 \operatorname{erf}(-Y^2) \operatorname{Co} \alpha}{\pi^{1/2} (r_g^2 - r_0^2 \operatorname{Co}^2 \alpha)^{3/2} \operatorname{erf} Y} \right]$ $Y = \operatorname{erf} \left[\frac{b \operatorname{Co} \alpha}{[r_g^2 - r_0^2 \operatorname{Co}^2 \alpha]^{1/2}} \right]$	$\ln \left[\frac{YN \operatorname{Se} \alpha}{2 \pi^{1/2} b r_g s} \right] =$ $\frac{1}{2} \left[1 + \frac{2b r_g^2 \operatorname{erf}(-Y^2) \operatorname{Co} \alpha}{\pi^{1/2} (r_g^2 - r_0^2 \operatorname{Co}^2 \alpha)^{3/2} \operatorname{erf} Y} \right]$	$r_g^2 = \frac{YN \operatorname{Se} \alpha}{2 \pi^{1/2} b s}$ $r_g^2 = r_0^2 + 4D t_{d=0}$

SUMMARY OF OPTICAL PROPERTIES

TABLE 2d. BEHAVIOR OF TOTAL FLUX

Type	$F(t)$ Total Flux/Sec	F_{max}	$t_{F_{max}}$ Time to Reach F_{max}	$F(t_{d_{max}})$
I.	$P\pi r_g^2 S_c \ln\left(\frac{eN}{\pi r_g^2 S_c}\right)$	PN	$\frac{1}{4D} \left(\frac{N}{\pi S_c} - r_0^2\right)$	$\frac{2}{e} PN, r_0^2 \ll 4DX$
II.	$P\pi r_g^2 S_c \ln\left[\frac{eN}{4D\pi r_g^2 S_c}\right]$	PN	$\frac{1}{4D} \left[\frac{N}{\pi S_c}\right]^{1/2}$	$\frac{2}{e} PN$
III.	$P\pi r_g^2 S_c \ln\left[\frac{eN\exp(-h\tau)}{\pi r_g^2 S_c}\right]$	$P\pi r_g^2 S_c \left(1 + \frac{C}{4D} r_g^2\right)$ $r_g^2 = r_0^2 + 4DX_{F_{max}}$	$\tau_{F_{max}} = \frac{1}{4D} \left[\frac{N}{\pi S_c} \exp(-2h\tau_{F_{max}} - \frac{hr_0^2}{4D}) - r_0^2\right]$	$P\pi S_c d_{max}^2$
IV.	$P\pi r_g^2 S_c \ln\left[\frac{eN[1-\exp(-h\tau)]}{\pi r_g^2 S_c}\right]$	$P\pi r_g^2 S_c \left[1 - \frac{5}{4D} \frac{h\exp(-h\tau)}{[1-\exp(-h\tau)]}\right]$ $\tau = \tau_{F_{max}}$ $r_g^2 = r_0^2 + 4DX_{F_{max}}$	$\frac{r_g^2 h \exp(-h\tau)}{4D[1-\exp(-h\tau)]} = \ln \frac{\pi r_g^2 S_c}{N[1-\exp(-h\tau)]}$ $\tau = \tau_{F_{max}}$ $r_g^2 = r_0^2 + 4DX_{F_{max}}$	$P\pi r_g^2 S_c \ln\left[\frac{eN[1-\exp(-h\tau)]}{\pi r_g^2 S_c}\right]$ $\tau = \tau_{d_{max}}$ $r_g^2 = r_0^2 + 4DX_{d_{max}}$
V.	Not suitable for total flux analysis			

APPENDIX C: SUMMARY OF PARAMETER EVALUATION

TABLE 3a. RESONANCE CLOUD TYPE I

APPENDIX C: SUMMARY OF PARAMETER EVALUATION

TABLE 3a. RESONANCE CLOUD TYPE I

Optical Data				r_0^2	N	D
Single Isophote Analysis $s = s(d_0, 0) \text{ at } t=0$ $s = s(d_{\max}, t_{d_{\max}})$				$d_0^2 = r_0^2 \ln \left[\frac{\exp(d_{\max}^2)}{r_0^2} \right]$	$e \pi S d_{\max}^2$	$\frac{1}{4 \lambda_{d_{\max}}} [d_{\max}^2 - r_0^2]$
MULTIPLE ISOPHOTE ANALYSIS	ISOPHOTE READINGS	$x=0$ $S_1 = S(d_{10}, 0)$ $S_2 = S(d_{20}, 0)$ $S_1 = e S_2$		$d_{20}^2 - d_{10}^2$		
		$S_1 = S(d_{11}, x_1)$ $S_1 = S(d_{12}, x_2)$ $S_2 = S(d_{21}, x_1)$ $S_2 = S(d_{22}, x_2)$ $S_1 = e S_2$	$\frac{(d_{21}^2 - d_{11}^2)x_1 - (d_{22}^2 - d_{12}^2)x_2}{x_1 - x_2}$	$\frac{\pi r_0^2 S_1}{r_0^3} \exp \left(\frac{d_{11}^2}{r_0^2} \right)$ $r_0^2 = r_0^2 + 4 \pi x_1$	$\frac{(d_{21}^2 - d_{11}^2) - (d_{22}^2 - d_{12}^2)}{4(x_1 - x_2)}$	
	TOTAL FLUX READINGS	$F_2 = F(x_2)$ $x_2 \neq 0, x_1$	$r_0^2 \ll 4 \pi x$	$\frac{F_1 x_2 - F_2 x_1}{e x_2 \ln \left(\frac{x_2}{x_1} \right)}$ $\times 4 \pi \left[\frac{F_1 x_2 \ln \left(\frac{x_2}{x_1} \right)}{F_1 x_2 - F_2 x_1} \right]$	$\frac{F_1 x_2 - F_2 x_1}{4 \pi P S_c x_1 x_2 \ln \left(\frac{x_2}{x_1} \right)}$	
		$F_1 = F(x_1)$ $x_2 = 0, x_1$	$r_0^2 \ll 4 \pi x$	$\frac{e F_1 - F_2}{e^2} \exp \left[\frac{e F_1}{e F_1 - F_2} \right]$	$\frac{e F_1 - F_2}{4 \pi e P S_c x_1}$	

SUMMARY OF PARAMETER EVALUATION				
TABLE 3b. RESONANCE CLOUD TYPE II				
Optical Data			v^2	H
Isophote Readings			$\frac{d_2^2 - d_1^2}{\lambda^2}$	$\pi(d_2^2 - d_1^2) \exp\left(\frac{d_1^2}{d_2^2 - d_1^2}\right)$
$s_1 = s(d_1, t)$				
$s_2 = s(d_2, t)$				
$s_1 = s_2$				
TOTAL FLUX READINGS	$F_2 = F(x_2)$	$x_2 \neq ex_1$	$\frac{F_1 x_2^2 - F_2 x_1^2}{2\pi p S_c x_1^2 x_2^2 \ln\left(\frac{x_2}{x_1}\right)}$	$\frac{F_1 x_2^2 - F_2 x_1^2}{2ep x_2^2 \ln\left(\frac{x_2}{x_1}\right)} \exp\left[\frac{2x_2^2 F_1 \ln\left(\frac{x_2}{x_1}\right)}{F_1 x_2^2 - F_2 x_1^2}\right]$
		$x_2 = ex_1$	$\frac{F_1 e^2 - F_2}{2\pi p S_c e^2 x_1^2}$	$\frac{F_1 e^2 - F_2}{2e^3 p} \exp\left[\frac{2e^2 F_1}{F_1 e^2 - F_2}\right]$
	$F_1 = F(x_1)$	$x_2 \neq ex_1$		
		$x_2 = ex_1$		

SUMMARY OF PARAMETER EVALUATION	
TABLE 3c. RESONANCE CLOUD TYPE III	
$F_i = F(x_i) = 4\pi p S_c x_i \ln \left[\frac{e N \exp(-\beta x_i)}{4\pi D S_c x_i} \right], \quad r_0^2 \ll 4 D x$	
$\alpha_i = \frac{F_i}{4\pi p S_c x_i} \quad \beta_i = \ln x_i \quad \gamma_i = x_i \quad i=1,2,3,$	
$\Delta = \begin{vmatrix} \alpha_1 & \gamma_1 & 1 \\ \alpha_2 & \gamma_2 & 1 \\ \alpha_3 & \gamma_3 & 1 \end{vmatrix}$	$\Delta_1 = \begin{vmatrix} \beta_1 & \gamma_1 & 1 \\ \beta_2 & \gamma_2 & 1 \\ \beta_3 & \gamma_3 & 1 \end{vmatrix}$
$\Delta_2 = \begin{vmatrix} \alpha_1 & \beta_1 & 1 \\ \alpha_2 & \beta_2 & 1 \\ \alpha_3 & \beta_3 & 1 \end{vmatrix}$	$\Delta_3 = \begin{vmatrix} \alpha_1 & \beta_1 & \gamma_1 \\ \alpha_2 & \beta_2 & \gamma_2 \\ \alpha_3 & \beta_3 & \gamma_3 \end{vmatrix}$
$D = -\frac{\Delta}{\Delta_1} \quad C = -\frac{\Delta_2}{\Delta} \quad N = \exp \left(-\frac{\Delta_3}{\Delta} + \ln D - \ln \frac{e}{4\pi S_c} \right)$	

SUMMARY OF PARAMETER EVALUATION	
TABLE 3d. RESONANCE CLOUD TYPE IV	
$F_i = F(x_i) = 4\pi p D S_c x_i \ln \left[\frac{e N [1 - \exp(-k x_i)]}{4\pi D S_c x_i} \right], \quad r_0^2 \ll 4 D x$	
<p>With</p> $\alpha_i = \frac{F_i}{4\pi p S_c x_i} \quad i=1,2,3, \quad k \text{ is the root of } G(k)=0,$ <p>where</p> $G(k) = \left[\frac{[1 - \exp(-k x_1)]}{[1 - \exp(-k x_2)]} \right]^{\alpha_1 - \alpha_3} \left[\frac{[1 - \exp(-k x_3)]}{[1 - \exp(-k x_1)]} \right]^{\alpha_1 - \alpha_2} = \left(\frac{x_3}{x_1} \right)^{\alpha_1 - \alpha_2} \left(\frac{x_1}{x_2} \right)^{\alpha_1 - \alpha_3}$	
$D = \frac{\alpha_1 - \alpha_2}{\ln \left(\frac{x_2}{x_1} \right) + \ln \left[\frac{[1 - \exp(-k x_1)]}{[1 - \exp(-k x_2)]} \right]}$	$N = \frac{4\pi D S_c x_1 \exp(\alpha_1 - 1)}{1 - \exp(-k x_1)}$

TABLE 4

RESONANCE CLOUDS
PARAMETERS USED IN ISOPHOTE ANALYSIS

h (km)	D (cm ² /Sec)	c (/Sec)	Minimum Size Cloud r ₀ (cm)	Over Expanded Cloud r ₀ (cm)
60	1.8×10^3	38	1.97×10^3	4.0×10^3
70	5.4×10^3	2.51	3.12×10^3	6.7×10^3
80	2.4×10^4	7.93×10^{-2}	5.55×10^3	1.2×10^4
90	1.7×10^5	2.50×10^{-3}	9.84×10^3	2.1×10^4
100	1.4×10^6	5.88×10^{-5}	1.60×10^4	3.4×10^4
110	1.1×10^7	1.99×10^{-6}	2.78×10^4	6.0×10^4
120	5.5×10^7	7.92×10^{-8}	4.40×10^4	9.5×10^4
200	3.5×10^9	8.46×10^{-11}	1.80×10^5	3.9×10^5
300	2.3×10^{10}	1.96×10^{-12}	3.37×10^5	7.3×10^5

FIGURE 2. VARIATION OF ISOPHOTE DISTANCE WITH TIME FOR VARIOUS ALTITUDES. INITIAL POINT SYMMETRIC GAUSSIAN RELEASE OF NEUTRALS IN AN OVER-EXPANDED CLOUD

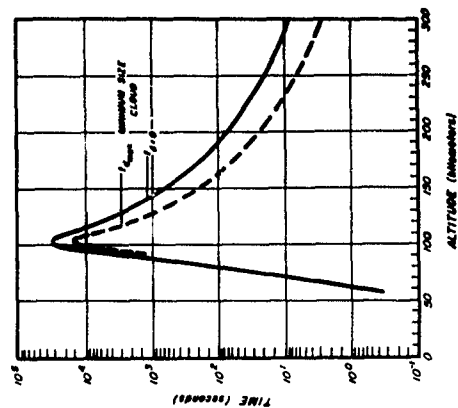


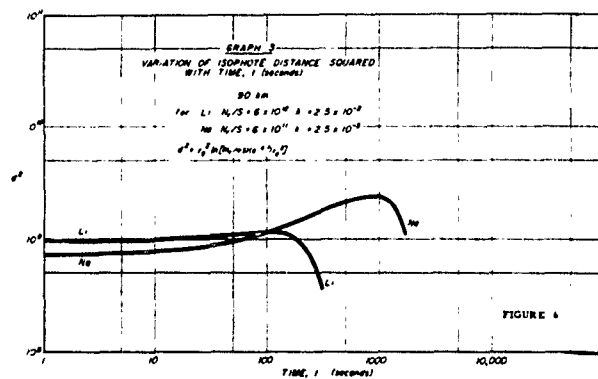
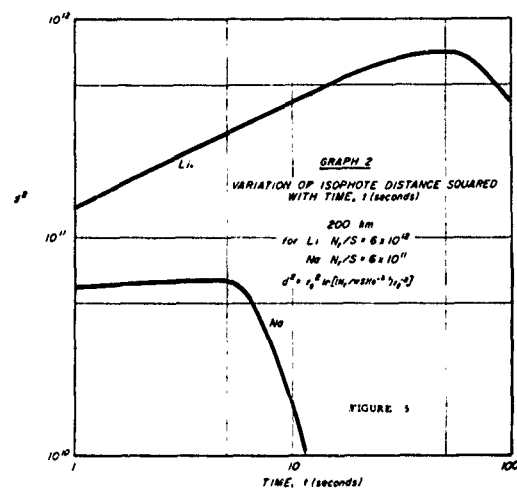
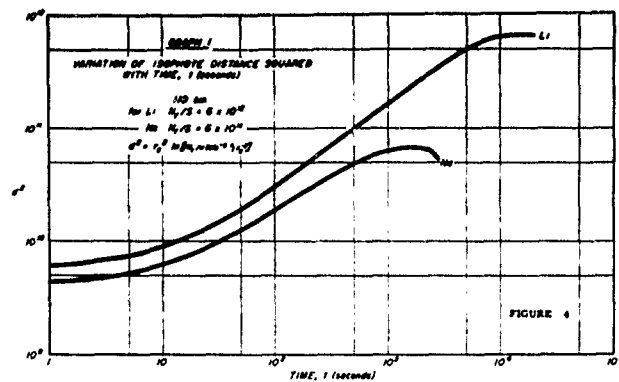
FIGURE 3. TIMES FOR RESONANT CLOUD BROWNE TO ATTAIN MAXIMUM AND ZERO DISTANCES AS A FUNCTION OF ALTITUDE FOR MAXIMUM SIZE CLOUD.

center-point density equals the unperturbed ambient density whereas reference to the "overexpanded cloud" indicates that the initial contaminant center-point density is taken to be only one-tenth of the ambient. In most instances, this range probably brackets the existing physical situation. In either case, the sensitivity to this parameter is indicated.

The data displayed in Figures 1-3 illustrate the several uses of optical observations on resonance clouds. For example, these or related data can serve to yield information on chemical yield, ionization yield (using resonant ions), diffusion, magnetic field alignment, chemical consumption rates, and many others discussed in AFCL 207 and AFCL 218.

An additional interesting use of these techniques is in the employment of resonant clouds for the determination of diffusion mechanisms; the following method may be employed. The payload could be doped with predetermined amounts of, say, two (or more) chemicals of widely different masses (which also possess different optical resonance excitation levels) and released under twilight conditions so as to generate detectable characteristic solar resonance radiations. Then, proper optical observations on the differential diffusion as related to the mass differences could be correlated to the diffusion mechanism. For example, in principle, it would be possible to compare the characteristic "constant intensity contours" (or isophotes) growth rates for the various chemicals of different masses and ascertain if any differences in the observed growths could be due to molecular diffusion. Although no details are given here, reference is now made to a specific example which has been investigated and reported in a note entitled "A Memo on the Use of Resonant Tracers for the Determination of Diffusion Mechanisms," GCA Technical Memo No. 61-1-AFM.

The memo examined the release of a payload which contained one mole each of Na and Li. It was assumed that both the chemical consumption rate and the solar resonance efficiency of lithium was one order of magnitude greater than those of sodium. Three release altitudes were considered; namely, 90, 110 and 200 km. For these cases, the time behavior of the radius of a given isophote (d^2) was investigated. These results are given in Figures 4, 5 and 6, which make evident the care that must be exercised in experiments of this kind. For example, the critical importance of understanding the roles of chemical consumption, solar resonance efficiency and diffusion is made evident in the figures. Finally, it should be noted that the resonance scattering work thus far deals



only with the case of back-scatter. Generalization should be extended to the cases of where the phase angle differs from 180° . Further a more exact treatment using radiative transfer techniques should be performed.

B. Chemiluminescence

1. Introduction

Artificial chemiluminescent clouds, produced by releasing known amounts of specific chemicals into the upper atmosphere, at prearranged heights, to react with an atmospheric in such a manner as to yield luminescence has been employed as an atmospheric probe. In addition to experiments performed according to the original suggestion of a sodium chemiluminescence reaction with atomic oxygen other chemiluminescent experiments have included the reaction of released nitric oxide with ambient atomic oxygen and of released ethylene with ambient atomic nitrogen. These initial exploratory experiments served to indicate the feasibility of successfully using the technique (of chemiluminescent clouds) for atmospheric experiments and also as an aid to understanding some current AF applied problems in missile trail technology. However, the initial work also did serve to indicate severe gaps in the necessary ground work for proper analysis of experiments of this design. Accordingly, some initial theoretical effort has been directed toward alleviating this situation. The details of this phase have been included in a recent AFCEC 201 Report entitled "Chemical Release Studies VI: Optical Properties of Chemiluminescent Clouds for Two-Body Chemical Reactions Without Diffusion". Several models are given in which the simplified concentration fields are presented; the continuity equations employed are limited to two-body chemical reactions. The initial conditions assumed are written in several terms of arbitrary initial release geometries. The optical properties of these chemiluminescent cloud models are then defined in terms of the density functions; these properties are (a) $F_{cc}(r,t)$, the photon flux per unit volume, (b) $B(d,t)$, the brightness per unit area along a line of sight through the cloud, and (c) $F_T(t)$, the total flux of the cloud. The model is specified to be that arising from spherically symmetric intermediate Gaussian releases of the contaminant where the dilution of the contaminant, at the center-point of the cloud, relative to the ambient density (λ) is left general; and accordingly, the ratio of the atmospheric reactant density to the ambient density (f_x) is also left general.

Later the generality of the initial density of the contaminant and atmospheric reactant is removed by assuming a symmetric Gaussian release; the formulas derived are transferred over in detail with the specification that $\lambda = 1$ and $f_x = 1$.

Another phase of the work deals with the chemiluminescent cloud models of finite extent (in one dimension, at least) and a finite homogeneous sphere is discussed. Next a spherical shell model with an unmixed core is discussed. Finally the properties of a finite spherical cloud is investigated for which the initial releases of contaminant are linear and parabolic, respectively. The details are not given in the present report but the reader is given reference to AFGL 201. However, it is appropriate here to include only the base results of the work cited.

2. Results

Because of the voluminous nature of the study only final results will be presented in a condensed form. Definitions of terms not previously mentioned are relegated to the glossary given at the end of this section.

a. Optical Properties of Chemiluminescent Clouds; General Considerations

(1) Photon Flux $F_{cc}(r,t)$ per Unit Volume

$$F_{cc}(r,t) = k_{p_2} n_c(r,0)x(r,0) \left[\frac{n_c(r,0) - x(r,0)}{n_c(r,0) - p x(r,0)} \right]^2 p. \quad (4)$$

(2) Brightness per Unit Area, $B(d,t)$

Along a line of sight L , a perpendicular distance $r=d$ from the origin $r=0$ of the chemiluminescent cloud, one can compute the line integral

$$B(d,t) = \int_{-\infty}^{\infty} F_{cc}(r,t) dS \quad (5)$$

to obtain $B=B(d,t)$, the chemiluminescent brightness per cm^2 , at the distance d , at times $t > 0$.

In terms of the initial concentration functions $n_c(r,0)$ and $x(r,0)$ and the chemical consumption and chemiluminescent rate k_{c_2} and k_{p_2} , respectively, at the time $t > 0$, the formula for the brightness, $B=B(d,t)$ per cm^2 along L , takes the imposing form

$$B(d,t) = 2k_{p_2} \int_d^{\infty} \frac{n_c(r,0)x(r,0) [n_c(r,0) - x(r,0)]^2 \exp[-k_{c_2}(n_c(r,0) - x(r,0))t]}{[n_c(r,0) - x(r,0) \exp(-k_{c_2}(n_c(r,0) - x(r,0))t)]^2} \frac{r dr}{[r^3 - d^2]^{1/2}} \quad (6)$$

(3) Total Flux, $F_T(t)$

The total photon flux, $F_T(t)$, from the luminescent cloud is expressed by the volume integral of $F_{cc}(r,t)$,

$$F_T(t) = \int_{-\infty}^{\infty} F_{cc}(r,t) dV \quad (7)$$

or by the area integral of $B(d,t)$.

$$F_T(t) = 2\pi \int_0^{\infty} r B(r,t) dr \quad (8)$$

Next are given the results of evaluating the above for various physical cases.

b. Symmetric Intermediate Gaussian Release. Initial Center-Point Density of the Contaminant Less than Ambient

(1) Photon Flux per Unit Volume, $F_{cc}(r,t)$

The formula for the photon flux, $F_{cc}(r,t)$, per unit volume (cm^3),

for the present case takes the explicit form

$$F_{cc}(r,t) = k_{p2} \lambda f_x n_a^2 E(1-\lambda E) \frac{[\lambda E - f_x(1-\lambda E)]^2 \exp[-k_{c2} n_a (\lambda E - f_x(1-\lambda E))t]}{[\lambda E - f_x(1-\lambda E) \exp[-k_{c2} n_a (\lambda E - f_x(1-\lambda E))t]]^2} \quad (9)$$

(2) Brightness per Unit Area, $B(d,t)$

The formula for $B(d,t)$ takes the explicit form

$$B(d,t) = 2k_{p2} \lambda f_x n_a^2 \int_d^{\infty} \frac{E(1-\lambda E) [\lambda(1+f_x)E - f_x]^2 \exp[-k_{c2} n_a t (\lambda(1+f_x)E - f_x)]}{[\lambda E - f_x(1-\lambda E) \exp(-k_{c2} n_a t (\lambda(1+f_x)E - f_x))]^2} \frac{r dr}{[r^2 - d^2]^{\frac{1}{2}}} \quad (10)$$

where

$$E \equiv \exp(-r^2/r_0^2).$$

c. Symmetric Gaussian Release: Initial Center-Point Density of the Contaminant Equal to the Ambient Density

The λ and f_x factors of b, in dealing with an intermediate Gaussian release, are now made equal to unity, so that the initial concentration of the contaminant is defined as

$$n_c(r,0) = n_a \exp(-r^2/r_0^2) \quad (11)$$

(1) Photon Flux per Unit Volume, $F_{cc}(r,t)$

$$F_{cc}(r,t) = k_{p2} n_a^2 E(1-E) \frac{(2E-1)^2 \exp[-k_{c2} n_a (2E-1)t]}{[E-(1-E) \exp[-k_{c2} n_a (2E-1)t]]^2} \quad (12)$$

where

$$E = \exp - \frac{r^2}{r_0^2}$$

(2) Brightness per Unit Area, $B(d,t)$

$$B(d,t) = 2k_{p2} n_a^2 \int_d^R \frac{E(1-E)(2E-1)^2 \exp[-k_{c2} n_a (2E-1)t]}{[E-(1-E)\exp[-k_{c2} n_a (2E-1)t]]^2} \frac{rdr}{[r^2-d^2]^{\frac{1}{2}}} \quad (19)$$

d. Homogeneous Finite Sphere Release

The contaminant is now assumed to be uniformly distributed inside a spherical region of radius $r=R$ at the instant $t=0$, so that $n_c(r,0) = n_c(0,0) = n_0$, $0 \leq r \leq R$. The atmospheric reactant has the initial concentration $x(r,0) = x(0,0) = x_0 = n_a - n_0$, $0 \leq r \leq R$ where $n_0 = \lambda n_a$, $0 \leq \lambda \leq 1$ so that $x_0 = (1-\lambda)n_a$, when $0 \leq 1-\lambda < 1$. Thus, now for the homogeneous case the following apply.

(1) Photon Flux per Unit Volume, $F_{cc}(r,t)$

$$F_{cc}(r,t) = k_{p2} n_a^2 \lambda(1-\lambda)(2\lambda-1)^2 \frac{\exp[-k_{c2} n_a (2\lambda-1)t]}{[\lambda-(1-\lambda)\exp[-k_{c2} n_a (2\lambda-1)t]]^2} \quad (14)$$

(2) Brightness per Unit Area, $B(d,t)$

$$B(d,t) = 2k_{p2} n_a^2 \lambda(1-\lambda)(2\lambda-1)^2 (R^2-d^2)^{\frac{1}{2}} \frac{\exp[-k_{c2} n_a (2\lambda-1)t]}{[\lambda-(1-\lambda)\exp[-k_{c2} n_a (2\lambda-1)t]]^2} \quad (15)$$

(3) Total Flux, $F_T(t)$

$$F_T(t) = \frac{4}{3} \pi R^2 F_{cc} \quad (16)$$

e. Homogeneous Spherical Shell Surrounding an Unmixed Ambient Spherical Core

The two-body chemical reaction is confined to a spherical shell region $R = r = R + T$, of wall thickness T ; the inner spherical core region, of radius R , is impervious to the reaction.

Initially one has the following concentration fields:

$$\begin{aligned} n_c(r,0) &= n_0 = \lambda n_a, & R \leq r \leq R+T \\ x(r,0) &= x_0 = n_a - n_0 = (1-\lambda)n_a, \end{aligned}$$

for the spherical shell region and

$$\begin{aligned} n_c(r,0) &= 0, & 0 \leq r < R \\ x(r,0) &= n_a \end{aligned}$$

for the spherical core region.

(1) Photon Flux per Unit Volume

In the spherical shell we have

$$F_{cc}(r,t) = k_{p2} n_0 x_0 \left[\frac{n_0 - x_0}{n_0 - p x_0} \right]^2 p \quad (17)$$

where

$$p = p(x,t) = \exp \left[-k_{c2} (n_0 - x_0) t \right] ;$$

(2) Brightness per Unit Area, $B(d,t)$

Case (a) $0 \leq d \leq R$

$$B = B(d,t) = 2 \left[\left[(R+T)^2 - d^2 \right]^{\frac{1}{2}} - \left[R^2 - d^2 \right]^{\frac{1}{2}} \right] F_{cc}(r,t) \quad (18)$$

Case (b) $R \leq d \leq R+T$

For case (b) the isophote $B = B(d,t)$ is defined by the formula

$$B = B(d,t) = 2 \left[(R+T)^2 - d^2 \right]^{\frac{1}{2}} F_{cc}(r,t) \quad (19)$$

f. Additional Models

There have been evaluated additional chemiluminescent clouds with different configurations. These include a finite sphere with a linear decrease of the contaminant and also the case of the parabolic initial distribution. These are given in "Chemical Release Studies VI" and for purposes of brevity will not be given here.

3. Parameterization

The evaluation of the various models has proceeded to the point of calculating the various kinds of brightness profiles and flux per unit volume. To indicate this, some selected graphs are included (Figs. 7-10). They are self-explanatory when used in conjunction with the text.

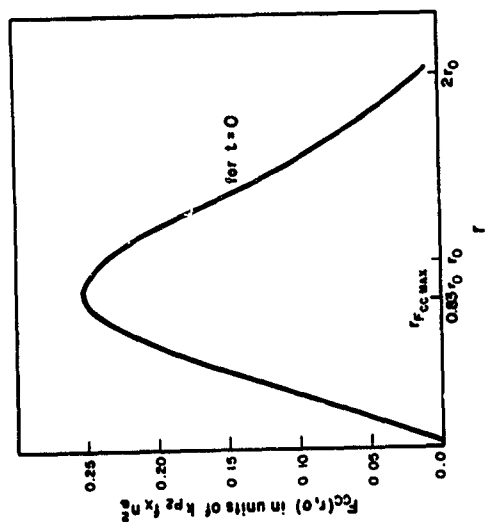


FIGURE 7: VARIATION OF $F(r, 0)$ FOR THE INITIAL GAUSSIAN CONTAMINANT CONCENTRATION WITH $n_c(00)_{0.25} = n_a$.

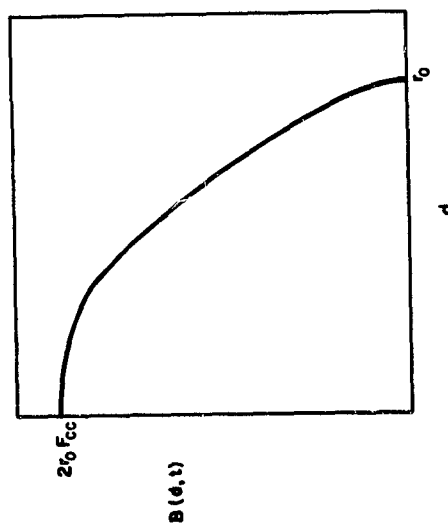


FIGURE 9: HOMOGENEOUSLY MIXED SPHERE BRIGHTNESS PROFILE.

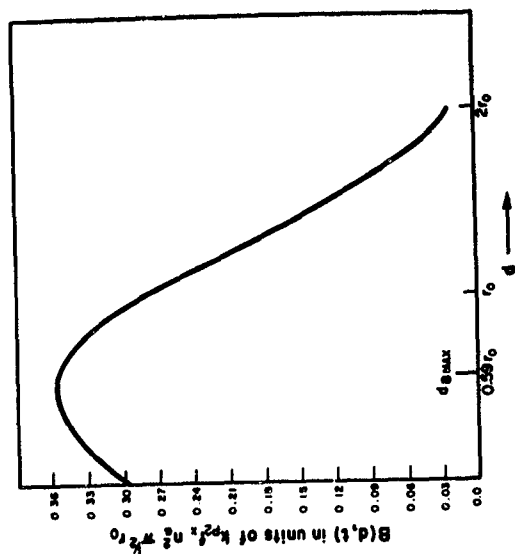


FIGURE 8: VARIATION OF BRIGHTNESS PROFILE $B(d, t)$ AS A FUNCTION OF d FOR INITIAL GAUSSIAN, CENTER DENSITY EQUALS AMBIENT DENSITY AT $t = 0$.

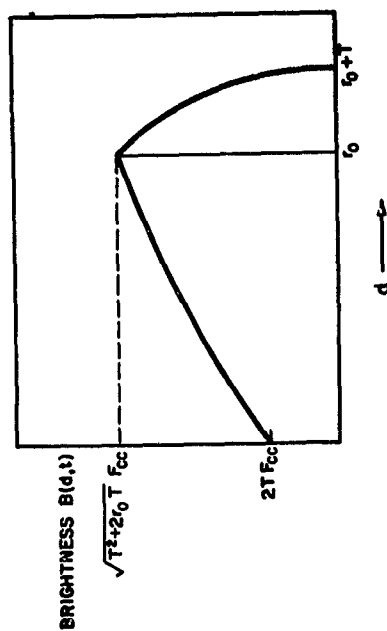


FIGURE 10: BRIGHTNESS PROFILE FOR HOMOGENEOUS MIXED SHELL WITH NON-REACTING CORE -- NO DIFFUSION.

GLOSSARY OF SYMBOLS (NOT PREVIOUSLY DEFINED) FOR CHEMILUMINESCENCE STUDY

<u>Symbol</u>	<u>Definition</u>
$B, B(d, t)$	brightness per unit area (cm^2) along line of sight L, a distance $r=d$ from origin $r=0$, at time $t > 0$
d	isophote distance, distance of line of sight L of brightness from origin
$d(B, t)$	isophote distance
$d_{t=0}$	isophote distance at time $t=0$
D	diffusion coefficient
$N_c(t)$	total number of contaminant molecules at time, t
f_x	$x(r, 0) / [n_a - n_c(r, 0)]$
S	parameter of length along line of sight, L
x	component of S in x direction
x_a	constant ($x, -, r, t$)
k_c	k_{c2}/x_a
k_{c2}	two-body consumption rate of contaminant
k_{p2}	two-body chemiluminescent rate
b_2	$k_{p2} x_a N_c(0)$
n_a	number density of ambient molecules in undisturbed environment
$n_c(r, t)$	concentration or number density of molecules (atoms) of contaminant per cm^3
$N_c(t)$	total number of molecules of contaminant at time $t \geq 0$
$p, p(r, t)$	$\exp [-k_{c2}(n_c(r, 0) - x(r, 0)t)]$
$P_{t_{d=0}}$	$\exp [-k_{c2}(n_0 - x_0) t_{d=0}]$
$P_{t_{d=R}}$	$\exp [-k_{c2}(n_0 - x_0) t_{d=R}]$
$u(r, t)$	number density of contaminant or reactant being consumed at $r \geq 0, t > 0$
$x(r, 0)$ or x_0	initial concentration of reactant at $t=0$
$x(r, t)$	concentration or number density of atmospheric reactant of species x within the cloud at $r \geq 0$ and $t \geq 0$

5. RF PROPAGATION STUDIES

The use of various RF equipments and experiments in the artificial electron cloud program is well known and requires no repetition here. It suffices to state that the several ionospheric sounders, back, forward (and side) scatter radar and communications experiments conducted during the Firefly programs have served, in consort with the optical measurements, as indicators of the degree of success of the individual shots with respect to cloud position, RF cross section, electron density contours, total electron content, etc. Most previous theoretical models which have been applied to the case of RF propagation have tacitly assumed a constant total number of electrons as well as a diffusion controlled model. It is therefore noteworthy that the initial mathematical models indicated the need for additional sophistication and more realistic models for day, night and twilight release conditions. The solutions of some of the general mathematical models presented earlier in this report have been oriented toward the determination of the electron density (at the center point, any point and/or any shell) for application to the RF problem, whereas other solutions have been directed for use in the optical cases where the integrated path length is the usual parameter to be applied.

A. RF Propagation Models

The simplest electromagnetic model applied to the electron cloud is the reflective one; this implies replacement of the cloud by a totally reflecting surface defined by the critical radius at the RF wavelength of interest. A more realistic treatment should take into account the refractive effects for more forward geometries by introducing the refractive bending of the incident energy from the underdense electron concentrations leading to greater values of cloud cross section and efficiency for propagation directions other than those from simple backscatter. It is felt that a natural extension of these electromagnetic models lies in the direction of a treatment of the problem by the techniques of geometric optics such that ray tracing should be applied. Before any complex analysis or indicated ray training can be employed, the requirement is for more realistic cloud models as exemplified by Section 2. Thus, the next stage suggests itself in the incorporation of geometric optics to the RF propagation case employing some of the models in this report.

The results of the general day and night time models in terms of the center point density normalized by the initial center point value are shown in Figures 11 through 14.

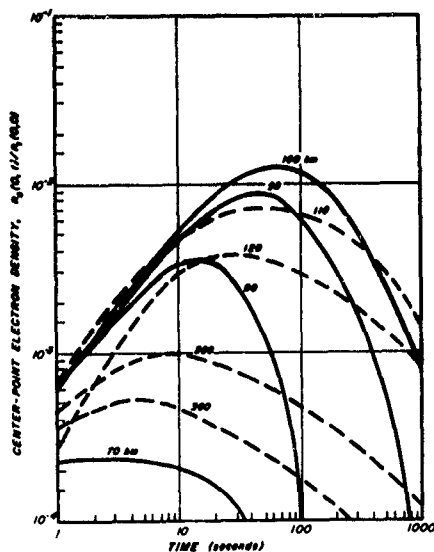


FIGURE 11. VARIATION OF CENTER-POINT ELECTRON DENSITY WITH TIME FOR DIFFERENT ALTITUDES: INITIAL SPHERICAL GAUSSIAN DAY-TIME RELEASE OF NEUTRALS FOR A MINIMUM IEE CLOUD.

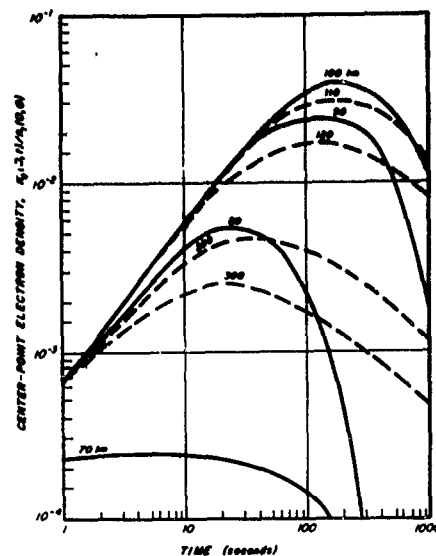


FIGURE 12. VARIATION OF CENTER-POINT ELECTRON DENSITY WITH TIME FOR DIFFERENT ALTITUDES: INITIAL SPHERICAL GAUSSIAN DAY-TIME RELEASE OF NEUTRALS FOR AN OVER-EXPANDED CLOUD.

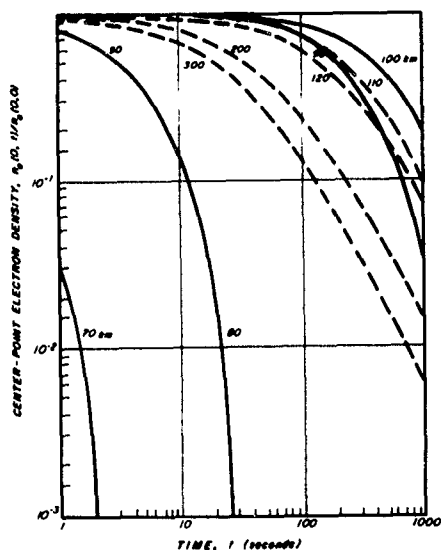


FIGURE 13. VARIATION OF CENTER-POINT ELECTRON DENSITY WITH TIME FOR DIFFERENT ALTITUDES: INITIAL SPHERICAL GAUSSIAN NIGHT-TIME RELEASES FOR A MINIMUM IEE CLOUD.

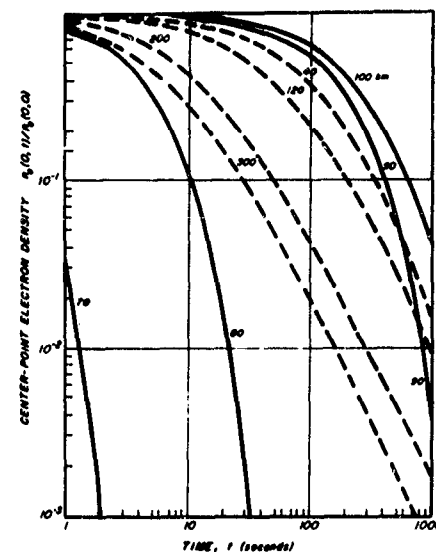


FIGURE 14. VARIATION OF CENTER-POINT ELECTRON DENSITY WITH TIME FOR DIFFERENT ALTITUDES: INITIAL SPHERICAL GAUSSIAN NIGHT-TIME RELEASES FOR AN OVER-EXPANDED CLOUD.

Tables 5 and 6 indicate the parameters employed for the graphs. The "minimum" and "over-expanded" clouds have been defined in the section on Optical Properties. Here, β is the attachment probability where γ is a pseudo recombination coefficient utilized to replace the non-linear $\propto n^2$ term. D , C and r_0 are diffusion coefficient, chemical consumption rate and initially Gaussian half width. With this information the Tables and Graphs are sufficiently labeled to be self-explanatory. The curves are of specific interest for the RF characteristics since if a reasonable, meaningful value of the initial center concentration, $n_e(0,0)$ is chosen, then the figures depict the variation of the center point electron density $n_e(0,t)$ with time. If the tacit assumption is made that the critical frequency of return is controlled by the center point density (since the spatial dimension requirement is at most a few wavelengths), then these figures can similarly be interpreted in terms of the C-3 results; i.e. critical frequency as a function of time for the several altitudes considered. It is to be noted that since the only assumption which has been made has been the assignment of a particular value to $n_e(0,0)$ and that the general forms of the curves in Figures 11 through 14 do not change when viewed in terms of critical frequency vs. time. From the above figures one can obtain knowledge of both the Gaussian half width, r_0 , and the time variation of the total electron content, and can then calculate the shell radius of any particular value of electron density and its time variation. This in turn is simply convertible into cloud cross section as a function of time. In other words, from the data which have been generated from the general models, the time and altitude variations of both critical frequency and cloud efficiency or cross section may be obtained. Extension of the present work will proceed in the indicated direction.

B. RF Applications

Having discussed the physical processes and models involved in the technology of artificial electron clouds it is of interest to summarize and review several aspects of RF propagation applications to existing military systems. In general the RF systems to which the artificially generated environment is most simply and naturally applied are in the areas of communications. Before discussing the above individually it is worthwhile stating several characteristics of the technology with respect to general military system interest. At frequencies above the MUF of the naturally existing F_2 layer, communications, for example, is limited by tropospheric (i.e. low altitude, therefore restricted range), ionospheric, meteor, etc. scatter systems ground to ground or by simple line-of-sight. The

TABLE 5
PARAMETERS USED IN CENTER-POINT EVALUATIONS
FOR AN OVER-EXPANDED CLOUD

DAY-TIME RELEASES OF NEUTRALS

h (km)	D (cm ² /Sec)	r_o (cm)	c (Sec ⁻¹)	$\gamma_1 = \alpha \bar{n}_e$ (Sec ⁻¹)	$n_1(o,o)$
60	1.10×10^3	4.0×10^3	38	5×10^{-3}	2.0×10^{14}
70	3.03×10^3	6.7×10^3	2.5	6×10^{-3}	1.8×10^{13}
80	1.32×10^4	1.2×10^4	8×10^{-2}	.015	3.2×10^{12}
90	9.40×10^4	2.1×10^4	3.1×10^{-3}	.010	5.6×10^{11}
100	7.80×10^5	3.4×10^4	7.1×10^{-4}	5×10^{-3}	1.3×10^{11}
110	6.25×10^6	6.0×10^4	6.5×10^{-4}	7×10^{-4}	2.5×10^{10}
120	3.16×10^7	9.5×10^4	6.5×10^{-4}	5×10^{-5}	6.3×10^9
200	2.04×10^9	3.9×10^5	6.5×10^{-4}	2×10^{-7}	9.2×10^7
300	1.34×10^{10}	7.3×10^5	6.5×10^{-4}	2×10^{-8}	1.4×10^7

NIGHT-TIME RELEASES OF ELECTRONS

h (km)	D_2 (cm ² /Sec)	r_o (cm)	β (/Sec)	$\gamma_2 = \alpha \bar{n}_e$ (/Sec)	$n_e(o,o)$
60	3.20×10^2	4.0×10^3	40	6×10^{-2}	2.0×10^{11}
70	6.5×10^2	6.7×10^3	3.5	5.4×10^{-3}	1.8×10^{10}
80	2.4×10^3	1.2×10^4	0.2	9.6×10^{-4}	3.2×10^9
90	1.8×10^4	2.1×10^4	3.0×10^{-3}	1.7×10^{-4}	5.6×10^8
100	1.6×10^5	3.4×10^4	9.2×10^{-4}	3.9×10^{-5}	1.3×10^8
110	1.5×10^6	6.0×10^4	8.5×10^{-4}	7.5×10^{-6}	2.5×10^7
120	8.2×10^6	9.5×10^4	3.2×10^{-4}	1.9×10^{-6}	6.3×10^6
200	5.8×10^8	3.9×10^5		2.8×10^{-7}	9.2×10^5
300	3.7×10^9	7.3×10^5		2.7×10^{-7}	1.4×10^5

TABLE 6
PARAMETERS USED IN CENTER-POINT EVALUATIONS
FOR A MINIMUM SIZE CLOUD

DAY-TIME RELEASE OF NEUTRALS

h (km)	D (cm ² /Sec)	r ₀ (cm)	c (Sec ⁻¹)	$\gamma_2 = \alpha \tilde{n}_e$ (Sec ⁻¹)	n ₁ (o,o)
70	3.03 x 10 ³	3.12 x 10 ³	2.51	.020	1.8 x 10 ¹⁴
80	1.32 x 10 ⁴	5.55 x 10 ³	8.0 x 10 ⁻²	.050	3.2 x 10 ¹³
90	9.4 x 10 ⁴	9.84 x 10 ³	3.15 x 10 ⁻³	.050	5.6 x 10 ¹²
100	7.8 x 10 ⁵	1.60 x 10 ⁴	7.09 x 10 ⁻⁴	.010	1.3 x 10 ¹²
110	6.25 x 10 ⁶	2.78 x 10 ⁴	6.52 x 10 ⁻⁴	.001	2.5 x 10 ¹¹
120	3.16 x 10 ⁷	4.40 x 10 ⁴	6.5 x 10 ⁻⁴	10 ⁻⁴	6.3 x 10 ¹⁰
200	2.04 x 10 ⁹	1.80 x 10 ⁵	6.5 x 10 ⁻⁴	5 x 10 ⁻⁷	9.2 x 10 ⁸
300	1.34 x 10 ¹⁰	3.37 x 10 ⁵	6.5 x 10 ⁻⁴	5 x 10 ⁻⁸	1.4 x 10 ⁸

NIGHT-TIME RELEASE OF ELECTRONS

(km)	D (cm ² /Sec)	r ₀ (cm)	β (Sec ⁻¹)	$\gamma_2 = \alpha \tilde{n}_e$ (Sec ⁻¹)	n _e (o,o)
70	6.5 x 10 ²	3.12 x 10 ³	3.5	5.4 x 10 ⁻²	1.8 x 10 ¹¹
80	2.4 x 10 ³	5.55 x 10 ³	0.2	9.6 x 10 ⁻³	3.2 x 10 ¹⁰
90	1.8 x 10 ⁴	9.84 x 10 ³	3.0 x 10 ⁻³	1.7 x 10 ⁻³	5.6 x 10 ⁹
100	1.6 x 10 ⁵	1.60 x 10 ⁴	9.2 x 10 ⁻⁴	3.9 x 10 ⁻⁴	1.3 x 10 ⁹
110	1.5 x 10 ⁶	2.78 x 10 ⁴	8.5 x 10 ⁻⁴	7.5 x 10 ⁻⁵	2.5 x 10 ⁸
120	8.2 x 10 ⁶	4.40 x 10 ⁴	3.2 x 10 ⁻⁴	1.9 x 10 ⁻⁵	6.3 x 10 ⁷
200	5.8 x 10 ⁸	1.80 x 10 ⁵		2.8 x 10 ⁻⁷	9.2 x 10 ⁵
300	3.7 x 10 ⁹	3.37 x 10 ⁵		2.7 x 10 ⁻⁷	1.1 x 10 ⁵

artificially generated ionosphere, however, offers a unique mode by establishing a novel geometry which does not naturally exist. It is certainly to be noted that a current proposal of interest, the 'Needles' concept, as well as satellites, balloons, etc. could conceivably perform similar missions. Operationally, however, the fact that initiation of transmission in the electron cloud system is determined (both in time and space) by the user, makes enemy detection, countermeasure, etc. extremely difficult. Therefore, although alternate technologies to the artificial cloud have been proposed which are frequently simpler to implement, cheaper, etc., most admit to the additional deficiency of easy enemy countermeasure.

1. Communications

There are generally three situations wherein the cloud could be conceived as a reflector in unique mode RF communications. The first of these is in a tactical situation where high reliability (i.e. high signal to noise operation), relatively high frequency (e.g. VHF-UHF), secure (i.e. relatively difficult to jam or countermeasure) communications is required. This may mean ground to ground, air to ground or ground to air as the situation requires. One may think of the natural application to very long distance (i.e. high altitude cloud generation) intercontinental links for this application. A second case involved the re-establishment of communications in a tactical situation, nuclear degraded environment. From the Hardtack data it is known that there existed some degradation of the normal RF propagation modes which varied as a function of the inverse square of the frequency. There is some discrepancy as to the degradation time at HF but outage periods on the order of a day seem appropriate. It is here that cloud communications could be initiated at a carrier frequency which is no longer suffering degradation ($> \text{HF}$). The final application is somewhat analogous to the previous one in that it is realized that during low sunspot activity periods the normal ionosphere does not support high MUF values. To supplement this electron deficiency during these periods artificially would, in effect, re-create a normal high sunspot ionosphere. Conceivably this could be performed on a routine basis with very small payloads.

2. Other Applications

The several other applications may be somewhat loosely grouped in terms of a unique geometry class and a proposed interaction class. The discrimination application, wherein a cloud is generated such that a decoy ensemble and warhead impinge the cloud upon re-entry, fit into the latter category. It is expected that many interactions between the

decoys and the artificial cloud will occur which will aid in discrimination.

6. SUMMARY

In this section is summarized the essential features of this report. For uniformity the summary is made to follow the format of the document. Accordingly, it is presented in the following phases: (1) Chemistry of Upper Atmosphere Releases, (2) Mathematical Models for Chemical Release Studies, (3) Optical Properties of Chemical Releases, and (4) RF Propagation Studies Including Applications.

(1) Chemistry of Upper Atmosphere Releases

Chemical releases are analyzed in terms of two successive processes: first, formation of the initial reaction products and second, evaluation of the non-equilibrium kinetic processes during expansion. Application of various models and comparison with experimental results provides the basis for recommendations for optimization for various types of releases.

Initial reaction product compositions and flame temperatures can be calculated on the basis of equilibrium processes with the aid of thermodynamical data. Details are given in AFCL Report No. 229 entitled "Chemical Release Studies IV: Chemistry of Upper Altitude Releases" by D. Golomb and A. W. Berger.

In the aluminum-alkali nitrate reaction maximum ionization is obtained with the stoichiometric reactant ratio. However, this reaction is relatively slow and therefore the reaction may be extinguished at burst of the canister, i.e. when the equilibrium pressure above the reacting mixture reaches the burst pressure of the canister. It is emphasized that it is probably difficult to assure reproducibility in a series of releases based upon detonating mixtures, unless the packaging, grain size, canister strength, etc. are completely equal. Furthermore, recombination losses of the ionized species (and neutral atoms) is increased in a high pressure release.

Propellant-type constant pressure releases have been shown to have potentially greater ionization efficiency than detonation systems. The disadvantage inherent in constant pressure (propellant-type) releases of having a long, narrow trail of relatively dilute plasma may be overcome by using a cluster of nozzles, or a large number of nozzles mounted on a spherical container (hedgehop bomb).

Concerning the problem of initial expansion, an accurate evaluation of the initial stages of an explosion is very complicated. However, specific models may be set up to

approximate the expected yield of chemical species (primarily electrons) which survive the recombination during expansion.

In one of the more sophisticated treatments (cf. AFCEC 202), correlation was obtained between the calculated number of electrons quenched in the cloud after expansion and the RF ground observations. Furthermore, the results suggest the following important conclusions:

1. The final degree of ionization in the expanded cloud is a direct function of initial energy and an inverse function of initial radius.
2. The initial expanded cloud distribution (neglecting turbulence) is non-homogeneous. The electron density is expected to decrease monotonically from the center point to the outer boundary.
3. The final degree of ionization is inversely proportional to the average specific heat ratio of the expanding gas.

The present work also contains some brief comments concerning the "India" release in which barium was not observed. It was shown that if thermodynamic equilibrium is maintained up to a temperature drop to 3000°K , then practically all of the elementary barium is recombined to BaO . Suggestions have been made for improvement of barium yield in future experiments. Finally, some brief effort was applied toward the determination of the physical state of various liquid releases. Within the approximations made, it was found that the several liquid releases considered were all feasible.

(2) Mathematical Models for Chemical Release Studies

In the systematic analysis of chemical releases an area of prime importance is the generation and proper utilization of appropriate theoretical models to compare to the experimental data.

The concentration field of the cloud, produced by the released contaminant can be used to measure rates, provided one knows the initial and boundary conditions which are associated with the continuity equations of the concentration fields of both the contaminant and any atmospheric reactant. The continuity equation for a particular substance can be viewed as a specification of the physico-chemical processes, assumed to be in action, controlling the time rate of change of density of the particular substance whereas the initial and boundary conditions assumed for the substance specify the constraints on the concentration field. In short, these specifications of continuity equation and initial

and boundary conditions specify a model for the artificial cloud. Additionally, for each plausible artificial cloud model one can associate the experimental data with the parameters of the model.

The current effort has generated a number of such models for a single substance (AFCL-222) and two substances (AFCL-223) and has derived the concentration field equation for each proposed model.

For the single substance treatment the most complicated model investigated (with respect to the chemi-physical processes assumed to be in action) is characterized by the partial differential equation

$$\frac{\partial n}{\partial t} = D \nabla^2 n - \alpha n^2 + \beta n + F(R, t) \quad t > 0$$

where the characteristic physical or chemical processes associated with the various terms of Equation (1) are respectively: (a) diffusion, $D \nabla^2 n$; (b) recombination, αn^2 ; (c) linear growth (or decay), βn ; and (d) some arbitrary generation (or decay) process at point R in space for $t \geq 0$, $F(R, t)$.

For the case of two substances (coupled and/or mutually coupled) an analogous treatment has been generated with appropriate mathematical compromises in view of the more complex physical situation. The details are treated extensively in AFCL-222 and AFCL-223. The most accurate summary is given by the appropriate Tables and Summaries included in this report in Section 3. Some specific plots were obtained to illustrate the utility of the models to day, night and twilight releases. Further, they include some initial basic models for the generation of theory applicable to particulate scattering, resonance scattering, chemiluminescence, radar propagation, etc. as associated with releases. The current theoretical models effort is better summarized by reference here to Summary Sections AFCL 222 and 223.

(3) Optical Properties of Chemical Releases

The value of an understanding of the optical behavior of planned experiments has been discussed. This phase represents a continuing effort for the understanding of the pertinent areas of resonance scattering and chemiluminescence.

A. Resonance Scattering

Optical properties of resonance clouds with diffusion has been discussed in some detail in AFCL 207; therefore, no details were included in the present report. However,

Tables 2a through 2d reproduced here from AFCL 207 serve as a convenient condensation of the technical area covered. The Tables identify the physical problems investigated, the corresponding defining equations, the derived concentration functions, and the pertinent solutions for the preceding cases. Tables 3a through 3d present a summary of the techniques to employ for reducing and analyzing the data.

However, aside from the theoretical approach, considerable parameterization was accomplished in order to better appreciate some of the practical implications of the theory as to proper experimental design related to the determination of geophysical constants and/or practical utility in systems. A few examples of this type of parameterization are summarized in Table 4 and plotted in Figures 1, 2 and 3.

The data displayed in these Figures illustrate the several uses of optical observations on resonance clouds. For example, these or related data can serve to yield information on chemical yield, ionization yield (using resonant ions), diffusion, magnetic field alignment, chemical consumption rates, and many others discussed in AFCL 207 and AFCL 218.

An additional interesting use of these techniques is in the employment of resonant clouds for the determination of diffusion mechanisms. For illustration, a specific case has been investigated in which specified releases were made at 90, 110 and 200 km. These results are given in Figures 4, 5 and 6, which make evident the care that must be exercised in experiments of this kind. For example, the critical importance of understanding the roles of chemical consumption, solar resonance efficiency and diffusion is made evident in the figures.

Finally, it has been noted that the resonance scattering work thus far has dealt only with the case of back-scatter. Generalization should be extended to the cases of where the phase angle differs from 180° . Further, a more exact treatment using radiative transfer techniques should be performed.

B. Chemiluminescence

Artificial chemiluminescent clouds, produced by releasing known amounts of specific chemicals into the upper atmosphere, at prearranged heights, to react with an atmospheric in such a manner as to yield luminescence can be employed for atmospheric experiments and also as an aid to understanding some current AF applied problems in missile trail technology. However, the present need for technical groundwork is evident. To this

end, the systematic study of chemiluminescence has been initiated. Here, use is made of some models generated in Section 3. These have been extended to incorporate the appropriate physics. In these, the initial conditions assumed are written in several terms of arbitrary initial release geometries. The optical properties of these chemiluminescent cloud models are then defined in terms of the density functions; these properties are (a) $F_{cc}(x,t)$, the photon flux per unit volume, (b) $B(d,t)$, the brightness per unit area along a line of sight through the cloud, and (c) $F_T(t)$, the total flux of the cloud. Several geometric models have been specified including spherically symmetric intermediate and total Gaussian releases.

Other models deal with the chemiluminescent cloud models of finite extent (in one dimension, at least) and a finite homogeneous sphere is discussed. Next, a spherical shell model with an unmixed core is discussed. Finally, the properties of a finite spherical cloud is investigated for which the initial releases of contaminant are linear and parabolic, respectively.

The evaluation of the various models has proceeded to the point of calculating the various kinds of brightness profiles and flux per unit volume. To indicate this, some selected graphs are included (Figs. 7-10). They are self-explanatory when used in conjunction with the text.

(4) RF Propagation Studies Including Applications

A. RF Propagation Models

The simplest electromagnetic model applied to the electron cloud is the reflective one; this implies replacement of the cloud by a totally reflecting surface defined by the critical radius at the RF wavelength of interest. A more realistic treatment should take into account the refractive effects for more forward geometries by introducing the refractive bending of the incident energy from the underdense electron concentrations leading to greater values of cloud cross section and efficiency for propagation directions other than those from simple backscatter. It is concluded that a fruitful extension of these electromagnetic models lies in the direction of a treatment of the problem by the techniques of geometric optics such that ray tracing should be applied. It is to this end that some of the mathematical models of Section 3 have been generated. This extension is left as a future effort. However, to demonstrate the utility of the RF center-point models some results are given here (in Figs. 11-14) of the general day and nighttime models in terms of the center-point density normalized by the initial center-point value.

From the above figures one can obtain knowledge of both the Gaussian half-width, r_0 , and the time variation of the total electron content, and can then calculate the shell radius of any particular value of electron density and its time variation. This in turn is simply convertible into cloud cross section as a function of time. In other words, from the data which have been generated from the general models, the time and altitude variations of both critical frequency and cloud efficiency or cross section may be obtained.

B. RF Applications

In general, the RF systems to which the artificially generated environment is most simply and naturally applied are in the areas of communications. These have been discussed individually, stating several characteristics of the technology with respect to the appropriate military system interest. Some discussion has been given to specific applications to communication systems. Finally, several other applications were grouped in terms of a unique geometry class and a proposed interaction class. The discrimination application, wherein a cloud is generated such that a decoy ensemble and warhead impinge the cloud upon re-entry, fit into the latter category. It is suggested that many interactions between the decoys and the artificial cloud will occur which may aid in discrimination.

C. Optical Applications

Several applications to missile trail technology, geophysical measurements (including diffusion, chemical rates, winds, shear, recombination, attachment, etc.) and other AF systems have been suggested at various places throughout the document. They are not well summarized out of context; thus, only reference is made here to their existence in the main text.

ROCKET MEASUREMENT OF CHARGE DENSITIES

Rita C. Sagalyn

Headquarters, Air Force Cambridge Research Laboratories,
Air Force Research Division (ARDC), Geophysics Research
Directorate, L.G. Hanscom Field, Bedford, Massachusetts

Instruments have been designed and constructed for the rocket measurement of positive and negative ion and electron densities and their energy distributions. Generating voltmeters modified for the measurement of ambient electric fields in the ionosphere have also been developed and successfully flown. The sensitivity range of these instruments is great enough to measure electrical properties both in the undisturbed atmosphere and in artificially produced ion or electron clouds.

In August 1960 during the field tests carried out under Project Firefly, a Nike Asp rocket instrumented for the measurement of positively and negatively charged particles was launched 10 seconds after another Nike Asp set for a chemical release at about 100 km. Due to malfunction of the first Nike, the artificially produced cloud was not sampled, however, valuable information on ionospheric charge density variations around sunset was obtained from the instrumented rocket.

Data was obtained between 40 and 210 km. On the ascent the ionosphere was sunlit above 80 km. A positive ion density peak of 1000 ions per cc was observed at approximately 70 km. A sharp increase in charge density concentrations was found between 90 and 105 km with a second ionization maximum (10^5 ions per cc.) at 125 km. A slight depression in the distribution was observed at 140 km; the charge density concentration then increased steadily with altitude to apogee at 210 km. The concentration gradients measured on this flight are about a factor of 5 lower than those observed with the same instrumentation on earlier flights launched around local noon.

Photocells mounted on the rocket showed that the ionosphere was not sunlit on the descent below 150 km. The charge densities were at least a factor of 5 lower than on the ascent between 150 and 80 km. Below 80 km the ascent and descent values were comparable. There was also a significant decrease in the concentration gradients at the base of the E region on the descent portion of this flight.

The flight data is not yet completely analyzed, however, the results are being applied to the interpretation of production and loss processes in the ionosphere near sunset. After evaluating effective recombination and diffusion coefficients from this data, the results will be examined to determine the specific collision processes which could account for the observed values.

PARTICLE SIZE ANALYSIS OF SOME OF THE SOLAR SCATTER
MATERIALS USED IN PROJECT FIREFLY 1960

J. L. Brown

Engineering Experiment Station
Georgia Institute of Technology
Atlanta, Georgia

Particle size analyses were made of the solar scatter materials used in the Firefly experiments to determine if any relationship might exist between particle size and solar scatter measurements.

The materials analyzed were aluminum oxides SS 1 (Frances), SS 2 (Lily), SS 3 (Mavis); cadmium sulphide (Hedy); and cobalt powder (Linda). The general particle size range was small enough to require electron microscopy.

The analytical procedures used are common to the field of electron microscopy and micromeritics and will not be dealt with in detail here.

All the aluminum oxide samples seemed to possess bimodal* particle size distributions. Sample SS 3 adhered most closely to the predicted size with a median size of 0.027 microns; sample SS 1 had a median size of 0.35 microns while SS 2 was extremely bimodal with 95% of the particles below 1 micron in size.

The cadmium sulphide contained a wide range of particle sizes with a median at 0.5 microns. Some particles were as large as 5 microns. This material consisted of brownish-orange transparent crystals as observed in an optical microscope. This property should be taken into account in analysis of solar scatter by these particles.

The cobalt powder could not be dispersed sufficiently for a good particle count; however, the particles are acicular (needle-like) in shape and range from 0.5 to 3 microns in length.

Particle size data are presented here in the form of size-frequency bar graphs. This form is probably the most convenient to relate size and scattering effects.

Electron micrographs representing typical views of the materials are included with this report.

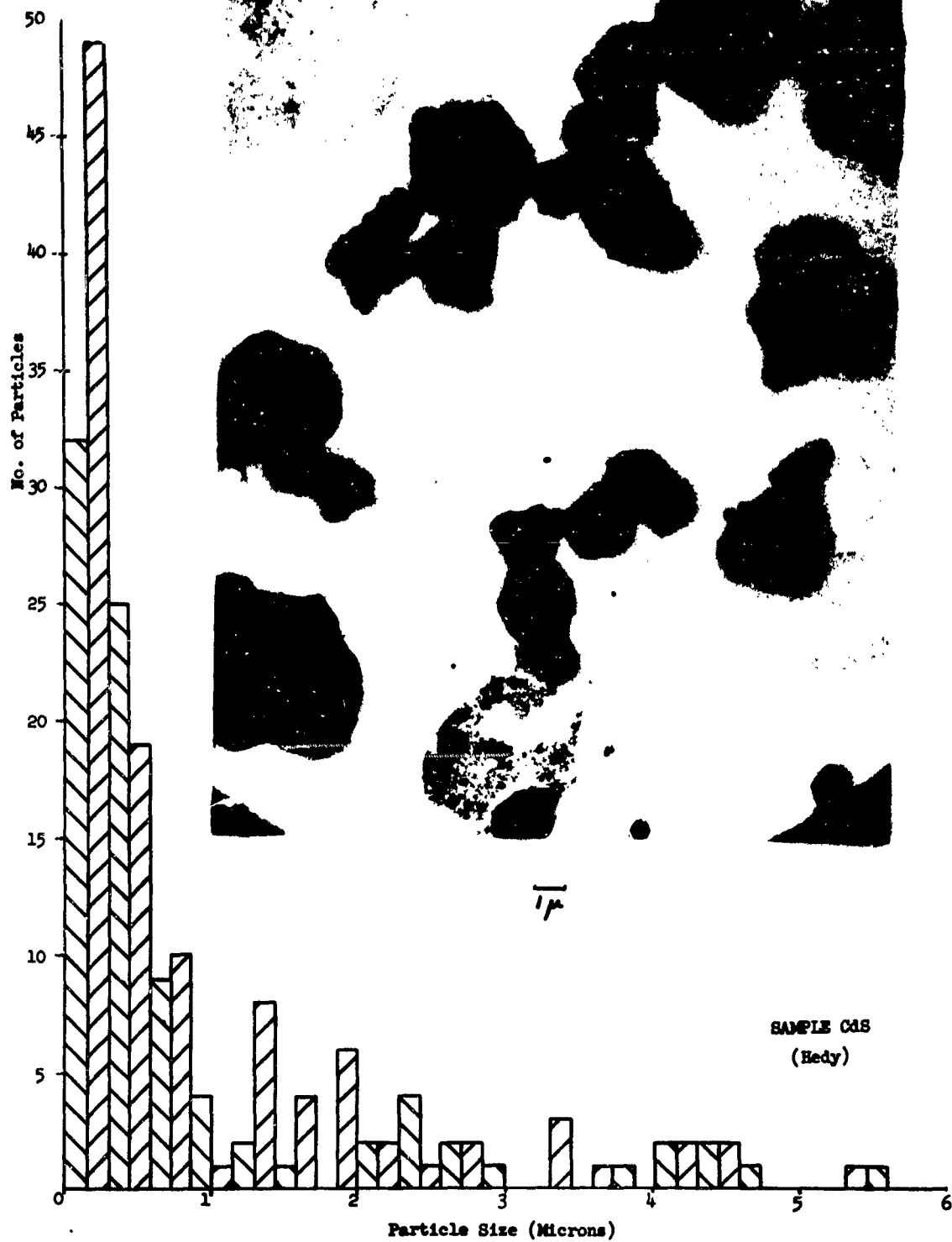
- - - - -

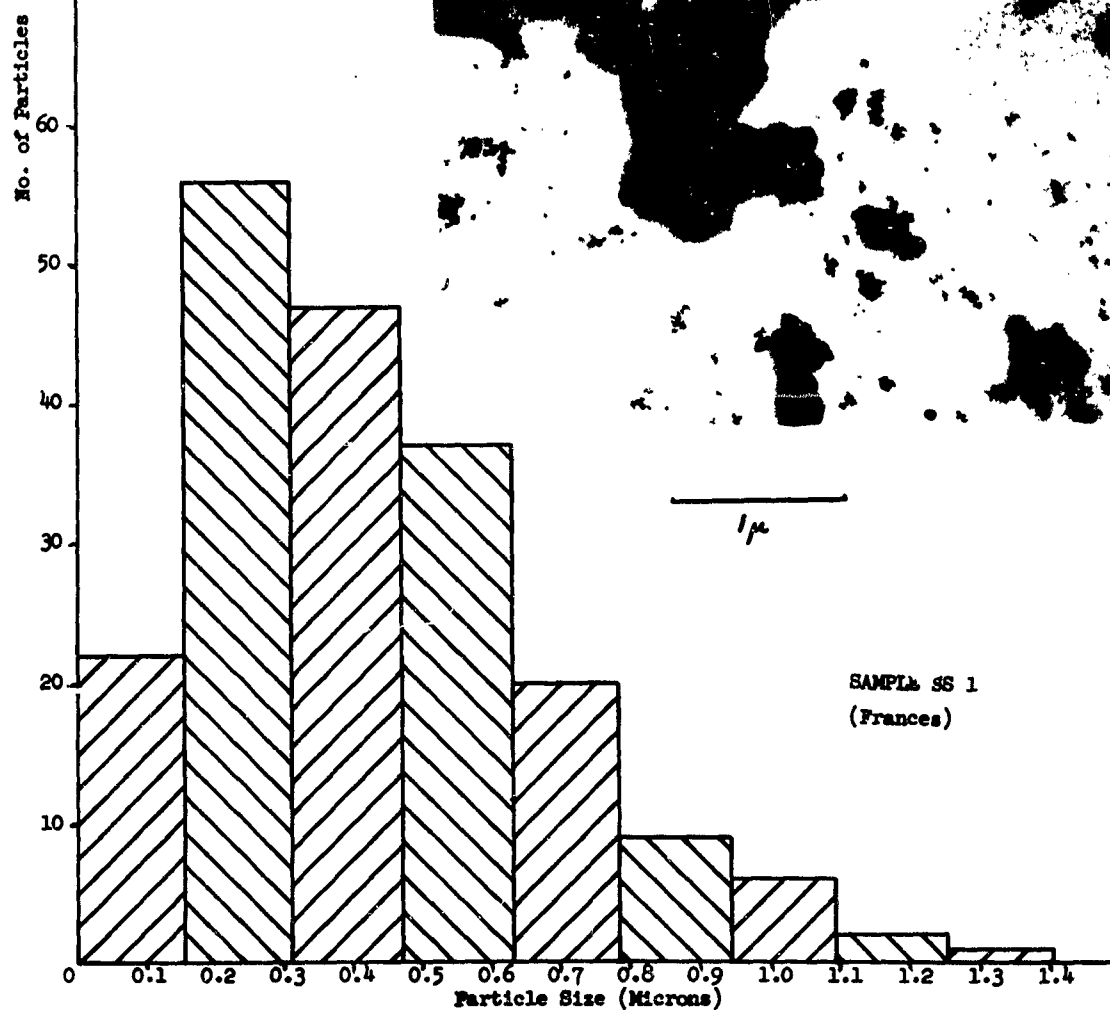
* A distribution lacking intermediate sizes; all particles either large or small.



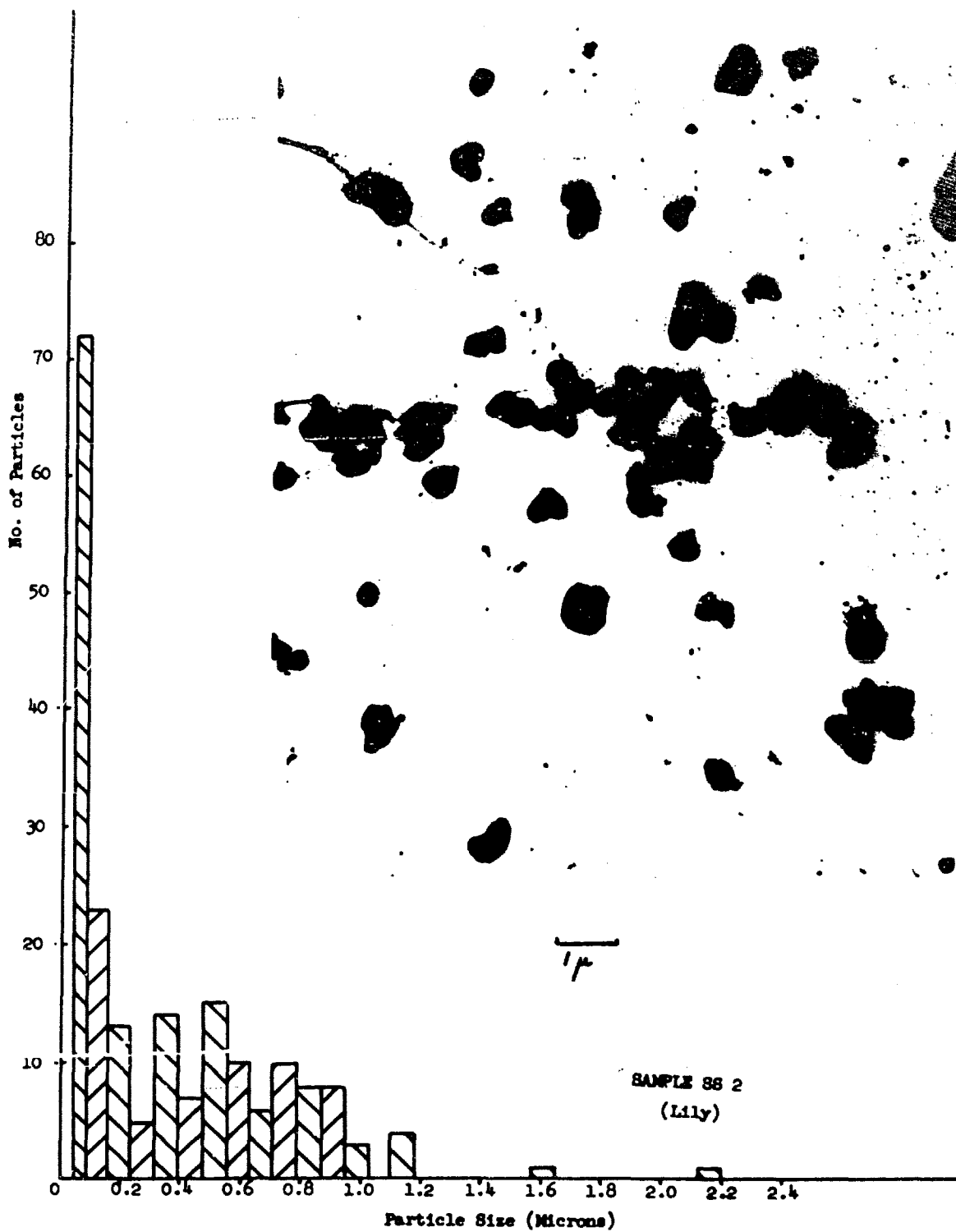
POWDERED COBALT

$\frac{1}{\mu}$



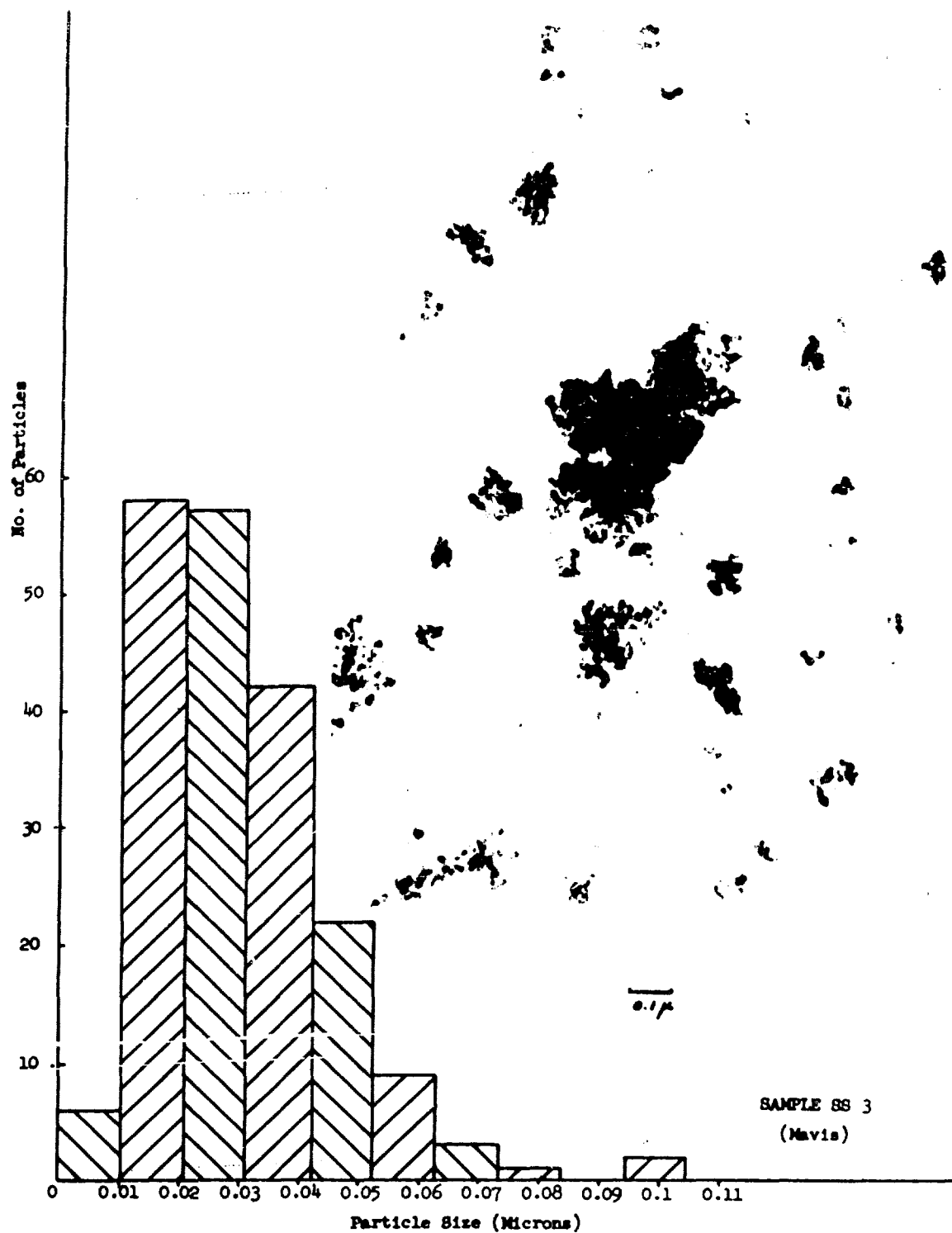


4076



Best Available Copy

4077



4678

Best Available Copy